The LINC complexe is a mechanotransducer that regulates catenin signaling during epithelial-mesenchymal transitions

Pietro Salvatore Carollo

Université de Paris

Ecole doctorale FIRE 474

Institut Jacques Monod / Mécanotransduction: de la surface de la cellule à son noyau - chef d'équipe: Dr. Nicolas Borghi

The LINC complex is a mechanotransducer that regulates catenin signalling during epithelial-mesenchymal transitions

Par Pietro Salvatore CAROLLO

Thèse de doctorat de Biophysique-Biologie Cellulaire

Dirigée par Dr. Nicolas BORGHI

Présentée et soutenue publiquement à Paris le 19/11/2019

Président du jury: Antoine GUICHET - Directeur de Recherche - IJM, Paris

Rapporteurs: Catherine COIRAULT - Directrice de Recherche - Institut de Myologie, Paris
Philippe CHAVRIER - Directeur de Recherche - Institut Curie, Paris

Examinateurs: Christophe GUILLUY - Chargé de Recherche - IAB, Grenoble
Sandrine ETIENNE-MANNEVILLE - Directrice de Recherche - Institut Pasteur, Paris

Directeur de thèse: Nicolas BORGHI - Chargé de Recherche - IJM, Paris

Title: The LINC complex is a mechanotransducer that regulates catenin signalling during epithelial-mesenchymal transitions

Abstract

In multicellular organisms, cells generate and experience mechanical forces. As a consequence, these forces can regulate cellular behaviour as well as tissue organization through a process known as "mechanotransduction", by which cells convert mechanical stimuli into biochemical signals. In animal cells, the nucleus is mechanically coupled by the cytoskeleton to cell adhesion complexes, such that extracellular mechanical cues can affect the position and shape of the nucleus. Such mechanical coupling is provided by outer nuclear transmembrane proteins, nesprins, whose KASH domain interacts with inner nuclear transmembrane SUN proteins in the perinuclear space. The cytoplasmic domain of nesprins can bind to the cytoskeleton and the nucleoplasmic domain of SUNs to the nucleoskeleton to form the so-called LINC complex: Linker of Nucleoskeleton and Cytoskeleton. Mutations in, or loss of LINC complex proteins impair nuclear envelope integrity, nucleus anchoring, chromosome positioning, DNA repair, genome transcription and replication and, in addition, LINC complex disruption negatively impacts nuclear translocation of transcription co-factors. However, it is still unclear whether the consequences of a dysfunctional LINC complex result from an impairment of mechanotransduction.

In this thesis, we focused on nesprin-2 giant (nesprin2G), which forms a complex with and regulates the nuclear localization of β-catenin, a major transcription co-factor in several morphogenetic processes. Upon induction of epithelial-mesenchymal transition (EMT) -a process through which epithelial cells can gradually acquire increased motility and decreased intercellular adhesion-, epithelial cell packing regulates β-catenin signalling. We thus hypothesized that the LINC complex could participate in this mechanical regulation. To this aim, we combined molecular tension microscopy, involving a genetically encoded FRET biosensor, with mechanical, genetic and pharmacological perturbations of fibroblastic and epithelial cells in culture.

We found that the LINC complex is mechanosensitive to cell packing. Moreover, nesprin2G tension increases upon induction of partial, but not complete EMT, thereby defining two mechanisms of β-catenin nuclear translocation. Upon induction of complete EMT, relaxed nesprin2G recruits α-catenin at the nuclear envelope, which results in nuclear translocation of both catenins. Upon partial EMT however, tensed nesprin2G does not recruit α-catenin and only β-catenin translocates to the nucleus. Finally, we found that α-catenin sequesters β -catenin in the nucleus in a transcriptionally less active form. We thus propose that, in a manner dependent on the EMT program, mechanosensitive nesprins may capture, at the nuclear envelope, the catenins and fine-tune their nuclear translocation and activities.

Keywords: Mechanotransduction/Nuclear Envelope/LINC complex/α and β-catenins/EMT/FRET biosensor/Microscopy

Titre: Le complexe LINC est un mécanotransducteur qui régule la signalisation de la caténine au cours des transitions épithélo-mésenchymateuses

Résumé

Dans les organismes multicellulaires, les cellules génèrent et subissent des forces mécaniques. En conséquence, ces forces peuvent réguler le comportement cellulaire ainsi que l'organisation des tissus grâce à un processus appelé «mécanotransduction», par lequel les cellules convertissent les stimuli mécaniques en signaux biochimiques. Dans les cellules animales, le noyau est couplé mécaniquement par le cytosquelette aux complexes d'adhésion cellulaire, de sorte que des signaux mécaniques extracellulaires puissent affecter la position et la forme du noyau. Un tel couplage mécanique est assuré par les protéines transmembranaires nucléaires externes, les nesprines, dont le domaine KASH interagit avec les protéines SUN transmembranaires nucléaires internes dans l'espace périnucléaire. Le domaine cytoplasmique des nesprines peut se lier au cytosquelette et le domaine nucléoplasmique des SUN au nucléosquelette pour former le complexe dit LINC: Linker of Nucleoskeleton and Cytoskeleton. Les mutations ou la perte de protéines du complexe LINC altèrent l'intégrité de l'enveloppe nucléaire, l'ancrage du noyau, le positionnement des chromosomes, la réparation de l'ADN, la transcription et la réplication du génome et, de plus, la rupture du complexe LINC a un impact négatif sur la translocation nucléaire des co-facteurs de transcription. Cependant, il n'est pas clair si les conséquences d'un complexe LINC dysfonctionnel résultent d'une déficience de la mécanotransduction.

Dans cette thèse, nous nous sommes concentrés sur la nesprine-2 géante (nesprine2G), qui forme un complexe avec et régule la localisation nucléaire de la β-caténine, un co-facteur de transcription majeur dans plusieurs processus morphogénétiques. Lors de l'induction de la transition épithélium-mésenchyme (TEM) -processus par lequel les cellules épithéliales peuvent acquérir progressivement une motilité accrue et une adhésion intercellulaire réduite- la compaction des cellules épithéliales régule la signalisation de la β-caténine. Nous avons donc émis l'hypothèse que le complexe LINC pourrait participer à cette régulation mécanique. À cette fin, nous avons combiné la microscopie de tension moléculaire, impliquant un biosenseur FRET codé génétiquement, à des perturbations mécaniques, génétiques et pharmacologiques de cellules fibroblastiques et épithéliales en culture.

Nous avons constaté que le complexe LINC est mécanosensible à la compaction des cellules. De plus, la tension de nesprin2G augmente lors de l'induction d'une TEM partielle, mais pas d'une TEM complète, définissant ainsi deux mécanismes de translocation nucléaire de la β-caténine. Lors de l'induction de la TEM complète, la nesprine2G détendue recrute l'α-caténine au niveau de l'enveloppe nucléaire, ce qui entraîne une translocation nucléaire des deux caténines. Cependant, en cas de TEM partielle, la nesprine2G sous tension ne recrute pas d'α-caténine et seule la β-caténine effectue une translocation dans le noyau. Enfin, nous avons constaté que l'α-caténine séquestrait la β-caténine dans le noyau sous une forme transcriptionnellement moins active. Nous proposons donc que, d'une manière dépendant du programme de TEM, les nesprines mécanosensibles peuvent capturer, au niveau de l'enveloppe nucléaire, les caténines et réguler finement leur translocations et activités nucléaires.

Mots-clés: Mécanotransduction/Enveloppe nucléaire/Complexe LINC/α et β-caténines /TEM/Biosenseur FRET/Microscopie

Acknowledgments

I would like to thank my PI, Dr. Nicolas Borghi, for his precious mentoring and scientific support provided to me throughout my PhD years.
I am thankful to all my co-workers, present and past, in the lab with whom I shared the researcher's daily routine.
I am very grateful to Imagoseine Facility at Institut Jacques Monod and, especially, I would like to thank Xavier Baudin, whose constant help let me carry out microscopy experiments.
My thanks go also to Dr. Matthieu Piel and Dr. Valérie Doye, my TAC members, whose insightful advices have been important for my PhD project.
Last, but not least, I deeply thank my mother and father, Maria Antonia and Filippo, and my brother, Riccardo, for their constant emotional support and I am very, very grateful to my fiancé, Viviana, whose presence in my everyday life is simply fundamental.

General table of contents

CHAPTER 1

Mechanotransduction: a growing field in biology

Table of contents

Premise

The study of biological phenomena in living organisms has been greatly focused, over the past 50 years, on unravelling the subtle molecular mechanisms underlying cellular functions. Indeed, scientists have made a great effort in deciphering the "hidden secrets" of the cellular genome and proteome, bearing in mind that understanding how nucleic acids and proteins work and interact together is the key to explain every shade of cell's behaviour. Despite the incomparable breakthroughs achieved with this approach in life sciences, a wider view to see and interpret cellular biology has been lacking for decades. Indeed, explaining cell's behaviour and functions by only using an "omic" approach, which involves a large-scale study of genomes and proteins, is somehow not complete, since a cell is not a single entity out of context but, on the contrary, it is surrounded by an environment, to which cell interacts by receiving inputs and giving outputs. If we just thought about the simplicity of the unicellular organisms or the complexity of the animals, we would be astonished by the fact that cells can literally shape and regulate themselves according to the plethora of stimuli they receive. From bacterial clones on a Petri dish to animal and plant cells organized in structured tissue and organs, it is extremely clear that cells must have developed some "tools" to be used, accordingly with a specific genetic and protein repertoire, to explore and interact among themselves as well as with their surroundings.

It is thus clear that the only "omic" approach is not sufficient to explain cell's behaviour in relation to its external environment and, therefore, a more specific and accurate way to study intracellular/extracellular interactions is needed.

Since cells respond to physical stimuli, we can therefore talk about "mechanobiology" and specifically "mechanotransduction", which is basically the way cells sense and respond to mechanical signals - coming from the cell's interior or its surroundings -, by converting them into biochemical signals (Donald E. Ingber, 2006; Ingber, 2003; Maurer & Lammerding, 2019). Actually, the term mechanotransduction refers to both physical stimuli and the consequent biochemical signalling, which can generate confusion. To be more accurate, we can talk about "mechanotransmission" and "mechanosensing" (Maurer & Lammerding, 2019), both of them part of the larger phenomenon that is the mechanotransduction. "Mechanotransmission" is the transmission, throughout the cell, of the

mechanical cues via the cytoskeletal elements (such as actin filaments, microtubules and intermediate filaments). "Mechanosensing" is, instead, the actual process of transduction through the activation of mechansensors or mechanotransducers, which fundamentally are the protein complexes located at one specific side of the cell, such as the Focal Adhesions (Fas) (N. Wang, Butler, & Ingber, 1993) on adherent animal cells, or the stretch-sensitive ion channels onto the plasma membrane of prokaryotes and eukaryotes (Martinac, 2004). Not only proteins are able to discriminate mechanical signals, indeed some organelles, such as the nucleus, are mechanosensitive (Isermann & Lammerding, 2013; N. Wang, Tytell, & Ingber, 2009).

Once mechanosensors are active, downstream signalling pathways can be activated, thus regulating multiple cellular functions.

To understand the great revolution that mechanotranduction has represented, over the years, in biology, it is worth to trace its historical path. Therefore, in the following paragraph, I will briefly discuss some works which have been extremely important in bringing pieces of evidences on mechanotransduction and its consequences.

1 Mechanotransduction through history: pioneering works

The first hints of mechanotransduction date back to the end of the 19th century, when the German surgeon Julius Wolff noticed that the trabecular bone forms load-bearing struts and continuously reshapes interstitially (Wolff, 2010a, 2010b, 2011; WOLFF & J, 1892).In his work, Wolff looked at the process of bone ossification due to mechanical loading/unloading as a consequence of geometric changes induced by mechanics (Wolff, 2010a, 2010b, 2011; WOLFF & J, 1892).

Some years later, at the beginning of the 20th century, D'Arcy W. Thompson proposed that the distribution of the surface tension is at the base of the organization of cells in tissues (Thompson, 1995). But Wilhelm Roux (1850-1924) was the first to associate mechanics with biology. Indeed, he proposed that direct physical forces caused biological processes: compression induces bone, tension induces connective tissue and, ultimately, shear plus compression or tension induces cartilage (Hamburger, 1997). Which can be therefore summarized as "form follows function" (Wall et al., 2018).

Despite these very early studies and theorizations, including the 1939 work by Moore and Burt on the forces causing gastrulation in embryos of *"Dendraster excentricus"* (Moore & Burt, 1939), mechanotransduction remained a relatively unexplored field till the 70s, when Beloussov et al. dissected embryos of *"Rana Temporaria"* to study tissue shape alterations (Beloussov, Dorfman, & Cherdantzev, 1975). From such experiments, the scientists were able to discriminate between two categories of deformations. The first one accounted for deformations happening just after dissection, which were identified as passive relaxations of previously established elastic tensile stresses; the second category listed deformations which were slow to happen. During these latter, cells elongated and migrated and, occasionally, isolated fragments of the dissected tissue underwent complex morphodifferentiations. Researchers considered these phenomena as the result of the contractile systems within the cell, either pre-existing or induced *de novo*.

In the meantime, Rodan et al. demonstrated that compressive forces in the order of 60g/cm^2 (that is of physiologic magnitude) determined a reduced concentration of both cyclic AMP (cAMP) in the epiphyses of 16-day-old chick embryos' tibiae (Fig 1A). In addition, they looked at cAMP and cyclic GMP (cGMP) levels in cells extracted from the distal, middle and proximal parts of the same epiphyses and subjected these cells to an equivalent hydrostatic pressure as above. Also in this case, cAMP plus

cGMP levels varied in respect to a control condition where pressure was not applied (Fig 1B). The authors thus concluded that the bone immediately responds to the applied pressure by altering the levels of cAMP and cGMP (Rodan, Bourret, Harvey, & Mensi, 1975) .

A

Time (min)	Cyclic AMP in control bones (pmole/epiphyses)	*N*	Cyclic AMP (exp/control)*	*P*
0	38.5 ± 13.2	6		
2	64.4 ± 4.9	15	0.98	†
4	78.5 ± 3.9	6	1.06	†
8	84.3 ± 7.1	6	0.80	< .01
12	92.7 ± 1.2	6	0.67	< .01
15	93.5 ± 10.6	6	0.72	< .01
18	82.2 ± 6.3	12	0.65	< .01
20	66.8 ± 8.4	4	0.87	†

*Mean ratio of experimental to control. †Difference is not statistically significant.

B

Segment	Accumulation in cells (pmole/10^6 cell)	
	Cyclic AMP	Cyclic GMP
Distal		
Pressure	61.7 ± 11.2	13.4 ± 1.8*
Control	88.0 ± 9.0	7.9 ± 1.7
Middle		
Pressure	105.5 ± 18.7*	5.5 ± 0.5*
Control	77.0 ± 13.5	3.6 ± 0.7
Proximal		
Pressure	106.2 ± 16.5	6.3 ± 0.7*
Control	104.3 ± 17.2	12.6 ± 1.9
No. experiments	15	

*$P < .05$.

Fig 1: Pressure applied, over time, on epiphyses of 16-day-old chick embryos' tibiae alters cAMP levels in bone (A) and cAMP plus cGMP levels in cells extracted from bone (B). In A, the significant differences are boxed in red. Adapted from (Rodan et al., 1975)

The next year, Bourret and Rodan demonstrated that the drop in cAMP concentration under pressure is due to calcium intake with a consequent inhibition of the membrane-associated adenyl cyclase (Bourret & Rodan, 1976).

The above studies gave an evidence which implied that, somehow, mechanical stimuli can affect cell's function, which results in variations in cellular metabolism.

A direct demonstration of the influence of mechanotransduction on cell's metabolism dates back to Frangos' work. This study revealed that human endothelial cells, subjected to a pulsatile flow shear stress, increased the production of the potent platelet aggregation inhibitor prostacyclin (PGI_2) (Frangos, Eskin, McIntire, & Ives, 1985) (Fig 2A). Some years later, the group of McIntire showed that in HUVEC cells subjected to arterial shear stresses of 15 and 25 dynes/cm^2, the tissue plasminogen activator (tPA) secretion rate was higher (2.1 and 3.0 times higher, respectively) than in in control condition with no shear stress(Diamond, Eskin, & McIntire, 1989) (Fig 2B).

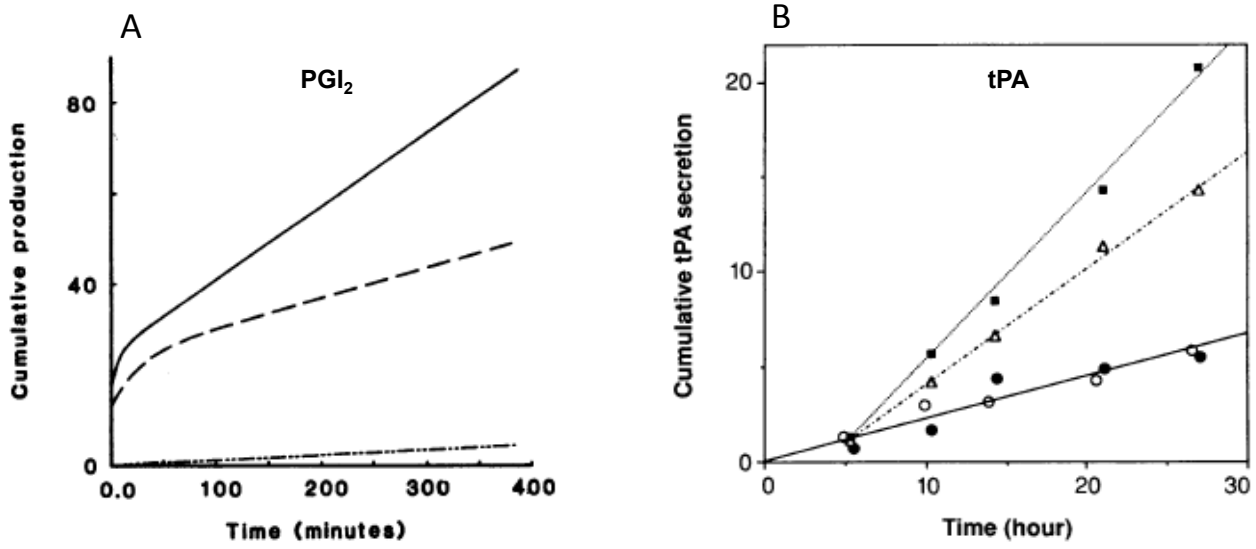

Fig 2. Shear stress influences cell's metabolism. A: cumulative production of PGI_2 in human endothelial cells subjected to pulsatile (straight line), steady (dashed line) and near-zero (dotted-dashed line) flow shear stress. From (Frangos et al., 1985). B: cumulative tPA production in HUVEC cells maintained in static culture (black circles) or exposed to different steady laminar shear stresses of 4 (open circles), 15 (open triangles) and 25 (black squares) dynes/cm^2. Note that with 4 dynes/cm^2 the authors reproduced venous shear stress. From (Diamond et al., 1989).

Mechanical cues thus do regulate cell's metabolism and as postulated by Diamond et al. in the case of tPA secretion, they must control mRNA transcription (Diamond et al., 1989) Therefore, can physical stimuli influence gene expression as well? A first answer to this question was given by Farge group in 2002. Indeed, Rauch et al. demonstrated that mechanically-inhibited endocytosis of BMP2 (bone morphogenetic protein 2) signalling protein determines nuclear translocation of Smad1 (mother against Dpp), with increased expression of *Jun b* gene in C2C12 mouse myoblasts (Rauch, Brunet, Deleule, & Farge, 2002). One year later, Emmanuel Farge showed the direct implication of mechanical forces on developmental gene expression. By applying a constraint to the fruitfly *Drosophila Melanogaster* embryos, the researcher was able to show that *Twist* gene and protein expression, involved in fruitfly development, is sensitive to mechanical forces via the nuclear accumulation of Armadillo, the homolog of mammalian β-catenin in *Drosophila* (Farge, 2003) (Fig 3A and B).

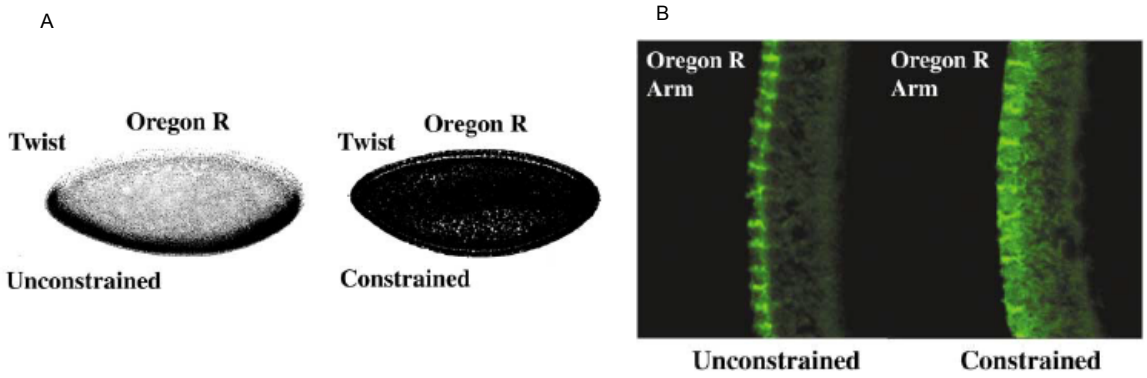

Fig 3: Mechanical stress induces Twist protein ectopic expression in Oregon R *Drosophila* embryos (A) via nuclear accumulation of Armadillo (B). Adapted from (Farge, 2003).

Force sensing has been also demonstrated to determine the differentiation fate of naive mesenchymal stem cells (MSCs). Indeed Engler et al. showed that naive MSCs differentiated towards neurons, myoblasts or osteoblasts if plated on a substrate with stiffness mimicking the one found in brain (0.1-1kPa), muscle (8-17kPa) or bone (25-40kPa), respectively (Engler, Sen, Sweeney, & Discher, 2006) (Fig 4A). In addition, this lineage specification was shown to be dependent on nonmuscle myosin II (NMM II) activity. Indeed, MSCs treated with the myosin II inhibitor blebbistatin failed to differentiate when seeded on the above substrate (Engler et al., 2006)(Fig 4B). Thus the activity of NMM II is required for matrix-lineage commitment.

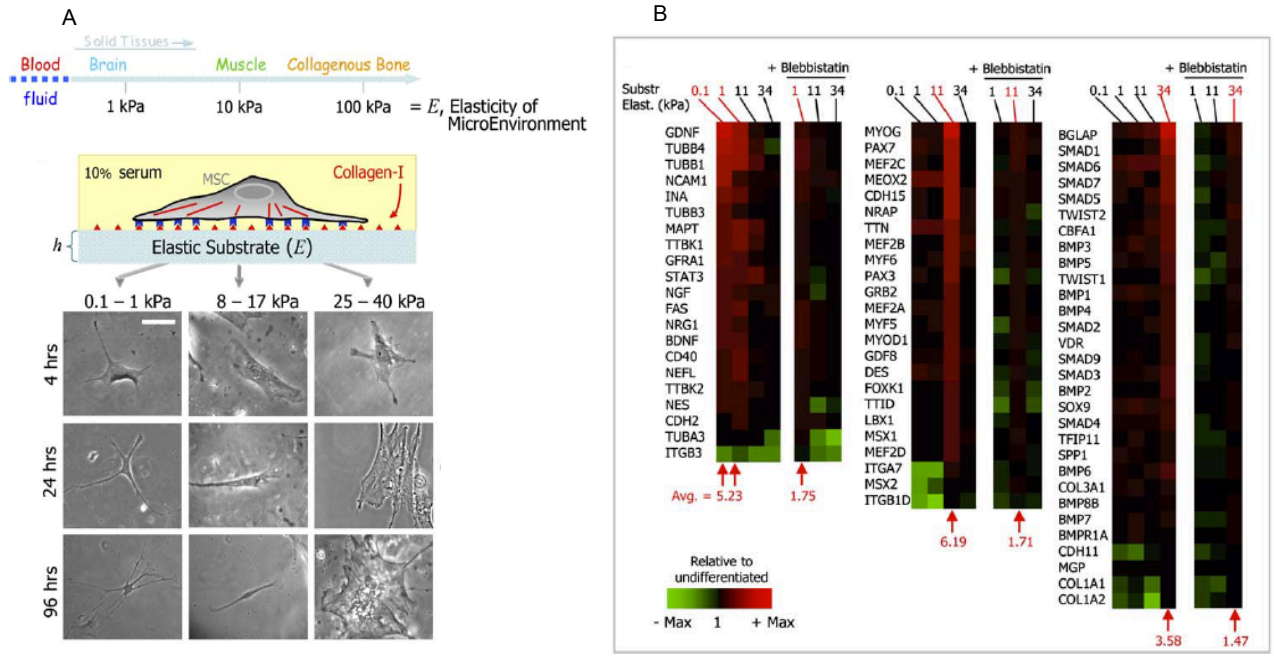

Fig 4: Substrate stiffness determines MSCs differentiation fate. A, above: schematic representing the different and increasing tissue stiffness (or elasticity "E") from brain to bone; middle: schematic depicting the substrate used to plate MSCs (h: substrate thickness); below: fate specification, over time, of MSCs seeded on the above substrate (see "middle") with increasing stiffness, mimicking brain (0.1-1kPa), muscle (8-17 kPa) or bone (25-40 kPa) elasticity, respectively. Scale bar: 20μm B: Microarray expression map for genes involved in neurogenic (left), myogenic (middle) or osteogenic (right) differentiation in MSCs at the indicated stiffness. Note that the presence of blebbistatin blocks lineage commitment. Adapted from (Engler et al., 2006).

The first demonstration of the existence of a protein able to act as a mechanosensor was given by Sheetz team, which demonstrated that the Focal Adhesion (FA) protein p130Cas undergoes tyrosine phosphorylation by Src family kinases (SFKs) after a 10% biaxial stretch in HEK cells (Sawada et al., 2006) (Fig 5A). Moreover, phosphorylated p130Cas involved the activation of the small GTPase RAP1 (Sawada et al., 2006) (Fig 5B), which is important in different signalling pathways as well as in integrin signalling (Hattori & Minato, 2003). Thus, a direct connection between mechanical cue sensing and consequent activation of intracellular signalling was demonstrated.

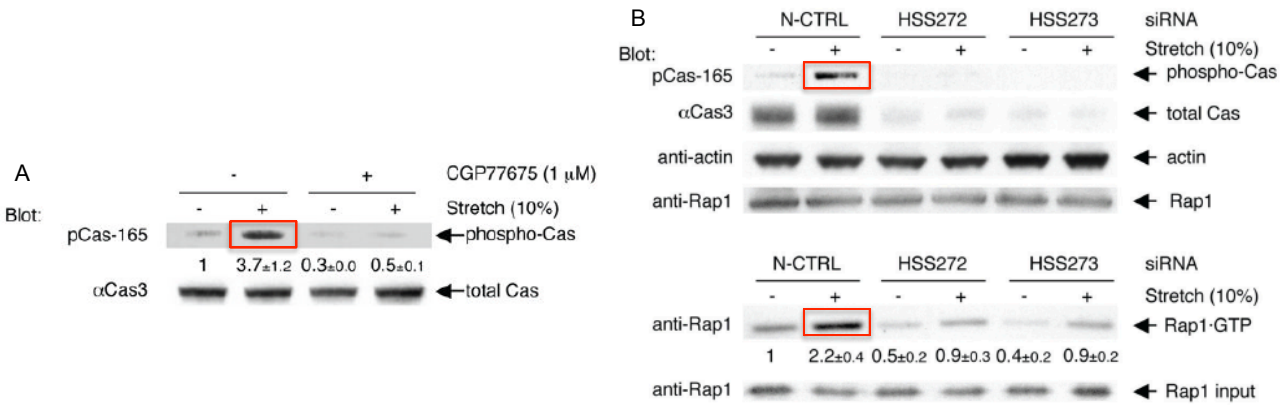

Fig 5: p130Cas is tyrosine phosphorylated upon stretch with consequent RAP1 activation. A: p130Cas phosphorylation (box in red) is mediated by SFKs (inhibited by CGP77675) upon stretch. B: Following p130Cas phosphorylation (box in red), the small GTPase RAP 1 is activated (box in red). Note that depletion (siRNA) of

p130Cas causes a significant reduction of RAP1 activation, even in presence of stretch. Adapted from (Sawada et al., 2006)

From the above studies, it is clear that the phenomenon of mechanotransduction influences many aspect of cell's behaviour -ranging from shape and metabolism to gene expression and cell fate decision- and, therefore, a deep comprehension of how it mechanistically works is of great importance in cell biology.

In the next paragraph, I will briefly discuss the different mechanistic models proposed to explain mechanotransduction.

2 Molecular scale mechanistic models of mechanotransduction

Daily, cells in our body continuously sense and respond to a plethora of mechanical stimuli. For instance, physical exercise generates and models muscle cells (Fitts & Widrick, 1996), which implies that muscles precursors must respond to mechanical forces, with their consequent expansion/contraction and differentiation (Lim, Jang, & Kim, 2018; Torgan, Burge, Collinsworth, Truskey, & Kraus, 2000) Endothelial cells in blood vessels are constantly subjected to a shear stress due to blood flow (Baratchi et al., 2017), whose change can determine atherosclerosis (Hajra et al., 2002). Also hearing and touch rely on mechanotransduction: vibration or pressure are forces sensed and interpreted by sensory neurons (Lim et al., 2018). It is intuitive to say that all the above forces cause a deformation in cell's structure and this deformation must be converted into biochemical inputs to execute cell's responses. We can thus conceive two ways of transferring physical stimuli to generate biochemical signals. The first one is referred to as the "tethered model"; instead we can call the second one as the "lipid bilayer model" (Lim et al., 2018).

In the "tethered model", when proteins tethered to the cell-cell contacts or to the interface between cell-extracellular matrix (ECM) are pulled by mechanical forces opposed to the tethering site, they can stretch with consequent conformational changes. These changes can involve the exposure of a protein-binding site or the disruption of a protein-protein interaction (Lim et al., 2018; Orr, Helmke, Blackman, & Schwartz, 2006) (Fig 6A and B). The latter can result in the release of a biochemical messenger, such as a growth factor, in the cell's interior with the consequent activation of signalling pathways.

In the "lipid bilayer model", cells can be entirely as well as locally deformed by applied mechanical forces and this can result in stretching and/or bending of the lipid bilayer in the plasma membrane. As such, this deformation in the cellular membrane can result in conformational changes in the integral plasma membrane proteins, with following changes in protein-protein interactions or enzymatic activity (Lim et al., 2018; Orr et al., 2006). Notably, the lipid bilayer model has been used to explain the opening or closing of "mechano-gated" ion channel (Haswell, Phillips, & Rees, 2011) (Fig 6D), even though their activity can be modulated by the tether model as well (Fig 6C).

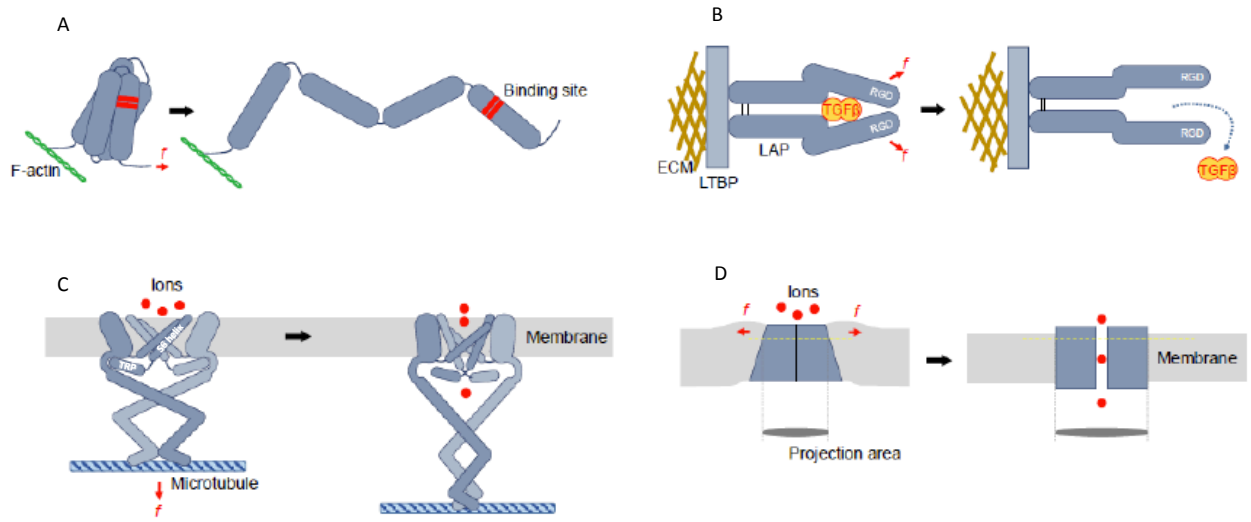

Fig 6: Tethered (A, B and C) and lipid bilayer (D) models used to describe conformational changes in mechanosensor proteins, leading to the activation of signalling pathways. A: A protein is stretched upon force application with the unmasking of a protein-binding site (in red). B: Mechanical force causes the transforming growth factor β (TGF β) release from the latency-associated peptide (LAP). C: NOMPC (no mechanoreceptor potential C) opening is associated with structural changes in the S6 helices. D: TRAAK and TREK-2 opening after plasma membrane stretching. Red arrows indicate force direction. Adapted from (Lim et al., 2018)

With the tethered model, one can explain, for instance, the molecular stretching of p130Cas, which results in its following phosphorylation (Sawada et al., 2006), or the binding of the Focal Adhesion (FA) protein vinculin to talin (another FA protein) after talin stretching, in vitro (Del Rio et al., 2009) (Fig 6A). Also, the tethered model can be used to understand the transforming growth factor β (TGF β) release from the "latency-associated peptide" (LAP) (Lim et al., 2018) Mechanical forces applied to LAP induce its conformational change, with consequent TGF β release (Buscemi et al., 2011) (Fig 6B).

The tether model can also explain the opening of some mechano-gated ion channels, such as the NOMPC (no mechanoreceptor potential C, also referred to as TRPN1), a mechanosensing-involved channel present in *Drosophila* (Walker, Willingham, & Zuker, 2000) (Fig 6C). Basically, the channel is made of four subunits, each of which comprises six alpha helices (S1-S6), with helices S5 and S6 forming the pore domain, where each S6 helix from each channel subunit blocks the passage of ions (Jin et al., 2017).

When a stretching force is applied to the channel, structural changes in the S6 helices cause the opening of the pore domain, with the subsequent entry of ions (Jin et al., 2017) (Fig 6C).

The lipid bilayer model can be used to describe the opening of some other mechano-gated channels, such as the mammalian K^+ channels TREK-1 (F Maingret, Patel, Lesage, Lazdunski, & Honoré, 1999; Patel et al., 1998), TRAAK (François Maingret, Fosset, Lesage, Lazdunski, & Honoré, 1999) and TREK-2 (Lesage, Terrenoire, Romey, & Lazdunski, 2000), each of them made of four transmembrane domains (TM1-TM4). It has been demonstrated that TRAAK and TREK-2 have an "up" and a "down" conformation (Brohawn, 2015; Brohawn, Campbell, & MacKinnon, 2014; Dong et al., 2015), corresponding to the "open" or the "close" state, respectively. In the "up" conformation, TM4 in the channels is moved upwards, whereas, in the "down" conformation, TM4 is moved downwards. These movements cause the opening (upon mechanical stretching) or closing of the channel, respectively, thus regulating ion entry (Fig 6D).

It is evident that cell's mechanosensors can work according to the tethered model or the lipid bilayer model, thus impacting cellular functions through mechanotransduction.

In the next paragraph, I will outline how mechanotransduction works in the cell, taking into account mechanosensing and mechanotransduction signalling.

3 Mechanotransduction in the cell: mechanosensors and mechanical signalling

As previously shown, mechanosensors can undergo conformational modifications if a mechanical stimulus is applied, with subsequent changes in cell's functions. As a consequence, cell's cytoskeleton can be imagined as a "hard-wired" network (N. Wang et al., 2009), which can induce variations in cellular, cytoskeletal and nuclear structures upon mechanical forces (Ingber, 2003) (Fig 7A). The meaning of "hard-wired" stands in the fact that cytoskeleton's filaments are strong enough to deal with mechanical stress cells undergo, thus keeping their shape stable (N. Wang et al., 2009). As such, cell's shape stability and mechanical force transmission throughout cell's interior are dictated by the level of isometric tension (also referred to as "prestress") in the cytoskeleton. We can define the prestress as the result of a force balance between opposing structural elements in the cell (namely cytoskeletal filaments and extracellular adhesions). Such a phenomenon happens because cell tenses and thus stiffens cytoskeleton's filaments relative to the surrounding cytoplasmic regions (Donald E. Ingber, 2006; Ingber, 2003; N. Wang & Suo, 2005). By virtue of the prestress in the cell's cytoskeleton, mechanical cues are faster in propagation than diffusion-based chemical signals (N. Wang et al., 2009) (Fig 7 B).

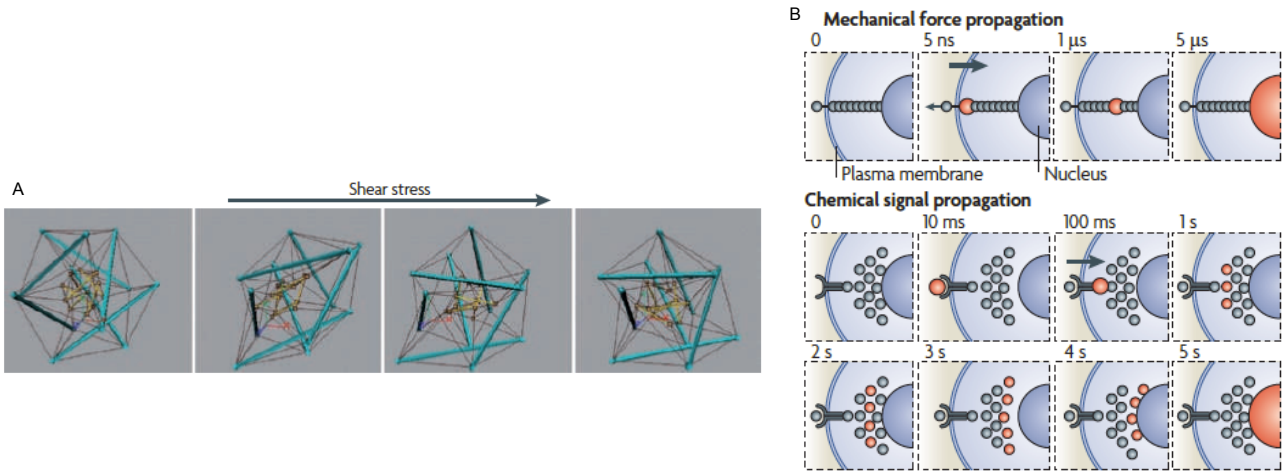

Fig 7: In cells, the "hard-wired" model accounts for mechanical force propagation (A), which is much largely faster than chemical signal propagation (B). Note that mechanical force propagation is in the order of micro-seconds, whereas chemical signal propagation is in the order of seconds. Adapted from (N. Wang et al., 2009).

In adherent animal cells, the first layer of extracellular mechanostranduction is represented by the interaction between ECM and cellular membrane via Focal Adhesions (FAs) (Fig 8). Indeed, FAs are multiprotein complexes through which extracellular mechanical stimuli can be perceived and, thus, transmitted to the cell's interior (Martino, Perestrelo, Vinarský, Pagliari, & Forte, 2018). Due to their complexity in structure, FAs can be split in a transmembrane and in an intracellular layer. Basically, the transmembrane layer is composed of integrins, which establish cell-ECM contacts, connected to the cytoskeletal actin filament via the intracellular layer of scaffolding, docking and signalling proteins (Martino et al., 2018) (Fig 8). ECM mechanics and structure influence FAs core

protein composition. Moreover, integrin clustering impacts the recruitment of proteins in FAs (Cavalcanti-Adam et al., 2007; Schiller & Fässler, 2013).

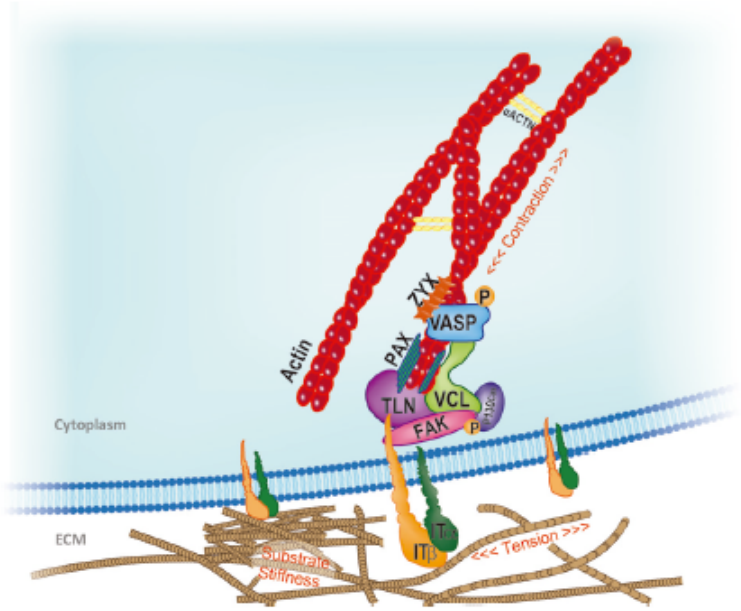

Fig 8: Focal Adhesion structure. See text for details. ACTN, actinin; FAK, focal adhesion kinase; IT,integrin; PAX, paxillin; TLN, talin; VASP, vasodilator-stimulated phosphoprotein; VCL, vinculin; ZYX, zyxin. Adapted from (Nardone et al., 2017).

3.1 Focal Adhesions

Assembly of FAs follows the interaction of the transmembrane proteins integrins with ECM proteins, such as fibro- and vitro-nectins, collagens and laminins. Basically, integrins are heterodimeric proteins made of α and β subunits (Fig 9A) and their assembly is dictated by ECM's molecular composition. Moreover, the combination of 24 α and 9 β subunits and alternative splicing events regulate integrins specificity in mammals (Martino et al., 2018).

The affinity between integrins and ECM can be modulated by both "inside-out" signalling and mechanical cues, which cause a high-affinity conformational change (Chen, Lou, Evans, & Zhu, 2012). This, in turn, elicits integrins activation (Fig 9B), due to increased integrin's affinity for extracellular ligands, with consequent clustering and reinforcement of molecular partners at the level of cell-ECM contacts (Oria et al., 2017; Strohmeyer, Bharadwaj, Costell, Fässler, & Müller, 2017), thus forming FAs. In these cellular structures, integrins connect the ECM to the actin cytoskeleton by interacting, through their cytoplasmic domain, with several docking proteins, which build up the inner core of FAs. As stated before, ECM's molecular composition regulates the specific assembly of the integrins' subunits, which then causes specific cellular signalling (Seetharaman & Etienne-Manneville, 2018). Because of the great number of subunit combinations that can be generated and the relative signalling pathways that can arise, integrins are "focal- points" of cellular mechanosensing (Martino et al., 2018).

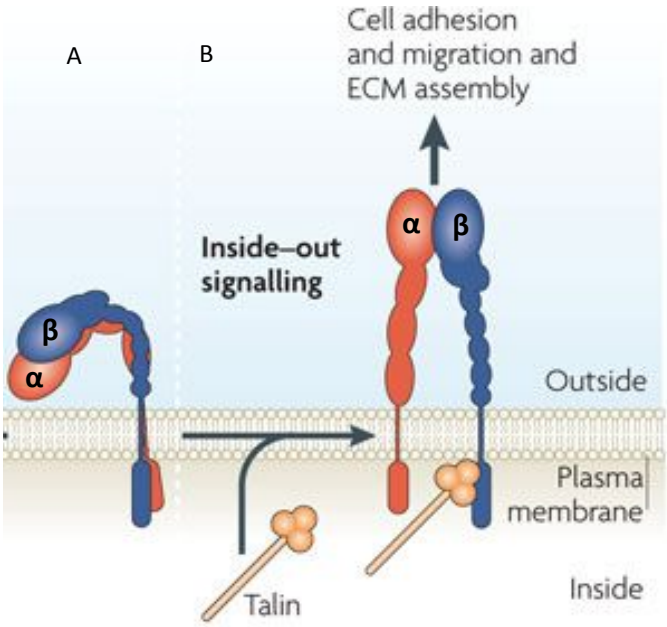

Fig 9: Integrins are heterodimeric proteins made of α and β subunits. A: integrins in their inactive form. B: following "inside-out" signalling, as well as mechanical cues, integrins are activated with consequent recruitment of FAs docking proteins, such as talin. Outside: extracellular side; inside: intracellular side. Adapted from (Shattil, Kim, & Ginsberg, 2010).

Another molecule involved in FAs composition is Focal Adhesion Kinase (FAK) (Fig 10), which is one of the first proteins to be recruited following externally applied forces. FAK is activated via autophosphorylation, which is thought to elicit intracellular mechanotranduction with following activation of cytoplasmic mechanotransducers (Lachowski et al., 2018). Contraction of the cytoskeleton as well as cell spreading can increase FAK activation, whose phosphorylation can be also enhanced by external applied mechanical forces (such as substrate rigidity or cell stretching) (Friedland, Lee, & Boettiger, 2009; Seong et al., 2013). Within the cell, FAK/cytoskeletal network interplay is strictly regulated in order to maintain tension at some critical cellular locations and regulate force transmission towards the nucleus (J. Zhou et al., 2015). Indeed, when cell polarizes or cell's nucleus deforms, FAK activation locally happens at cellular sites, thus eliciting cytoskeleton local rearrangement and nucleus squeezing (Jung et al., 2012). FAK activity has also been shown to influence nuclear morphology, as recently demonstrated by Yang team. Indeed, the authors found that in A549 lung carcinoma cells, inhibition of FAK with the competitive ATP-inhibitor PF-573228 (Slack-Davis et al., 2007) resulted in nuclei with aberrant shapes (Fig 11 A), which the authors claimed to be the a consequence of the decreased expression of the nuclear lamins A and C (Chuang et al., 2019) (Fig 11 B).

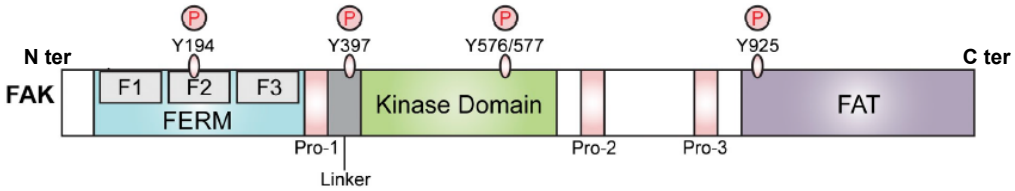

Fig 10: Schematic representing focal adhesion kinase (FAK). Starting from the N-terminus, FAK 's structure displays an autoinhibitory FERM domain, comprising three lobes (F1-F3), followed by a first proline-rich domain (Pro-1), a linker domain, a central kinase domain, two other proline-rich domains (Pro-2 and Pro-3) and the focal adhesion targeting domain (FAT). Tyrosine phosphorylation sites (Y) are displayed. Adapted from (Lawson & Schlaepfer, 2013).

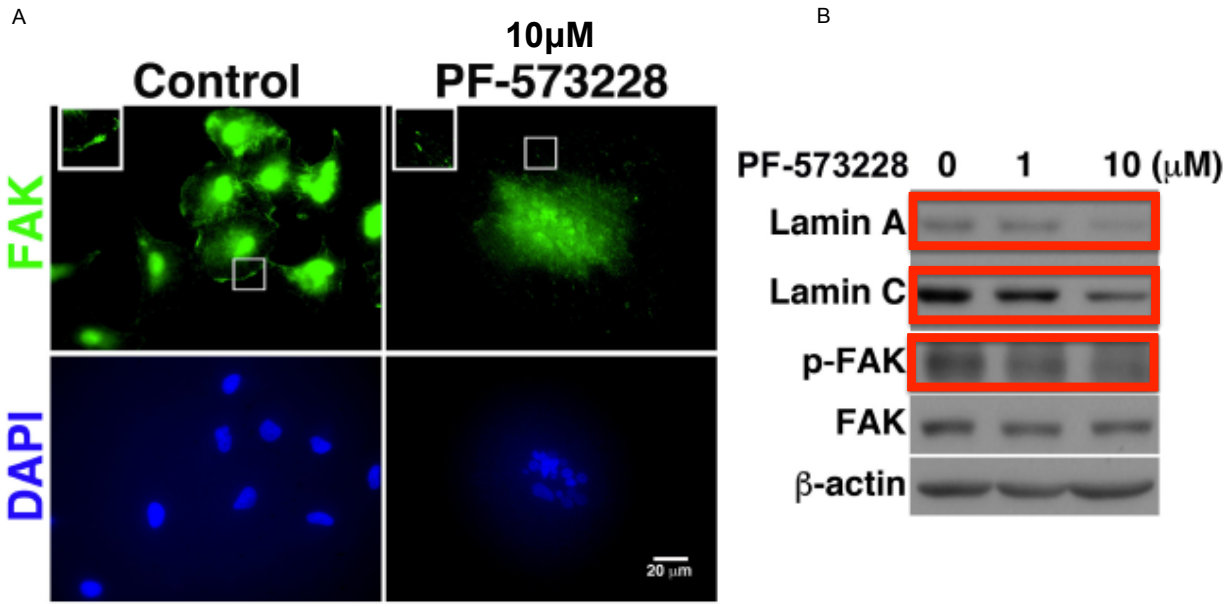

Fig 11: FAK inhibition induces nuclear aberrant morphology due to the decreased expression of nuclear lamins A and C. A: In A549 lung carcinoma cells treated with FAK inhibitor PF-573228, FAK distribution at the FAs is greatly reduced compared to control (see insets in the FAK immunostaing) and this correlates with aberrant nuclear morphology (nuclei counterstained with DAPI). B: PF-573228 decreases protein levels of nuclear lamins A and C as well as of active (phosphorylated) FAK (p-FAK) (boxes in red) in A549 lung carcinoma cells. Scale bar 20 μ m. Adapted from (Chuang et al., 2019).

FAs also comprise the 270 kDa protein talin, which binds both filamentous actin (F-actin) and the FA protein vinculin. Talin is also responsive to force. Indeed upon mechanical force application, it unfolds and unmasks cryptic hydrophobic biding sites for vinculin (Del Rio et al., 2009; Hirata, Tatsumi, Lim, & Sokabe, 2014). Once vinculin is recruted to talin, talin/F-actin interaction is stable with consequent force transmission into cell's interior (Humphries et al., 2007).

Vinculin recruitment in FAs is directly dependent on the forces applied to the FAs (Dumbauld et al., 2013). Vinculin is basically made of a head domain, with which is connected to talin (Price et al., 1989), a rod-like tail domain, with which vinculin is also connected to paxillin (Turner, Glenney, & Burridge, 1990) -a docking protein residing in the intracellular layer of FAs- and a flexible linker between head and tail domains (Fig 12). The tail domain in vinculin is important for force transmission to the actin cytoskeleton (Dumbauld et al., 2013).

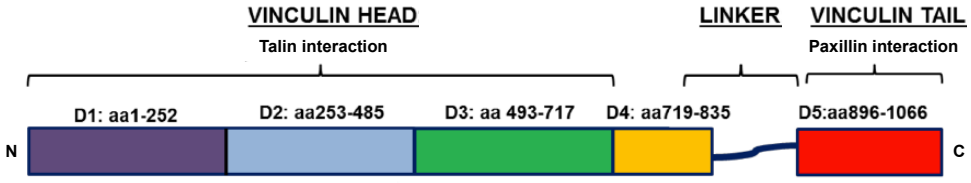

Fig 12: Schematic representing vinculin's structure. Vinculin head is made of 3 domains (D1-D3), whereas one domain (D5) composes vinculin tail. A flexibile linker is in between vinculin head and vinculin tail. aa=amino acids. N: N-terminus. C: C-terminus. Adapted from (Bays & DeMali, 2017).

Other proteins present at the FAs sites are Zyxin, which promotes filamentous-actin (F-actin) polymerization, α-actinin, which cross-links F-actin and p130Cas which, following cell stretching, is phosphorylated to regulate signalling pathway (Sawada et al., 2006).

3.2 Adherens junctions

Besides the ECM, in cohesive animal tissues, cells can interact among them via intercellular adhesion complexes, whose the best understood example is represented by adherens junctions (AJs) (Nicolas Borghi & James Nelson, 2009). Ajs mediate cell-cell interaction via "classical cadherins" (Fig 13), single-span transmembrane glyocoproteins which share a highly conserved cytoplasmic domain (M Takeichi, 1995). Classical cadherins are named according to the tissue they derive: this is why one can talk about E-cadherin (from epithelial tissue), N-cadherin (from neural tissue) and R-cadherin (from retinal tissue), for instance (Baranwal & Alahari, 2009). Hereafter, with "cadherins" I will refer to classical cadherins. With the five extracellular repeats domains, cadherins present on one cell engage the cadherins residing on the opposing cell via Ca^{2+} dependent trans-binding (Shapiro & Weis, 2009; M Takeichi, 1988; Masatoshi Takeichi, Atsumi, Yoshida, Uno, & Okada, 1981)(Fig 13). Cadherins' cytoplasmic domain is involved in the interaction with p120 and β-catenins; the further interaction of β-catenin with α-catenin permits the link of cadherins to the actin cytoskeleton (Baranwal & Alahari, 2009; Nelson, 2008) (Fig 13).

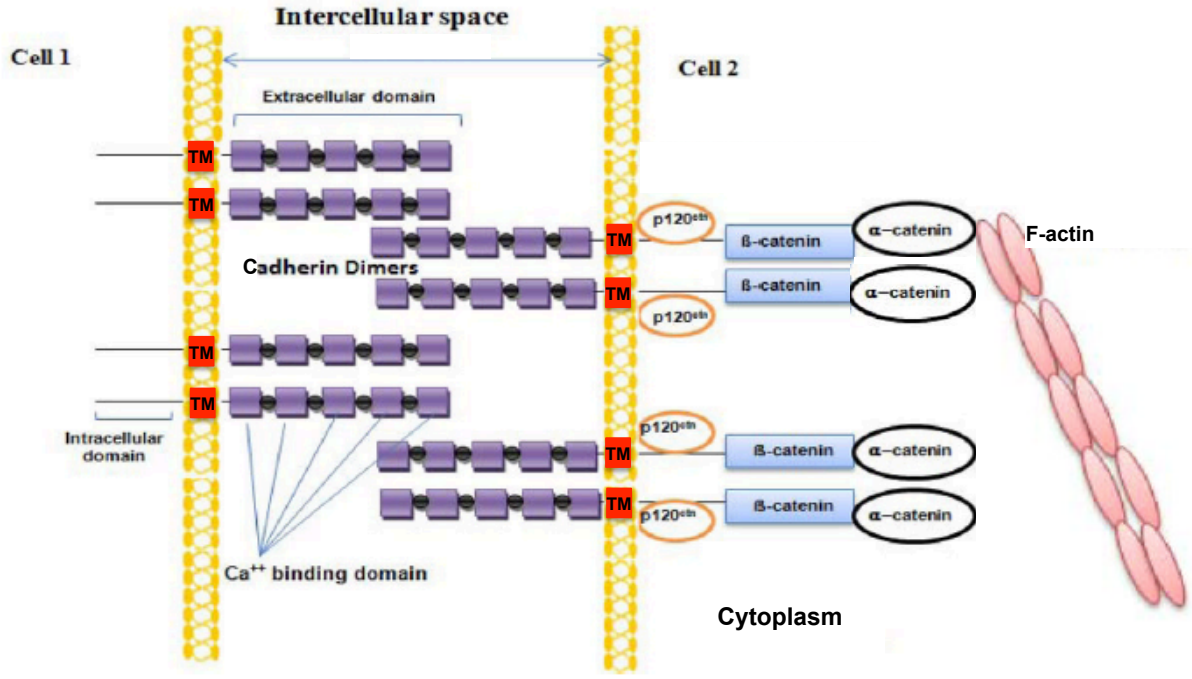

Fig 13: The adherens junction. See text for details: TM: transmembrane domain. p120 ctn: p120 catenin. F-actin: filamentous actin. Adapted from (Baranwal & Alahari, 2009)

AJs are involved in mechanical coupling of plasma membrane with the cytoskeleton via cadherins' cytoplasmic domain (Tabdanov, Borghi, Brochard-Wyart, Dufour, & Thiery, 2009) and, moreover, if mechanically stimulated via cadherins' extracellular domain, cells stiffen in a vinculin-dependent manner (le Duc et al., 2010). In addition, E-cadherin was demonstrated to be under cytoskeleton generated tension in epithelial MDCK type IIG cells. Indeed, by using a FRET TSMod biosensor (Grashoff, Hoffman, Brenner, Zhou, Parsons, Yang, McLean, Sligar, Chen, Ha, & Schwartz, 2010) inserted into full length as well as β-catenin binding domain deleted E-cadherins (EcadTSMod and EcadTSModΔcyto, respectively), Borghi et al demonstrated that the FRET index measured at the level of the cell-cell contacts (namely adherens junctions) was lower (meaning higher tension) in MDCK cells stably expressing EcadTSMod compared to those cells stably expressing EcadTSModΔcyto

(N. Borghi et al., 2012) (Fig 14A). This reported variation in tension through FRET was associated to the lost connection between the cytoskeleton and the truncated E-cadherin construct, suggesting that E-cadherins are under constitutive cytoskeleton-generated tension at the cell-cell contacts. This was then confirmed by the authors treating MDCK cells stably expressing EcadTSMod with the actin polymerization inhibitor cytochalasin B (Cooper, 1987) (Fig 14B). Compared to untreated cells, drug-treated cells displayed a higher FRET index difference, meaning that tension in E-cadherin decreased (Fig 14B). Thus, the authors concluded that E-cadherin is under constitutive actin cytoskeleton-generated tension at the cell-cell contacts (N. Borghi et al., 2012).

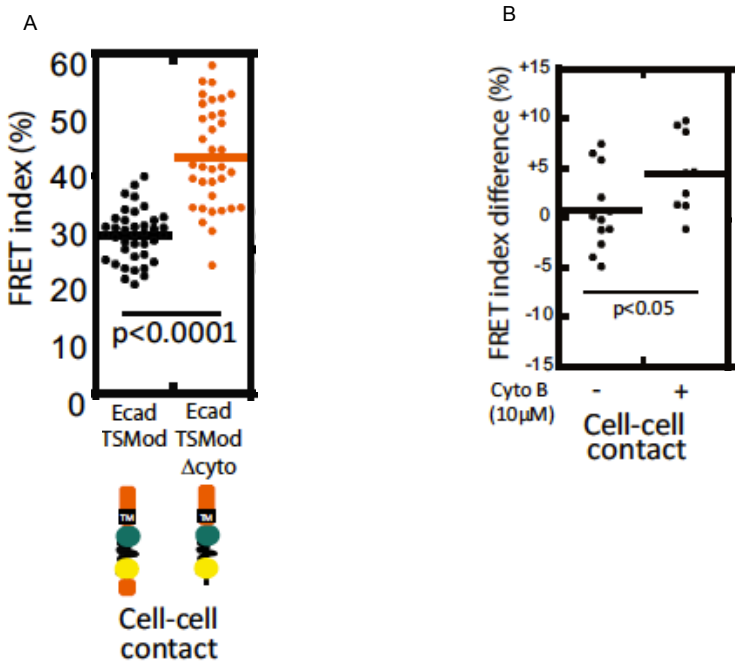

Fig 14: E-cadherin is under constitutive cytoskeleton-generated tension at the cell-cell contacts. A: FRET index measurements in MDCK type IIG cells stably expressing EcadTSMod (full length) and EcadTSMod Δ cyto (deletion of the β-catenin binding domain) constructs at the cell-cell contacts (AJs). Due to the lack of cytoskeleton connection, cells expressing EcadTSMod Δ cyto show a higher FRET index, which means lower tension, compared to EcadTSMod expressing cells. B: cytochalasin b treatment induces actin polymerization inhibition, which determines a reduction in tension (measured as FRET index difference) applied by the cytoskeleton to E-cadherin at the cell-cell contacts. Adapted from (N. Borghi et al., 2012).

3.3 Cytoskeleton

Force transmission, as well as force generation, within the cell is assured by the presence of the cytoskeleton, whose tensional state is highly regulated (Discher, Janmey, & Wang, 2005). The cytoskeleton gives the cell mechanical support and, among others, regulates its shape and motility (Fletcher & Mullins, 2010). Impairment of cytoskeletal structure has been shown to impact gene expression and cell signalling (Dupont et al., 2011; Jaalouk & Lammerding, 2009). Basically, the dynamic cytoskeletal network comprises actin filaments (F-actin, filamentous actin, also referred to as microfilaments), microtubules (MTs, made of α and β tubulin monomers) and intermediate filaments (IFs) (Fig 15). Through this organized filaments network, the cytoskeleton is able to keep the integrity of cell's organelles (Martino et al., 2018).

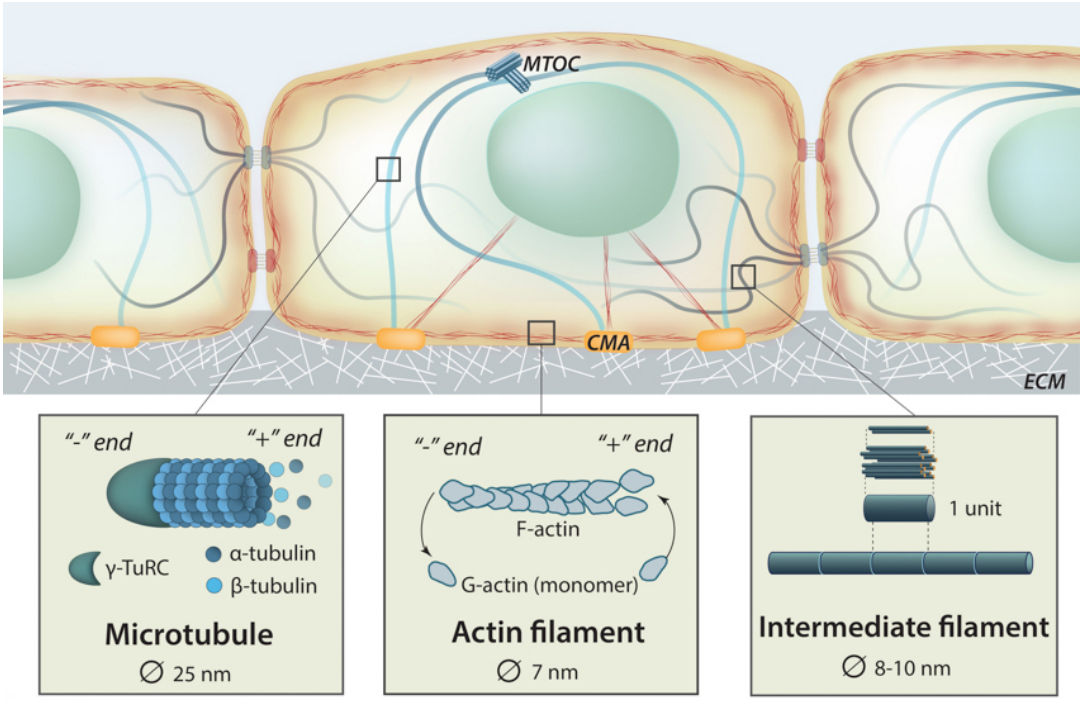

Fig 15: Schematic representing cell's cytoskeleton with insets showing microtubules and actin filaments with their dynamical polymerization and intermediate filaments. MTOC: microtubule organizing center. CMA: cell-matrix adhesion. ECM: extracellular matrix. Adapted from Mechanobio.info.

Microfilaments and the motor protein myosin II, important for cytoskeletal contractility, are cross-linked by α-actinin in complex structures know, in mammals, as stress fibers (SFs), which have been shown to transmit force from ECM to cell and from cell to ECM when FAs are pulled (Cramer, Siebert, & Mitchison, 1997; Naumanen, Lappalainen, & Hotulainen, 2008; Pellegrin & Mellor, 2007).

SFs are defined as dorsal SFs, transverse arcs and ventral SFs (Naumanen et al., 2008). Dorsal SFs, which lack myosin II, have just structural function at the level of FAs -to which are connected- and do not contract (Tojkander, Gateva, & Lappalainen, 2012).Transverse arcs interact with dorsal SFs and are, instead, contractile and indirectly connected to FAs through dorsal SFs (Martino et al., 2018). Lastly, ventral SFs are both contractile and directly connected to the FAs (Martino et al., 2018) (Fig 16). Contraction of SFs has been shown to elicit vinculin recruitment to the FAs (H. Yamashita et al., 2014).

It has been demonstrated that the Nuclear Envelope (NE) is connected to FAs via a particular subtype of actin fiber, namely the perinuclear actin cap, which wraps around the nucleus (Khatau et al., 2009) (Fig 16). Mechanical stimuli have been shown to be directly transferred from the FAs to the nucleus via the perinuclear actin cap (D. H. Kim et al., 2012; Q. Li, Kumar, Makhija, & Shivashankar, 2014).

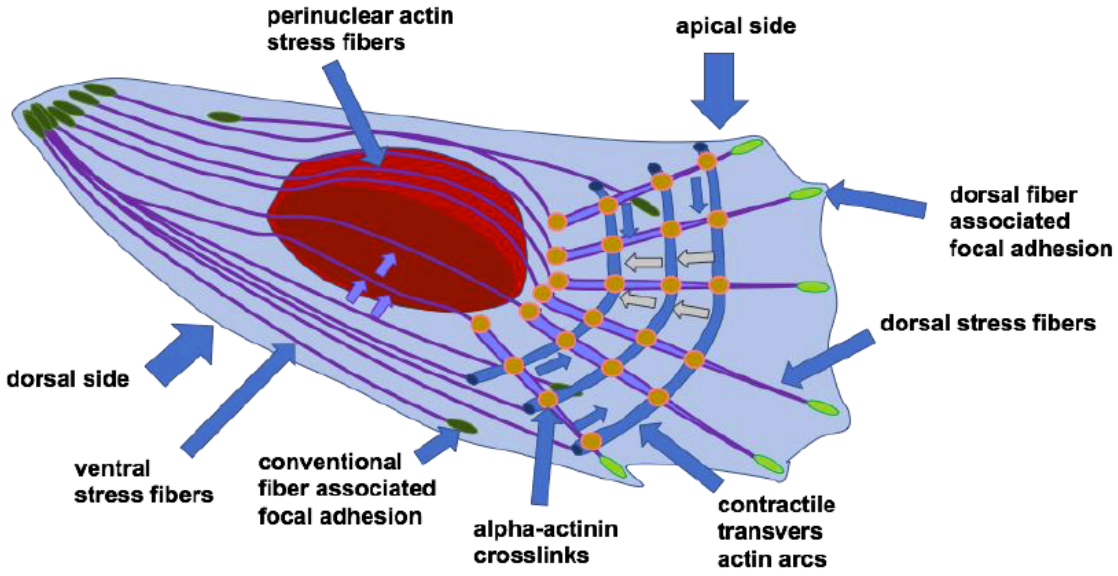

Fig 16: Stress fibers and formation of the perinuclear actin cap. Transverse arcs and dorsal fibers are cross-linked via α-actinin (orange dots). Transverse arcs contraction promotes the movement of the cross-linking points and the stress fibers from cell's periphery in front of cell's nucleus (bleu and white arrows). Transverse arcs and dorsal fibers move stress fibers above the nucleus (purple arrows), thus leading to the perinuclear actin cap formation. From (Tanja Mierke, 2018).

Actin dynamics is regulated by the Rho/ROCK pathway. Indeed, the ROC Kinase (ROCK) activates myosin II via myosin light chain (MLC) phosphorylation or MLC phosphatase inhibition (Feng et al., 1999; Mutsuki et al., 1996), thus resulting in F-actin contraction.

In addition, Rho/ROCK pathway activates the formin Diaphanous (mDia) which, in turn, elicits microfilament polymerization (Watanabe et al., 1997) (Fig 17). Rho/ROCK pathway also regulates F-actin stabilization by activating LIM kinase (LIMK) (Ohashi et al., 2000), which phosphorylates and inhibits the actin-severing protein cofilin (Bamburg, Harris, & Weeds, 1980)(Fig 17).

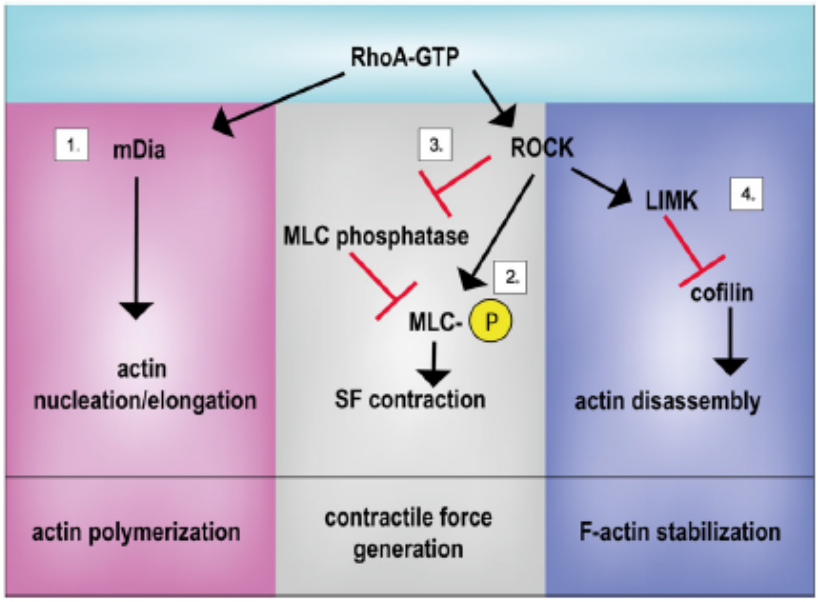

Fig 17: Rho/ROCK pathway regulates actin cytoskeleton dynamics by 1) inducing actin polymerization through mDia activation; 2) stimulating F-actin contraction via either direct MLC phosphorylation or 3) inhibition of MLC phosphatase; 4) determining F-actin stabilization via LIMK activation which, in turn, inhibits cofilin through

phosphorylation. mDIA: Diaphanous; MLC: myosin light chain; LIMK: LIM Kinase. SF: stress fiber. From (Martino et al., 2018).

It has been shown that microfilaments interact with MTs (Dugina et al., 2016) ,which are the stiffest cytoskeletal filaments. MTs regulate intracellular trafficking, mitotic spindle formation and cellular polarity (Fletcher & Mullins, 2010; J. Zhang, Guo, & Wang, 2014). Moreover, MTs have been shown to be mechanoresponsive when mitotic cells are stretched. Indeed, Fink et al. demonstrated that mitotic spindle aligns parallel to the stretch direction (Fink et al., 2011).

Lastly, IFs are more flexible and stable than microfilaments and MTs. Also, post-translational modifications govern IFs' dynamics and implication in different cellular pathways (Snider & Omary, 2014).

3.4 Signalling upon mechanotransduction

Mechanical cues, perceived by the cell via mechanosensors, can let other mechanorensposive proteins undergo conformational changes and/or post-translational modifications with consequent nuclear shuttling (Martino et al., 2018). An example of this shuttling was given by Gottardi et al., who showed that the tight junction protein zonula occludens-1 (ZO-1) accumulates into the nuclei of subconfluent MDCK epithelial cells but not in confluent monolayers (Gottardi, Arpin, Fanning, & Louvard, 1996). Furthermore, Lewis et al found that cell-cell adhesion induced by integrins determines the translocation of the FA tyrosine kinase c-Abl from the nucleus to the early focal contacts and then back to the nucleus, in C3H 10T1/2 mouse fibroblasts plated onto fibronectin (Lewis, Baskaran, Taagepera, Schwartz, & Wang, 1996). Recently, β-catenin, which interacts with the E-cadherin at the AJs, has been demonstrated to undergo nuclear accumulation upon E-cadherin tension relaxation in MDCK type IIG epithelial cells (Gayrard, Bernaudin, Déjardin, Seiler, & Borghi, 2018).

The FA protein Zyxin, was also demonstrated to shuttle between nucleus and the cytoplasmic focal contacts in primary CEFs (chicken embryo fibroblasts) (Nix & Beckerle, 1997). Moreover, it has been suggested that, once in the nucleus of rat aortic smooth muscle cells (SMCs) upon cyclic stress, zyxin may regulate few mechanoresponsive genes, such as endothelin B receptor (ETB-R) and matrix protein tenascin-C (Cattaruzza, Lattrich, & Hecker, 2004). Another FA protein demonstrated to undergo nuclear translocation is paxillin, whose nuclear shuttling has been shown to be regulated, in fibroblasts, by cell geometry and be independent of ECM composition (Sathe, Shivashankar, & Sheetz, 2016).

Other mechanoresponsive proteins not associated to FAs demonstrated to undergo nuclear shuttling are the transcriptional co-activators Yes-associated protein (YAP) and WW Domain-Containing Transcription Regulator Protein 1 (WWTR1/TAZ), playing the role of downstream effectors in the Hippo pathway (Huang, Wu, Barrera, Matthews, & Pan, 2005; Oka & Sudol, 2009) (Fig 17), known to limit organ size in animals (Yu, Zhao, & Guan, 2015).

YAP and TAZ are intended as molecular relays for ECM mechanics. Indeed, Dupont et al showed that human mesenchymal stem cells (MSCs) grown on hard substrates displayed YAP/TAZ nuclear accumulation, compared to YAP/TAZ cytoplasmic localization in MSCs grown on soft subtrates (Dupont et al., 2011). Moreover, YAP localization has been also shown to be regulated by E-cadherin. Indeed, Kim et al found that inducible expression of E-cadherin in human breast cancer cells (MDA-MB-231), grown at high density, determined cytoplasmic localization of YAP, which was instead nuclear in the parental, E-cadherin negative cells (N.-G. Kim, Koh, Chen, & Gumbiner, 2011). YAP

nuclear translocation has been also associated with cell area. To this regard, Nardone et al showed that adipose tissue-derived mesenchymal stem cells (AD-MSCs), grown onto fibronectin-coated micropatterns, presented an increasing YAP nuclear localization when cell's area increased (Nardone et al., 2017) In addition to mechanical regulation, Hippo pathway can be also controlled by G-protein-coupled receptor signalling and cell's energy status (Y. Zhang, Zhang, & Zhao, 2018) (Fig 18), as well as by insulin/IGF signalling (IIS) (Straßburger, Tiebe, Pinna, Breuhahn, & Teleman, 2012).

When Hippo pathway is active, MST1/2 phosphorylates SAV1, MOB1A/B and LATS 1/2, whose kinase activity is thus activated. Consequentially, LATS1/2 phosphorylates YAP/TAZ, which can be either retained in the cytoplasm by interacting with 14-3-3 protein or degraded via E3 ligase SCF $^{\beta\text{-TRCP}}$. When Hippo pathway is not active, YAP/TAZ are then no more phosphorylated, which results in their nuclear accumulation. Once in the nucleus, YAP/TAZ can bind to transcription factors, such as TEADs or others having PPXY motif, in order to allow gene transcription (Y. Zhang et al., 2018) (Fig 18).

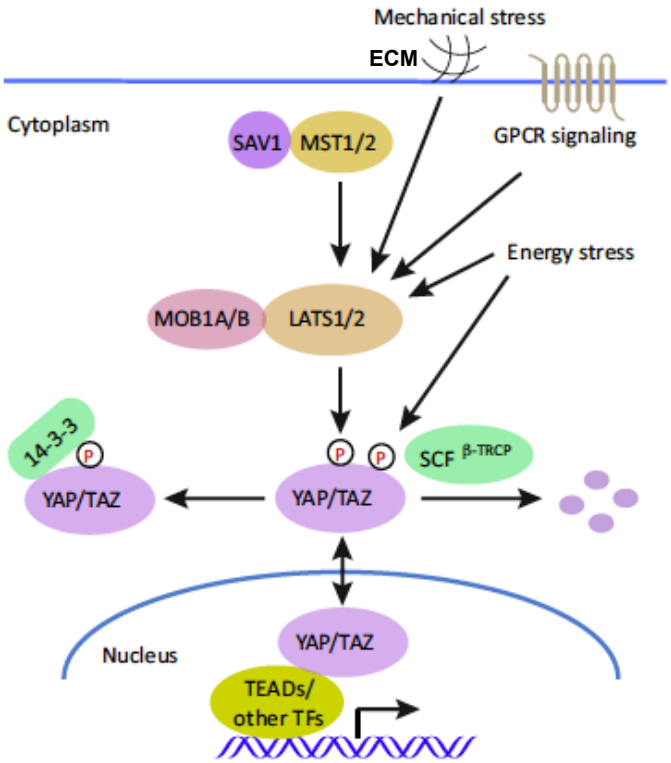

Fig 18: Hippo pathway regulation. See text for details. Adapted from (Y. Zhang et al., 2018).

It has also been shown that a complex of YAP/TAZ/SMAD can undergo nuclear shuttling via cell density regulation. Indeed, YAP/TAZ/SMAD complex translocates into the nucleus of sparse HaCaT cells, which do not perceive cell-cell connection (Grannas et al., 2015).

Co-transcriptional activity of nuclear YAP/TAZ has been connected to cell growth and tumor spreading (Zanconato et al., 2015). Nevertheless, recent findings proved that YAP activity in mechanotransduction is related to its capability to directly elicit transcription of genes involved in cell-matrix interaction and ECM composition (Nardone et al., 2017), as well as cytoskeleton integrity during cardiomyocyte renewal and regeneration (Morikawa et al., 2015).

In summary

- Mechanotransduction refers to the way cells sense and respond to external and internal mechanical cues by converting these physical stimuli into biochemical signals.
- Mechanosensors or mechanotransducers are the protein complexes, as well as cell's organelles, being able to transduce mechanical stimuli.
- Pioneering works showed that mechanotransduction is involved in tissue shaping, cellular metabolism, embryo development, gene expression and lineage commitment.
- Mechanistically, two ways of transferring physical stimuli can be conceived: the tethered model and the lipid bilayer model.
- Mechanical force propagation in cells is possible since cell's cytoskeleton is prestressed.
- Extracellular matrix, focal adhesions and adherens junctions participate in mechanotransduction.
- Signalling upon mechanical cues is highly regulated and can imply protein shuttling between nucleus and cytoplasm.

CHAPTER 2

The nuclear envelope: what wraps the cell's nucleus

In this chapter, I will discuss the structure of NE focusing on its molecular components in normal as well as in diseased conditions. Nucleo-cytoplasmic shuttling and mechanotransduction in the nucleus will be also taken into account.

Table of contents

1 Nuclear envelope's structure

1.1 Outer nuclear membrane (ONM), inner nuclear membrane (INM) and nuclear lamina.

Cell's nucleus is surrounded by the nuclear envelope (NE) consisting of two different lipid membranes, the outer nuclear membrane (ONM) and the inner nuclear membrane (INM). INM and ONM are in continuity with the endoplasmic reticulum (ER) (Schirmer & Gerace, 2002) and separated by the perinuclear space (PNS) (Fig 19), which is 30-50 nm in width (Maurer & Lammerding, 2019). This structure allows the chromatin to be well separated, in the nucleus, from the cytoplasm (Osorio & Gomes, 2013) and the presence on the NE of the selective barrier of the nuclear pore complex (NPC) permits to control the inwards/outwards nuclear shuttling of molecules larger than 30 kDa (Maurer & Lammerding, 2019).

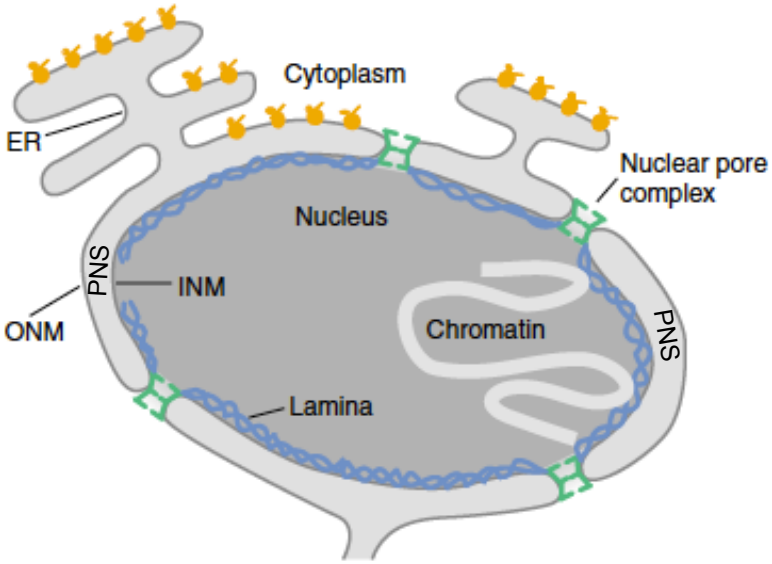

Fig 19: The nucleus, surrounded by the inner nuclear membrane (INM) and the outer nuclear membrane (ONM), which, with the nuclear pore complex (NPC), form the nuclear envelope (NE). Underneath the INM there lays the nuclear lamina. Note that INM and ONM are in continuity with the endoplasmic reticulum (ER). On ER surface, ribosomes are displayed in ochre. PNS: perinuclear space. Adapted from (Schirmer & Gerace, 2002).

Underneath the INM, there lays the nuclear lamina (Fig 20), a protein meshwork with a thickness of 10-30 nm (Turgay et al., 2017). Basically, the proteins composing the nuclear lamina, called lamins, are type V nuclear intermediate filaments and are present in the greatest part of the differentiated cells (Maurer & Lammerding, 2019).

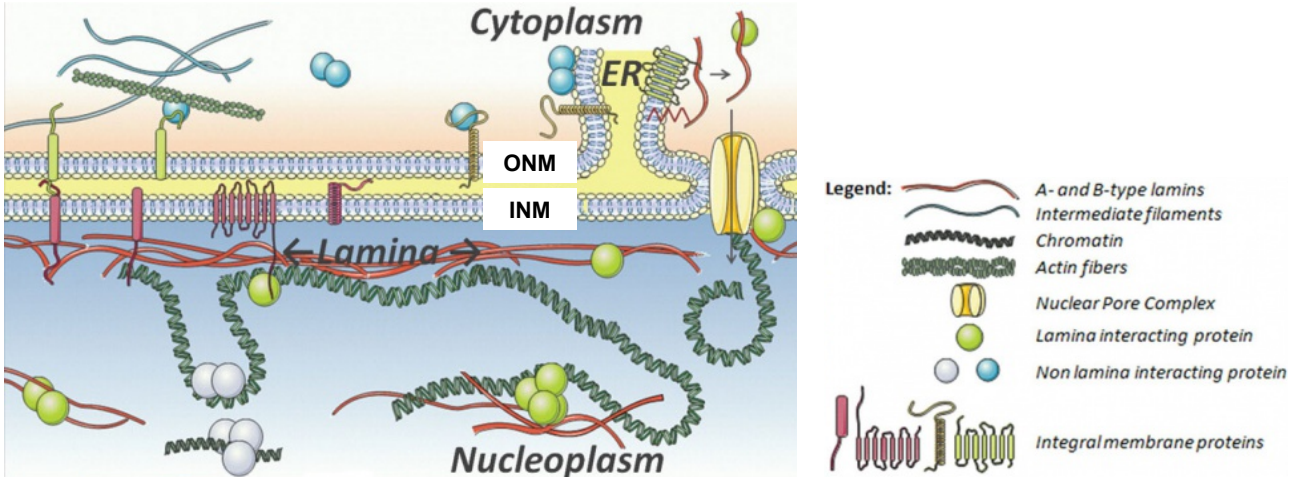

Fig 20: Nuclear lamina is located underneath the inner nuclear membrane (INM) and interacts with chromatin as well as with different proteins. ER: endoplasmic reticulum. ONM: outer nuclear membrane. Adapted from: cellbiology.med.unsw.edu.au

In mammals, lamins are fundamentally divided into A-type lamins and B-type lamins (Janin & Gache, 2018) (Fig 21). A-type lamins, which are encoded by the gene *LMNA*, produce the major isoforms lamin A and C and other less common ones (Maurer & Lammerding, 2019). Lamins A and C are generated by an alternative splicing event occurring on exon 10. As such, lamins A and C share a similar structure from the N-terminus till the amino-acid position 556 at the C-terminus. However, while lamin C presents just five additional amino-acids, lamin A shows an extra domain encoded by exons 11 and 12 of the *LMNA* gene (Janin & Gache, 2018). Lamins A and C have a development-dependent regulation and are present during cellular differentiation (Maurer & Lammerding, 2019). Regarding B-type lamins, they are divided into lamins B1 and B2 encoded by *LMNB1* and *LMNB2*

genes, respectively (Maurer & Lammerding, 2019). Being themselves intermediate filaments, nuclear lamins dimerize via their central rod domain (Herrmann & Aebi, 2016) (Fig 21).

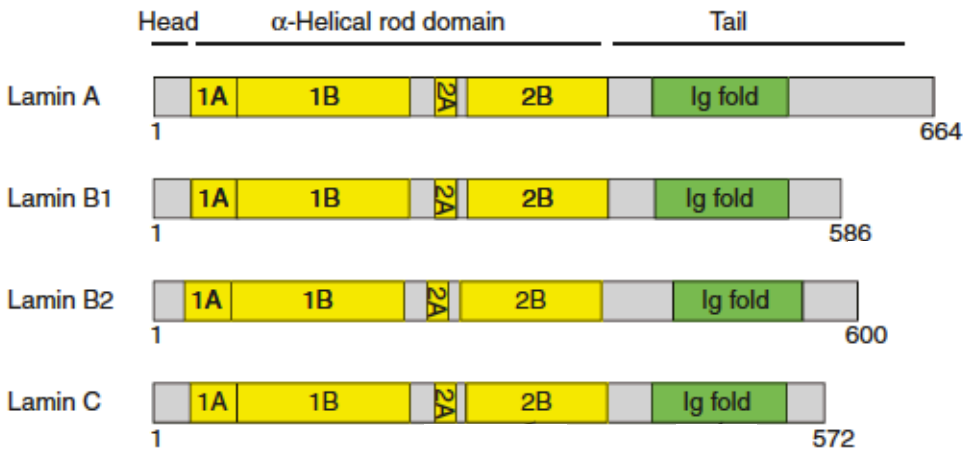

Fig 21: Lamins A and B structures. With the rod domain, nuclear lamins dimerize. Ig:immunoglobulin. Adapted from(Dittmer & Misteli, 2011)

Nuclear lamins interact with different partners, such as chromatin, transcription factors and LEM (LAP2, Emerin and MAN1) proteins, the latter being critical in gene regulation (Dorner, Gotzmann, & Foisner, 2007). It is thus clear that nuclear lamins are important in terms of genome regulation and chromatin organization (de Leeuw, Gruenbaum, & Medalia, 2018; Gruenbaum & Foisner, 2015).

Lamins and heterochromatin interact either in specific lamin-associated-domains (LADs)-genomic regions involved in molecular contact with nuclear lamina (Pickersgill et al., 2006; van Steensel & Belmont, 2017)-or through the LEM protein lamin-associated protein 2 (LAP2) and its partner, BAF (barrier to autointegration factor) (Goldman, Gruenbaum, Moir, Shumaker, & Spann, 2002; Shumaker, Lee, Tanhehco, Craigie, & Wilson, 2001). Both A-type and B-type lamins, by binding nucleoporin 153 (Nup153) – one of the protein composing the NPC – place the NPC at the level of the NE (Maurer & Lammerding, 2019). Nuclear lamina was postulated to have elastic extensibility and limited compressibility, as proposed by Dahl et al. following osmotic swelling experiments involving *Xenopus* oocyte nuclear envelopes (Dahl, 2004). In addition, Disher team also showed that 3D migration of lung carcinoma-derived A549 cells is influenced by Lamin A levels (Harada et al., 2014). Indeed, Harada et al. found that cell migration through 3-μm pore Transwell filters increased upon Lamin A depletion and reached a peak when depletion was partial (Fig 22). On the contrary, Lamin A overexpression impeded migration (Harada et al., 2014)(Fig 22).

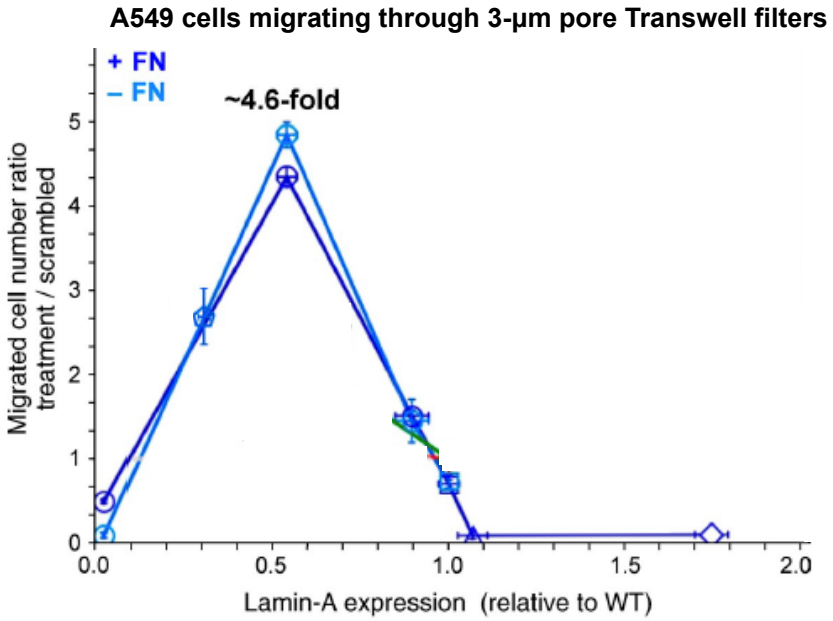

Fig 22: Lamin A expression influences 3D migration. Note that the highest migration level (≈4.6 fold) is reached when Lamin A depletion is partial (0.5 Lamin A expression on x axis). Overexpression of Lamin A impedes migration. Pre-coating filters with fibronetcin (+FN) does not exert any variation on migration compared to uncoated filters (-FN). Adapted from (Harada et al., 2014).

Among those proteins interacting with lamins, we find emerin, which is encoded by the *EMD* gene (Bione et al., 1994; Janin & Gache, 2018). Beside being involved in gene regulation (Holaska, Lee, Kowalski, & Wilson, 2003; Wilson et al., 2005), emerin regulates cell signalling as well as nuclear architecture (Berk, Tifft, & Wilson, 2013). With its LEM domain located at the N-terminus (Fig 23), emerin interacts with BAF, which, in turn, is important for post-mitotic nuclear assembly, cell viability and cell cycle progression (Janin & Gache, 2018). Additionally to its presence at the nuclear lamina, emerin has been also found at the level of ONM and ER, where it directly interacts with the centrosome (Salpingidou, Smertenko, Hausmanowa-Petrucewicz, Hussey, & Hutchison, 2007).

Fig 23: Emerin's structure. The interaction with BAF (barrier to autointegration factor) occurs at the LEM (LAP2, Emerin and MAN1) domain. With the TM (transmembrane) domain, emerin is inserted into the inner nuclear membrane (INM). APC-L: Adenomatous poliposis coli-like domain. N: N-terminus. C: C-terminus. Adapted from (Berk et al., 2013).

Emerin has also a role in β-catenin's activity regulation. Indeed, by using human fibroblasts, both wild-type or null for emerin, Markiewicz et al. found that a β-catenin antibody co-immunoprecipitated emerin in cell extracts from wild-type human fibroblasts but did not in cell extracts from emerin null human fibroblasts (Fig 24A),thus demonstrating that emerin interacts with β-catenin. Moreover, the researchers showed that this interaction is mediated by an APC-like domain in emerin (Fig 24B) whose deletion increased β-catenin's activity (Fig 24C) and stimulated β-catenin nuclear accumulation in HEK 293 cells (Fig 24D). The authors thus concluded that emerin negatively regulates β-catenin's activity (Markiewicz et al., 2006).

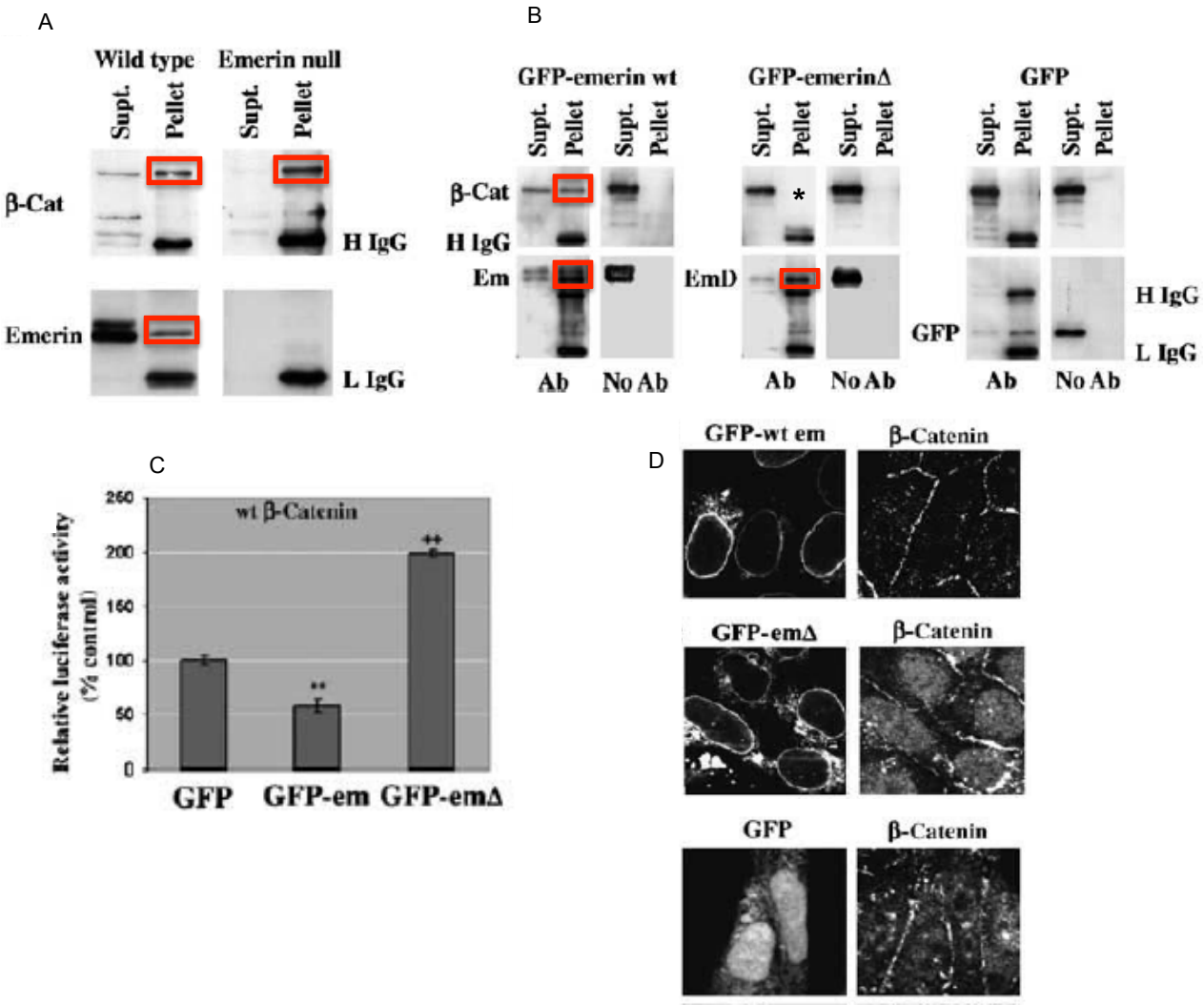

Fig 24: Emerin interacts with β-catenin and regulates its activity and nuclear accumulation. A: emerin co-immunoprecipitates with β-catenin in cell extracts from wild type human fibroblasts but it did not in emerin null human fibroblasts B: cell extracts from HEK 293 cells co-transfected with β-catenin plus GFP-emerin wt (wild type emerin), GFP-emerinΔ (emerin with deletion in the APC-like domain) or GFP alone were used for immunoprecipitation with an anti-GFP antibody. In GFP-emerinΔ extracts, β-catenin was not co-immunoprecitated with the anti-GFP antibody (see asterisk in "pellet" lane). In A and B red boxes to indicate (co)immunopreciptated emerin and β-catenin; H and L to indicate "heavy" and "light" IgG chains, respectively. C: luciferase assay to estimate β-catenin's acitivity in HEK 293, co-transfected with wt (wild type) β-catenin and TOPGLOW (to measure β-catenin's acitivity) plus the GFP-emerin (or GFP alone) constructs (GFP-em: wild type emerin; GFP-emΔ: APC-like domain deleted emerin). Note that GFP-emΔ increases β-catenin's acitivity compared to GFP-em. D: in HEK 293 cells co-transfected with β-catenin plus GFP-wt em (wild type emerin), β-catenin localizes at the cell-cell contacts (β-catenin immunostaining panel,above), whereas in the presence of GFP-emΔ (APC-like domain deleted emerin) co-transfected β-catenin is mostly nuclear (β-catenin immunostaining panel, middle). ** p<0.001. Adapted from(Markiewicz et al., 2006).

1.2. The LINC complex: nesprin and SUN proteins

Embedded into the ONM and the INM, the LINC (Linker of Nucleoskeleton and Cytoskeleton) complex spans the NE and assures coupling between the cytoskeleton and the nucleus (Crisp et al., 2006; Starr & Han, 2002).This function is made possible because of the presence of the nesprin (nuclear envelope spectrin repeat proteins,) proteins (Q Zhang et al., 2001) and the SUN (Sad1p and UNC-84 homology) domain proteins(Lygerou, Christophides, & Séraphin, 1999; Malone, Fixsen, Horvitz, & Han, 1999).

Nesprin proteins are inserted into the ONM and connect it with the cytoskeletal filaments; whereas SUN domain proteins (simply referred to as SUN proteins) reside in the INM and interact both with the nesprin proteins in the PNS- via the KASH (Klarsicht, ANC-1 and Syne homology) domain of nesprins- and with the nuclear lamina underneath the INM. Thus, the LINC complex creates a bridge between the lamins nucleoskeleton and the cytoskeleton (Maurer & Lammerding, 2019) (Fig 25).

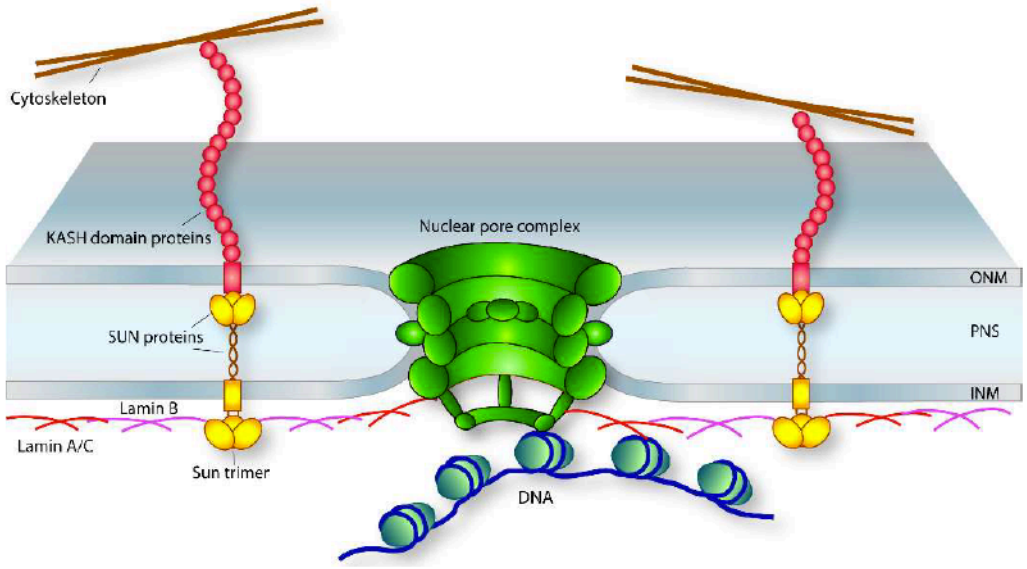

Fig 25: LINC complex organization: spanning the nuclear envelope, the LINC complex connects the lamins nucleoskeleton with the cytoskeleton via nesprin proteins (KASH domain proteins) in the outer nuclear membrane (ONM) and SUN domain proteins in the inner nuclear membrane (INM). Note that SUN proteins form trimers and interact with nesprins in the perinuclear space (PNS). From (Preston & Faustino, 2018).

The first demonstration of the existence of a complex connecting the nucleus with the cytoskeleton in mammalian cells was given by Crisp et al. in 2006. By transfecting HeLa cells, which expressed a GFP-KASH construct under the induction of a tetracycline promoter, with a plasmid harbouring a HASun1 construct, the authors were able to spot a colocalizing signal coming from the two proteins.(Fig 25A). Moreover, they found the same colocalization signal when the same cells were transfected with a HASun2 construct (Fig 25A). Finally, the direct interaction between nesprin proteins and SUN proteins was demonstrated by co-immunopreciptation (Co-IP) assay (Fig 25B). Since nesprins interacted with cytoskeletal filaments and since both nesprin and SUN proteins were present at the nucleus- with SUN proteins interacting with the nuclear lamina- the authors proposed the existence of the LINC complex as a bridge between the nucleoskeleton and the cytoskeleton (Crisp et al., 2006).

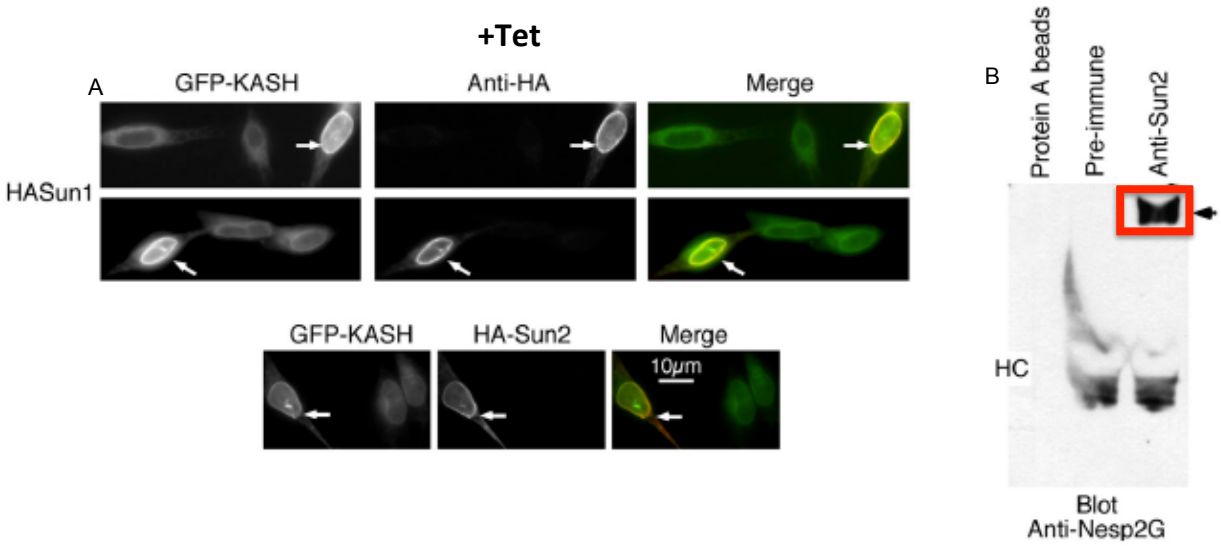

Fig 25: Nesprin proteins and SUN proteins interact together to determine nucleo-cytoskeleton coupling. A: in HeLa cells expressing a GFP-KASH construct (upon tetracyclin induction), HASun1 (above) and HASun2 (below) chimera proteins colocalize with GFP-KASH (see arrows). B: nesprin 2G co-precipitates with SUN2. The red box and the arrow indicate the presence of nesprin 2G in the SUN2 IP. HC indicates the position of immunoglobulin heavy chains. Adapted from (Crisp et al., 2006).

As stated above, nesprins are KASH domain proteins and, up to now, six of these proteins have been described: nesprins 1-4, KASH 5 and LRMP (Lymphoid-Restricted Membrane Protein) (Fig 26), respectively encoded by *SYNE1-4*, *KASH 5* and *LRMP* genes (Janin & Gache, 2018). Among these proteins, nesprins 1,2 and 3 are ubiquitously expressed (Janin & Gache, 2018), while nesprin 4, KASH 5 and LRMP are restricted to secretory epithelia and mechanosensory cochlea hair cells (Horn et al., 2013; Roux et al., 2009), meiotic cells (C. L. Stewart & Burke, 2014) in and in some taste cells in mammal tongue (Shindo et al., 2010), respectively.

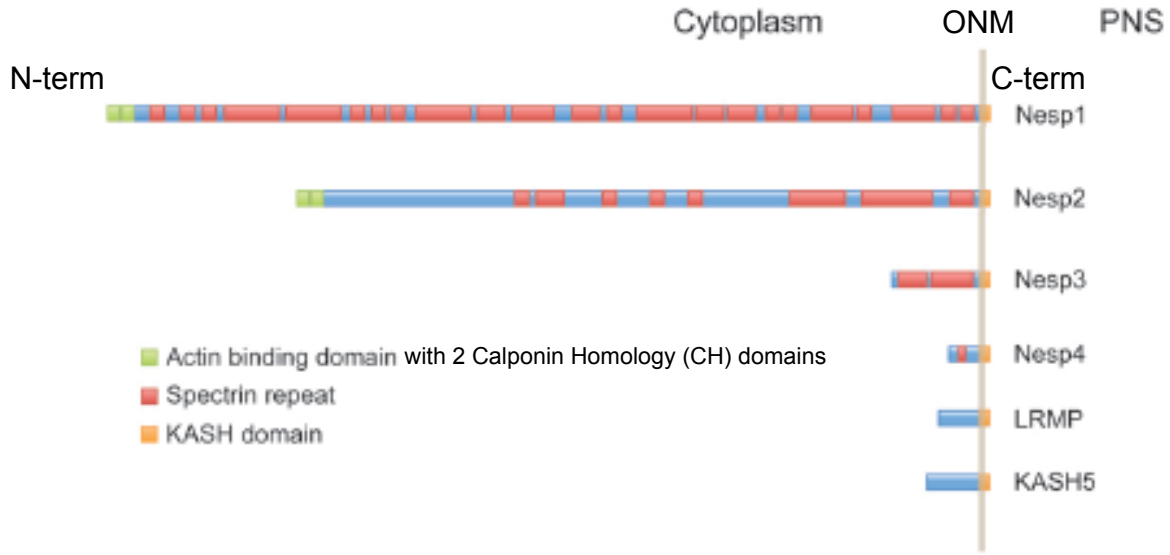

Fig 26: Schematic representing the six different nesprins described up to now. Note that the KASH domain, important for nesprin connection with SUN proteins, is found in all the six proteins, whereas the CH domains or the spectrin repeats are not always present. Blue spaces to indicate weak similarity with spectrin repeats. ONM: outer nuclear membrane. PNS: perinuclear space. Adapted from (C. L. Stewart & Burke, 2014).

Nesprins 1 and 2, in human, are classified as the "giant" isoforms, because of their molecular weight which is 1MDa for nesprin 1 (coding sequence of 146 exons) and 800 kDa for nesprin 2 (conding sequence of 116 exsons) (Janin & Gache, 2018). These isoforms are made of three major domains, which are, starting from the N-terminus: the actin-binding domain (ABD) with 2 calponin homology (CH) domains, connecting nesprins to the actin cytoskeleton; a central rod domain, made of 74 spectrin repeats (SRs) in nesprin 1 and 56 in nesprin 2, which permits interaction with other proteins such as emerin and nuclear lamins; and the KASH domain, inserted into the ONM, which connects nesprin proteins with SUN 1/2 proteins in the PNS (Janin & Gache, 2018; Rajgor & Shanahan, 2013) (Fig 27). Moreover, an additional domain, named "adaptive domain" (AD), is present in the C-terminus with the function of stabilizing the SRs by increasing their overall helicity, thermal stability and cooperativity of folding (Zhong, Chang, Kalinowski, Wilson, & Dahl, 2010). Although *SYNE 1* and *SYNE 2* genes share about 60% of homology, nesprin 1 is more conserved than nesprin 2 (Janin & Gache, 2018).

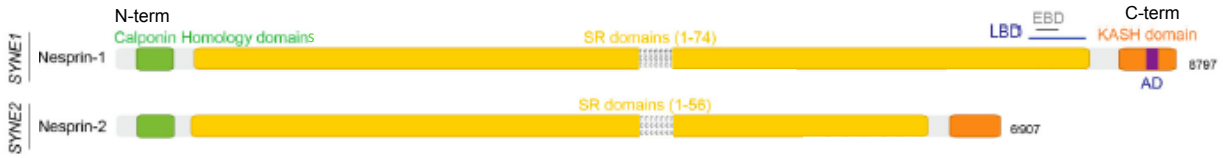

Fig 27: Nesprins 1 and 2. Note that KASH domain is displayed in orange in both the proteins. See text for details. SR: spectrin repeat. LBD: lamin binding domain. EMD: emerin binding domain. AD: adaptive domain. Adapted from (Janin & Gache, 2018).

There exist multiple nesprin 1/2 isoforms, coming from alternative splicing of the genes *SYNE1/2* or alternative initiation/termination events of transcription (Janin & Gache, 2018). These nesprin variants can be different in size, with the large ones only speculated and the small ones demonstrated to exist. To this regard, Rajgor et al showed that these small isoforms can retain the KASH domain plus some spectrin repeats (the case for p53KASH^{Nesp1}), a spectrin repeat plus the CH domains (the case for p56CH^{Nesp1}), only the CH domains (the case for p32CH^{Nesp2}), or just some spectrin repeats (the case for different nesprin 1 derived small variants) (Rajgor, Mellad, Autore, Zhang, & Shanahan, 2012) (Fig 28).

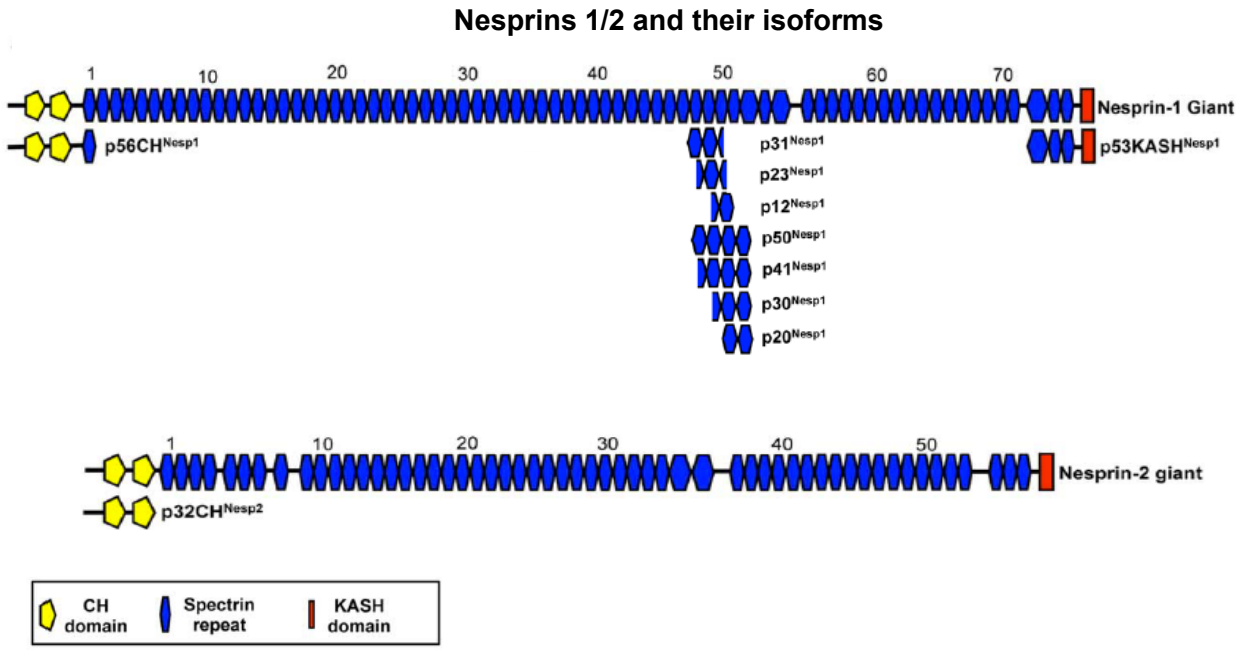

Fig 28: Nesprin 1/2 isoforms. See text for details. Adapted from (Rajgor et al., 2012).

These alternative isoforms are found in specific subcellular localizations, such as stress fibers (SFs), focal adhesions (FAs) and microtubule and are tissue-specific as well (Rajgor et al., 2012). For instance, nesprin-1α_1 is greatly expressed in skeletal and cardiac muscles (Duong et al., 2014). Moreover, nesprin-1α, which is present at the ONM and interacts with the microtubule via the centrosomal protein akap450 (Gimpel et al., 2017) and the motor protein kinesin (Janin & Gache, 2018), can be also localized to the INM, where it directly interacts with emerin (Janin & Gache, 2018) (Fig 29).

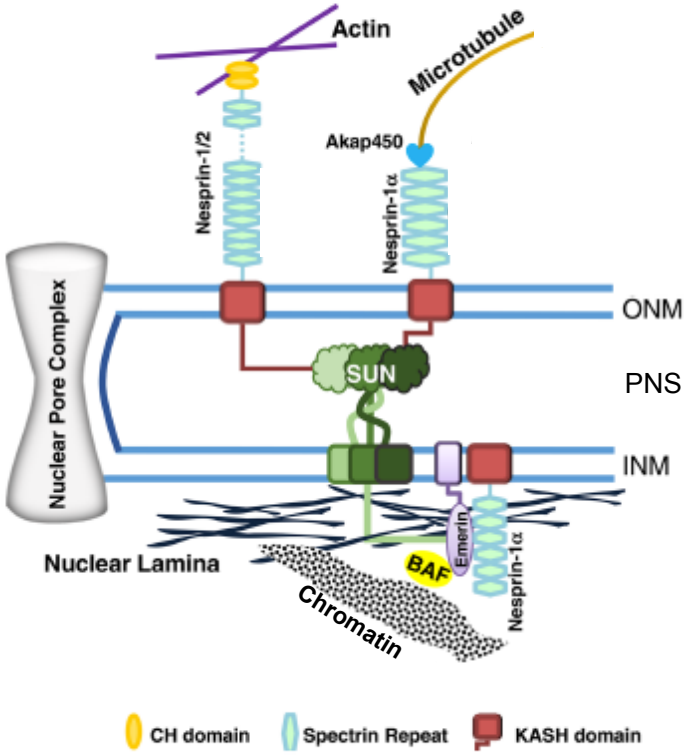

Fig 29: The giant nesprins (1and 2) are inserted into the outer nuclear membrane (ONM) and directly interact, via the calponin homology (CH) domains, with cytoskeletal actin, whereas the small isoform nesprin-1α is linked to the microtubules via the centrosomal protein akap450. Nesprin-1α can be also found associated to the inner nuclear membrane (INM), where it interacts with emerin through the spectrin repeats. The KASH domain in nesprins permits the interaction of these proteins with SUN proteins in the perinuclear space (PNS). BAF: barrier to autointegration factor. Adapted from (C. Zhou, Rao, Shanahan, & Zhang, 2018).

Besides being connected to the actin cytoskeleton, nesprins 1/2 can be also linked to the microtubules via the motor proteins dynein and kinesin (Janin & Gache, 2018; Maurer & Lammerding, 2019) (Fig 30).

Like nesprin 1 and 2, nesprin 3 is also ubiquitous and was discovered in association with the ABD of plectin (Wilhelmsen et al., 2005), the protein which links the intermediate filaments (IFs) with different cellular structures (Janin & Gache, 2018). Thus, nesprin 3 interacts with IFs via plecitn (Fig 30).

Nesprin 4 interacts with the microtubules via kinesin (Roux et al., 2009) (Fig 30); KASH 5 interacts with the microtubules through the dynein/dynactin complex (Morimoto et al., 2012); and LRMP also interacts with microtubules (Lindeman & Pelegri, 2012).

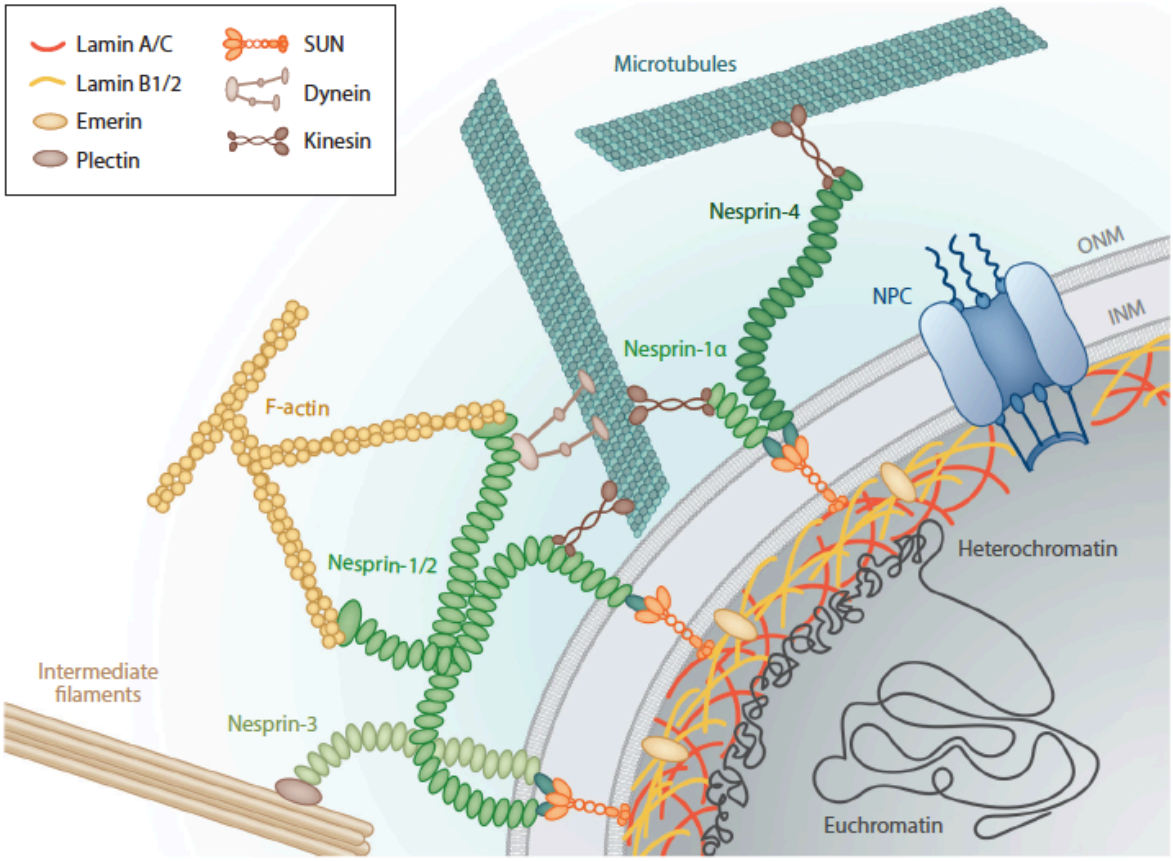

Fig 30: Different forms of nesprin and SUN proteins can build different forms of the LINC complex. Note that nesprins 1/2 are directly connected to the actin filaments (F-actin), whereas nesprins 3, 4 and 1α are indirectly linked to the intermediate filaments and the microtubules via the cytoskeletal linker plectin or the motor protein kinesin, respectively. A connection between nesprins 1/2 and the microtubules is also possible via kinesin or dynein (another motor protein). The interaction between nesprin proteins and SUN proteins is also displayed. SUN proteins directly interact with the nuclear lamina, which, in turn, binds chromatin and emerin. NPC: nuclear pore complex. ONM: outer nuclear membrane. INM: inner nuclear membrane. From (Maurer & Lammerding, 2019).

As previously stated, nesprins interact with SUN proteins in the PNS. In all eukaryotes, SUN proteins are widely conserved and, moreover, they share at their C-terminus a motif of roughly 175 amino-acids, referred to as the SUN domain (Tapley & Starr, 2013).

In mammals, five genes, *SUN1-5*, encode the SUN proteins (Hieda, 2017). Among these genes, we can identify *SUN1-2* which are largely expressed in somatic cells; *SUN3*, *SUN 4* (also referred to as *SPAG4*) and *SUN 5* (also referred to as *SPAGL*) are, instead, associated to gametes (Hieda, 2017).

Basically, the SUNs are made of an N-terminus domain, which protrudes in the nucleoplasm and interacts with the nuclear lamins as well as with chromatin-biding proteins; a transmembrane domain, which is important for the insertion of the SUN protiens into the INM; and the already cited C-terminus, which protrudes into the PNS and displays, besides the SUN domain -which interacts with the KASH domain in nesprins-, coiled-coils domains (Hieda, 2017) (Fig 31), important for SUN trimerization (Sosa, Rothballer, Kutay, & Schwartz, 2012).

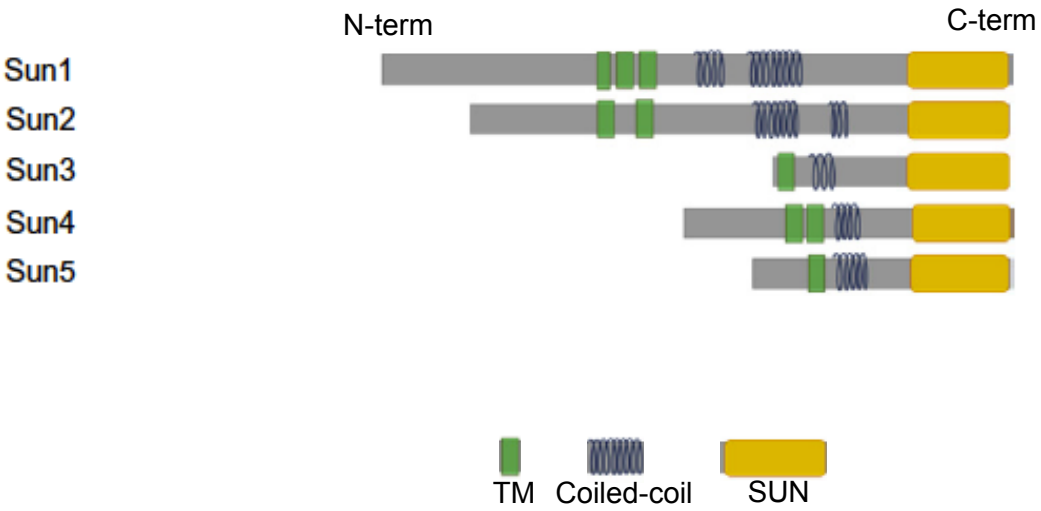

Fig 31: The mammalian SUN proteins. which form trimers via the coiled-coil domains. TM: transmembrane domain. SUN: SUN domain. Adapted from (Kracklauer, Link, & Alsheimer, 2013).

Because of SUNs' capability to form trimers, it is thought that SUN and nesprin proteins interact according to the stoichiometry of 3:3 (Hieda, 2017), which means that for each SUN trimer, 3 nesprins can be associated (Fig 32).

Anyway, the ratio can be varied and stoichiometries of 3:2 or 3:1 can be also possible (Hieda, 2017). In addition, there could exist SUN1dimers or tertramers in particular cellular conditions (Lu et al., 2008).

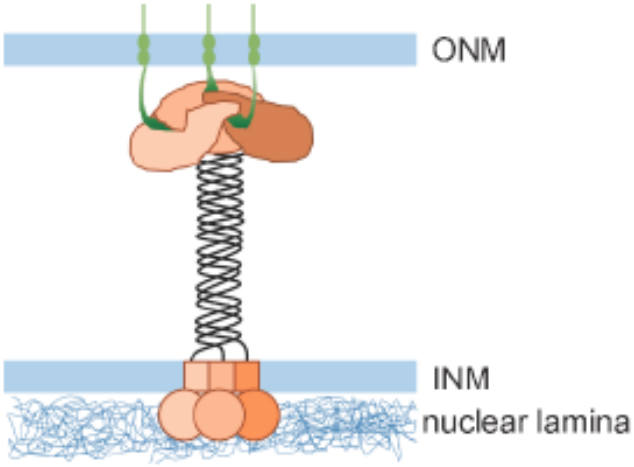

Fig 32: SUNs and nesprins combine in a ratio of 3:3. Nesprins are depicted in green. From (Hieda, 2017).

By referring to Crisp et al. work, we know that the LINC complex bridges the nucleoskeleton and the cytoskeleton. But what happens if the LINC complex is disrupted? That is what I will explore in the next sub-paragraph.

1.3. The LINC complex: when the LINC is perturbed

A proper connection between nucleus and cytoskeleton is important for transmitting forces from the cell's surface to the cell's nucleus. If this connection is impaired, force transmission is lost, which can have multiple consequences for the cell. Nevertheless, it is not totally clear if these cellular

consequences are strictly associated to force-transmission impairment. To this regard, it is worth quoting Lombardi's et al. work (Lombardi et al., 2011) . In this paper, the researchers took advantage of a form of nesprin which was totally devoid of the N-terminus and just retained the KASH domain (Luxton, Gomes, Folker, Vintinner, & Gundersen, 2010). This particular construct was able to dislodge the endogenous nesprins from the nuclear envelope (shown for the first time in 2008 by Hodzic team (Stewart-Hutchinson, Hale, Wirtz, & Hodzic, 2008))in MEFs (murine embryonic fibroblasts), thus acting as dominant negative (DN)(Luxton et al., 2010) (Fig 33A). Therefore, the chimera protein was referred to as DN KASH (Lombardi et al., 2011). DN KASH was able to disrupt nucleo-cytoskeletal coupling: indeed nucleus displacement via microneedle manipulation of cytoskeleton was impaired in cells stably expressing DN KASH compared to control cells, whereas cells transiently expressing a mini Nesprin-2 Giant (miniNes2G) construct (Luxton et al., 2010; Ostlund et al., 2009) (whose protein localized to the NE not displacing endogenous nesprin 2G) had a higher nuclear displacement due to an increased nucleo-cytoskeleton coupling (Lombardi et al., 2011) (Fig 33B). Moreover, DN KASH MEFs, seeded onto fibronectin crossbow patterns, had random-oriented centrosomes and failed to polarize compared to MEFs expressing a mock construct (Lombardi et al., 2011) (Fig 33C).

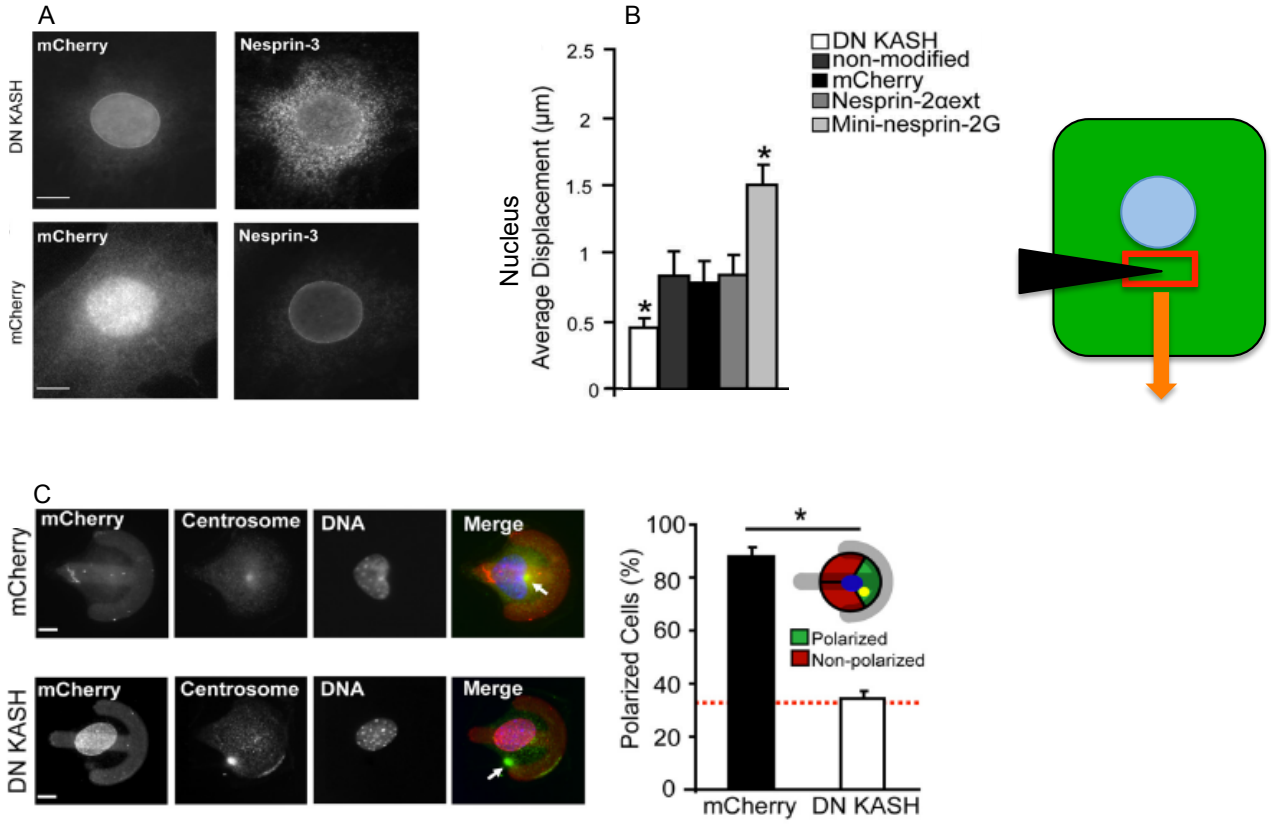

Fig 33: LINC complex disruption impairs nucleo-cytoskeleton coupling thus impacting force transmission, centrosome orientation and cell polarization. A: immunofluorescence showing that in MEFs (mouse embryonic fibroblasts) expressing the DN KASH construct (tagged with mCherry), nesprin-3 is no more present around the nuclear envelope, whereas cells expressing the mock construct (mCherry) present a regular nesprin-3 rim around the nucleus. B: DN KASH impairs force transmission in microneedle manipulation assay. Nucleus displacement is reduced in MEFs expressing DN KASH compared to control cells (non-modified), to cells expressing the mock construct (mCherry) or to cells expressing a modified version of nesprin-2α (Nesprin-2α ext) that cannot bind SUN proteins. In contrast, when nucleo-cytoskeleton coupling is enhanced by overexpressing a Mini-nesprin-2G construct, nucleus displacement is higher compared to the other conditions. In the sketch on the right, the red box represents the microneedle insertion and the strain application site in the cell, whereas the orange arrow represents the direction of the applied strain C: on the left, immunofluorescence showing that MEFs plated onto fibronectin crossbow patterns and expressing DN KASH construct present a random orientation of the centrosome compared to the same cells but harbouring the mock construct

(mCherry); on the right, MEFs expressing DN KASH construct failed to polarize compared to MEFs harbouring the mock construct (mCherry). Scale bars 10 μm in A and 5 μm in B. *p<0.05. Adapted from (Lombardi et al., 2011).

Lombardi et al. also showed that DN KASH expressing MEFs displayed aberrant cytosketal morphology, with discontinuous and fragmented actin stress fibers at the perinuclear area (Fig 34A) and disrupted perinuclear vimentin organization (Fig 34B).

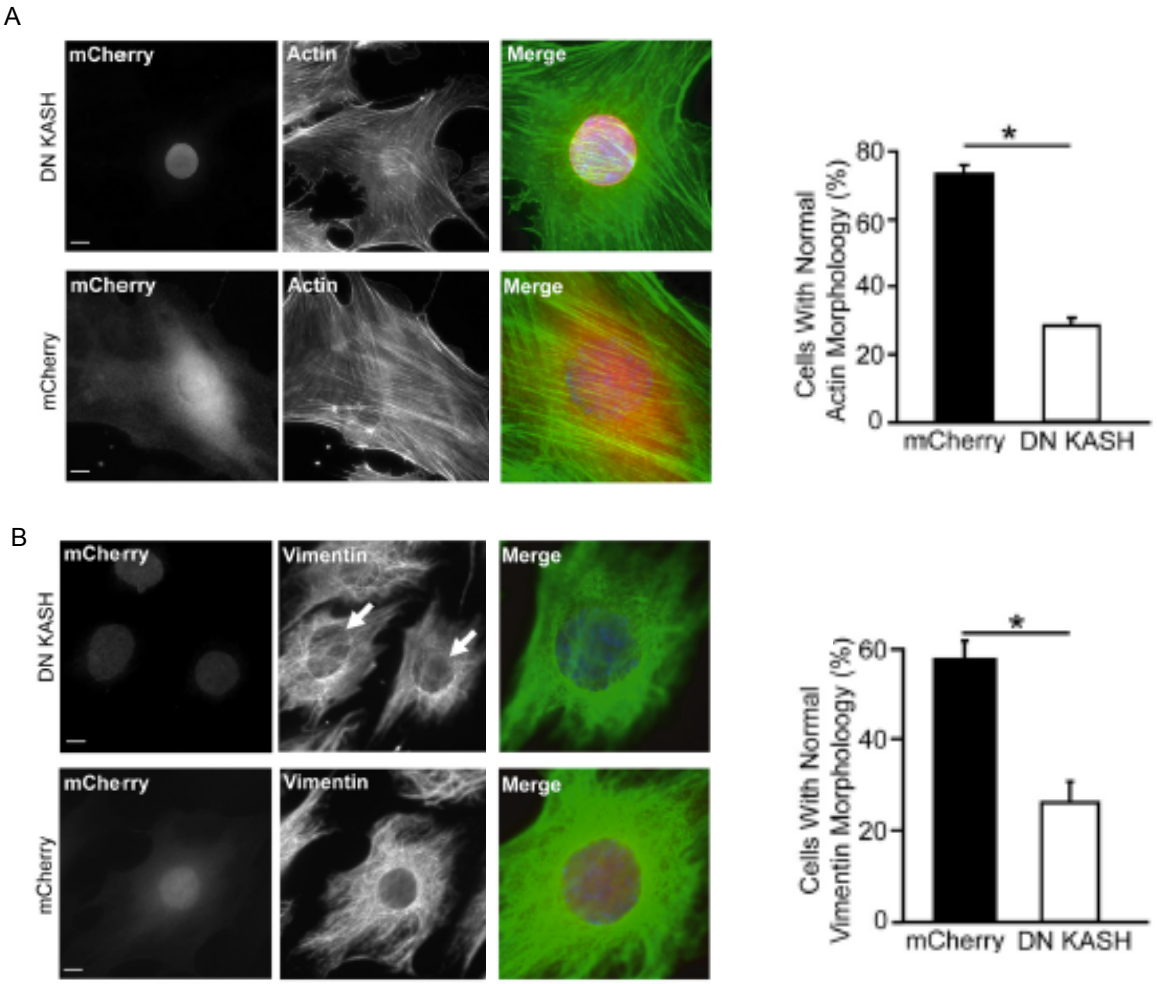

Fig 34: DN KASH expressing MEFs display cytoskeletal morphology defects, with both aberrant perinuclear actin filaments (A) and perinuclear vimentin organization compared to mock expressing cells. Scale bars in the immunostaining panels are 10μm. P<0.05. Adapted from (Lombardi et al., 2011).

It has to be pointed out that before Lombardi et al., Luxton et al. showed that defects in nucleo-cytoskeleton coupling, due to LINC complex disruption, impaired nuclear movement (Luxton et al., 2010).

Nucleo-cytoskeleton connection is not the only thing to be impaired when LINC complex is disrupted. Indeed, it has been demonstrated that a non-functioning LINC is also the cause of a deregulated cellular signalling. To this regard, Neumann et al. showed that depletion of nesprin-2G in HEK (human embryonic kidney) cells decreased the rate of TOP/FOP gene reporter assay, which measures the co-transcriptional activity of β-catenin (Neumann et al., 2010) (Fig 35A). More recently, Uzer et al. found that following LINC complex disruption in mouse MSCs (mesenchymal stem cells) by SUN1/2 co-depletion, β-catenin colocalized with the nuclear-envelope displaced nesprin-2G (Uzer et al., 2018) (Fig 35B).

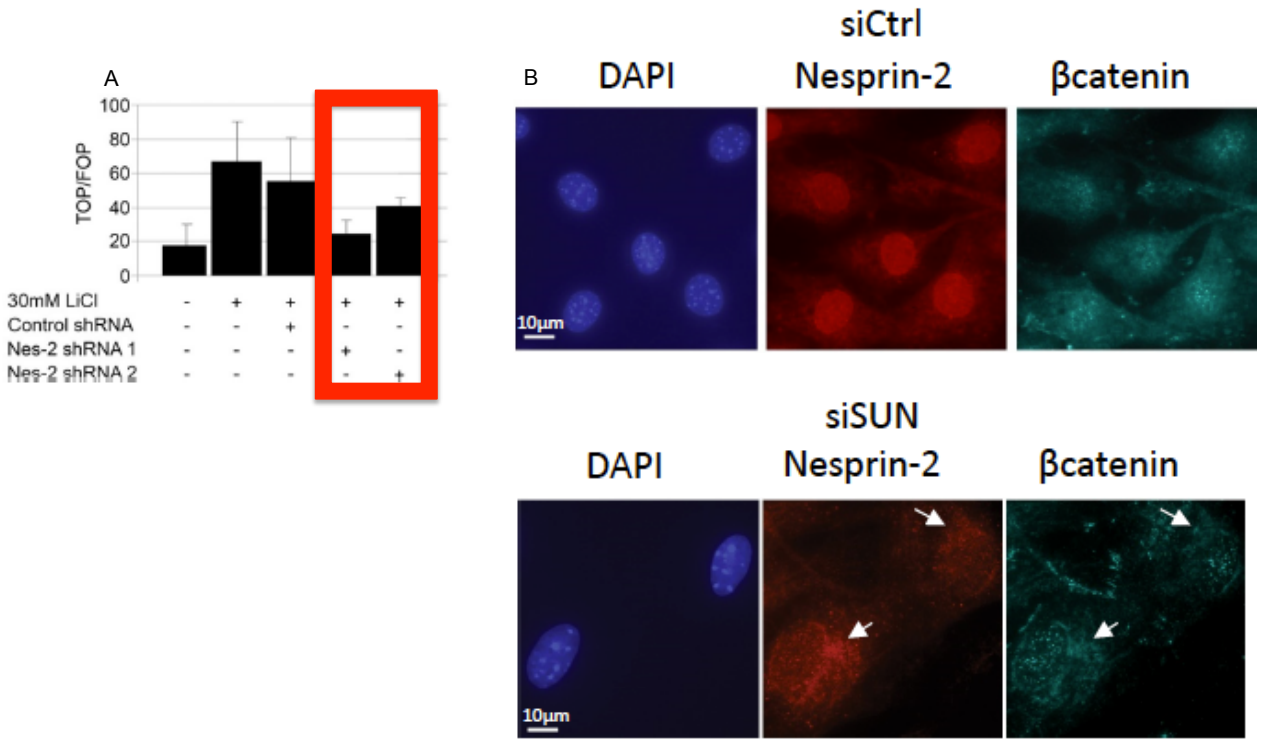

Fig 35: LINC complex disruption impairs β-catenin signalling and its localization. A: in HEK cells stimulated with lithium chloride (LiCl) to induce WNT pathway, depletion of nesprin-2G (Nes-2-shRNA1/2) decreased TOP/FOP ratio (red box) compared to the control (control shRNA), thus resulting in a reduction of β-catenin signalling. B: in MSCs, following co-depletion of SUN 1/2 (siSUN), β-catenin colocalizes with nuclear envelope-displaced nesprin-2G (see arrows in the below immunostaining panel). DAPI used to counterstain nuclei. Adapted from (Neumann et al., 2010) (A) and (Uzer et al., 2018) (B).

Impairment of cellular signalling due to LINC complex disruption has also been demonstrated for the Hippo pathway co-transcription factor YAP (Yes associated protein, see section 3.4 "Signalling upon mechanotransduction" in Chapter 1). Indeed Elosegui-Artola et al. demonstrated that in MEFs transfected with dominant negative constructs of nesprin and seeded onto rigid substrates, accumulation of nuclear YAP was impaired in comparison to mock transfected cells (Elosegui-Artola et al., 2017) (Fig 36).

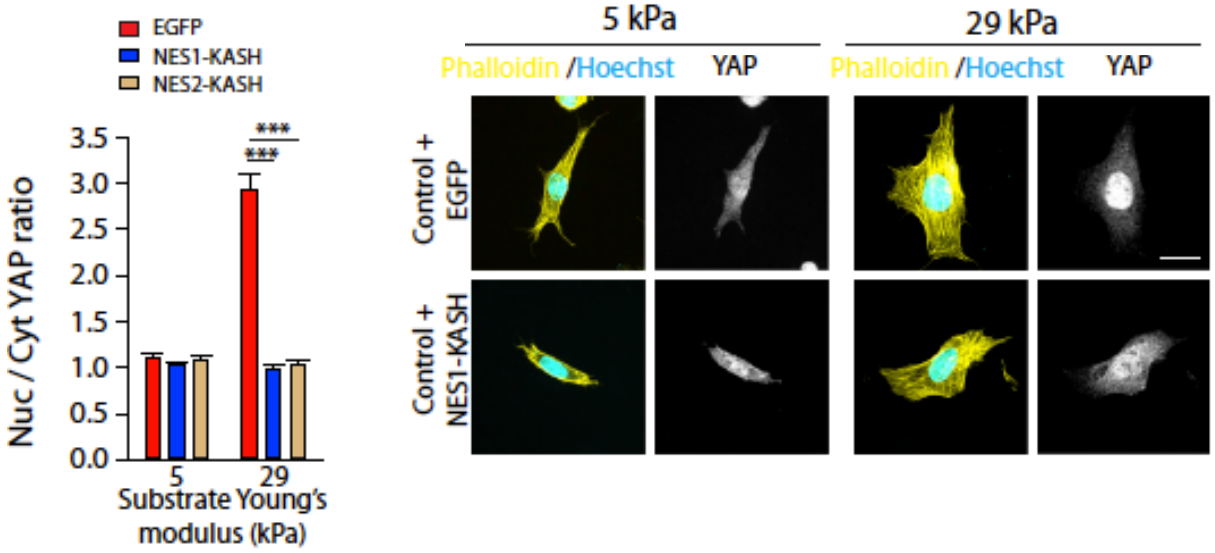

Fig 36: LINC complex disruption through dominant negative constructs of nesprin (NES1-KASH and NES2-KASH, both constructs harbouring an EGFP tag) impairs nuclear YAP accumulation in MEFs seeded onto stiff (29kPa) substrates, compared to the mock (EGFP) control in the same condition. Note that a lower substrate rigidity (5kPa) does not trigger nuclear accumulation of YAP in any condition (NES1/2-KASH and EGFP). Phalloidin is used to stain actin and Hoechts to counterstain nuclei. ***p<0.001. Scale bar: 20 μm. Adapted from (Elosegui-Artola et al., 2017).

It is thus conceivable that, because of the altered cell signalling, LINC complex disruption can impact gene transcription as well. Indeed, Alam et al. showed that in NIH 3T3 fibroblasts expressing a doxycycline-inducible SUN1 construct (SUN1 protein luminal domain, SUN1L), which acted as dominant negative by dislodging nesprin-3 (Fig 37A), expression of genes related to focal adhesions (FAs), cytoskeleton and nuclear envelope was altered on both soft and stiff substrates (Fig 37B), in comparison to control cells expressing a doxycycline-inducible GFP (Alam et al., 2016)

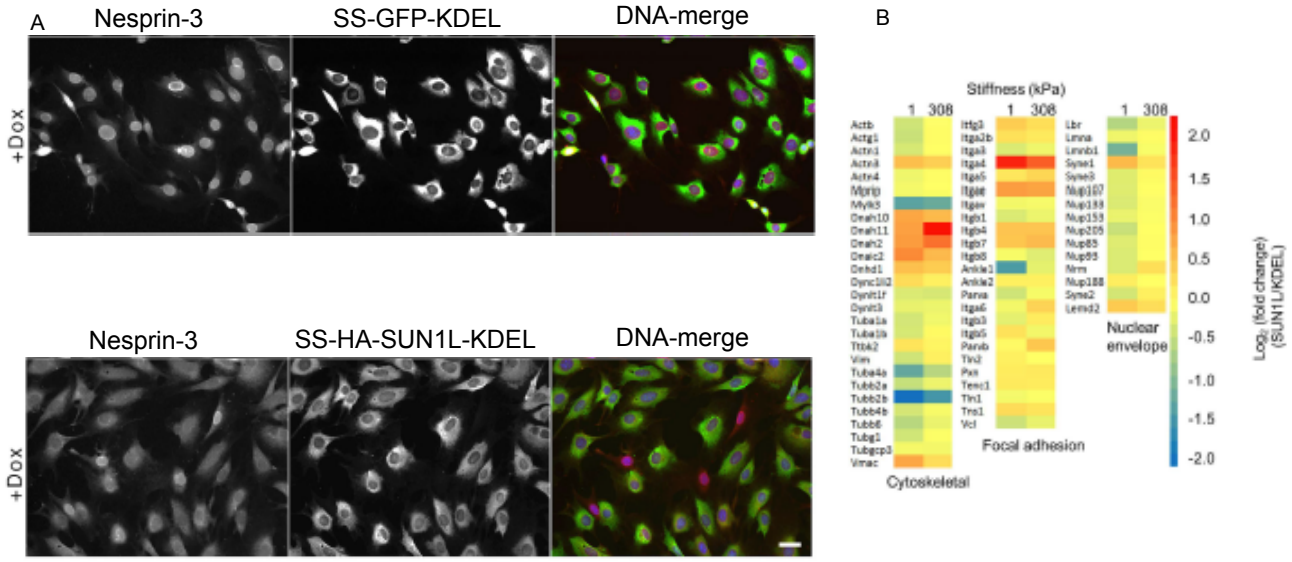

Fig 37: LINC complex disruption alters gene expression. A: doxycycline-inducible SS-HA-SUN1L-KDEL (signal sequence-HA epitope tag-SUN1 protein lumenal domain- ER retrieval amino acid sequence) construct dislodges nesprin-3 from the nuclear envelope (below), whereas the doxycycline-inducible SS-GFP-KDEL does not (above). B: heat maps depicting gene expression variations upon LINC complex disruption for NIH 3T3 fibroblasts seeded onto soft (1kPa) and stiff (308 kPa) substrates. Note that the values on the heat maps are already normalized to the SS-GFP-KDEL control. Scale bar in immunostaining panel: 30 μm. Adapted from (Alam et al., 2016).

Beside what shown above, LINC complex alterations can also impact nucleus anchoring (Grady, Starr, Ackerman, Sanes, & Han, 2005; Starr & Han, 2002) , chromosome positioning (Chikashige et al., 2006), DNA repair (Swartz, Rodriguez, & King, 2014) and cell cycle and DNA replication (S. Wang et al., 2018).

Therefore, a properly working LINC complex is important for a variety of cellular functions that can then be thus impacted upon LINC complex disruption/alteration.

1.4 The nuclear pore complex: structure and nucleo-cytoplasmic shuttling

As stated before, the nuclear pore complex (NPC) is the selective barrier embedded into the nuclear envelope (NE), which permits to selectively control the inwards/outwards nuclear shuttling of molecules larger than 30 kDa (Maurer & Lammerding, 2019). Basically, the NPC is made up of roughly 30 different proteins called “nucleoporins” (Nups) and, in vertebrates, reaches a size of around 125

MDa (OKA & YONEDA, 2018). The NPC can be split in eight repeating subunits called "spokes" (Alber et al., 2007), which compose three distinct parts: the central channel, the cytoplasmic filaments (protruding towards the cytoplasm) and the nuclear basket (Jahed, Soheilypour, Peyro, & Mofrad, 2016) (Fig 38).

In the NPC, an outer ring, made of Nups and known as coat Nup complex (CNC), is present both at the cytoplasmic and nuclear sides of the NPC (Lin et al., 2016) (Fig 38). In the central channel, concentric cylinders are formed by two different layers of Nups, that is the central channel Nups (also known as FG layer) and adapter proteins (Jamali, Jamali, Mehrbod, & Mofrad, 2011; Lin et al., 2016) (Fig 38). The presence, in the central channel, of Nups containing phenylalanine-glycine repeats (FG repeats), gives the NPC its capability to selectively block passive diffusion of macromolecules (OKA & YONEDA, 2018). There exists a third Nups layer, named POMs (Fig 38), which comprises transmembrane proteins with the role of anchoring the NPC into the NE (Jahed et al., 2016).

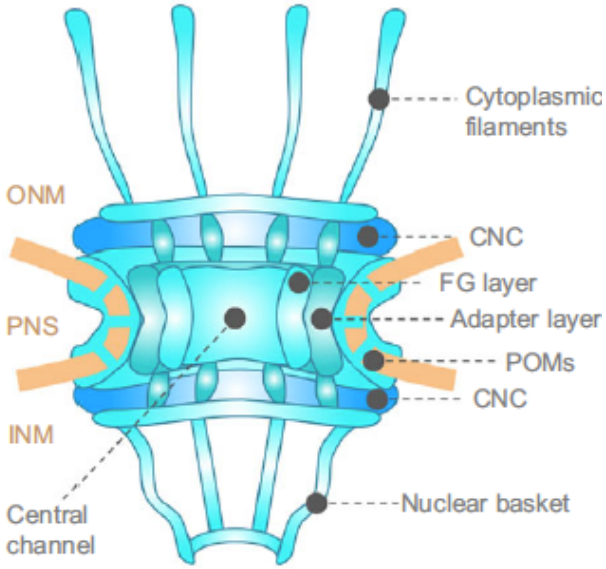

Fig 38: NPC's structure. See text for details. CNC: coat Nup complex. ONM: outer nuclear membrane. PNS: perinuclear space. INM: inner nuclear membrane. From (Jahed et al., 2016).

The process of protein nuclear import via the NPC is accomplished thanks to the existence of nucleocytoplasmic transport receptors (NTRs), know as karyopherines or, more commonly, importins α and β (OKA & YONEDA, 2018), as well as thanks to the presence of a Ran-GTP/GDP gradient between nucleus and cytoplasm(Harel & Forbes, 2004; OKA & YONEDA, 2018).

Generally, proteins that can be translocated into the nucleus (also named as cargoes or cargo proteins) harbour a particular amino-acid sequence, namely the nuclear localization signal (NLS) (Kalderon, Roberts, Richardson, & Smith, 1984) , which is greatly characterized by the presence of basic amino-acids, such as lysine (K) and arginine (R) (OKA & YONEDA, 2018). These sequences are referred to as classical NLS (cNLS) and are divided into monopartite, which display only a cluster of basic amino-acids, and bipartite, which harbour two clusters of basic amino-acid spaced by an amino-acidic linker (Robbins, Dilworth, Laskey, & Dingwall, 1991). Beside cNLSs, non-classical NLSs (ncNLSs) also exist (Cingolani, Bednenko, Gillespie, & Gerace, 2002). cNLSs are recognized by importin α, which comprises an N-terminal importin β binding (IBB) domain, a central domain composed of armadillo (Arm) repeats, important for cNLSs binding, and the C-terminus involved in the interaction with CAS/CSE1L, the importin α nuclear export factor (Kutay, Bischoff, Kostka, Kraft, & Görlich, 1997; OKA & YONEDA, 2018) (Fig 39).

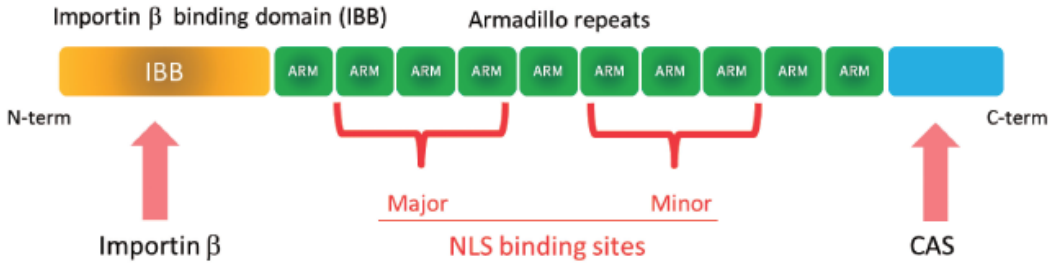

Fig 39: Importin α's structure. See text for details. From (OKA & YONEDA, 2018).

Specifically, the central cNLS-binding domain of importin α comprises 10 Arm repeats, which are divided into major (repeats 2-4) and minor (repeats 6-8) NLS binding sites (OKA & YONEDA, 2018) (Fig 39). Bipartite cNLSs bind both major and minor sites, whereas monopartite cNLSs bind the major site only (OKA & YONEDA, 2018; M. Stewart, 2007).

The other importin involved in the protein nuclear import is importin β, which can transport, across the NPC, different cargoes either in association with importin α or by its own (OKA & YONEDA, 2018). Basically, importin β is made of 19 HEAT (huntingtin, elongation 3 factor, PP2A regulatory A subunit, TOR1(Andrade & Bork, 1995)) repeats, consisting in A and B helices connected by a short turn (Ström & Weis, 2001) (Fig 40). Specifically, HEAT repeats 1-8 bind Ran-GTP; HEAT repeats 7-19 are involved in the interaction with importin α (bound to the cargo); and HEAT repeats 4-8 determine the interaction of importin β with the Nups in the NPC (Ström & Weis, 2001)(Fig 40). Moreover, HEAT repeats are also important to let importin β overcome the selective filter of the NPC, via the interaction with the FG repeats (Bayliss, Littlewood, & Stewart, 2000; Bayliss, Littlewood, Strawn, Wente, & Stewart, 2002; OKA & YONEDA, 2018).

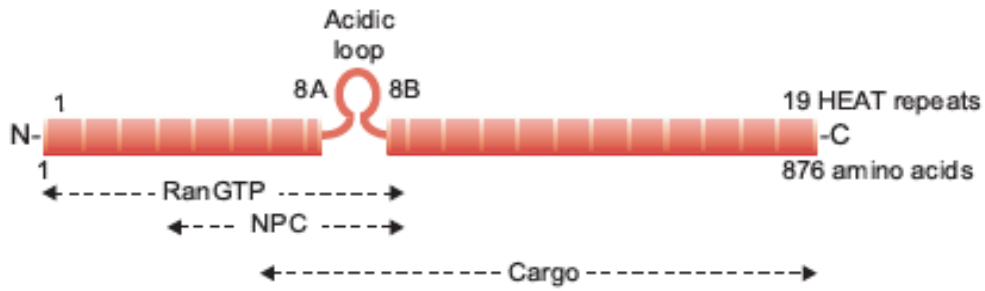

Fig 40: importin β's structure. Note that helices 8A and 8B are linked by an acidic loop instead of a short turn. See text for details. NPC: nuclear pore complex. N: N-terminus. C: C-terminus. Cargo: importin α binding sites. From (Ström & Weis, 2001).

Besides the complex of cargo protein-importin α-importin β, another molecular partner is involved in regulating nuclear import, that is the small GTPase Ran, whose activity is dictated by binding either GTP or GDP (OKA & YONEDA, 2018) (Fig 41). Basically, in the nucleus, the presence of the Ran-GEF (guanine-nucleotide exchange factor) RCC1 (which is associated to the chromatin), permits the conversion of Ran-GDP to Ran-GTP (Harel & Forbes, 2004)(Fig 41). On the contrary, in the cytoplasm, the presence of Ran-GAP (GTPase-activating protein, also presents at the level of the NPC cytoplasmic filaments (Harel & Forbes, 2004) (Fig 41)) enhances the weak intrinsic GTPase activity of Ran, thus resulting into the hydrolysis of Ran-GTP to Ran-GDP (OKA & YONEDA, 2018). In this way, a Ran-GTP/GDP gradient is estabilshed between the nucleus and the cytoplasm (Harel & Forbes, 2004; Kassianidou, Kalita, & Lim, 2019; OKA & YONEDA, 2018) (Fig 41).

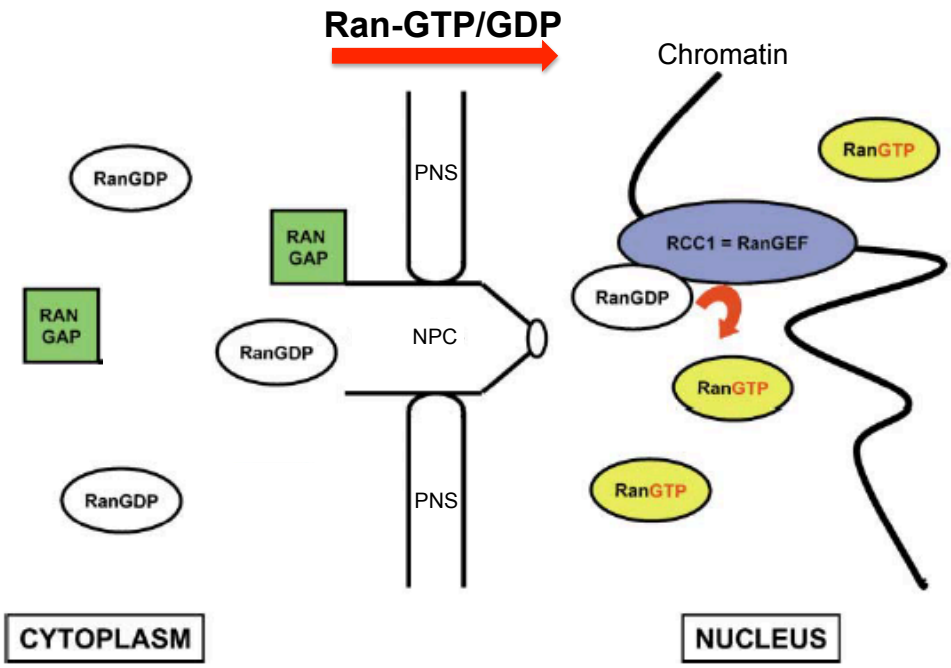

Fig 41: Ran-GTP activity triggerd by RCC1 and Ran-GAP, with the estabilishment of a Ran-GTP/GDP gradient between nucleus and cytoplasm. The arrow points to the gradient. See text for details. Ran-GAP: Ran-GTPase-activating protein. Ran-GEF: Ran-guanine-nucleodite exchange factor. PNS: perinuclear space. NPC: nuclear pore complex. Adapted from (Harel & Forbes, 2004).

Because of the presence of different molecular players, the nuclear import is highly regulated. When a cargo protein,harbouring a cNLS, has to be translocated into the nucleus, it is recognized by importin α, which is then bound by importin β, thus creating a ternary complex called "nuclear pore-targeting complex" (OKA & YONEDA, 2018) (Fig 42). Once importin β mediates the translocation of the ternary complex into the nucleus, Ran-GTP binds to importin β, which triggers the dissociation of the ternary complex with the consequent release of the cargo protein (Görlich, Panté, Kutay, Aebi, & Bischoff, 1996) (Fig 42). Importin α is then recycled back to the cytoplasm by forming a ternary complex with Ran-GTP and the export factor CAS/CSE1L (Kutay et al., 1997), whereas importin β reaches the cytoplasm just by the interaction with Ran-GTP(Izaurralde, Kutay, von Kobbe, Mattaj, & Görlich, 1997) (Fig 42). Once in the cytoplasm, both the complexes are dissociated due to Ran-GTP hydrolysis to Ran-GDP mediated by Ran-GAP and, therefore, importins α and β are ready for the next round of nuclear transport (OKA & YONEDA, 2018) (Fig 42).

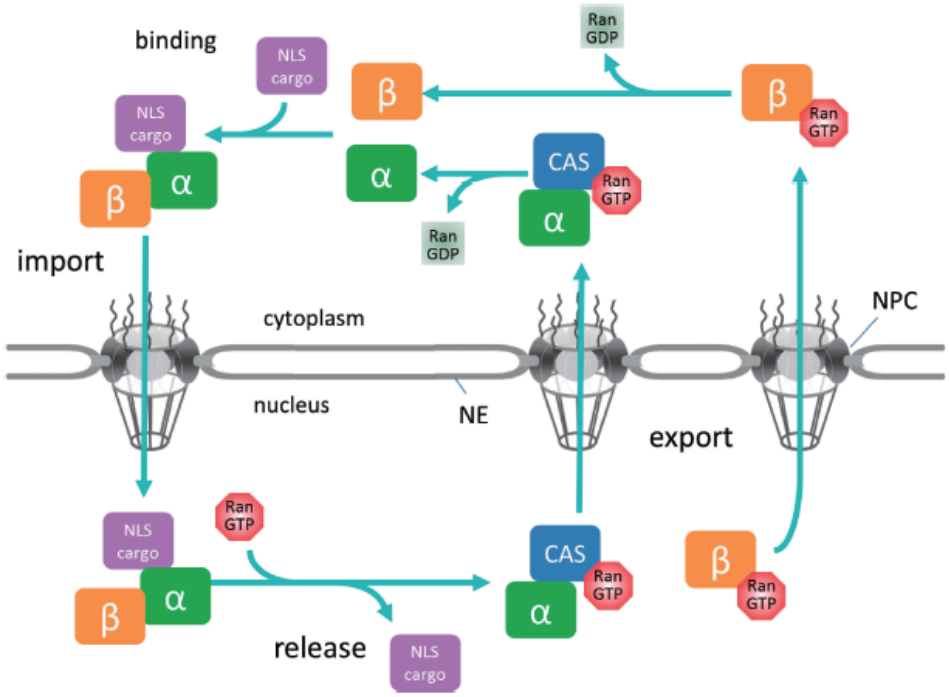

Fig 42: Schematic representing the nuclear import. See text for details. α and β: importins α/β. NPC:nuclear pore complex. NE: nuclear envelope. NLS cargo: cargo protein with classical nuclear localization signal. CAS: importin α nuclear export factor. Adapted from (OKA & YONEDA, 2018).

Above, I have described the canonical pathway to transport proteins with cNLS. However, cargoes harbouring an ncNLS can directly bind importin β to be translocated into the nucleus without the presence of importin α (Kassianidou et al., 2019; Marfori et al., 2011) (Fig 43). Moreover, a third nuclear transport pathway exists, where karyopherin-independent (Kap-independent) proteins are able to cross the NPC by directly interacting with the FG Nups (Nups containing the FG repeats in the central channel of NPC (OKA & YONEDA, 2018))(Whitehurst et al., 2002) by, maybe, not using the Ran-GTP/GDP gradient (Kassianidou et al., 2019) (Fig 43).

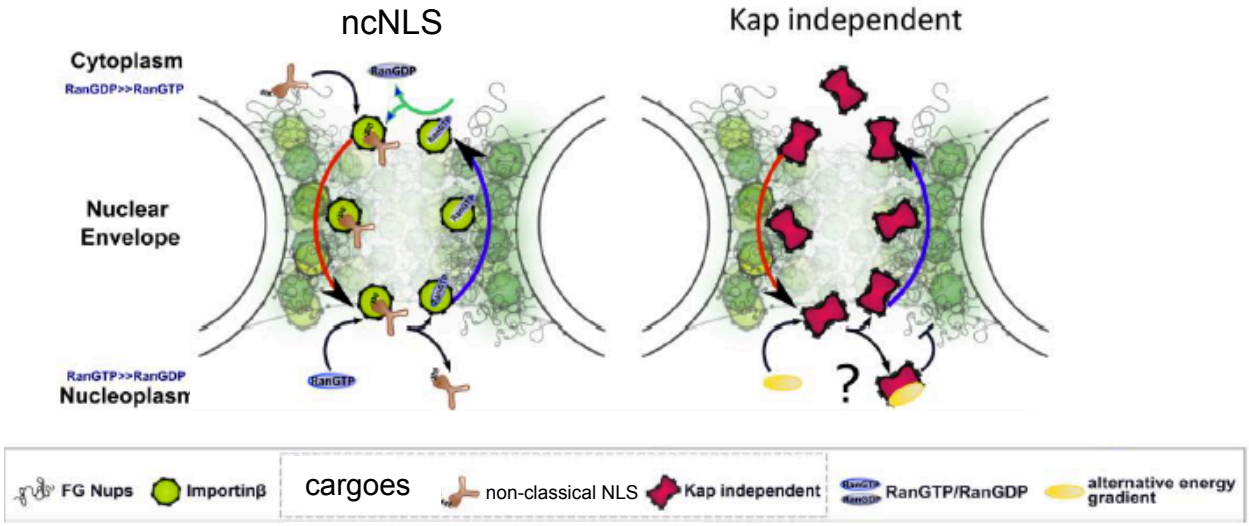

Fig 43: Schematic representing nuclear import of cargoes harbouring a non-classical NLS (ncNLS) or cargoes able to directly interact with the FG Nups in the NPC (Kap independent) without using the RanGTP/GDP gradient. In

this case, an alternative energy gradient (question mark) may be used. FG Nups: nucleoporins containing FG repeats. Adapted from (Kassianidou et al., 2019).

Another protein thought to use a kap-independent nuclear transport is β-catenin. Indeed, even though β-catenin does not contain any cNLS , it is able to undergo nucleo-cytoplasmic shuttling (François Fagotto, 2013), which does not rely on any nuclear transport receptor (François Fagotto, Glück, & Gumbiner, 1998; Yokoya, Imamoto, Tachibana, & Yoneda, 1999). β-catenin would rather undergo nucleo-cytoplasmic shuttling in a free diffusion manner, since its transport is indepedent of Ran-GTP and does not require energy (François Fagotto, 2013; Yokoya et al., 1999). In addition, β-catenin would enter the NPC by directly interacting, via its Arm repeats, with Nups (François Fagotto, 2013). Moreover, β-catenin, similarly to importins α/β ,could work as nuclear import receptor. To this regard, Asally and Yoneda showed that a mutant LEF1 (lymphoid enhancement factor 1, a transcription factor interacting with β-catenin in the nucleus (Behrens et al., 1996)), devoid of its NLS, was translocated into the nucleus of living NIH 3T3 cells when β-catenin was co-expressed (Asally & Yoneda, 2005).

In this section, I have explored the structure of the nuclear envelope, taking into account the nuclear lamina and,in particular, the LINC complex. I have also described few papers where the LINC complex was disrupted, with its subsequent consequences on cell's functions. I have also taken a look into the NPC and how the nucleo-cytoplasmic shuttling is regulated.

Cell's nucleus can also participate in the process of mechanotranducstion. Therefore, in the next paragraph, I will briefly cover the aspects of nuclear mechanotransduction.

2 Nuclear mechanotransduction

The first evidence of the existence of a mechanical connection between cytoskeleton and nucleus was given by Maniotis et al., in 1997. In this work, the researchers, by using microbeads coated with the RGD pepitide -an integrin binding domain present in several ECM protein such as fibronectin (Pierschbacher & Ruoslahti, 1984) - were able to displace the nucleus of intact endothelial cells by simply pulling on the microbeads (Maniotis, Chen, & Ingber, 1997) (Fig 44A and B).

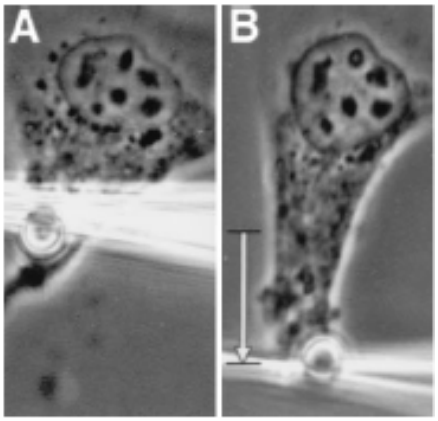

Fig 44: Cell's nucleus at rest (A) and displaced (B) upon pulling on microbeads with a glass micropipette. From (Maniotis et al., 1997)

From the above study, it is clear that force transmission from plasma membrane to cell's interior make the nucleus respond to the applied pulling force. The consequences of nuclear responses

to applied stimuli were explored by Guilluy et al., who showed that successive force pulses application on isolated HeLa cell's nuclei, via magnetic beads coated with anti nesprin 1 antibody (Fig 45A), induced increased nuclear stiffness (Fig 45B). In addition, magnetic force application promoted emerin phosphorylation in the same isolated nuclei (Guilluy et al., 2014) (Fig 45C).

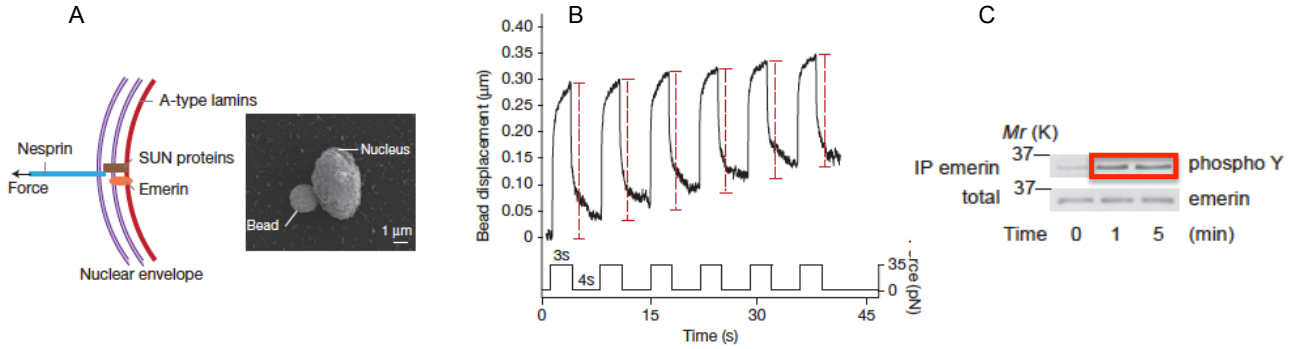

Fig 45: Isolated nuclei (A) displayed increased stiffness upon force pulse application (B), which correlates with force-induced emerin phosphorylation (red box). Adapted from (Guilluy et al., 2014).

Emerin is also involved in nuclear mechanotransduction. Indeed, Essawy et al. recently found that the small deletion ΔK37 in emerin LEM-domain impacts actin fiber organization on the top of nuclei of myofibroblasts derived from human immortalized fibroblasts. Indeed, when plated onto a rigid substrate (glass), cells harbouring ΔK37 emerin mutation (Em ΔK37) displayed less and not well-organized actin stress fibers compared to wt cells in the same condition (Fig 46A). Moreover, upon cyclic stretching events, cells harbouring the mutant emerin scored lower for the number of actin stress fibers compared to wt cells (Fig 46B). Thus, ΔK37mutation alters emerin function upon mechanical cues (Essawy et al., 2019).

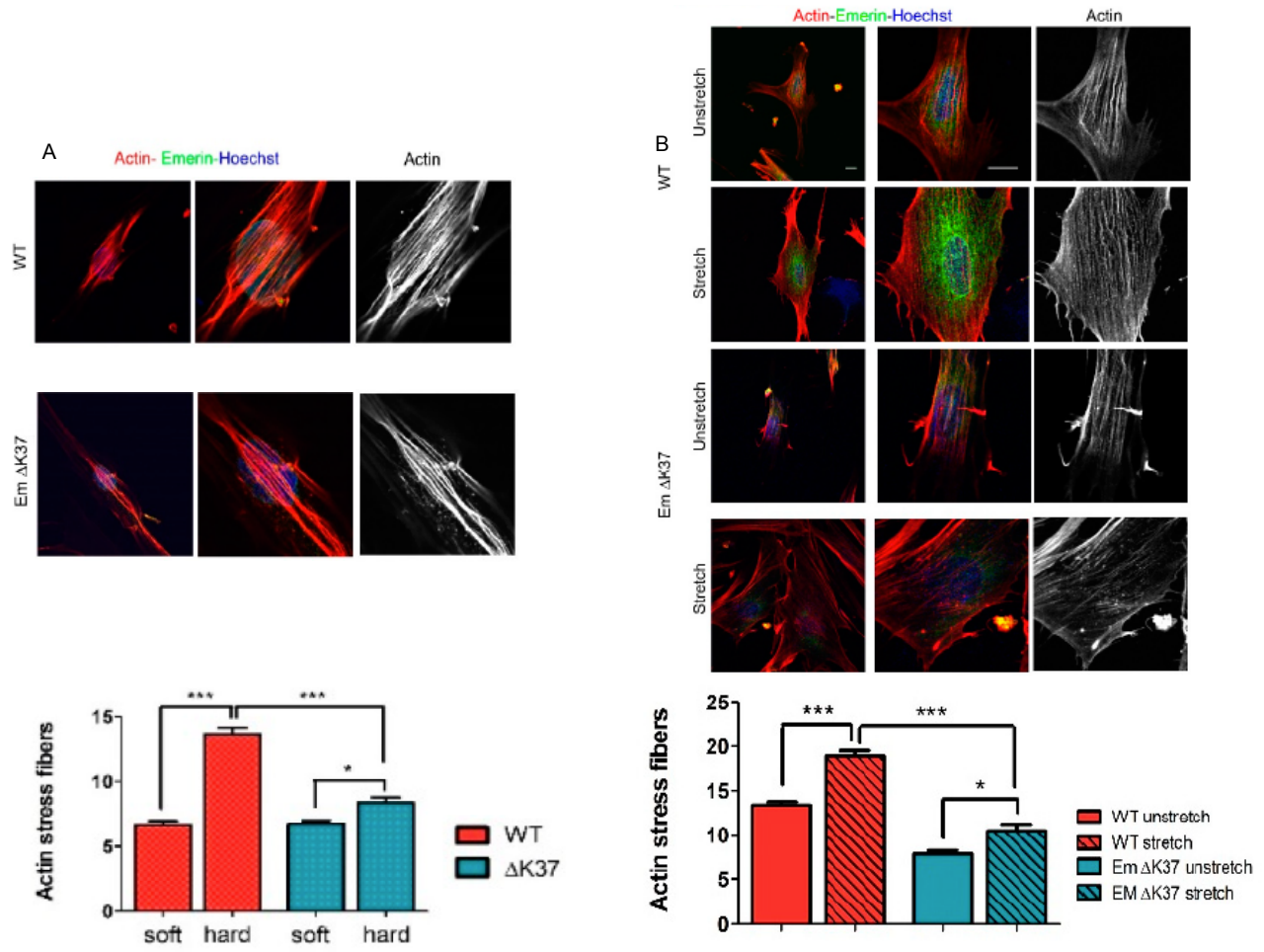

Fig 46: Response to mechanical cues is altered in cells harbouring ΔK37 mutation in emerin LEM-domain. A: in myofibroblasts derived from human immortalized fibroblasts, the small deletion ΔK37 in emerin (Em ΔK37) impairs the organization of the perinuclear actin stress fibers (immunonstaining panel above) as well as their number (graph below) in cells plated onto a hard (glass) substrate, compared to wt cells in the same condition. The soft substrate displays a stiffness of 8kPa. B: upon 10% cyclic stretch (4 hours at 0.5 Hertz), myofibroblasts (the same as in A) harbouring ΔK37 mutation in emerin (Em ΔK37) scored less for actin stress fibers (graph below) compared to wt stretched cells. In A and B panels, phalloidin is used to stain actin fibers, whereas Hoechst to counterstain nuclei. Scale bars in B: 10µm. *p<0.05; ***p<0.001. Adapted from (Essawy et al., 2019).

Mechanical cues can also regulate NPC permeability and, thus, influence protein accumulation into the nucleus, as recently demonstrated by Elosegui-Artola et al for YAP (Elosegui-Artola et al., 2017). Indeed, by plating mouse embryonic fibroblasts onto soft (5kPa) and stiff (150 kPa) substrates, the authors found that the size of the NPCs (measured through transmission electron microscopy (TEM)) was larger on stiffer substrates (Fig 47A). In addition, perturbation of NPC permeability barrier by disrupting FG interactions with trans 1,2 cyclohexanediol (CHD)(Ribbeck & Gorlich, 2002) and Pitstop2 (Liashkovich et al., 2015), did not increase YAP nucleo/cytoplasmic ratio in mouse embryonic fibroblasts plated onto stiff (150 kPa) substrates, compared to the same cells treated with the same drugs but seeded onto soft (5 and 29 kPa) substrates (Fig 47B).

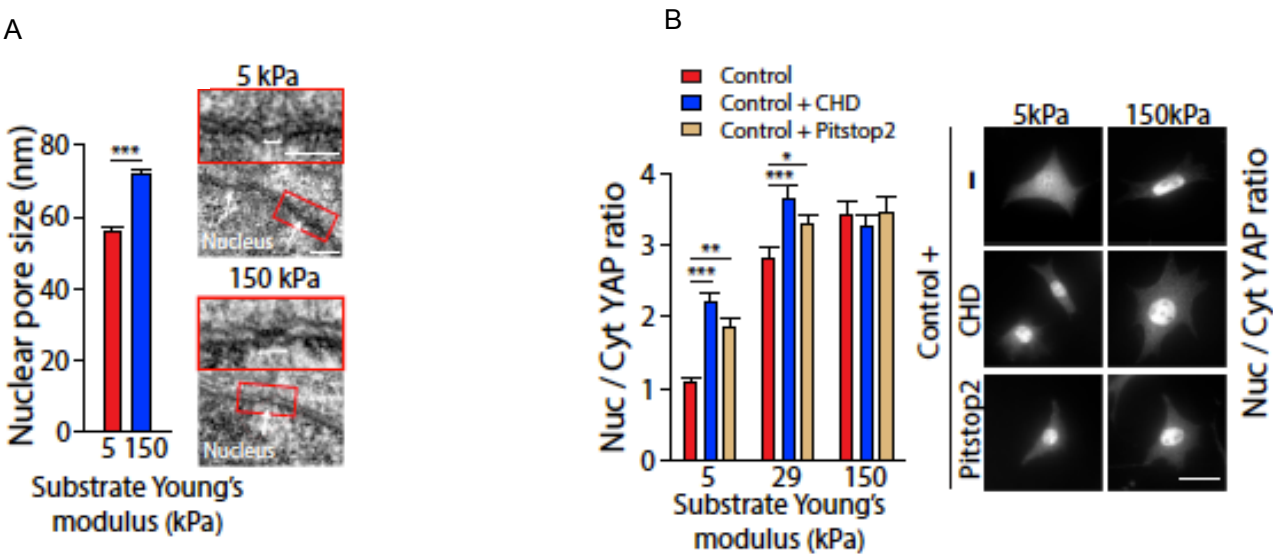

Fig 47: NPC permeability is influenced by mechanical cues. A: Nuclear pore size is higher in mouse embryonic fibroblasts plated onto a rigid substrate (150 kPa), compared to the same cells seeded onto a soft (5 kPa) substrate. B: YAP nucleo/cytoplasmic ratio increases in the presence of either of CHD (trans 1,2 cyclohexanediol) or Pitstop2, which perturb NPC permeability barrier, in mouse embryonic fibroblasts seeded onto soft (5 and 29 kPa) substrates (fibronectin-coated gels). Note that in cells seeded onto a stiffer (150 kPa) substrate, treatment with the drugs does not elicit any increase in nuclear YAP , which is already elevated in the control condition (see also YAP immunostaining on the right). Scale bars are 200nm in A and 20 μm in B. *p<0.05; **p<0.01; ***p<0.001. Adapted from (Elosegui-Artola et al., 2017).

Mechanical cues can also perturb chromatin arrangement and transcription events. In this case, chromatin conformational changes upon mechanical force application can be assessed by surrounding a chosen reporter gene with arrays of the lac operator (LacO) sequences. These, in turn, can be bound by a fluorescently-tagged lac inhibitor (LacI), such as a GFP-LacI. By measuring the distance between adjacent fluorescent LacI spots, it is possible to correlate chromatin stretching with the rate of gene transcription induction, which can be measured by RNA fluorescent *in situ* hybridization (RNA FISH) (Kirby & Lammerding, 2018; Tajik et al., 2016)(Fig 48).

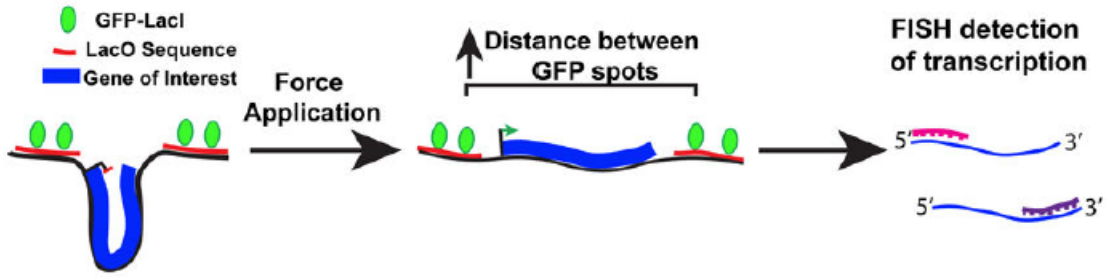

Fig 48: Schematic representing how to measure transgene transcription rates upon force-induced chromatin stretching. To detect nascent transcripts, 5' or 3' FISH probes can be used. From (Kirby & Lammerding, 2018).

This assay was used by Wang team to estimate gene induction upon external mechanical force application onto living cells (Tajik et al., 2016). Indeed, by using three-dimensional magnetic twisting cytometry (3D-MTC) (Hu et al., 2004) to locally apply shear stress via integrins on CHO cells, Tajik et al. were able to stretch the chromatin around the insertion site of the DFHR (dihydrofolate reductase) transgene, which resulted in rapid DHFR transcription induction (Fig 49A). Moreover, DHFR transcriptional induction was abolished when LINC complex was perturbed (Fig 49B), meaning that LINC complex was involved in force propagation towards the chromatin (Tajik et al., 2016).

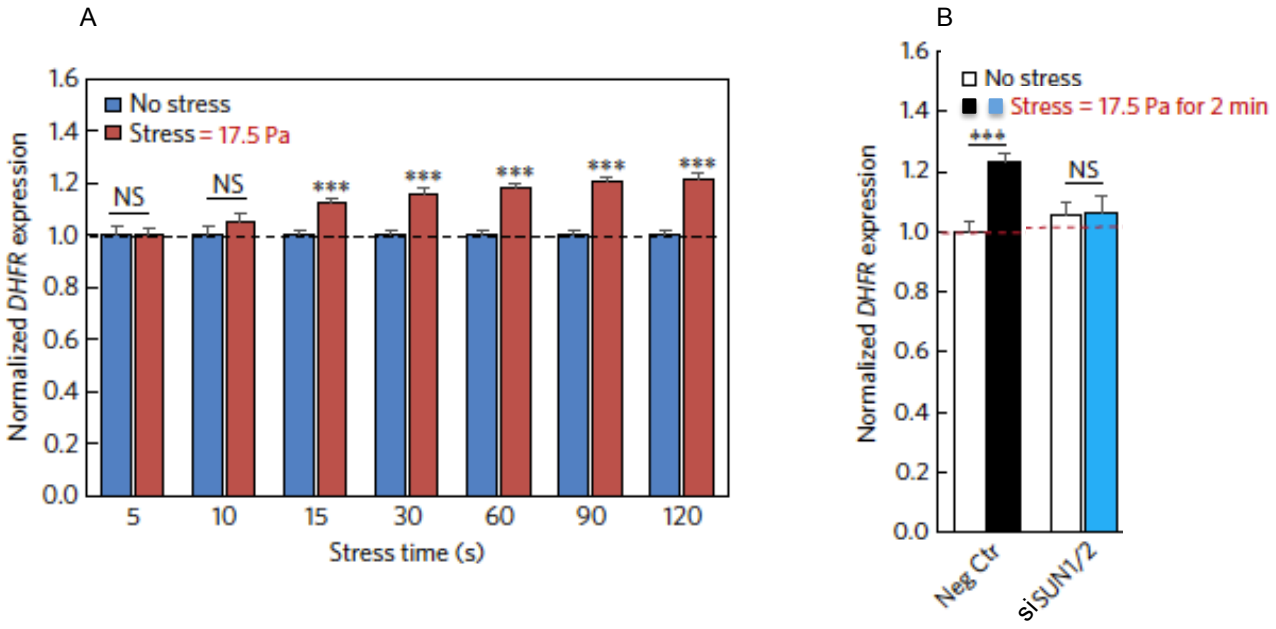

Fig 49: DHFR transgene induction upon chromatin stretching is rapid (seconds) (A) and depends on an intact LINC complex (B). siSUN1/2= small interfering RNA against SUN1/2. ***p <0.001. NS= Not statistically significant. Adapted from (Tajik et al., 2016).

Recently, the development of a FRET (Förster Resonance Energy Transfer) based biosensor, namely Tension Sensor Module (TSMod) (Grashoff, Hoffman, Brenner, Zhou, Parsons, Yang, McLean, Sligar, Chen, Ha, & Schwartz, 2010), has made it also possible to measure forces across the LINC complex. Indeed, by inserting a the TSMod into a MiniNesprin 2 Giant (MiniN2G) construct (Ostlund et al., 2009) -which was demonstrated to act as the endogenous Nesprin 2G (Luxton et al., 2010; Ostlund et al., 2009)- Arsenovic et al. showed that nesprin 2G is under constitutive tension in resting NIH 3T3 mouse fibroblasts (Fig 50A) and that this tension depends on actomyosin contractility (Arsenovic et al., 2016) (Fig 50B).

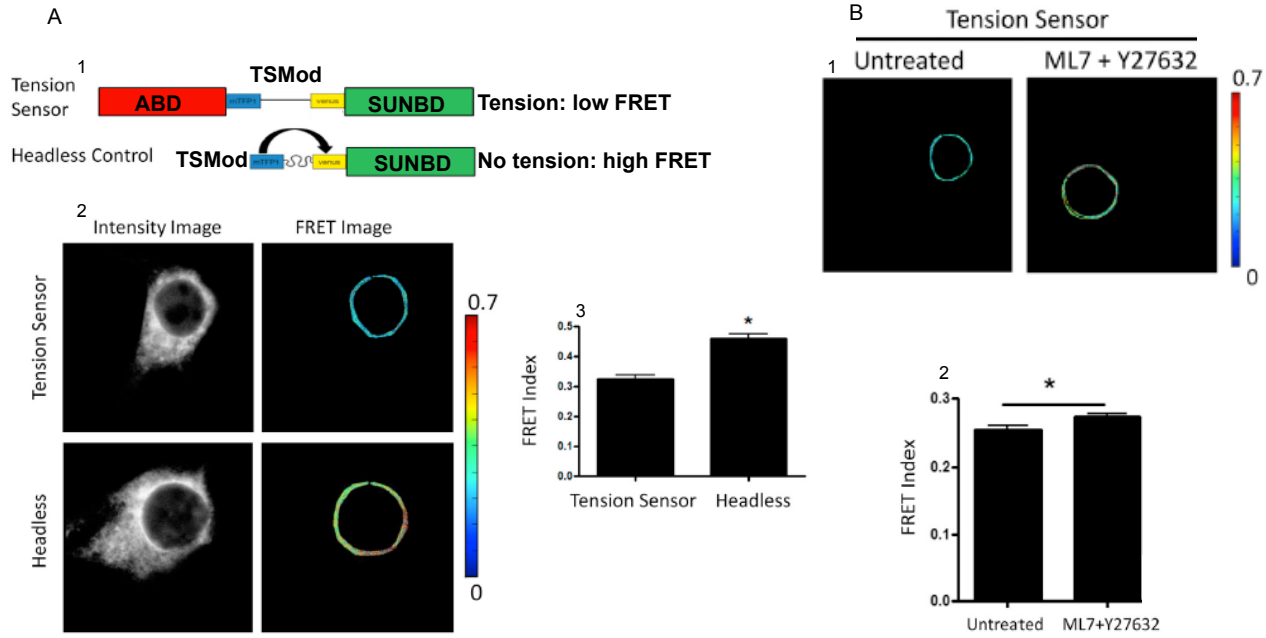

Fig 50: Nesprin 2G is under constitutive actomyosin-generated tension in resting NIH 3T3 mouse fibroblasts. A1: schematic of the MiniNesprin 2 Giant (miniN2G) with the TSMod inserted in between the acting binding domain (ABD) and the SUN binding domain (SUNBD), referred to as "Tension Sensor" and the same construct but devoid of the ABD, referred to as the "Headless Control". Note that the Headless Control cannot feel tension because of the lack of the ABD. A2 and A3: Tension Sensor and Headless Control localizes both at the nuclear envelope (intenisity image) but the Tension Sensor displays a low FRET in comparison to the high FRET coming from the Headless Control (FRET image in A2 and FRET index quantification in A3). B1 and 2: actomyosin contractility inhibition by means of ML7 (which inhibits myosin light chain kinase (MLCK)) plus Y27632 (which inhibits ROC Kinase (ROCK)) determines a higher FRET in the Tension Sensor in comparison to the untreated control. *p<0.01. Adapted from (Arsenovic et al., 2016).

Cell's nucleus can thus respond and adapt to mechanical forces by increasing its stiffness, varying the size of its pores as well as inducing gene expression following chromatin stretching. It is therefore clear that functional and structural integrity of the nuclear envelope has to be preserved and that mutations associated to nuclear envelope components may impair this integrity, resulting in a plethora of diseases.

Thus, in the next paragraph, I will briefly cover the pathological aspects associated to the mutations in the proteins composing the nuclear envelope.

3 Nuclear envelope associated pathologies: the envelopathies

The term "envelopathies" indicates the wide spectrum of diseases associated with alterations in the molecular components of the ONM, the INM and the nuclear lamina (Janin, Bauer, Ratti, Millat, & Méjat, 2017). The greatest part of these diseases is tissue-related, negatively impacting skeletal muscles, heart, peripheral nerves, bones or the adipose tissue (Janin et al., 2017). It has been thought that envelopathies could be caused either by deregulation in gene expression (gene regulation hypothesis), due to, for instance, mutations in nuclear lamins (Janin & Gache, 2018; Maurer & Lammerding, 2019), or by the impaired nucleo-cytoskeleton coupling (structural hypothesis), determined by mutations in nesprins and SUN proteins (Janin et al., 2017; Janin & Gache, 2018). However, the above hypoteses can be merged into a third one, which involves mechanotransduction (Maurer & Lammerding, 2019). Indeed, deregulation of gene expression may arise from an impaired nucleo-cytoskeleton coupling (Maurer & Lammerding, 2019) (Fig 51). To this regard, Banerjee et al. demonstrated that loss of nesprin 1 and 2 in murine cardiomyocytes abrogated biomechanical gene response following strain application, with consequent cardiomyopathy development in mice (Banerjee et al., 2014).

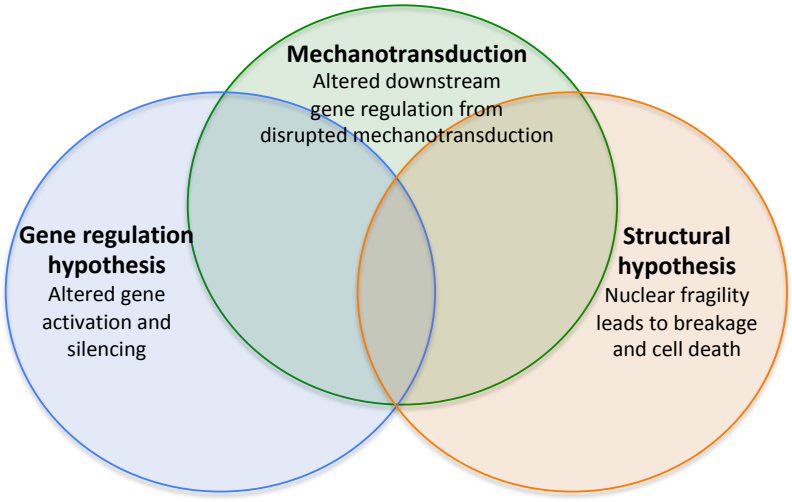

Fig 51: Proposed hypotheses leading to envelopathies. Note that impairements in mechanotransduction could bridge the gap between gene regulation hypothesis and structural hypothesis. Adpated from (Maurer & Lammerding, 2019).

Mutations in the *EMD* gene, which encodes emerin (Bione et al., 1994; Janin & Gache, 2018), are estimated to be the cause, in around 60% of the cases (Janin et al., 2017), of Emery-Dreifuss Muscular Distrophy (EDMD) (Emery, 1989). Most of these mutations are null mutations, resulting in a complete emerin loss (Janin et al., 2017). EDMD is characterized by a triad of symptoms, which are rigidity of spine, progressive muscle wasting and weakness and cardiomiopathy, the last one usually present as a heart block (Emery, 1989; Janin et al., 2017). A clinical hint of EDMD is the increased level of creatine-kinase (CK) in serum or plasma, which is a sign of a lytic process involving the muscular cells (Janin et al., 2017). Nevertheless, variations in muscle fiber size, fibrosis or necrosis are not found through histolgical examinations; however, hypercondensed chromatin, nuclear invagination/fragmentation and intranuclear filaments are spotted (Janin et al., 2017).

Mutations in genes encoding nuclear lamins determine a wide range of rare genetic disorders called "laminopathies" (Janin et al., 2017; Janin & Gache, 2018; Maurer & Lammerding, 2019). Mutations affecting *LMNA* gene, are mostly missense, even though abnormalities in RNA splicing, in-frame deletions and haploinsufficiency are also documented (Janin et al., 2017). There exist multiple diseases related to *LMNA* gene mutations, such as the muscle laminopathies Autosomal Dominant form of EDMD (referred to as EDMD2), Dilated CardioMyopathy with Conduction Defect disease (DCM-CD) and Limb-Girdle Muscular Distrophy 1B (LGMD1B), all of them dysplaying joint contractures and progressive muscle weakness and wasting (Janin et al., 2017); the autosomal dominant Dunningan-type Familial Partial Lipodystrophy (FPLD), involving the loss of adipose tissue at the extremities (Dunnigan, Cochrane, Kelly, & Scott, 1974; Garg, Vinaitheerthan, Weatherall, & Bowcock, 2001; Janin et al., 2017); and the neuropathy Charcot-Marie-Tooth syndrome 2B1 (CMT2B1), which determines a progressive muscular and sensory loss in the distal extremities with chronic distal weakness (De Sandre-Giovannoli et al., 2002; Janin et al., 2017).

Another form of laminopathy is Hutchinson-Gilford progeria syndrome (HGPS), a sporadic, autosomal-dominant syndrome characterized by premature ageing, with sclerotic skin, joint contractures,micrognathia, alopecia, distal-joint abnormalities, growth impairment and vascular abnormalities (DeBusk, 1972; Gerber et al., 2008; Janin et al., 2017; Worman, 2012). Generally, death occurs at the age of 13 and is due to myocardial infarction or stroke (Gerber et al., 2008; Janin et al., 2017; Worman, 2012). The molecular mechanism behind HGPS is the occurrence of a *de novo* point mutation in exon 11 of the *LMNA* gene, which activates a cryptic splicing site, thus resulting in the production and accumulation of an abnormal lamin A, called progerin (De Sandre-Giovannoli et al., 2003; Eriksson et al., 2003; Janin et al., 2017).

Some laminopathies are also associated with mutations in *LMBN1* gene. For instance, Autosomal Dominant LeukoDystrophy (ADLD), a rare genetic disorder resulting in central nervous system (CNS) demyelination, is characterized by the duplication of *LMBN1* genic locus (Padiath et al., 2006), which leads to increased LMBN1 RNA levels and lamin B1 protein levels in patients (Schuster et al., 2011). Interestingly, high levels of lamin B1 are also found in patients affected by ataxia telangiectasia (AT), an autosomal recessive disorder -due to a mutation in the DNA Damage Response (DDR) protein ATM (ataxia telangiectasia mutated)(Janin et al., 2017; Shiloh & Ziv, 2013)-,characterized by cerebellar ataxia, telangiectasia, immune defects and predisposition to malignancy (Gatti & Perlman, 1993; Janin et al., 2017; Shiloh & Ziv, 2013).

Taking into account the LINC complex, mutations in *SUN* genes, by their own, are not disease relevant (Janin et al., 2017). Indeed, *SUN1* and *SUN2* are considered as "modifier-genes" (Meinke et al., 2014), whose mutations exacerbate pre-exisisting diseases, caused, for instance, by alterations in *LMNA* or *EMD* genes (Janin et al., 2017; Meinke et al., 2014; Taranum et al., 2012).

Mutations are also found in genes enconding nesprin proteins (Janin et al., 2017; Janin & Gache, 2018). For instance, in *SYNE1* gene, non-sense and intronic mutations, leading to translation premature termination, have been found to cause Autosomal Recessive Cerebellar Ataxia type 1 (ARCA1), also known as "recessive ataxia of Beauce" (Gros-Louis et al., 2007; Janin et al., 2017). This disorder presents diffuse pure cerebellar atrophy and dysarthria (Janin et al., 2017).

Mutations in *SYNE1* gene have also been associated to psychiatric disorders (Janin et al., 2017). Indeed recent genome-wide association studies (GWAS) identified a polymorphism within *SYNE1* gene as a risk factor for Bipolar Disorder (BD) (Green et al., 2013; Janin et al., 2017).

Mutations in *SYNE1* gene are also the cause of Arthrogryposis Multiplex Congenital (AMC), a group of non-progressive diseases displaying congenital joint contractures (Baumann et al., 2017; Janin et al., 2017).

Heterozygous missense mutations in *SYNE1* and *SYNE2* genes have been found in EDMD-like phenotypes, resulting in mislocalization of SUN 2 protein, emerin as well as altered nuclear morphology in fibroblasts from these patients (Qiuping Zhang et al., 2007).

Considering *SYNE3* gene, no diseases have been reported to be associated with its mutations (Cartwright & Karakesisoglou, 2014; Janin et al., 2017).

Lastly, mutations in *SYNE4* gene, leading to truncation of nesprin 4 protein, are associated to hearing loss with hereditary and progressive high frequence impairement (Cartwright & Karakesisoglou, 2014; Horn et al., 2013; Janin et al., 2017).

In the next figure, all the pathologies discussed above are summarized (Fig 52).

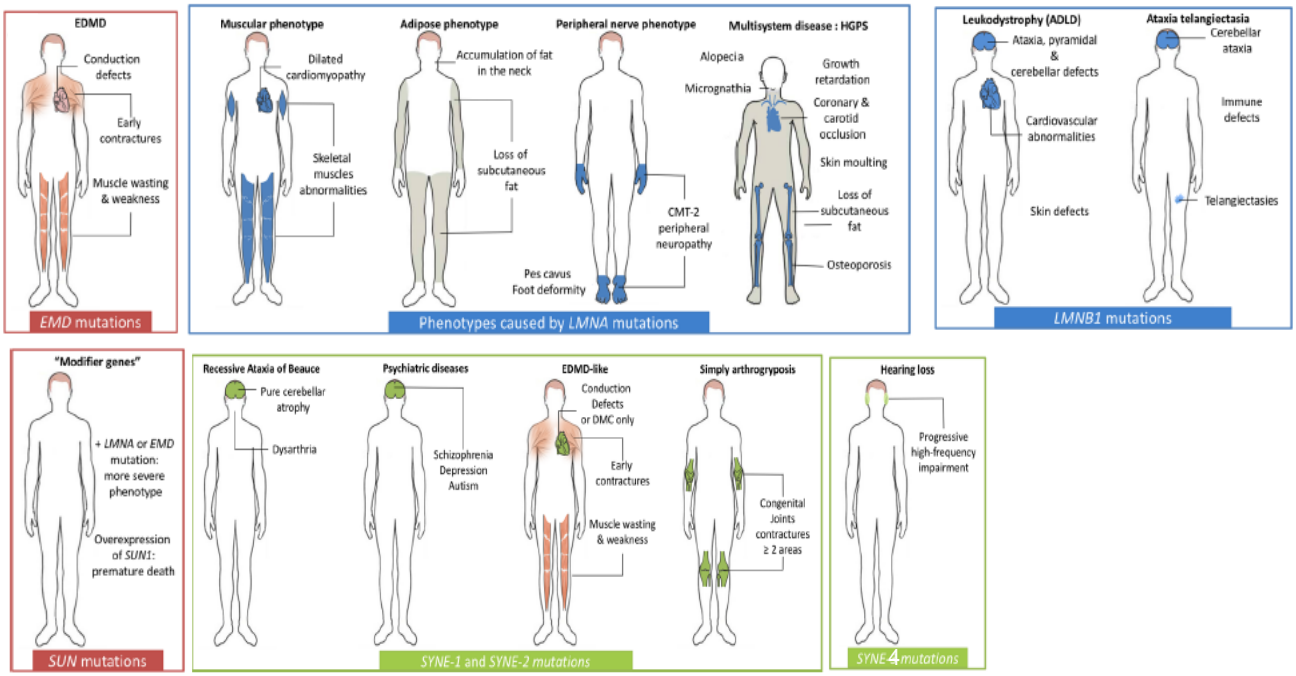

Fig 52: Envelopathies are rare genetic disorders involving multiple genes encoding nuclear envelope proteins.

Adapted from (Janin et al., 2017).

In summary

- The cell's nucleus is surrounded by a double lipid membrane called nuclear envelope (NE), which comprises the outer nuclear membrane (ONM) and the inner nuclear membrane (INM), separted by the perinuclear space (PNS).
- Nuclear pore complexes (NPCs) are embedded into NE and work as selective filter for molecules shuttling in and out the nucleus.
- Underneath the INM, a meshwork of proteins, nuclear lamins, forms the nuclear lamina.
- Nesprin proteins and SUN proteins, by interacting together in the PNS, form the LINC complex, which connects the lamins nucleoskeleton (via SUN proteins) with the cytoskeleton (via nesprin proteins).
- The LINC complex ensures mechanical coupling between nucleoskeleton and cytoskeleton.
- LINC complex perturbations can impact force transmission, cell signalling and gene transcription.
- The cell's nucleus can respond to mechanical cues by stretching, stiffening as well as increasing NPCs permeability.
- Mutations in NE components cause a plethora of diseases, collectively called envelopathies.

CHAPTER 3

Alpha- and beta- catenins: structure and functions

In this chapter, I will briefly cover the structure of α- and β- catenins as well as their involvement in cell signalling. I will also take into account those mutations in α- and β- catenins which lead to cancerous diseases.

Table of content

1 What are the catenins?

With the name of "catenins"(from the latin word *catena*, meaning "chain" (Valenta, Hausmann, & Basler, 2012)) one refers both to those proteins that bind the cytoplasmic domain of classical cadherins, (those cadherins present at the adherens junctions, such as the epithelial cadherins "E-cadherins"; see paragraph 3.2 in Chapter 1) and to those proteins that connect cadherins to the actin cytoskeleton. In this way, the formation of the cadherin-catenin complex is established (Fig 53) (Ishiyama et al., 2013; Masatoshi Takeichi, 2018).

Catenins are divided into 3 groups, represented by p120, β-catenin (β-cat) and α-catenin (α-cat) (Masatoshi Takeichi, 2018). Specifically, p120 and β-cat directly bind the cytoplasmic domain of cadherins (H Aberle et al., 1994; Daniel & Reynolds, 1995; Shibamoto et al., 1995), whose stability on the plasma membrane is thereby regulated (Ishiyama et al., 2010, 2013); whereas α-cat, which binds actin (Rimm, Koslov, Kebriaei, Cianci, & Morrow, 1995), interacts with β-cat (H Aberle et al., 1994) and, thus, as a monomer, links the cadherins to the actin cytoskeleton (Desai et al., 2013; Rimm et al., 1995) (Fig 53).

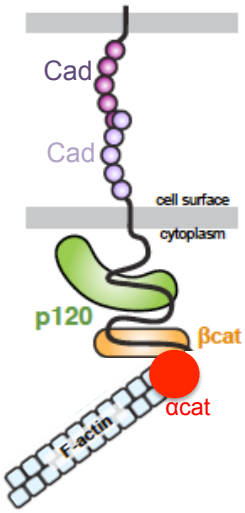

Fig 53: The cadherin-catenin complex, which connects the cadherins (Cad) with the actin cytoskeleton (F-actin). The black string represents the cytoplasmic domain of cadherin (namely "tail") with which p120 and β-cat interact. Adapted from (Ishiyama et al., 2013).

2 β-catenin's structure

β-catenin, known as the mammalian homolog of Armadillo in *Drosophila* (Mccrea, Turck, & Gumbiner, 1991), was first discovered in association with uvomorulin (i.e. Epithelial cadherin (E-cadherin)) in 1989 by Kemler group (Ozawa, Baribault, & Kemler, 1989).

Encoded by the *CTNNB1* gene in human (Nollet, Berx, Molemans, & van Roy, 1996), β-cat comprises a central region consisting of 12 imperfect Armadillo repeats (R1-R12) (referred to as ARM repeats) (Peifer, Berg, & Reynolds, 1994; Riggleman, Wieschaus, & Schedl, 1989)-each of them made of around 42 amino-acids-, flanked by the N-terminal and the C-terminal domains (NTD and CTD) (Valenta et al., 2012) (Fig 54). Between the last ARM repeat and the CTD, there lays a specific and conserved helix, named "Helix-C"(Fig 54), which packs on the C-terminal end of the ARM repeats domain (Xing et al., 2008). The ARM repeats domain can be seen as a rigid scaffold mediating the interaction with different β-cat binding partners (Fig 54), present at different subcellular locations (plasma membrane, cytosol and nucleus)(Huber, Nelson, & Weis, 1997; Valenta et al., 2012). It is important to stress that these molecular partners share overlapping binding sites and, therefore, cannot bind β-cat at the same time (Valenta et al., 2012).

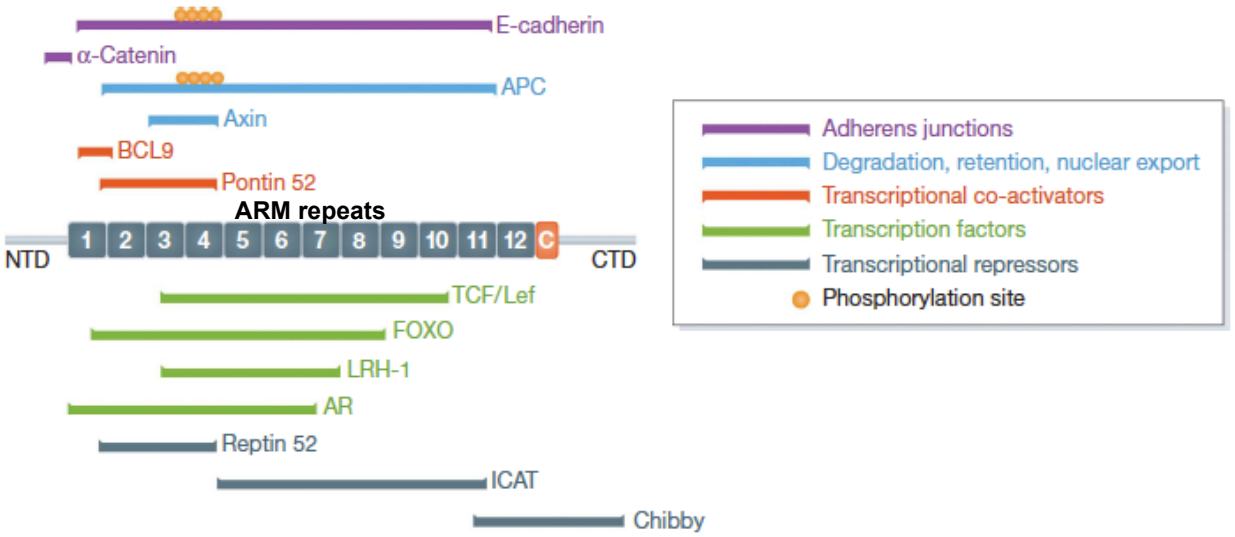

Fig 54: β-catenin's structure presents 12 ARM repeats (1-12) flanked by the N and the C terminal domains (NTD and CTD). Note that the ARM repeats domain mediate interaction with different β-cat binding partners. C: Helix C. APC: Adenomatous Polyposis Coli. TCF/Lef: T-cell factor/Lymphoid enhancement factor. AR: androgen receptor. LRH-1: liver receptor homologue-1. ICAT: inhibitor of β -catenin and TCF. BCL9: B-cell lymphoma-9. Adapted from (Valenta et al., 2012).

Besides its structural function in cell adhesion (Ozawa, Ringwald, & Kemler, 1990) (see paragraph 3.2 in Chapter 1), β-cat is also a transcription co-factor (Valenta et al., 2012) and has a central role in the Wnt signalling, as demonstrated in the 90s by Gumbiner team (Funayama, Fagotto, McCrea, & Gumbiner, 1995; P D McCrea, Brieher, & Gumbiner, 1993).

3 β-catenin's signalling activation

3.1 Activation through Wnt

β-cat can be activated in response to the Wnt pathway, which plays a major role in cell fate (Siegfried, Chou, & Perrimon, 1992) and development (McMahon & Moon, 1989; Noordermeer, Klingensmith, Perrimon, & Nusse, 1994) in different organisms (McMahon, 1992), as well as in cancer (Rubinfeld et al., 1993; L. K. Su, Vogelstein, & Kinzler, 1993).

Wnt signalling is based on the synthesis and secretion of Wnt proteins, ligands encoded by the *WNT* genes, which are 19 in most of the mammals (Clevers H & Nusse R, 2012). Wnt proteins, whose molecular weight is around 40 kDa, comprise many cysteins (Tanaka, Kitagawa, & Kadowaki, 2002) and are modified through the attachment of a palmitoleic acid chain to one of these cysteins (cysteine 77 in Wnt3a) (Large-scale et al., 2003). Palmitoylation is possible because of the presence on the ER (endoplasmic reticulum) of the Wnt ligand producing cells (Clevers H & Nusse R, 2012) of a dedicated multipass transmembrane O-acyltransferase, known as Porcupine (Porc) (K. Hofmann, 2000; Kadowaki, Wilder, Klingensmith, Zachary, & Perrimon, 1996) (Fig 55). Once palmitoylated, Wnt proteins leave the ER towards the Golgi, where they are bound by Eveness (Evi)/Wintless (Wls) (Bartscherer, Pelte, Ingelfinger, & Boutros, 2006; Clevers H & Nusse R, 2012) , a multipass transmembrane protein involved in Wnt ligands secretion (Bänziger et al., 2006; Bartscherer et al., 2006) (Fig 55). After Wnt proteins bind to Wls in a vescicle, the latter moves Wnt ligands towards the plasma membrane (Clevers H & Nusse R, 2012), thus resulting in Wnt exocytosis (Fig 55). After this event, Wls can be cycled back towards the Golgi in an intracellular trafficking complex called

"retromer" (Belenkaya et al., 2008; Clevers H & Nusse R, 2012; Franch-Marro et al., 2008; Haft et al., 2000) (Fig 55).

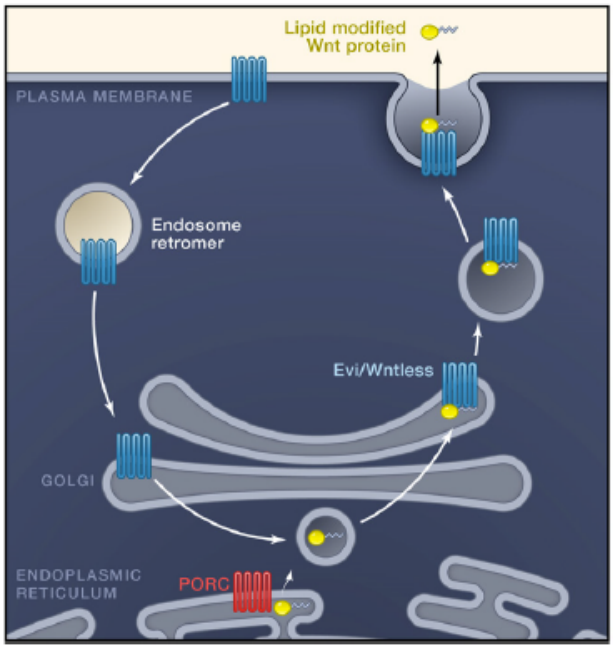

Fig 55: Secretion of palmitoylated Wnt protein. Eveness (Evi)/Wintless (Bartscherer et al., 2006), in a vescicle, determines Wnt ligand exocytosis and, after that, the transmembrane protein is cycled back, towards the Golgi, via the endosome retromer. Porc: porcupine. From (Clevers H & Nusse R, 2012).

On cell's surface, a heterodimeric receptor complex, comprising Frizzled and LRP5/6 proteins (Clevers H & Nusse R, 2012; Wiese, Nusse, & van Amerongen, 2018) (Fig 56A), responds to Wnt ligands. Frizzled is a seven-transmembrane (7TM) receptor protein -encoded, in mammals, by 10 different *Frizzled* genes (Koike et al., 1999; Y. K. Wang et al., 1997; Y Wang et al., 1996; Yanshu Wang, Chang, Rattner, & Nathans, 2016)- and with its cysteine-rich domains (CRD)(Bhanot et al., 1996),located at the N-terminus, binds Wnt proteins (Clevers H & Nusse R, 2012; Dann et al., 2001; Janda, Waghray, Levin, Thomas, & Garcia, 2012). LRP (low-density lipoprotein related receptor protein)(Angers & Moon, 2009) 5/6 are single pass transmembrane proteins which act as Frizzled co-receptors in vertebrates (X. He et al., 2000; Tortelote, Reis, de Almeida Mendes, & Abreu, 2017). Therefore, Frizzled and LRP5/6 are the binding platform for Wnt signalling (Clevers H & Nusse R, 2012).

In the cytoplasm, when there is no binding of Wnt to the Frizzled-LRP5/6 complex, cytosolic β-cat engages a protein complex, referred to as the "destruction complex", to be proteasome degraded (Clevers H & Nusse R, 2012; Shang, Hua, & Hu, 2017; Tortelote et al., 2017) (Fig 56A, "Wnt OFF"). The destruction complex comprises five proteins which are the tumour suppressor protein APC (Adenomatous Poliposis Coli), Dishevelled (Dvl), the scaffolding protein Axin and the serine-threonine kinases GSK3β (glycogen synthase kinase 3 β) and CK1 (Casein Kinase 1)(Clevers H & Nusse R, 2012; Duchartre, Kim, & Kahn, 2016; Shang et al., 2017; Tortelote et al., 2017) (Fig 56A, "Wnt OFF"). Specifically, Axin interacts with β-cat, APC, GSK3β, CK1 and Dvl- this latter binds Axin via an N-terminal DIX (Dishevelled Interaction with Axin) domain (Kishida et al., 2015)-; whereas APC interaction with β-cat is mediated by 15-20 amino-acids stretches interspersed within 3 Axin-binding motifs in APC (Clevers H & Nusse R, 2012; L. K. Su et al., 1993; Tortelote et al., 2017). In the destruction complex, GSK3β and CK1 phosphorylate β-cat, at its N-terminus, which is then targeted for

the proteasome degradation (Clevers H & Nusse R, 2012; Shang et al., 2017; Tortelote et al., 2017). Specifically, β-cat phosphorylation by CK1 at serine 45 is a priming site for the subsequent GSK3β-mediated phosphorylation events (Amit et al., 2002) at threonine 41, serine 37 and, lastly, serine 33 (Hagen, Daniel, Culbert, & Reith, 2002) (Fig 56B). These phosphorylations generate the binding site for the β-TrCP (β-transducin repeat containing protein), an E3 ubiquitin ligase that mediates β-cat poly-ubiquitination with subsequent β-cat proteasome degradation (Hermann Aberle, Bauer, Stappert, Kispert, & Kemler, 1997; Marikawa & Elinson, 1998; Tortelote et al., 2017) (Fig 56A, "Wnt OFF"), thus preventing β-cat from undergoing nuclear translocation and activating gene transcription (Clevers H & Nusse R, 2012) (Fig 56C, "Wnt OFF"). In this case, gene transcription is blocked because of the interaction of the DNA-bound TCF/LEF (T-cell factor/lymphoid enhancement factor) transcription factors (Behrens et al., 1996; Molenaar et al., 1996) with Groucho transcriptional co-repressor (Cavallo et al., 1998; Roose et al., 1998) (Fig 56C, "Wnt OFF").

Upon Wnt ligand binding to the Frizzled- LRP5/6 heterodimeric receptor complex, a conformational change in this latter mediates the consequent phosphorylation of the cytoplasmic tail of the LRP5/6 co-receptors (Tamai et al., 2004), which results in the recruitment of Axin to LRP5/6 (Mao et al., 2001) (Fig 56A, "Wnt ON"). Frizzled, instead, facilitates the interaction between Axin and LRP5/6 by interacting, via its cytoplasmic domain, with Dishevelled (Rothbächer et al., 2000) (Fig 56A, "Wnt ON"). This event determines the disaggregation of the destruction complex: β-cat is no more phosphorylated and no more proteasome degraded, which makes it stable (G. Wu, Huang, Abreu, & He, 2009) and free to undergo nuclear translocation, upon its cytoplasmic accumulation (Clevers H & Nusse R, 2012; Shang et al., 2017; Tortelote et al., 2017) (Fig 56A, "Wnt ON"). Once in the nucleus, β-cat displaces Grouch from TCF/LEF, thus activating the transcription of Wnt target genes (Fig 56C, "Wnt ON"), such as *c-Myc*, *CyclinD1* (for cell cycle regulation)(Shang et al., 2017) and *Axin2* genes, the latter being considered as a general indicator of Wnt pathway activity (Lustig et al., 2002). Once in complex with TCF/LEF, β-cat can also interact with other molecular partners, such as Bcl9/Legless - which bridges the other molecular component Pygopus to β-cat (Kramps et al., 2002)- and the histone modifiers CBP,Brg-1 (Städeli, Hoffmans, & Basler, 2006) and Parafibromin/Hyrax, homologs of yeast Cdc73 (Mosimann, Hausmann, & Basler, 2006)(Fig 56C, "Wnt ON").

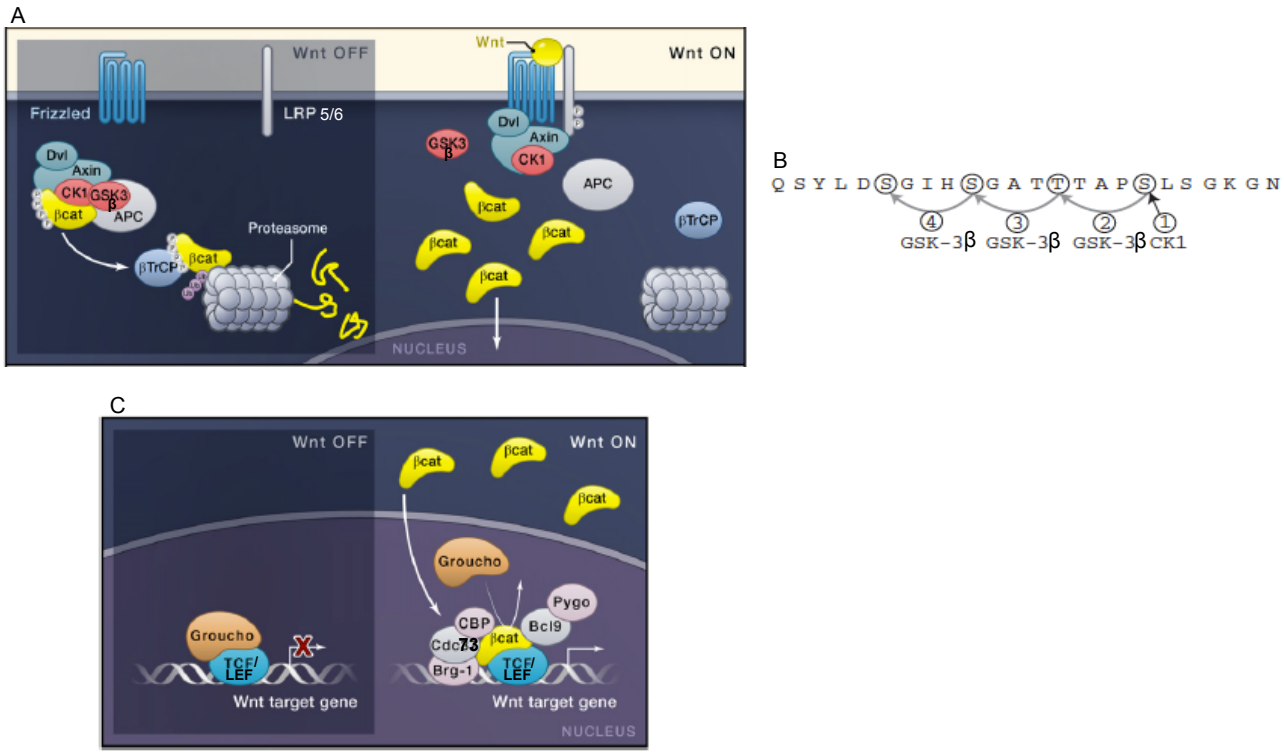

Fig 56: β-cat regulation in absence/presence of the Wnt ligand. A: In absence of Wnt protein (Wnt OFF), β-cat is retained in the cytoplasmic destruction complex, where it is phosphorylated (by CK1 and GSK3 β) and tagged by poly-ubiquitination for proteasome degradation. When Wnt ligand is present (WNT ON), its binding to the Frizzled-LRP5/6 heterodimeric receptor complex determines the disaggregation of the destruction complex, with the cytoplasmic accumulation of not phosphorylated, stable β-cat, which can undergo nuclear shuttling. B: amino-acidic sequence showing the phosphorylation sites (circled in chronological order of phosphorylation, from 1 to 4) in β-cat to prime it for poly-ubiquitination. C: in absence of Wnt signal (Wnt OFF), TCF/LEF transcription factors are bound by the co-repressor Groucho, which results in no transcription of Wnt targent genes. In the presence of Wnt ligand (Wnt ON), β-cat displaces Groucho and binds TCF/LEF, thus activating Wnt target genes transcription. Once associated to TCF/LEF, β-cat can interact with other molecular partners, such as Bcl9, Pygopus (Pygo), Brg1, CBP and CdC 73, the yeast homolog of Parafibromin/Hyrax. APC: Adenomatous Poliposis Coli. β-TrCP: β-transducin repeat containing protein. CK1: casein kinase 1. GSK3 β: glycogen synthase kinase 3 β. Dvl: Dishevelled. LEF: lymphoid enhancement factor. LRP5/6: low-density lipoprotein related receptor protein 5/6. TCF: T-cell factor. Adapted: A and C from (Clevers H & Nusse R, 2012); B from (Stamos & Weis, 2013).

3.2 Mechanical activation

Mechanical cues can induce β-cat nuclear translocation. An example of that it is the already discussed Farge's work (see paragraph 1 in Chapter 1), where it was demonstrated that the nuclear accumulation of the *Drosophila* homolog of β-cat, namely Armadillo, follows mechanical constraint, in fruit fly embryos. This resulted in the induction of the development-associated *Twist* gene (Farge, 2003).

Mechanical induction of β-cat has also been demonstrated to counteract adipogenesis (Sen et al., 2008). Indeed, Rubin's team showed that 2% uniform biaxial strain application on mouse C3H10T1/2 MSCs (mesenchymal stem cells) cultured in highly adipogenic medium blocked the accumulation of cytoplasmic triglyceride droplets (in comparison to control, unstrained cells) and this event was associated to an increase of active (hypophosphorylated) β-cat into cells' nuclei (Sen et al., 2008) (Fig 57).

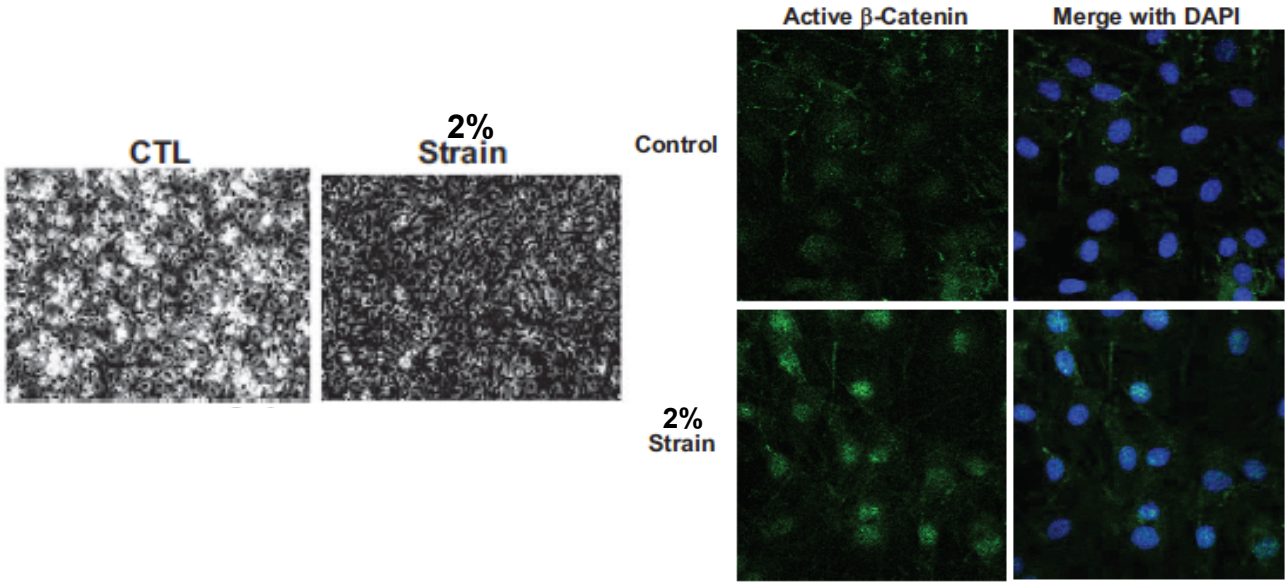

Fig 57: Application of mechanical strain blocks adipogenesis differentiation (accumulation of white cytoplasmic lipid droplets) in mouse C3H10T1/2 MSCs in comparison to unstrained control cells (left), with nuclear accumulation of active (hypophosphorylated) nuclear β-cat (right). DAPI was used to counterstain nuclei in the immunofluorescence assay (right). Adapted from (Sen et al., 2008).

Increased levels of nuclear β-cat can be also obtained by applying fluid shear stress (FSS). Indeed, Norvell et al. showed that the application for 1 hour of 10-dynes/cm^2 laminar FSS on mouse MC3T3-E1 osteoblasts resulted in high levels of nuclear β-cat in comparison to the same cells, but subjected to 1 hour of static conditions (Fig 58 A and B). Moreover, the application of the same type, as above, of FSS onto UMR 106.01 rat osteosarcoma cells increased the TCF luciferase reporter gene activity (which measures the β-cat-dependent gene transcription activity), compared to the same cells but in static conditions (Norvell, Alvarez, Bidwell, & Pavalko, 2004) (Fig 58 C).

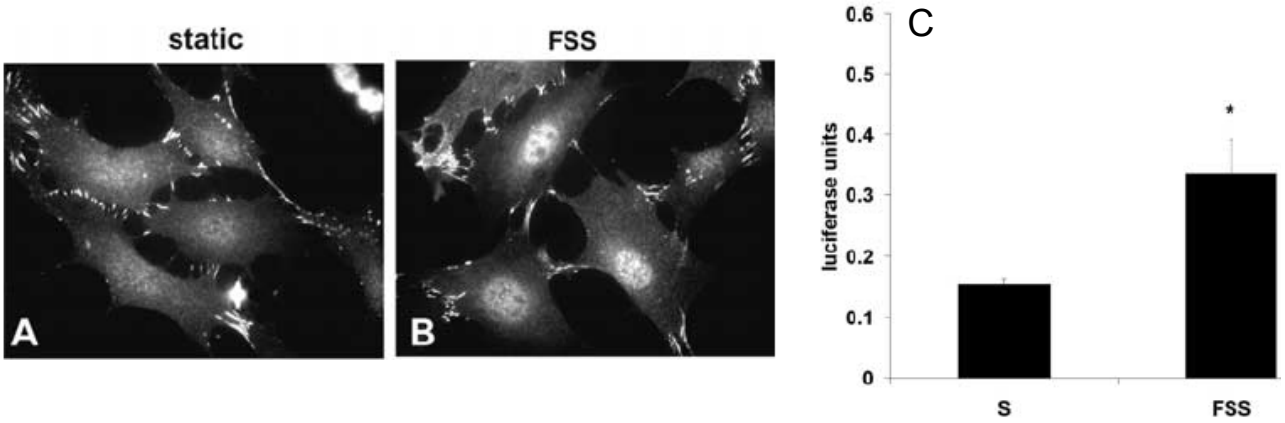

Fig 58: β-cat level (immunodetection) in nuclei is increased in mouse MC3T3-E1 osteoblasts after 1 hour of 10-dynes/cm^2 laminar FSS (B), compared to the same cells but in static conditions (1 hour) (A). Application of the same FSS onto UMR 106.01 rat osteosarcoma cells determines an increased activity of the TCF luciferase reporter gene, which corresponds to an increased β-cat transcriptional activity compared to the same cells in static (s) conditions (C). *$p<0.05$. Adapted from (Norvell et al., 2004).

β-cat nuclear translocation can be also induced by the application of low intensity vibration (LIV), which means applying low strain at high frequency (Sen et al., 2011). To this regard, Uzer et al. demonstrated that after the application of 20 minutes of LIV (0.7g, 90Hz) onto mouse marrow-derived MSCs, β-cat enriched the nuclear fraction of LIV stimulated cells compared to not stimulated cells. In

addition, LIV application resulted in an increased mRNA level of Axin-2, which is positively regulated by β-cat (Uzer et al., 2018) (Fig 59).

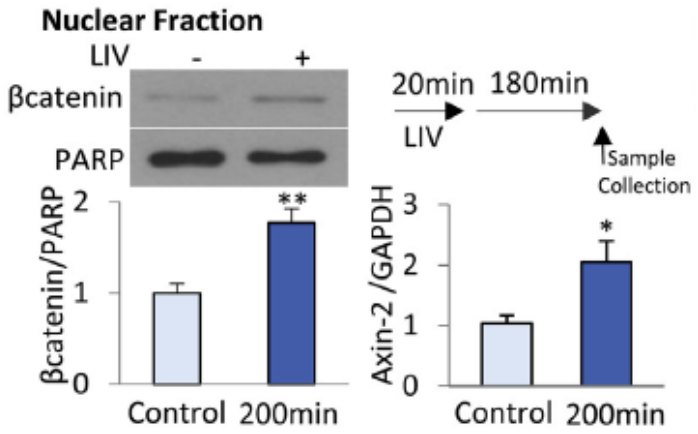

Fig 59: 20 min LIV application onto mouse marrow-derived MSCs resulted in increased β-cat in cells' nuclear fraction, with a concomitant increase of Axin-2 mRNA level. PARP (poly ADP-ribose polymerase) was used as loading control in western blotting, whereas GAPDH (glyceraldehyde 3-phosphate dehydrogenase) was used to normalize Axin-2 mRNA level in qPCR. * $p<0.05$; ** $p<0.01$. From (Uzer et al., 2018).

Mechanical induction of β-cat has also been demonstrated to happen in mammalian epithelial cells, as shown by Nelson group. Indeed, Benham-Pyle et al. demonstrated that when a biaxial stretching of 15% strain is applied onto a dense monolayer of epithelial cells (MDCKs type IIG), β-cat, normally associated with the Epithelial cadherin (E-cad),-accumulates into the nucleus and activates gene transcription (Benham-Pyle, Pruitt, & Nelson, 2015) (Fig 60).

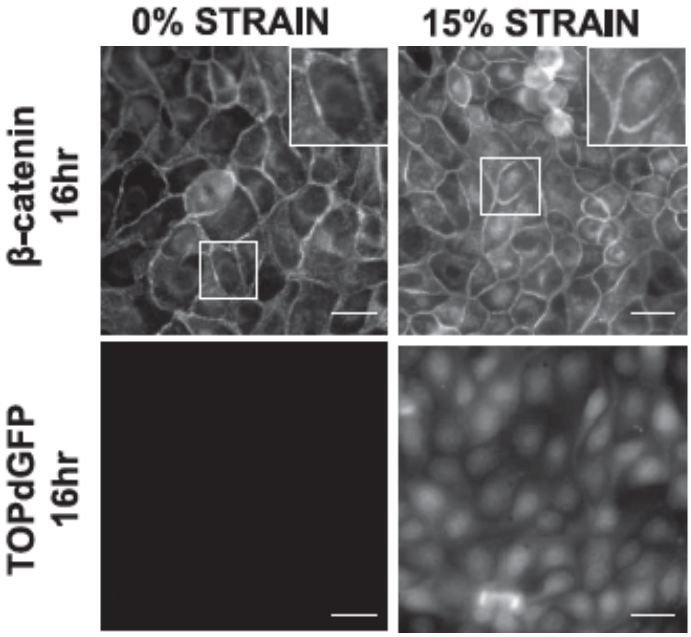

Fig 60: After 16 hours of biaxial 15% strain applied onto MDCK cells monolayers, β-cat (immunodetected) translocates into cells' nuclei (15 % strain image and inset) with concomitant activation of gene transcription (measured with TOPdGFP). Scale bars: 25 μm. Adapted from (Benham-Pyle et al., 2015).

Very recently, the former PhD student in my laboratory, Charlène Gayrard, has shown that the promotion of partial (via wound healing (WH) assay) as well as complete (through hepatocyte growth factor (HGF) stimulation) epithelial-mesenchymal transition (EMT) in MDCK type IIG cells determines E-cad tension relaxation with concomitant β-cat nuclear translocation and activity (Gayrard et al.,

2018)(Fig 61). Specifically, upon wounding of a monolayer of MDCK cells stably expressing the FRET biosensor TSMod (Grashoff, Hoffman, Brenner, Zhou, Parsons, Yang, McLean, Sligar, Chen, Ha, & Schwartz, 2010) inserted into the E-cad protein (N. Borghi et al., 2012) (see section 3.2 "Adherens junctions" in Chapter 1), Charlène demonstrated that cells at the front of the wound (leaders) exhibited a decreased tension in E-cad (high FRET index), compared to cells at the back which displayed, on the contrary, an increased tension in E-cad (low FRET index) (Fig 61A). Decreased tension in E-cad correlated with β-cat nuclear translocation (Fig 61B) as well as β-cat dependent gene transcription activation (Fig 61C), both at the front of the wounded sheet of MDCK cells (leaders). Moreover, induction of total EMT through treatment of MDCK cell colonies with HGF (+HGF), resulted, again, in decreased tension in E-cad (high FRET index change) with β-cat nuclear translocation, compared to untreated colonies (-HGF), where E-cad tension was higher (low FRET index change) and β-cat did not translocate into cell's nuclei Fig (61 D and E).

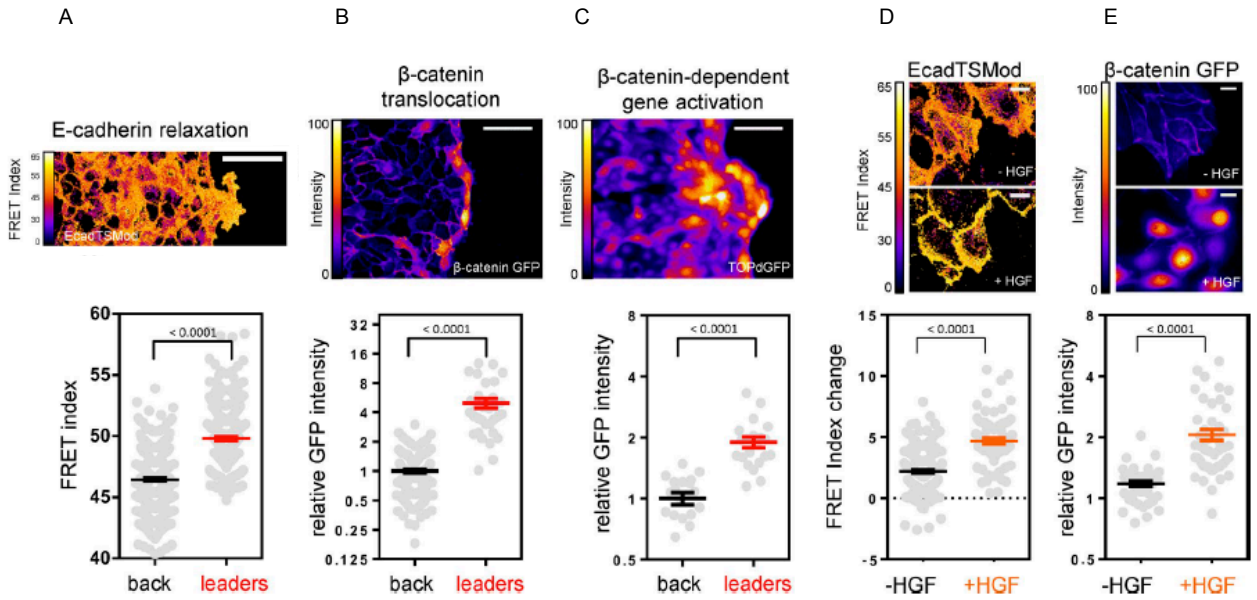

Fig 61: E-cad tension relaxation promoted by partial (A, B and C) or total (D and E) EMT correlates with nuclear β-cat translocation (measured with β-cat-GFP fusion protein) and β-cat-dependent gene transcription activation (measured with TOPdGFP (Dorsky, Sheldahl, & Moon, 2002)). Note that in B and C GFP intensity for leader cells is presented as relative to the cells at the back of the wound. In E, for both –/+HGF conditions, GFP intensity is presented as the ratio nucleus/cytoplasm. HGF: hepatocyte growth factor. Scale bars: A, B and C: 100 µm; D and E: 20 µm. Adapted from (Gayrard et al., 2018).

In addition, the pool of β-cat undergoing nuclear translocation comes from cell membrane, as shown by Charlène with a phoconversion assay. Indeed, by using a β-cat fused with the photoconvertible protein mMaple (McEvoy et al., 2012), Charlène demonstreated that, in HGF treated MDCK cells, photoconverted cell-cell contact β-cat-mMaple translocated into the nucleus (Fig 62A) with higher nuclear concentration than in unstimulated cells (Fig 62B).

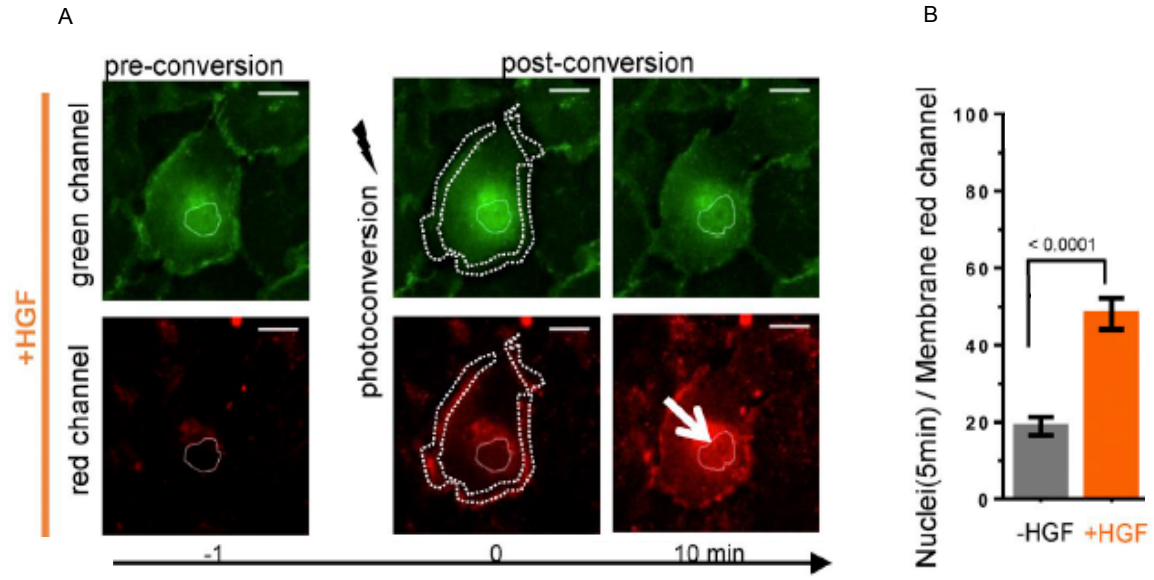

Fig 62: Membrane-bound β-cat translocates into the nucleus upon HGF treatment. A: photoconvertible β-cat-mMaple residing at the plasma membrane (dotted line, time 0) of HGF treated (50ng/mL, 4 hours) MDCK cells translocates from cell-cell contacts towards the nucleus within 10 minutes after photoconversion (see arrow). B: HGF treatment (50 ng/mL, 4 hours) in MDCK cells significantly increases Nucleus/Membrane ratio of the photoconvertible β-cat-mMaple, already 5 minutes after photoconversion, Scale bars: 20 µm. Adapted from (Gayrard et al., 2018).

Furtherhmore, nuclear localization of photoconverted β-cat-mMaple fusion protein was also spotted in leader cells in WH assay (Fig 63).

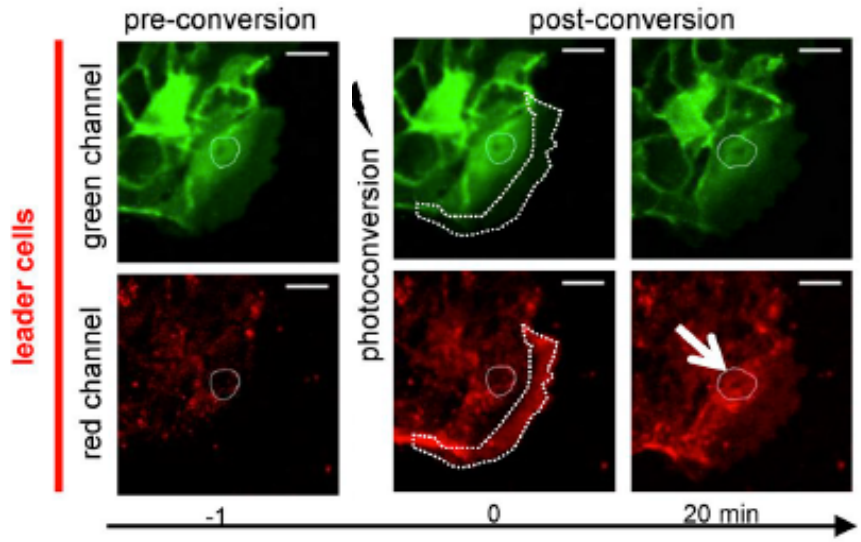

Fig 63: Membrane-bound β-cat translocates into the nucleus of leader cells in wound healing assay. Photoconvertible β-cat-mMaple residing at the plasma membrane of the lamellipodium (dotted line, time 0) in a leader cell translocates into the nucleus within 20 minutes after photoconversion (see arrow). Scale bars: 20 µm. Adapted from (Gayrard et al., 2018).

Thus, Charlène concluded that, upon EMT promotion, it is the membrane-bound β-cat to accumulate into cells'nuclei. In addition, β-cat is released from plasma membrane concomitantly with E-cadherin tension relaxation (Gayrard et al., 2018).

Mechanical cues and Wnt ligands can also synergize to activate β-cat. To this regard, Nelson group recently demonstrated that, when biaxial stretching with a strain of 15% was applied, super-confluent monolayers of MDKC type IIG cells, expressing TOPdGFP β-cat activity reporter (Dorsky et al., 2002) and grown in Wnt3a-conditioned medium, displayed an increased number of cells positive for the reporter compared to the same stretched monolayers but grown in absence of Wnt3a (Fig 64A). This increased β-cat activity correlated with an increased number of cells undergoing progression from G1 into S/G2 cell cycle phases, following a biaxial stretch of ≈8.5% strain applied to super-confluent monolayers of MDCK cells, grown in the same Wnt3a-conditioned medium as above and expressing FUCCI cell cycle reporter (Sakaue-Sawano et al., 2008) (Fig 64B). In the end, the researchers concluded that the combination of both mechanical strain plus Wnt3a induced higher levels of β-cat signalling which let cells go through the cell cycle. (Benham-Pyle, Sim, Hart, Pruitt, & Nelson, 2016).

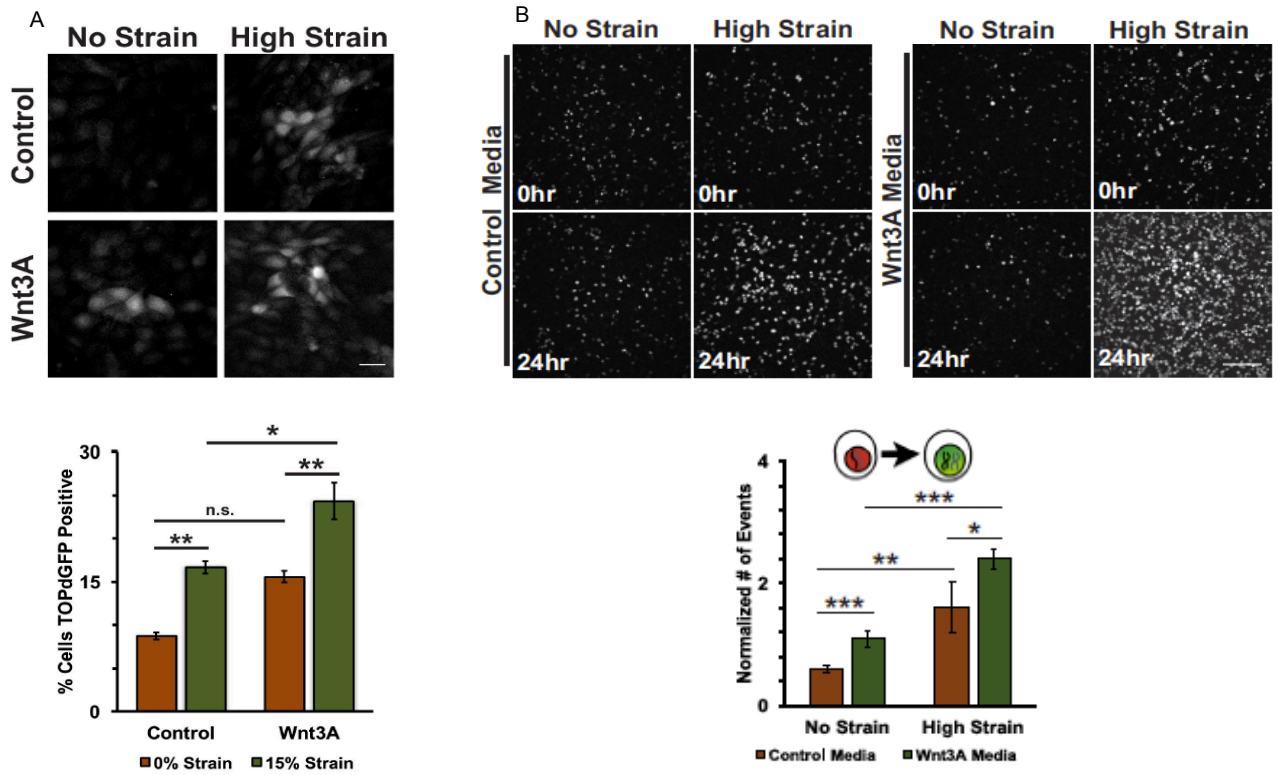

Fig 64: Mechanical cues and Wnt3a synergize to activate β-cat and promote cell cycle progression. A: super-confluent monolayers of MDCK cells, expressing TOPdGFP β-cat activity reporter and grown in Wnt3a-conditioned medium (Wnt3A) or control medium (Control), with or without application of strain (high strain=15% strain for 8 hours). Note that the application of strain determined a higher number of TOPdGFP positive cells in monolayers grown in presence of Wnt3a, compared to the same strained monolayers but grown in control medium (live cell imaging above and quantification below). B: super-confluent monolayers of MDCK cells, expressing FUCCI cell cycle reporter and grown in Wnt3a-conditioned medium or control medium as in A, with or without strain application for 24hours (high strain: ≈8.5% strain). Note that monolayers grown in Wnt3a conditioned-medium and subjected to strain displayed a greater number of cells progressing from G1 into S/G2cell cycle phases, compared to the same monolayers only grown in the presence of Wnt3a or only subjected to strain (live cell imaging above and quantification below). Scale bar in B: 150μm. n.s: not statistically significant. *p<0.05; **p<0.01; ***p<0.001. Adapted from: (Benham-Pyle et al., 2016).

β-catenin signalling activation is therefore highly and differentially regulated and involves Wnt ligands, mechanical cues as well as a combination of both.

As previously pointed out, β-cat at the cadherin-catenin complex has a structural role that permits a connection between the cadherins, residing on the plasma membrane, and the actin cytoskeleton. Specifically, this connection in mediated by α-cat (Desai et al., 2013; Rimm et al., 1995), that is the topic of the next paragraph.

4 α-catenin's structure

In mammals, three distinct α-catenins exist, encoded by three different genes: *CNNT1*, which codes for the epithelial α-cat (referred to as E α-cat) that is ubiquitously expressed and not only restricted to the epithelia; *CNNT2*, coding for the neural α-cat (N- α-cat), which is largely restricted to brain; and *CNNT3*, encoding testis α-cat (T α-cat), particularly present in the testis but also expressed in the brain, the spinal cord and the peripheral nerve (Chiarella, Rabin, Ostilla, Flozak, & Gottardi, 2018; Hirano, Kimoto, Shimoyama, Hirohashi, & Takeichi, 1992; Janssens et al., 2001; Nagafuchi & Takeichi, 1989).

Although the three α-catenins share high levels of amino acid identity/similarity (Janssens et al., 2001), my focus will be on E α-cat, which, because of its ubiquitous expression in mammalian cells (Chiarella et al., 2018),has been used in my PhD project. Hereafter, with "α-cat" I will refer to E α-cat.

α-cat's structure comprises an N-terminal (N) domain, a modulatory (M) domain and a C-terminal (C) domain, each of which having distinct roles (Ishiyama et al., 2013) (Fig 65). Specifically, the N-terminal domain is involved in β-cat binding and α-cat homodimerization (H Aberle et al., 1994; Koslov, Maupin, Pradhan, Morrow, & Rimm, 1997); the M-domain serves for interactions with several actin-binding proteins, such as vinculin (Watabe-Uchida et al., 1998); and the C-terminal domain determines α-cat interaction with F-actin (Rimm et al., 1995) (Fig 65).

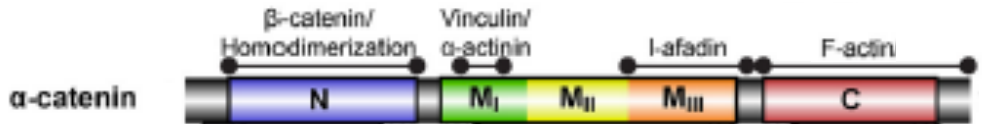

Fig 65: α-cat's structure. Note that the modulatory (M) domain (divided into M_I,M_{II} and M_{III}), besides vinculin, also interacts with α-actinin and afadin, two actin binding proteins (Mandai et al., 1997; Maruyama & Ebashi, 1965).See text for detail. N:N-terminal domain. C: C-terminal domain. Adapted from (Ishiyama et al., 2013).

5 α-catenin regulates β-cat signalling

Besides its structural role at the cadherin-catenin complex (Desai et al., 2013; Yonemura, Wada, Watanabe, Nagafuchi, & Shibata, 2010), α-cat has been demonstrated to be implied in β-cat signalling. Indeed, α-cat was shown to colocalize with β-cat in the nuclei of human colon cancer cell line SW480 (A L Giannini, Vivanco, & Kypta, 2000) (Fig 66, left). Moreover, Gottardi laboratory demonstrated that this colocalization was abolished in SW480 β-cat depleted cells, where α-cat was found redistributed to the cytoplasm (Rebecca L Daugherty et al., 2014) (Fig 66, right).

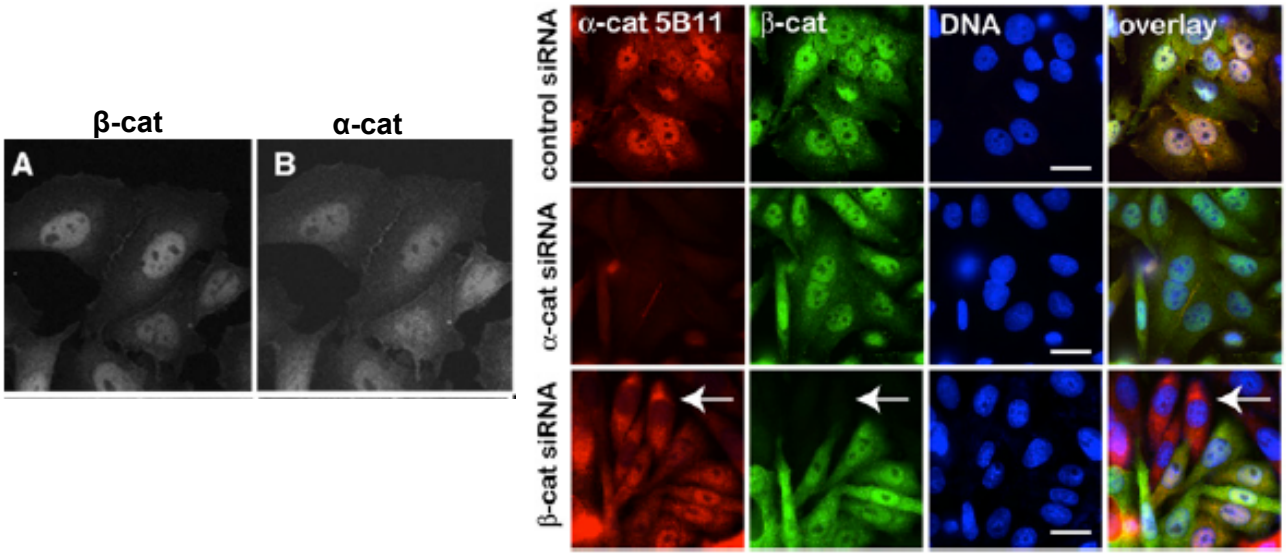

FIG 66: α-cat colocalization with β-cat in SW480 cells' nuclei (immunostaining, left) is lost upon β-cat depletion (see arrow in β-cat immunostaining panel, right), with consequent α-cat redistribution to the cytoplasm (see arrow in α-cat immunostaining panel, right). Note that, in the right panel, the "5B11" is the antibody used to stain α-cat. DNA is counterstained with Hoechst 33342. Scale bars: 10 μm. The immunostaing shown on the left is adapted from (A L Giannini et al., 2000), whereas the one on the right is from (Rebecca L Daugherty et al., 2014).

Gottardi team also showed that a stable knockdown of α-cat in SW480 cells upregulated some established Wnt target genes (Fig 67A). Increased mRNA levels of *Axin2*, *NKD1* and *LEF1* genes, considered more selective to Wnt activation (that is directly activated by Wnt pathway), were also found in normal (non cancerous) human skin fibroblasts, transiently depleted for α-cat and activated with recombinant Wnt3a (Roelink & Nusse, 1991) (Fig 67B). Moreover, α-cat transient depletion with siRNA in SW480 cells determined an overall increase of RNA synthesis, in vivo (Rebecca L Daugherty et al., 2014) (Fig 67C).

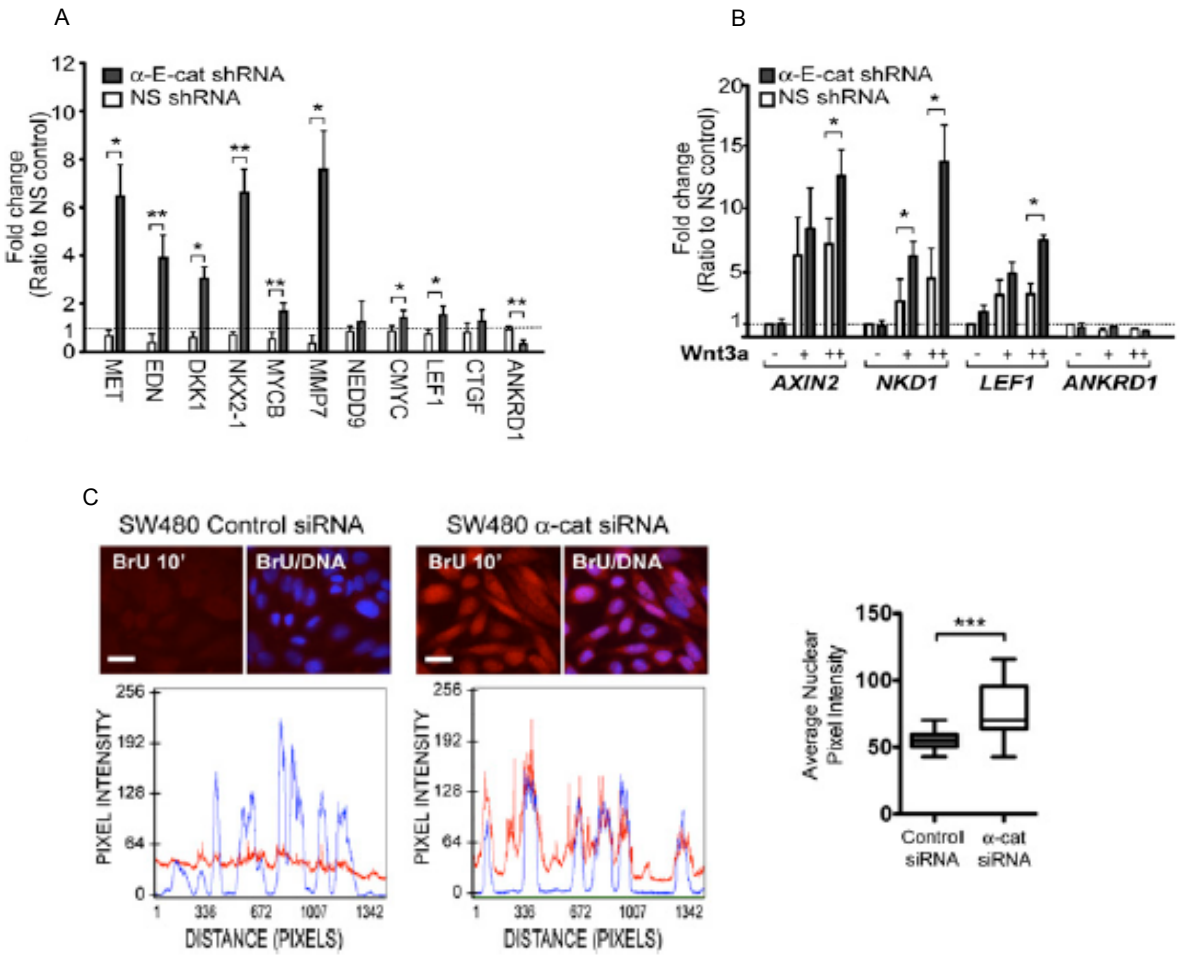

Fig 67: α-cat depletion (via short hairpin (sh) or small interfering (si) RNA) upregulates Wnt target gene expression and induces an overall increase of RNA synthesis, in vivo. A: qRT-PCR carried out on SW480 cells stably knockdowned for α-cat (α-E-cat shRNA; E: epithelial) shows the upregulation of some established Wnt target genes, compared to the mock control (NS shRNA; NS: nonspecific). B: induction of α-cat transiently depleted (α-E-cat shRNA) normal human skin fibroblasts with Wnt3a (+,++: 50, 100 ng/mL) results in the increased transcription (measured via qRT-PCR) of genes more selective to Wnt stimulation. C: transient α-cat depletion (α-cat siRNA) increased in vivo RNA synthesis (visualized after 10 minutes incubation with 2mM Bromouridine (BrU)) in SW480 cells compared to mock control (control siRNA). DNA is counterstained with Hoechst 33342. Scale bars: 10 μm *p<0.05; ** p<0.01;***p<0.001. Adapted from (Rebecca L Daugherty et al., 2014).

It is thus clear that α -and β-catenins colocalize in the nucleus, with α-cat involved in the regulation of both Wnt target gene expression and global RNA synthesis. But how mechanistically could α-cat regulate β-cat signalling? It has been proposed that α-cat, by binding the destruction complex via APC, could promote β-cat proteasome-dependent degradation in the cytoplasm (Choi, Estarás, Moresco, Yates, & Jones, 2013) (Fig 68**a**).In another way, α-cat could also block β-cat activity in the nucleus. In this case, α-cat could destabilize TCF/LEF-bound β-cat, as being part of a histone H3 Lys4 demethylase transcriptional repressor complex, made of APC, C-terminal binding protein (CtBP), CoREST and Lys-(lysine)specific demethylase 1 (LSD1). As such, α-cat could mediate gene transcription repression (Choi et al., 2013) (Fig 68**b**). To this regard, it has also been proposed that α-cat could repress β-cat dependent gene transcription by sequestering nuclear monomeric G (globular)-actin and promoting its polymerization into F-actin. Indeed, it has been demonstrated that nuclear α-cat causes the formation of nuclear actin filaments (NAFs), thus inhibiting RNA synthesis (Rebecca L Daugherty et al., 2014). Therefore, since monomeric actin is incorporated into RNA

polymerase II as well as into chromatin remodelling complexes (W. A. Hofmann et al., 2004; Kukalev, Nord, Palmberg, Bergman, & Percipalle, 2005; Zhao et al., 1998), the resulting actin depletion from the transcriptional machinery could repress β-cat dependent gene expression (Rebecca L Daugherty et al., 2014) (Fig 68**c**).

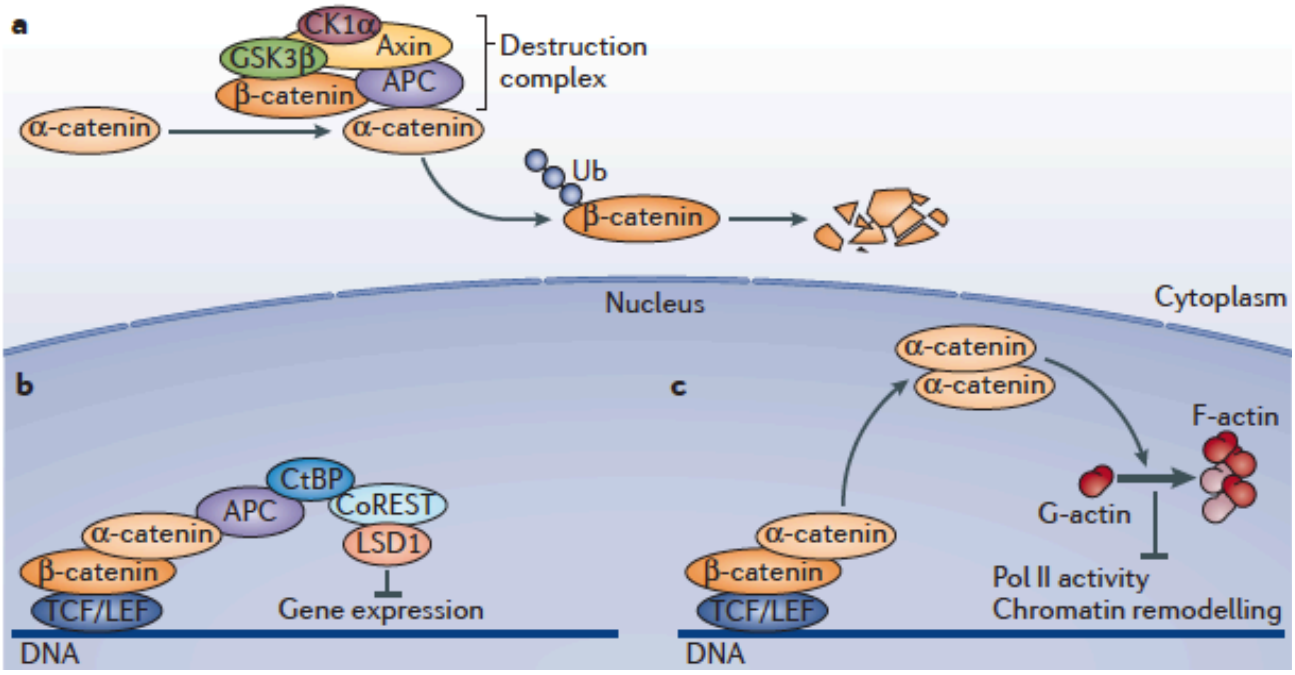

Fig 68: α-cat could regulate β-cat signalling: by promoting cytoplasmic β-cat degradation via destruction complex interaction (**a**); by destabilizing TCF/LEF-bound β-cat through the histone H3 Lys4 demethylase transcriptional repressor complex (APC+CtBP+CoREST+LSD1), which could lead to gene expression repression (**b**) or by sequestering monomeric G (globular)-actin from the transcriptional machinery (Poll II + chromatin remodelling factors), thus likely resulting in gene expression repression as well (**c**). APC: Adenomatous Poliposis Coli. CK1α: casein kinase 1α. GSK3β: glycogen synthase kinase 3β. LEF: lymphoid enhancement factor. TCF: T-cell factor. From: (Pierre D. McCrea & Gottardi, 2016).

Besides binding β-cat, α-cat has also been shown to bind nesprin 2, as demonstrated by Karakesisoglou group (Neumann et al., 2010) (Fig 69A and B). Moreover, the authors suggested that, since β-cat is bound by emerin (Markiewicz et al., 2006) which, in turn, is associated with nesprin 2 (Wheeler et al., 2007), a quaternary complex made of α-cat- β-cat-emerin-nesprin 2 and residing on the nuclear envelope may form, in conditions when Wnt pathway is active (Fig 69C). In this case, the complex would facilitate β-cat nuclear translocation, which is impaired when the complex is disrupted due to loss of nesprin 2 (Fig 69D).

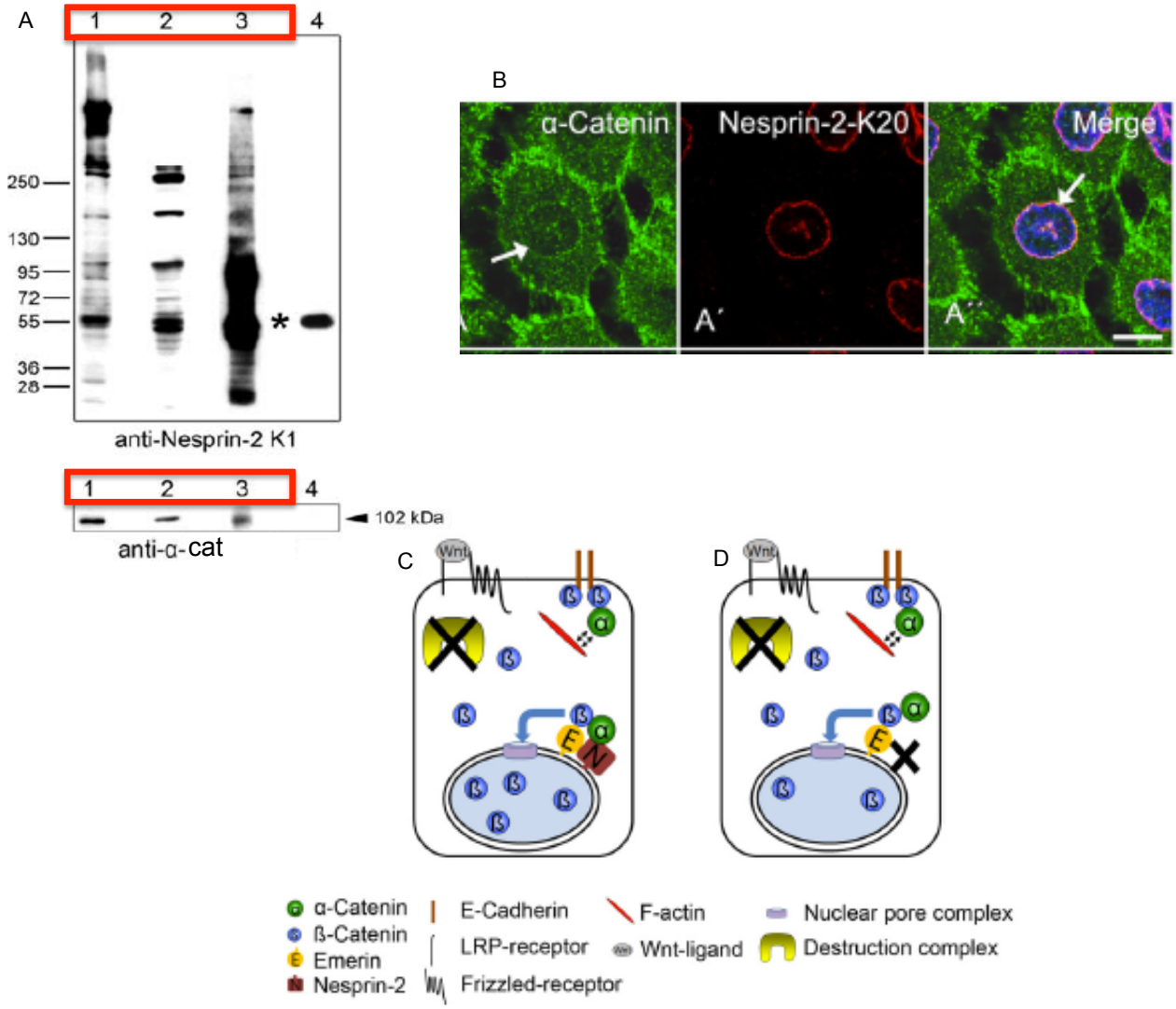

Fig 69: α-cat interacts with nesprin 2. A: lysates from HaCaT cells were subjected to co-immunoprecipitation with a nesprin 2 antibody (K1) and then immunoblotted both for nesprin 2 and α-cat. Note that the nesprin 2 antibody recognizes different isoforms of nesprin. Red boxes to indicate the lysates with the co-immunoprecipitated α-cat. B: primary human keratinocytes immunostained for α-cat and nesprin 2 (K20 antibody) present α-cat colocalizing with nesprin 2 at the nuclear envelope (see arrows and merge image). C: upon Wnt ligand binding, the formation, at the nuclear envelope, of a quaternary complex made of α-cat- β-cat-emerin-nesprin2 would facilitate β-cat nuclear translocation. D: when Wnt pathway is activated but nesprin 2 is lost, the quaternary complex would be disrupted thus resulting in impaired β-cat nuclear translocation. LRP:low-density lipoprotein related receptor protein. Scale bar: 10 μm. Adapted from (Neumann et al., 2010).

α-cat acts as a regulator of β-cat by likely promoting its cytoplasmic degradation (Choi et al., 2013) or by repressing β-cat dependent gene transcription (Choi et al., 2013; Rebecca L Daugherty et al., 2014). Moreover, the formation of an α-cat–β-cat–emerin–nesprin2 quaternary complex at the nuclear envelope could be important for β-cat nuclear translocation when Wnt signalling is active (Neumann et al., 2010). It is thus conceivable that mutations impairing β- and α-catenins functions/signalling could lead to cellular dysfunctions, therefore resulting in diseases such as cancer. That is the topic I will briefly explore in the next paragraph.

6 Cancerous diseases associated to impaired functions/signalling in β- and α-catenins

6.1 β-catenin

Mutations in genes leading to constitutive activation of the Wnt pathway are indicated as early events promoting the development of some cancers in human (Gao et al., 2018). Additionally, high β-cat activity levels are important for tumour initiation (Gao et al., 2018). Mutations (frequently missense) in β-cat encoding gene *CTNNB1* have been found occurring at the exon 3 (Machin et al., 2002). This exon codes for those serine-threonine sites recognized and phosphorylated by GSK3β, thus regulating β-cat degradation(Hermann Aberle et al., 1997; Hagen et al., 2002). First cases of *CTNNB1* mutations and impaired regulation of the Wnt pathway were reported in colorectal cancer (Rubinfeld et al., 1993; Zhenghe Wang, Vogelstein, & Kinzler, 2003). Same type of mutations/alterations was found in other human cancers (Koch et al., 2001; Rubinfeld et al., 1997; T.-H. Su et al., 2003; Udatsu, Kusafuka, Kuroda, Miao, & Okada, 2001). For instance, a β-cat mutation (S37F) was found to activate Wnt pathway in melanoma cells (Rubinfeld et al., 1997). These mutations/signalling alterations determine β-cat stabilization and nuclear accumulation, thus resulting in tumorigenesis (Jiang et al., 2014; Morin et al., 1997). Indeed, in a murine model of MEN1-deficient pancreatic neuroendocrine tumours (PNETs), which lack the scaffolding protein menin and display β-cat nuclear accumulation (Cao et al., 2009), β-cat ablation was found to inhibit tumour cell proliferation with suppression of pro-proliferative gene expression (Jiang et al., 2014).

Besides mutations in β-cat, those inactivating APC can also lead to the deregulation of β-cat proteasome-mediated degradation (Gao et al., 2018; Morin et al., 1997). Indeed, in colon carcinoma cells, APC loss is associated with nuclear β-cat, whose stability is counteracted when APC is reintroduced (Korinek et al., 1997). Stable nuclear β-cat elicits activation of human proto-oncogenes, such as *c-myc* and *cyclin D1*, thus promoting cell proliferation (Gao et al., 2018; Korinek et al., 1997). This is why abnormal accumulation of β-cat (both in the cytoplasm and in the nucleus) is seen as a tumour marker (Ziyi Wang et al., 2015; Xia et al., 2006).

Aberrant nuclear β-cat accumulation can be also caused by mutations in other molecular components of the Wnt pathway. Indeed, this latter can be triggered by mutations in *Axin 1/2* genes, which have been linked to the promotion of a series of carcinomas (liver, colon and ovary) and medulloblastoma (Dahmen et al., 2001; W. Liu et al., 2000; Satoh et al., 2000; R. Wu, Zhai, Fearon, & Cho, 2001). In addition, nuclear β-cat accumulation due to GSK3β inhibition has been associated with hepatocarcinogenesis (Desbois-Mouthon et al., 2001).

Mechanical cues can also contribute to tumour formation due to deregulated β-cat signalling. Indeed, Farge team recently showed thatβ-cat nuclear accumulation -with increased expression of β-cat target genes- contributed to tumour transformation of mouse colonic tissue when subjected to a pressure mimicking the one exerted by surrounding endogenous early growing tumours. Thus, tumour growth can induce tumour transformation in the surrounding healthy tissue via mechanical pressure (Fernández-Sánchez et al., 2015).

Lastly, it has been shown that, in colon and small intestine of mouse, E-cadherin reduction can synergize with an activating mono-allelic mutation in β-cat, thus leading to cancer initiation. Indeed, E-cadherin can sequester mutated β-cat, which can thus be stopped undergoing nuclear accumulation and consequently promoting malignant transformation (Huels et al., 2015).

6.2 α-catenin

Loss of α-cat has been linked to tumorigenesis in human (Vite, Li, & Radice, 2015). Indeed, α-cat loss has been associated to different cancers, such as myelodysplastic syndrome (MDS, a preleukemic disorder) and acute myeloid leukemia (AML), where *CTNN1* gene expression was found to be low (T. X. Liu et al., 2007). Additionally, restoration of *CTNN1* gene expression in a myeloid leukemia cell line (HL-60) determined reduced cell proliferation with apoptosis (T. X. Liu et al., 2007). Therefore, α-cat loss is thought to provide a growth advantage, thus contributing to MDS or AML in human (T. X. Liu et al., 2007).

α-cat loss, as well as its reduced expression, was found to promote colon cancer progression (Raftopoulos, Davaris, Karatzas, Karayannacos, & Kouraklis, 1998; Vermeulen et al., 1995). Indeed, α-cat has invasion suppression function in colon cancer (Vermeulen et al., 1999). α-cat loss was also shown to determine global loss of cell-cell contacts in E-cadherin expressing human breast carcinoma cells (Bajpai, Feng, Krishnamurthy, Longmore, & Wirtz, 2009). Moreover, α-cat expression acts as tumour suppressor in E-cadherin-negative basal like breast cancer (Piao et al., 2014).

In summary

- α-, β- and p120-catenins form a complex with the classical cadherins called the "cadherin-catenin complex".
- β- and p120-catenins directly interact with the cytoplasmic tail of classical cadherins, whereas α-catenin assures the connection between cadherins and actin cytoskeleton by binding actin and interacting with β-catenin.
- β-catenin is also a transcription co-factor and its signalling can be activated in response to Wnt ligands as well as mechanical cues.
- α-catenin can negatively regulate β-catenin signalling either via proteasome-dependent degradation or target gene expression repression.
- Cancerous diseases can be a consequence of deregulation/mutations of α-/β-catenins functions/signalling.

CHAPTER 4

The Epithelial-Mesenchymal Transition (EMT)

In this last introduction chapter, I will briefly cover the aspect of the epithelial-mesenchymal transition (EMT), taking into account its definition and the experimental approaches exploited to define it.

Table of content

1 Epithelial versus mesenchymal cells

Before focusing on what EMT is, it is worth giving some background on the cells which are the actors in the EMT, that is the epithelial and the mesenchymal cells.

In animals, epithelial cells are those cells forming epithelia, the tissues lining the outer surface of organs and blood vessels. Epithelia can be simple, composed of a single layer of cells, or stratified, made of multiple layers of cells stacked on top of each other (Fig 70A). Underneath the epithelia, an organized layer of Extracellular Matrix (ECM) protein molecules forms the basal lamina (Fig 70 B), which gives structural support to the epithelia and protects them from biochemical and biophysical stress (Mouw, Ou, & Weaver, 2014).

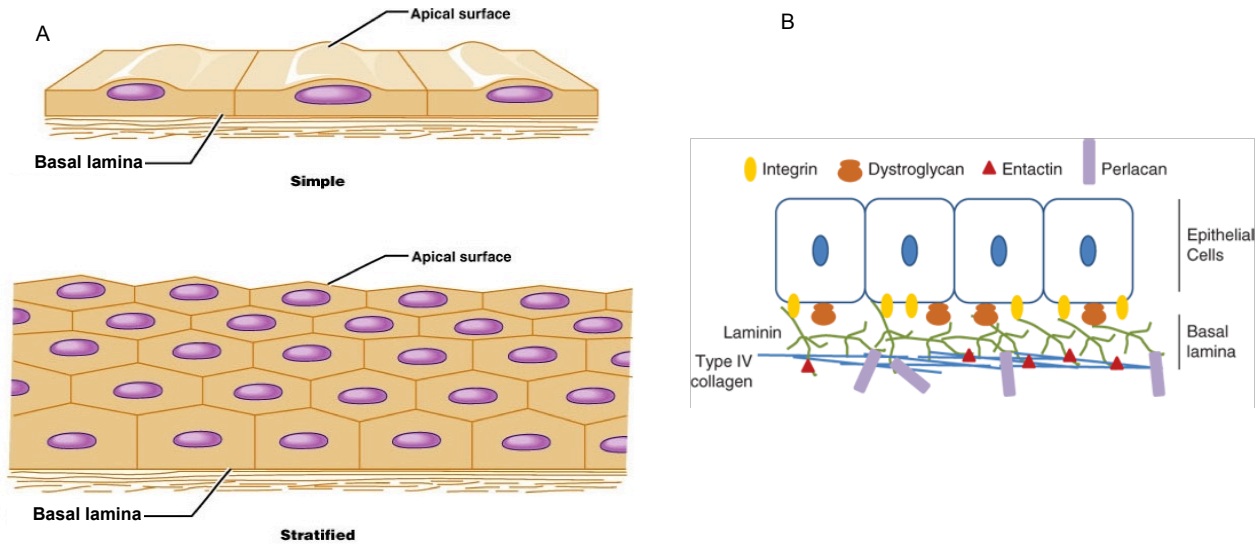

Fig 70: A: simple (up) and stratified (down) epithelia. B: Basal lamina, composed of different layers of ECM proteins (type IV collagen, perlecan, entactin and laminin), gives support to the epithelia. A, adapted from: Pearson Education, 2004. B from: Harper's Illustrated Biochemistry, 31st edition. McGraw-Hill education.

Epithelial cells present apical-basal polarity, (that is the unequal distribution of proteins between the apical/basal cellular sides) and are able to form layers via cell-cell junctions (Fig 71), such as adherens and tight junctions, desmosomes and gap junctions (Lamouille, Xu, & Derynck, 2014; Thiery & Sleeman, 2006). Even though they are motile, in normal conditions epithelial cells do not detach from the layer they form (Thiery & Sleeman, 2006), but they do if dying.

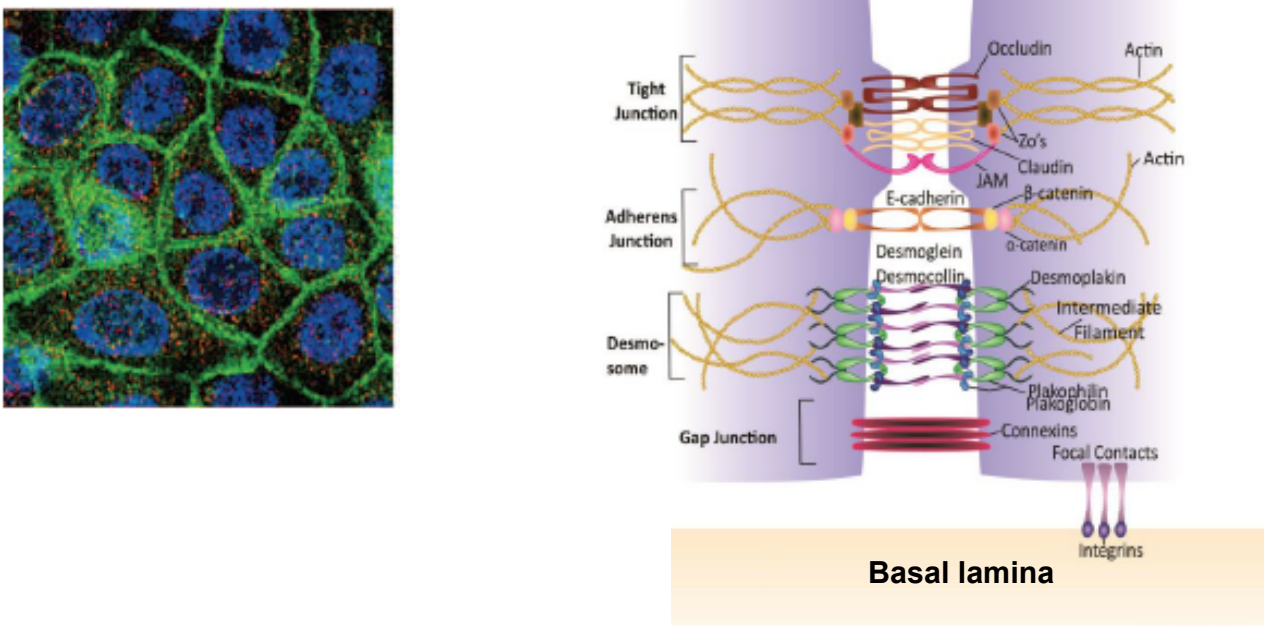

Fig 71: Left: monolayer of epithelilal Eph4 V12-transformed murine mammary cells, stained for E-cadherin (green), vimentin (red) and counterstained for nuclei with DAPI (blue). Note the clear presence of adherens junctions (E-cadherin) within the cell monolayer. Adapted from (Thiery & Sleeman, 2006). Right: cell-cell junctions assure the connection of cells in the epithelia. Adapted from: (Singh, Yelle, Venugopal, & Singh, 2018).

Mesenchymal (from "Mesenchyme", a connective tissue in animals) cells, on the contrary, are not able to form a monolayer nor they have the capability to polarize (Lamouille et al., 2014; Thiery & Sleeman, 2006), even though they display a front-to-rear polarity (J. M. Lee, Dedhar, Kalluri, & Thompson, 2006). These cells, in culture, present an elongated, spindle-shaped morphology compared to epithelial cells (Fig 72, left and right) and have high motility, with single cell or cell cluster migration (Friedl, 2004).

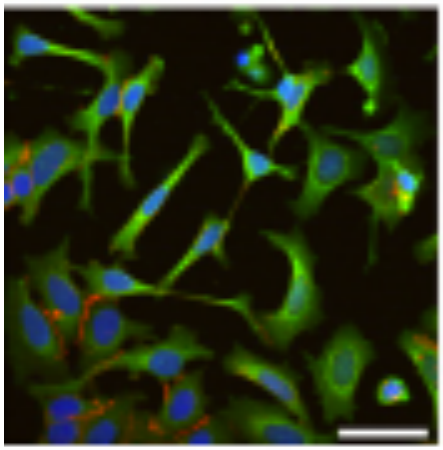

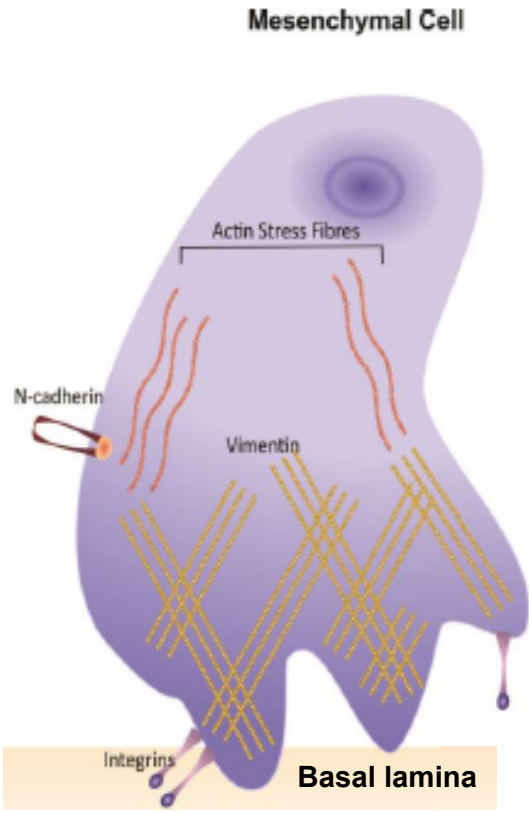

Fig 72: Left: MCF-7 cells (mammary epithelial adenocarcinoma cells), undergone EMT, display spindle-shaped morphology and express increased expression of vimentin (stained in green) as well as decreased expression of E-cadherin (stained in red), all typical features of mesenchymal cells. Nuclei stained with Hoechst 33342. Scale bar: 50 μm. Adapted from (L. Zhang & Min, 2017). Right: Increased vimentin expression gives mesenchymal cell's cytoskeleton more flexibility and less susceptibility to damage during migration (Mendez, Kojima, & Goldman, 2010). Adapted from: (Singh et al., 2018)

2 The EMT

The term "EMT" refers to a series of biological changes through which epithelial cells can gain mesenchymal phenotype, with the acquisition of high migratory capacity, invasiveness, resistance to apoptosis and ability to degrade the extracellular matrix (ECM)(Kalluri & Weinberg, 2009; Książkiewicz, Markiewicz, & Zaczek, 2012; Strutz et al., 2002). As such, cell-cell contacts are weakened, as marked by the downregulation of E-cadherins (adherens junctions) as well as claudins, occludins and ZO-1 (zonula occludens 1) (tight junction proteins)(Jechlinger et al., 2003) (Fig 73). Cells with an acquired mesenchymal phenotype display high levels of N (neural)-cadherins, ECM proteins such as fibronectin, tenascin c, collagen VI-α and laminin-β1 (ECM molecular composition remodels during the EMT process (Lamouille et al., 2014)) and intermediate filament protein vimentin (Jechlinger et al., 2003; Książkiewicz et al., 2012; Park & Schwarzbauer, 2014) (Fig 73). Transcription factors, such as TWIST1, SNAIL, SLUG and SIP1 (survival of motor neuron protein interacting protein 1)(Carver, Jiang, Lan, Oram, & Gridley, 2001; Comijn et al., 2001; Leptin, 1991; M A Nieto, Sargent, Wilkinson, & Cooke, 1994) (Fig 73), as well as soluble ligands, such as Wnt and TGF-β (transforming growth factor-β) (McMahon, Takada, Ikeya, Lee, & Johnson, 1997; Romano & Runyan, 2000; Spagnoli, Cicchini, Tripodi, & Weiss, 2000), regulate EMT, which is also characterized by changes in microRNAs (miRNAS) expression (Kalluri & Weinberg, 2009) (Fig 73). Among the mentioned transcription factors, SLUG, which binds DNA via five zinc-fingers (Laity, Lee, & Wright, 2001; M. S. Lee, Gippert, Soman, Case, &

Wright, 1989; M A Nieto et al., 1994), is known to repress E-cadherin expression (Bolós et al., 2003),promote EMT (P Savagner, Yamada, & Thiery, 1997) and be implied in tumour progression and invasiveness (Côme, Arnoux, Bibeau, & Savagner, 2004). Moreover, soluble ligands such as BMPs (bone morphogenetic proteins), HGF (hepatocyte growth factor) and TGFβ2 (transforming growth factor beta2) are involved in SLUG regulation in different cell types (Liem, Tremml, Roelink, & Jessell, 1995; Romano & Runyan, 2000; P Savagner et al., 1997).

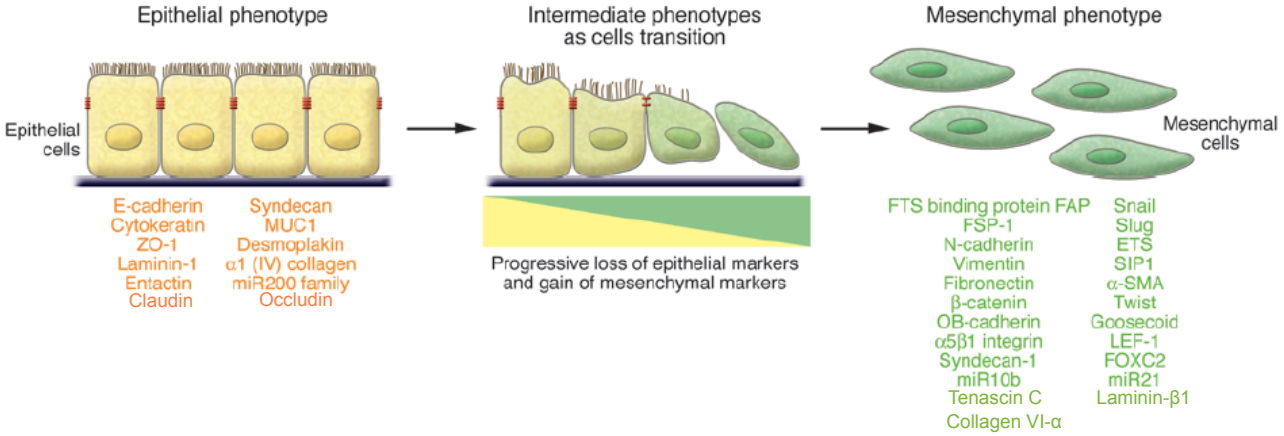

Fig 73: Schematic of the EMT process: epithelial cells are converted into mesenchymal cells via the downregulation of epithelial markers (orange) and the acquisition of mesenchymal ones (green). To reach the mesenchymal phenotype, epithelial cells pass through an intermediate state, where they progressively lose epithelial markers while acquiring mesenchymal markers. ZO-1: zona occludens 1. MUC1: mucin 1, cell surface associated. miR200: microRNA 200. SIP1: survival of motor neuron protein interacting protein 1. FOXC2: forkhead box C2. Adapted from (Kalluri & Weinberg, 2009).

The idea that epithelial cells could undergo mesenchymal transition dates back to the early 80s. Indeed, in 1982, Hay group showed that, when cultured in a collageneous gel matrix, explants from chick embryonic notochord and limb ectoderm as well as adult chick anterior lens epithelia gave rise to elongated bipolar cells, which migrated individually away from the explant and became mesenchymal in appearance (Greenburg & Hay, 1982) (Fig 74).

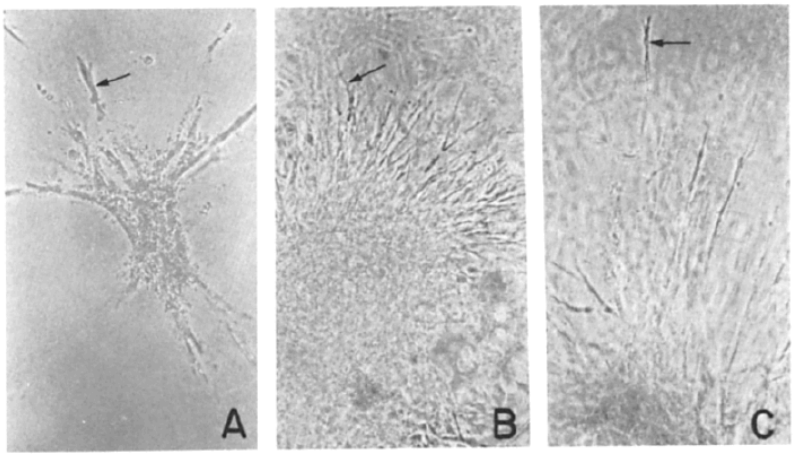

Fig 74: In explants from chick embryonic notochord (A), chick embryonic limb ectoderm (B) and adult chick lens epithelia (C), elongated bipolar cells (see arrows) start migrating away from the explants after 5 (A and C) and 4 (B) days of culture in a collagenous gel matrix. Phase-contrast micrographs from (Greenburg & Hay, 1982).

The term proposed to describe this process was initially “transformation” (Hay, 1995). However, “transformation” was then replaced by “transition”, indicating the plasticity of the phenomenon (Kalluri & Weinberg, 2009; Lamouille et al., 2014). Indeed, once cells become mesenchymal, they can be reverted to the epithelial state (Ekblom, 1989; Hay, 1995) via MET (mesenchymal-epithelial transition), the inverse of EMT (Kalluri & Weinberg, 2009; Lamouille et al., 2014; Thiery & Sleeman, 2006).

EMT has been shown to play a fundamental role in embryonic development (Ciruna & Rossant, 2001), wound healing (Yan et al., 2010), fibrosis (Y. Li, Yang, Dai, Wu, & Liu, 2003) and cancer progression (Xue, Plieth, Venkov, Xu, & Neilson, 2003).

Due to its widespread biological implications, EMT can be classified as type 1 EMT, associated with embryonic development, type 2 EMT, linked to wound healing and fibrosis and type 3 EMT, involved in cancer progression (Kalluri & Weinberg, 2009; Książkiewicz et al., 2012).

An example of type 1 EMT is the differentiation of the mesoderm and endoderm (the two of the three embryonic germ layers (Kiecker, Bates, & Bell, 2016)) following primitive streak formation upon gastrulation of the fertilized egg (Kalluri & Weinberg, 2009). Type 1 EMT is also involved when migratory neural crest cells are generated from neuroectoderm (which derives from ectoderm and forms nervous system) (Duband & Thiery, 1982; Kalluri & Weinberg, 2009).

Tissue injury due to trauma or inflammation triggers type 2 EMT, which is aimed to repair the damaged tissue (Kalluri & Weinberg, 2009). In this case, for instance, the EMT can be triggered by the recruitment, at the site of injury, of macrophages and activated fibroblasts which release growth factors (such as TGFβ and FGF-2 (fibroblast growth factor 2)) as well as metalloproteinases (MMPs)(Strutz et al., 2002). Such an environment can stimulate epithelial cells to degrade basal membrane and migrate (Strutz et al., 2002).

If EMT is continuously triggered by inflammation, organ fibrosis can happen with consequent organ disruption (Kalluri & Weinberg, 2009). Organ fibrosis due to EMT program has been found in lung and liver (K. K. Kim et al., 2006; Zeisberg et al., 2007).

Activation of the EMT process in epithelial cancer cells (type 3 EMT) has been thought to be a critical step for the acquisition of malignant phenotypes (Thiery, 2002). To this regard, studies in mouse have pointed out that carcinoma cells can display a mesenchymal phenotype, with the expression of the mesenchymal markers vimentin and α-SMA (Kalluri & Weinberg, 2009). In this context, EMT would work as a facilitator of cancer progression towards metastasis, especially because of the genetic and epigenetic alterations cancer cells undergo (during primary tumour formation), which renders them more responsive to the EMT-inducting signals (that is, for instance, growth factors) coming from the surrounding tumour stroma (Kalluri & Weinberg, 2009). As a consequence, activation of transcription factors promoting EMT (such as SNAIL, SLUG and TWIST) can be induced (Lo, Lee, Lee, & Hsieh, 2017).

It has also been shown that E-cadherin loss, in cancer cells, can promote EMT (Theys et al., 2011). Moreover, increased β-catenin nuclear accumulation, that can also arise from loss of E-cadherin (Huels et al., 2015; Orsulic, Huber, Aberle, Arnold, & Kemler, 1999), has been associated with EMT promotion and acquisition of an invasive phenotype (K. Kim, Lu, & Hay, 2002; Thiery, 2002).

It is thus clear that EMT is an event characterizing physiological processes as well as pathologies (Thiery, Acloque, Huang, & Nieto, 2009). Nevertheless, EMT can be also experimentally induced, as explained in the following paragraph.

3 The EMT is induced following wound healing and HGF exposure

An example of experimental EMT induction through wound healing dates back to 2005, when the Hudson team studied the implication of SLUG transcription factor on skin re-epithelialization (Pierre Savagner et al., 2005). By wounding a monolayer of human SCC 12 keratinocytes, the authors found that SLUG transcription factor enriched the margin of the wound but was not present where cells were confluent (Fig 75A). In addition, SCC 12 cell clones stably overexpressing SLUG exhibited faster wound closure capacity compared to the same cells used as control (only expressing the empty vector) (Fig 75B). Furthermore, the authors found that in a wounded monolayer of HaCaT cells, the expression of the desmosome protein desmoplakin was lower at the wound margin compared to the confluent region of the monolayer (Fig 75C). In addition, immunostaining wounded HaCaT cells for E-cadherin revealed no reduction of this protein at the wound margin (Fig 75D). The authors thus concluded that, after wound healing, SLUG expression regulates re-epithelialization which is marked by the reduction of desmosome number (Pierre Savagner et al., 2005).

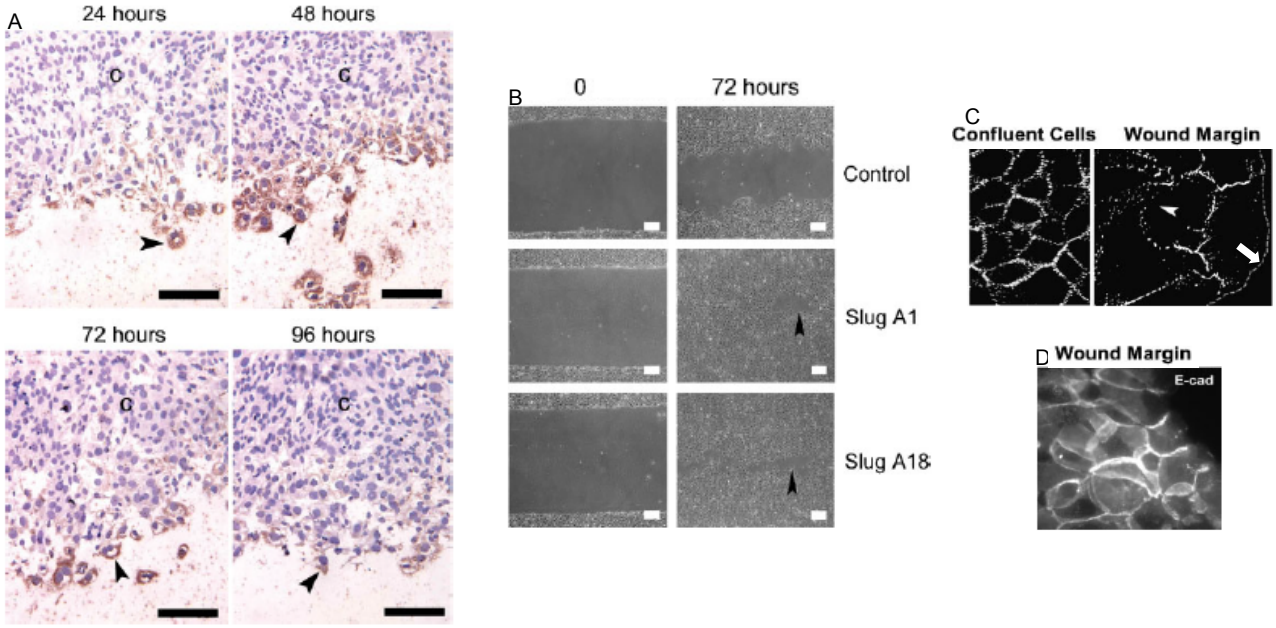

Fig 75: SLUG is involved in skin re-epithelialization upon wound healing. A: human SCC 12 keratinocytes were probed for SLUG mRNA (brown) at 24, 48, 72 and 92 hours post-wound. Note that SLUG mRNA enriched wound margins (arrowheads) whereas it was not present in the remaining confluent part of the monolayer (marked by **C**). SLUG expression in wound margins stayed elevated till 72 hours, then decreased (92h). Hematoxylin used to counterstain nuclei in the shown immunohistochemistry image. B: human SCC 12 keratinocyte clones stably overexpressing SLUG (Slug A1 and Slug A18 clones) were faster in wound closure (72h post-wound) compared to the same control cells. Arrowheads point to the cell-free areas in the SLUG-expressing clones. C: HaCaT cells immunostained for the desmosome marker desmoplakin showed less signal for this protein in the wound margin compared to the remaining confluent cells. In the wound margin field, the arrowhead shows a gap in desmoplakin staining at the cell-cell contact, whereas the dotted line (arrow) marks the wound edge. D: E-cadherin immunostaining in HaCaT cells revealed no signal reduction of this protein at the wound margin. Scale bars: 200μm. Adapted from (Pierre Savagner et al., 2005).

EMT promotion can be also achieved via the scattering factor HGF (Thiery & Sleeman, 2006; Weidner et al., 1993). To this regard, Lehembre team showed that treatment of HepG2 (epithelial liver cancer) cells with HGF determined an upregulation of the transcription factor SNAIL (a zinc finger protein, like SLUG, which induces EMT through repression of E-cadherin (Cano et al., 2000)), both at the protein as well as at the mRNA levels (Grotegut, Von Schweinitz, Christofori, & Lehembre, 2006)(Fig 76A and B). HGF treatment also directly activated SNAIL, as reported by the increased

SNAIL promoter activity via a luciferase assay in HEK cells (Fig 76C). Furthermore, this upregulation in SNAIL levels correlated with decreased transcription levels of E-cadherin (Fig 76D). In addition, upon stable depletion of SNAIL in HepG2 cells (sh(short hairpin)Snail S-3 clones), HGF was not able to determine cell scattering in comparison to control cells (control vector, C-1 clones) (Fig 76E-H). Thus, the authors concluded that HGF induced an increase in SNAIL expression (protein and mRNA), which leads to E-cadherin downregulation and cell scattering (Grotegut et al., 2006).

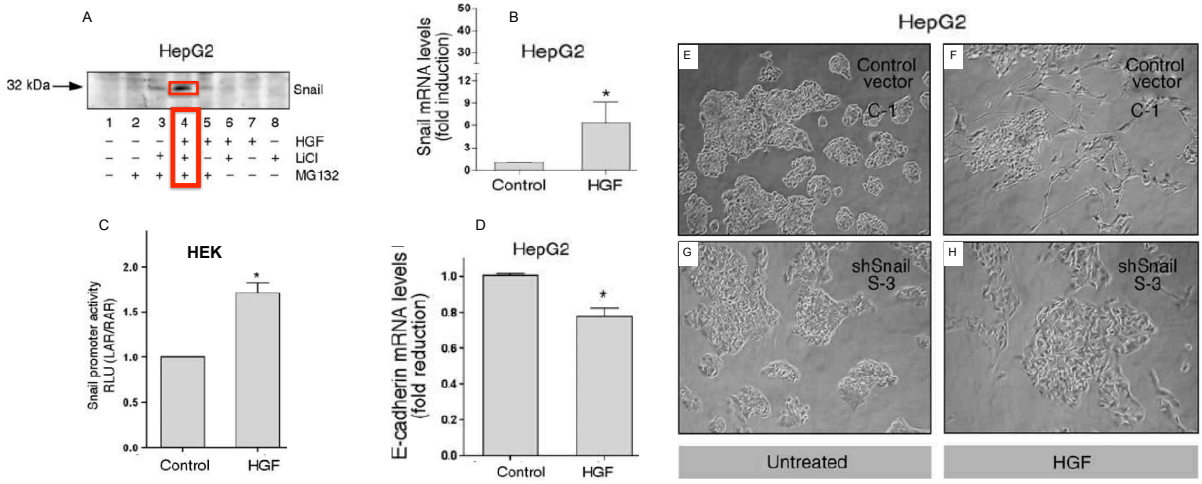

Fig 76: HGF induces increased SNAIL (both protein and mRNA) levels, which leads to E-cadherin downregulation and cell scattering. A: SNAIL protein levels are upregulated upon combined treatment (8h) of HGF, LiCl (GSK-3β inhibitor) and MG132 (proteasome inhibitor) (red boxes). Note that SNAIL protein is rapidly proteasome degraded upon GSK-3β phosphorylation, which explains why its increase is only visible upon triple treatment. B: HGF (8h) induces increased SNAIL mRNA levels. C: SNAIL is directly regulated by HGF (24h), as displayed by the increased SNAIL promoter activity measured with a luciferase assay. D: upon HGF treatment, E-cadherin mRNA levels are downregulated. E-F: in HepG2 clones (C-1) expressing a control sh(short hairpin)RNA (control vector), HGF promoted scattering (observed after 72h HGF incubation) compared to untreated cells. G-H: in HepG2 clones (S-3) expressing a sh(short hairpin) targeting SNAIL (shSnail), HGF did not promote scattering, compared to untreated cells. Magnification: x200. *p<0.05. Adapted from (Grotegut et al., 2006).

HGF is able to trigger EMT via the interaction with the c-met tyrosine kinase receptor, an RTK (receptor tyrosine kinase) on the plasma membrane, which is the product of the *c-met* proto-oncogene (Bottaro et al., 1991). Once HGF binds c-met receptor, the RAS-RAF-MEK-ERK MAPK cascade signalling is activated, which promotes the expression of EMT transcription factors as well as regulators of cell migration and invasion (Lamouille et al., 2014) (Fig 77).

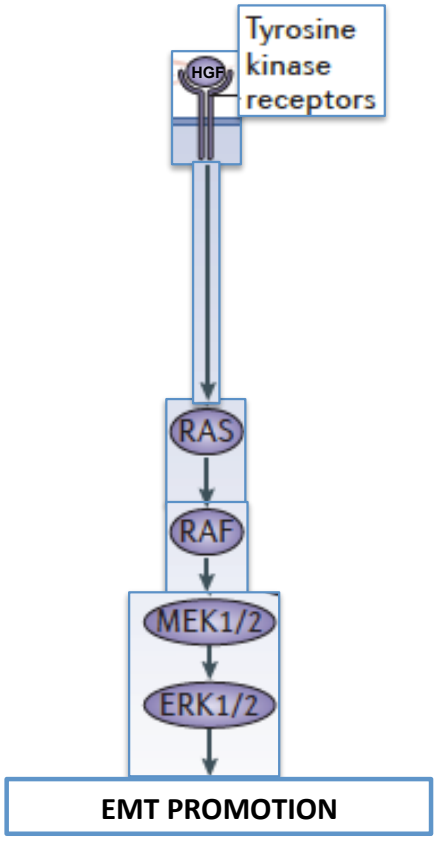

Fig 77: HGF triggers EMT via the MAPK cascade signalling. Adapted from (Lamouille et al., 2014).

Wound healing as well as HGF treatment can be thus used to experimentally induce EMT. Indeed, in her work, Charlène Gayrard use both of them to trigger epithelilal cell unpacking, which resulted in E-cadherin tension relaxation and β-catenin signalling (Gayrard et al., 2018) (see section 3.2 "mechanical activation" in "β-catenins's signalling activation", Chapter 3). In this case, however, mesenchymal phenotype acquisition is rapid (10 hours in wound healing assays and 5 hours in HGF treatments) and, either in wound healing assays or in HGF treatments, both FAK (Focal Adhesion Kinase; see section 3.1 "focal adhesions", Chapter 1) and Src activities are required to promote actomyosin cytoskeleton remodelling (Gayrard et al., 2018). This adds an upstream regulatory layer in the EMT process not addressed by both Hudson and Lehembre teams, which only answered the question if SLUG and SNAIL transcription factors were required to promote EMT during skin re-epithelization and upon cell-scattering (Grotegut et al., 2006; Pierre Savagner et al., 2005), thus exploring only the function of the the two downstream players of the EMT induction. In addition, in Charlène's work, it has to be noted that, although wounded cells acquire a mesenchymal phenotype at the wound margin, they, however, still migrate as a cohesive group (Gayrard et al., 2018). This can be thought as a model of partial EMT compared to HGF treatment which determines cell-cell contact disruption and lets cells migrate individually, a sign of complete EMT (Gayrard et al., 2018).

In the next paragraph, I will briefly clarify the meaning of partial EMT.

4 Partial EMT: meaning and experimental evidence

EMT has long been thought as a binary process, where epithelial cells can be converted into fully mesenchymal cells (Thiery & Sleeman, 2006). However, mounting evidence supports the idea that epithelial cells may not necessarily achieve a full mesenchymal phenotype, rather they can acquire a hybrid state between epithelial and mesenchymal states, named as "partial-EMT" (also referred to as

P-EMT)(Jolly, Ware, Gilja, Somarelli, & Levine, 2017; M. Angela Nieto, Huang, Jackson, & Thiery, 2016). As a consequence, cells can move back and forth through a spectrum of different intermediate phases (M. Angela Nieto et al., 2016) (Fig 78), which renders them "metastable" (J. M. Lee et al., 2006), that is cell's capability to induce or reverse the EMT process (Rosanò et al., 2005). In other words, P-EMT can be seen as a condition where the acquired intermediate phenotype is the result of the different gene expression profiles determined by the overexpression of EMT-inducing transcription factors (EMT-TF), such as SNAIL and SLUG (Jolly et al., 2017). Acquisition of this intermediate phenotype has been found in many different carcinoma cell lines as well as in cancer tissue and patients (Jolly et al., 2017), which reflects an important role of P-EMT in tumorigenicity.

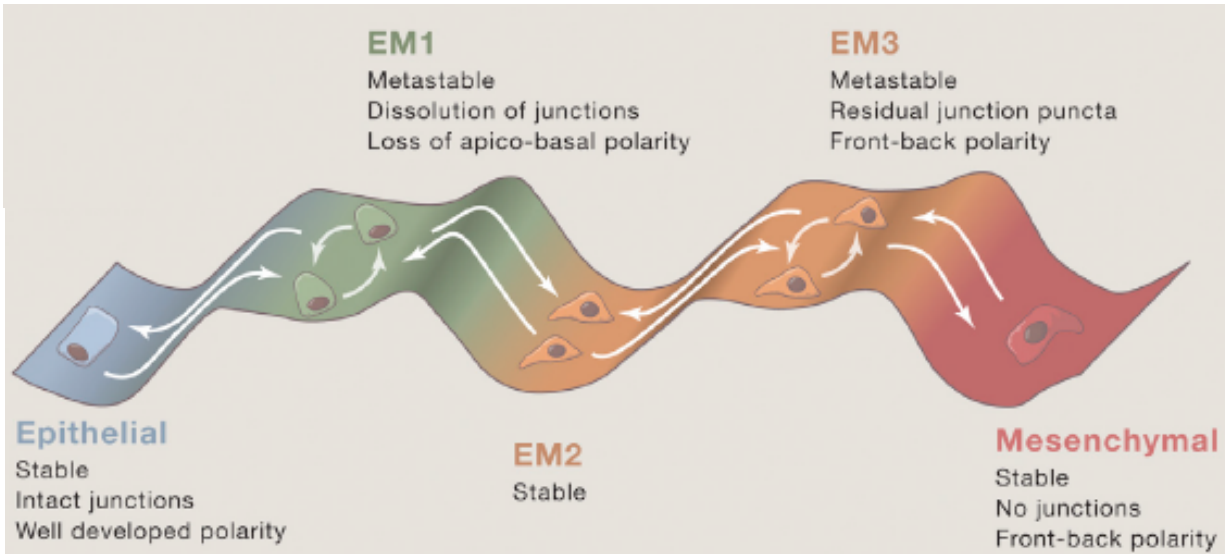

Fig 78: EMT is not a binary process, bur rather it involves a series of intermediate metastable as well as stable states (EM), through which a cell can navigate before reaching the mesenchymal (or the epithelial) phenotype. Adapted from (M. Angela Nieto et al., 2016).

Recent evidence on the existence of P-EMT has been given by Aiello et al. In this work, the researchers took advantage of the KPCY mouse model, where pancreatic tumours can be induced - through a pancreas-specific Cre recombinase activity which triggers the expression of a mutant form of Kras oncogene ($Kras^{G12D}$) and the concomitant deletion of a single p53 allele- and tumour cells can be easily recognized through the expression of YFP. In these KPCY tumour sections, the authors found that most of the tumour cells (expressing YFP) which exhibited EMT features (such as spindle-shaped morphology) also lacked membrane E-cadherin (M-ECAD),whose loss is considered a hallmark of EMT (Aiello et al., 2018)(Fig 79A). This loss correlated also with an increased expression of SLUG (Fig 79B, B' and C), that, however, was not present in the tumour cells which did not lose E-cadherin (M-ECAD+) (Fig 79A, B, B' and C). Subsequently, RNA sequencing for genes involved in the EMT process was carried out on tumour cells sorted from KPCY tumours. The sequencing revealed that some cells exhibited a downregulation in genes characterizing the epithelial state (E-cadherin expression was also repressed) with a concomitant upregulation in those genes related to the mesenchymal state, which marked these cells as undergone complete EMT (C-EMT) (Fig 79D). Other cells (a much bigger group), instead, while upregulating mesenchymal state genes, did not display reduced expression levels of the epithelial state genes (E-cadherin expression was also maintained) (Fig 79D), which meant these cells underwent partial EMT (P-EMT). The authors thus concluded that KPCY tumours exhibited two distinct EMT processes, with overlapping mesenchymal programs (Aiello et al., 2018) (Fig 80).

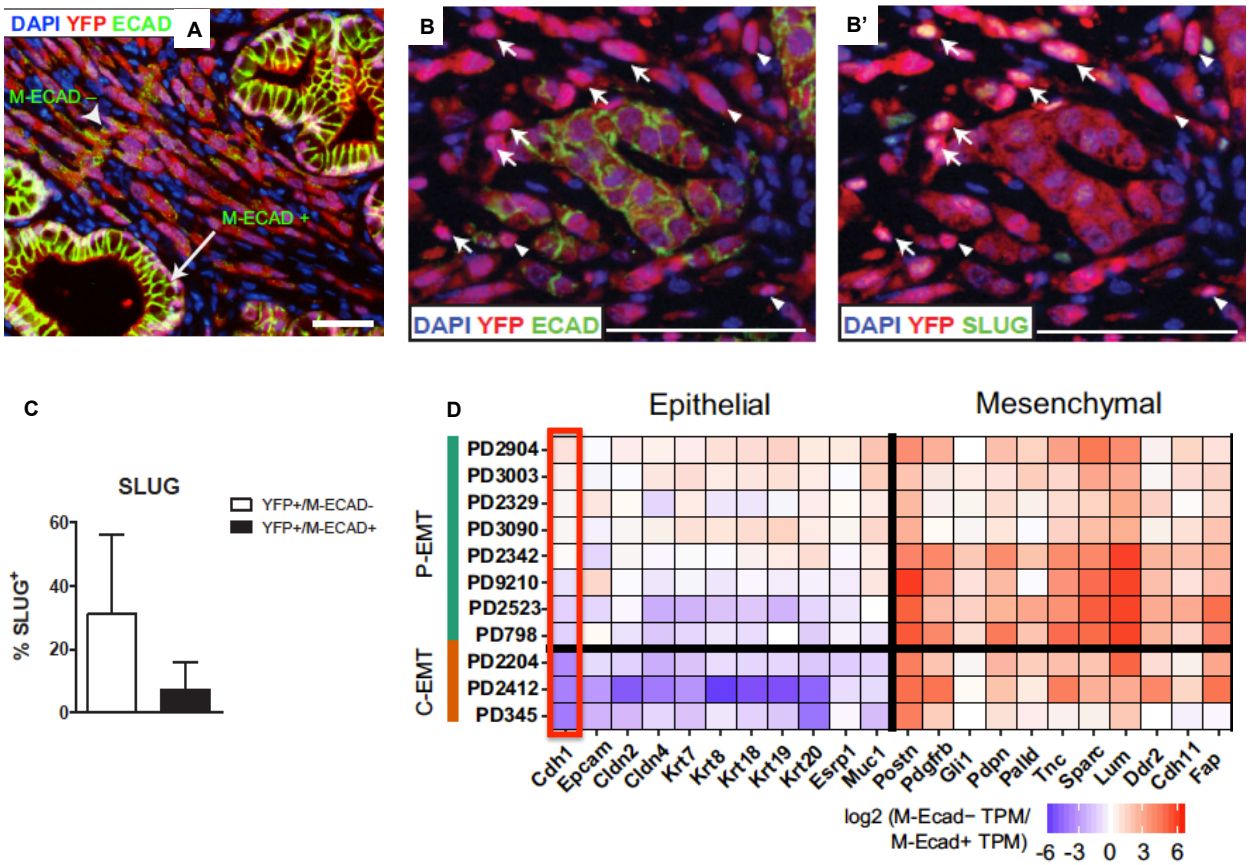

Fig 79: KPCY tumour cells (YFP positive, immunostained in red) exhibiting loss of membrane E-cadherin (M-ECAD-, immunostained in green) (A and B) correlate with increased SLUG expression (immunnostained in green) (B' and quantification in C) compared to those tumour cells still expressing E-cadherin (M-ECAD+) (A and B) which did not present SLUG (B' and quantification in C). Subsequent RNA sequencing of all these cells revealed that a group of them underwent complete EMT process (C-EMT), whereas another, bigger group displayed partial EMT (P-EMT) (D). Arrowhead in A points to M-ECAD- cells, whereas arrow indicates M-ECAD+ cells. In B and B', arrows denote M-ECAD- cells positive for SLUG, whereas arrowheads indicate M-ECAD- cells negative for SLUG. In A, B and B' DAPI is used to counterstain nuclei. In D, E-cadherin expression levels are boxed in red. Scale bars: 25µm in A and 50µm in B and B'. TPM: transcripts per million. Adapted from (Aiello et al., 2018).

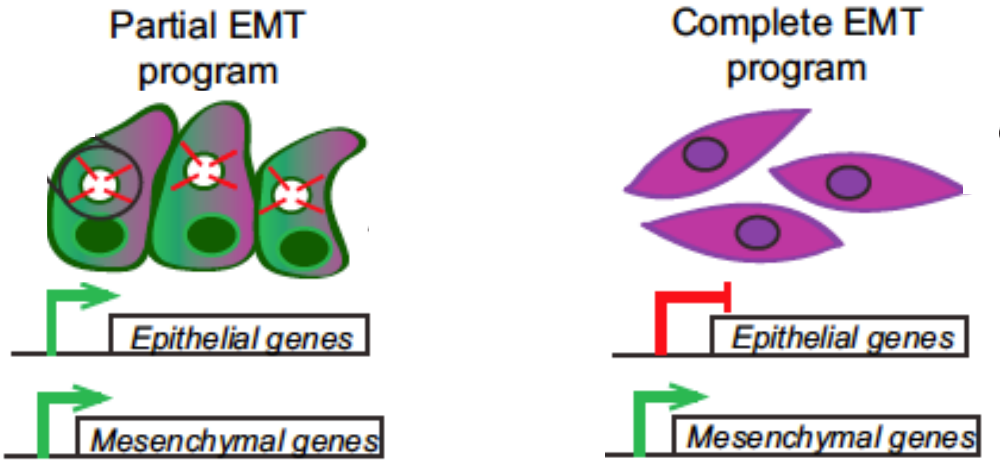

Fig 80: KPCY tumours undergo EMT via a partial EMT program (left), where both epithelial as well as mesenchymal genes are transcribed, or through a complete EMT program (right), which permits only mesenchymal gene transcription while repressing epithelial genes. Adapted from (Aiello et al., 2018).

It is thus clear that EMT is not a static, simple process through which cells can only acquire a definite state. It is, instead, a very plastic process, where cells can both retain epithelial features while acquiring mesenchymal traits (Aiello et al., 2018; Jolly et al., 2017; M. Angela Nieto et al., 2016).

In summary

- In animals, epithelial cells are the cells that form epithelia, by connecting each other through cell-cell junctions, display apical-basal polarity and are motile but do not leave the layer they reside in.
- Mesenchymal cells do not form layers nor have an apical-basal polarity, are highly motile and, in culture, present a spindle-shaped morphology.
- Epithelial cells can acquire a mesenchymal phenotype through the process of EMT, characterized by the gradual loss of epithelial markers and the concomitant acquisition of mesenchymal markers.
- EMT is found in physiological as well as pathological process, such as embryo development, tissue re-epithelialization after injury, organ fibrosis and cancer progression.
- EMT can be experimentally induced through wound healing or cell treatment with scattering factors, such as HGF.
- Recently, the concept of EMT has been revised putting the stress on partial EMT (P-EMT), an intermediate, highly plastic state between the epithelial and the mesenchymal ones resulting from an overlap of different gene expression profiles.

Thesis objectives

The importance of mechanotransduction in a plethora of cellular responses has been discussed so far, especially in the context of the nuclear envelope. Indeed, the role of the LINC complex in assuring mechanical connection between nucleoskleton and cytoskeleton (Lombardi et al., 2011; Maniotis et al., 1997) from one hand and its function in regulating cellular signaling, through nuclear translocation of β-catenin (Neumann et al., 2010; Uzer et al., 2018) for instance, from the other the one, has been addressed. I have also focused on the mechanical activation of β-catenin, which can be promoted by strain application, (Benham-Pyle et al., 2015), a combination of this latter plus extracellular ligands (Benham-Pyle et al., 2016) or by decreased cell packing with consequent E-cadherin tension relaxation in the process of epithelial-mesenchymal transition (EMT)(Gayrard et al., 2018). To this regard, however, it is unknown if the LINC complex mechanically induces β-catenin signaling. Nesprin 2 Giant (N2G) has been recently shown to be under tension (Arsenovic et al., 2016) and, moreover, an interaction between this protein and α-catenin, whose nuclear localization depends on β-catenin (Rebecca L Daugherty et al., 2014),has been demonstrated (Neumann et al., 2010). Thus, we asked ourselves if, in the context of partial as well as complete EMT induction, nesprin 2G could, as a function of its tension, capture and thus regulate α/β-catenin signaling and nuclear translocation. To this aim, we tried to answer the following questions:

1. Is the LINC complex under specific cytoskeleton-generated tension and can this tension be influenced by cell-cell junctions?

2. Is the LINC complex sensitive to mechanical cues and how does the LINC complex respond to them?

3. Is the LINC complex, through nesprin 2G tension, involved in regulating α/β-catenin signaling upon EMT-induced decreased cell packing?

4. Provided an evidence of LINC complex regulation in α/β-catenin signaling, what is the implication of α-catenin on β-catenin activity?

To answer these questions, we relied on Molecular Tension Microscopy (MTM)(Gayrard & Borghi, 2016) through FRET TSMod (tension sensor module) biosensors (Grashoff, Hoffman, Brenner, Zhou, Parsons, Yang, McLean, Sligar, Chen, Ha, & Schwartz, 2010), which have been largely exploited to asses mechanical forces exerted onto proteins. They are cloned into miniN2G (a short variant of N2G (Luxton et al., 2010; Ostlund et al., 2009) and SUN2 LINC complex proteins, in order to retrieve changes in tension upon mechanical (nuclear confinement/cell stretching assays), genetic (mutant N2G) and pharmacological (cytoskeleton drug) perturbations, in absence or presence of partial as well as complete EMT induction. In addition, we used GFP-tagged α and β-catenin proteins, in the same context of EMT induction as above, to evaluate the response of α/β -catenins to LINC complex perturbation as well as to assess α-catenin influence (through its nuclear ovexpression or depletion all-over the cell) on β-catenin signaling. Finally, by using a β-catenin transcriptional activity reporter, we also evaluated how β-catenin dependent gene transcription is affected by either nuclear α-catenin overexpression or LINC complex perturbation.

CHAPTER 5

Materials and Methods

In this chapter, I will describe the experimental procedures carried out for this thesis work. Some background concepts related to the FRET phenomenon will be also discussed.

Table of contents

1 Cell cultures

Our research has been based on mammalian cells as model system. Most of the experiments have been carried out by exploiting the well-known MDCK (Madin-Darby Canin Kidney) type II G cell line, and, in some cases, to assess the conservation of biological mechanisms, we also relied on NIH 3T3 mouse fibroblasts. Indeed fibroblasts, contrary to MDCK, have been widely used to study nesprins' biology (Lombardi et al., 2011; Luxton et al., 2010; Ostlund et al., 2009). MDCK cells are epithelial cells from kidney tubules of cocker spaniel dog (Fig 81A) which, once at confluence in culture, create a full monolayer and display typical apical-basal polarity, with presence of adherens and tight junctions (Howard, Deroo, Fujita, & Itasaki, 2011). MDCK cells have also a rapid doubling time of roughly 21h (Cho, Thompson, Cramer, Vidmar, & Scieszka, 1989).

NIH 3T3 fibroblasts, instead, are derived from a Swiss mouse embryo (Jainchill, Aaronson, & Todaro, 1969) (Fig 81B).

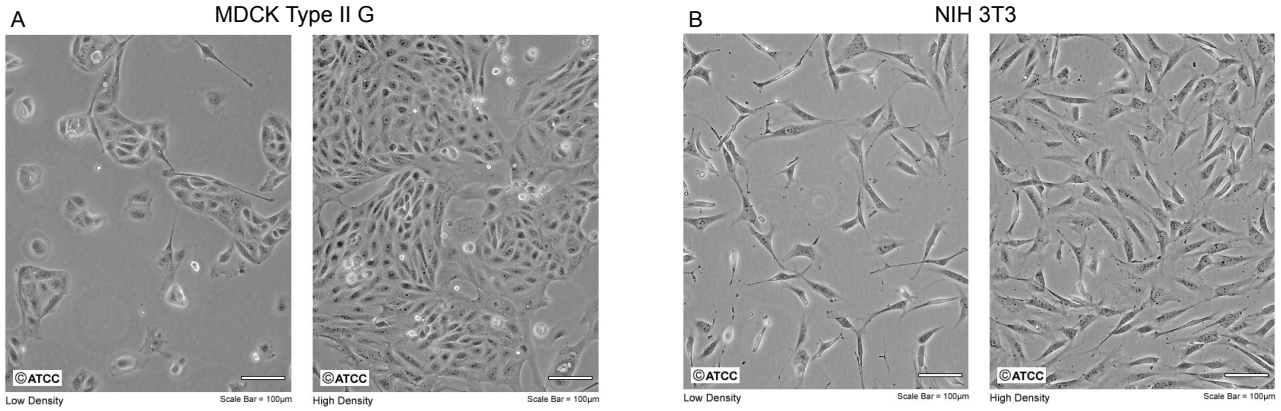

Fig 81: Cell lines used in this project. A: MDCK type II G at low (left) and high (right) density. B: NIH 3T3 at low (left) and high (right) density. Scale bars: 100µm. From: ATCC.

MDCK and NIH 3T3 cells are cultured at 37 °C and 5% CO_2 in DMEM (Dulbecco's Modified Eagle Medium), supplemented with 10% (vol/vol) FBS with 1g/L glucose, and are normally passaged three times a week. To obtain lines stably expressing the different constructs exploited in this work (see paragraph 2 in this chapter), cells were transfected by using Turbofect reagent (Thermo Fisher Scientific). Cells were FACS sorted after a two- week selection with 200µg/mL hygromycin (InVivoGen, France). After that, in order to avoid constructs loss, the new cell lines are maintained under a basal selective pressure of 100 µg/mL hygromycin.

MDCK type II G cells expressing β catenin-GFP and α catenin-GFP are gifts from W.J. Nelson (Stanford University, Stanford, CA). MDCK type II G cells expressing TOP-dGFP are a gift from C. Gottardi (Northwestern University, Chicago, IL). All these three cell lines are cultured in presence of G418 at 200mM.

For live cell imaging experiments, cells were seeded onto glass coverslips coated with 50µg/mL human type IV collagen (Sigma C7521). DMEM Fluorobrite (Life Technologies), without phenol red, was used as imaging medium, supplemented with 10% or 0.5% FBS (fetal bovine serum) -depending on experiments-, 1U/mL of penicillin, 20 mM Hepes and 2.5mM L-glutamine. Live cell imaging was then carried out at 37°C and with 5% CO2.

2 Plasmid constructs

In order to test the hypothesis if the LINC complex works as a mechanotransducer, a FRET TSMod biosensor, which can report FRET variations according to the mechanical stress applied to it (Grashoff, Hoffman, Brenner, Zhou, Parsons, Yang, McLean, Sligar, Chen, Ha, & Schwartz, 2010) (Fig 82, left), was inserted into a Mini Nesprin 2G (MiniN2G) construct (Luxton et al., 2010; Ostlund et al., 2009). In comparison to Nesprin 2G full length, MiniN2G is almost devoid of the cytoplasmic domain. Indeed, it only retains the Calponin Homology Domains (CHs)-which connect Nesprin 2G to the actin cytoskeleton and work as an Acting Binding Domain (AB)- plus the Spectrin Repeats (SRs) 1,2 and 55,56 and conserves all the Transmembrane (TM)/KASH (Klarsicht, ANC-1, SYNE, Homology) domain (Fig 82, right).

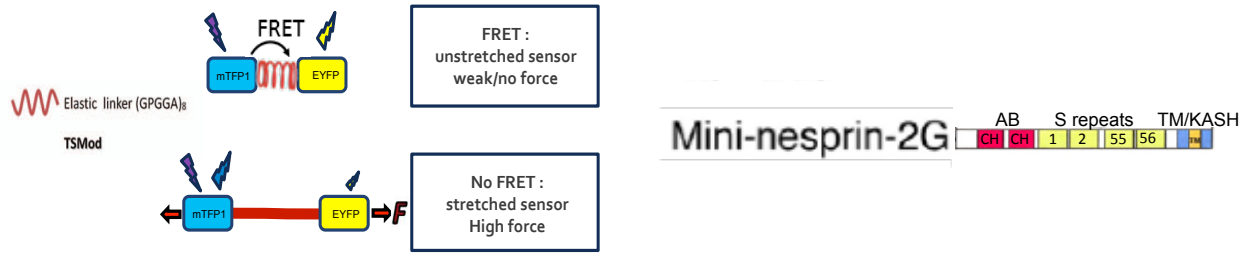

Fig 82: On the left, the FRET TSMod biosensor under rest (above) or under mechanical force (tension, below). Note that the FRET is higher in the resting state because of the close vicinity of the donor fluoropohore (mTFP1 protein, in blue) to the acceptor (EYFP protein, in yellow) fluorophore. On the right, MiniN2G, adapted from (Ostlund et al., 2009). See text for details.

To measure the mechanical force transmission through the LINC complex, the TSMod biosensor was inserted between the SR56 and the TM/KASH domain. The lab thus generated four MiniN2G FRET TSMod constructs (CB,CH, DNKASH and Beyond) (Fig 83A), whose TSMod was obtained from the EcadTSMod construct (N. Borghi et al., 2012) by digestion with the restriction enzymes BspEI and SpEI.

To generate the CB (cytoskeletal binding) construct, which has an intact CH domain, is connected to the actin cytoskeleton and thus can sense mechanical tension, a PCR was carried out on the MiniN2G-GFP construct (Luxton et al., 2010), with the primer pairs indicated in the table 1, in order to obtain the cytoplasmic and the TM/KASH domains. The PCR products and the TSMod were then cloned into a pcDNA3.1 hygro(-) vector (ThermoFisher Scientific), previously digested with the restriction enzyme BamHI, by using In-fusion HD cloning kit (Clontech Laboratories, TaKaRa Bio Inc., Shiga, Japan).

The CH mutant, whose interaction with the actin cytoskeleton is impaired due to two point mutations in the Actin Binding Domain (Ile128 to Ala128 and Ile131 to Ala131) (Luxton et al., 2010) and thus it has been used as "tension-less" control, was made from the CB construct through site-directed mutagenesis (Quikchange II XL, Agilent), by using the primer pair indicated in the table 1.

The lab also generated two other presumed "tension-less" controls: DNKASH-TSMod and "Beyond".

The DNKASH-TSMod construct, which is basically a TSMod biosensor attached to the TM/KASH domain and, thus, cannot undergoing mechanical stretching, was made by ligation, after digestion with the restriction enzyme ClaI, of a PCR product from the CB construct with the primer pair indicated in the table 1.

The "Beyond" construct, displaying the TSMod "beyond" the CH in the N terminus and thus not undergoing mechanical stretching as well, was obtained by PCR amplification on the mN2G-GFP construct with the primer pair indicated in the table 1. The PCR product and the TSMod with a synthetized dsDNA linker were then cloned into a pcDNA3.1 hygro(-) vector as above.

Also, to test the hypothesis if mechanical force sensitivity is propagated within the nucleus through the LINC complex, the lab generated a SUN2-TSMod construct (Fig 83B). In this chimera protein, SUN2 transmembrane and nucleoplasmic domains were obtained from a SUN2-V5 construct (Hodzic, Yeater, Bengtsson, Otto, & Stahl, 2004) by PCR, with the primer pair indicated in the table 1. The PCR products and the TSMod were then cloned into a pcDNA3.1 hygro(-) vector as above.

To understand if LINC complex perturbation is important in terms of α/β-catenin signaling, I replaced the TSMod in the above DNKASH construct with the fluorescent protein mCherry, thus generating the mCherry-DNKASH construct (Fig 83C). I chose the mCherry tag in order to co-express the construct with GFP-tagged α and β-catenins. To do so, the DNKASH-TSMod construct was digested by the restriction enzymes AgeI and HpaI and the mCherry sequence of an mCherry-cSrc construct (from M. Davidson, Florida State University, Tallahassee, FL; 55002; Addgene) was PCR amplified by using the primer pair indicated in the table 1. The digestion and the PCR product were then subjected to homologous recombination by In-fusion.

Lastly, to understand the impact of nuclear α-catenin on β -catenin signaling, I generated an NLS-iRFP-α catenin construct (Fig 83D), by digesting an α catenin-GFP plasmid (a gift from W.J.Nelson) with the restriction enzymes AgeI and SalI and PCR amplifying the cDNA sequence of the iRFP (infraRed Fluorescent Protein) (Filonov et al., 2011) with the primer pair indicated in the table 1. In the forward primer, the NLS (Nuclear Localization Signal) sequence of the oncogene c-myc (Dang & Lee, 1988) was inserted in order to restrict α-catenin into the nuclear compartment. The digestion and the PCR product were then subjected to homologous recombination by In-fusion.

I also employed a plasmid expressing a shRNA directed to α-catenin (a gift from I.G. Macara, University of Virginia, Charlottesville, VA),in order to understand α-catenin's influence on β-catenin nuclear shuttling.

DNA fragment		Sequence 5'→3'
MiniN2G cytoplasmic domain	Fw	CTGGACTAGTGGATCCGAATTCGAGATGGCTAGCCCTGTGCTGCCC
	Rev	CTTTCGAGACTCCGGAGCCTGCTCCTGCTCCTCCACCGGTGTGGGGCATCCTGCTGTCT
MiniN2G TM/KASH domain	Fw	GCTGTACAAGACTAGTGGTGCTGGAGGTGGTGCTGTTAACCTCGACAGCCCCGGCAGC
	Rev	TACCGAGCTCGGATCCCTAGGTGGGAGGTGGCCCGT
CH mutant	Fw	CCATTATCCTTGGCCTGGCTTGGACCGCTATCCTGCACTTTCATATTG
	Rev	CAATATGAAAGTGCAGGATAGCGGTCCAAGCCAGGCCAAGGATAATGG
DNKASH-TSMod	Fw	ACCATCGATGAATTCGAGATGACCGGTGGA
	Rev	TGCAATCGATGGATCCACTAGTCCAGTGTG
Beyond	Fw	GCTGTACAAGACTAGTGGTGCTGGAGGTGGTGCTGTTAACGCTAGCCCTGTGCTGCCC
	Rev	TACCGAGCTCGGATCCCTAGGTGGGAGGTGGCCCGT
dsDNA linker		CTGGACTAGTGGATCCGAATTCGAGATGACCGGTGGAGGAGCAGGAGCAGGCTCCGGAGTCTCGAAAG
SUN2 transmembrane domain	Fw	GCTGTACAAGACTAGTGGTGCTGGAGGTGGTGCTGTTAACACGGACTCAGACCAGCACAG
	Rev	TACCGAGCTCGGATCCCTAGTGGGCAGGCTCTCCGT
SUN2 nucleoplasmic domain	Fw	CTGGACTAGTGGATCCAAGCTTACCATGGGTAAGCCTATCC
	Rev	CTTTCGAGACTCCGGAGCCTGCTCCTGCTCCTCCACCGGTGTAGCCTGCAAGGTCATCCTCTGA
mCherry	Fw	ATTCGAGATGACCGGTATGGTGAGCAAGGGCGAGGAGGATA
	Rev	GGGGCTGTCGAGGTTAACAGCACCACCTCCAGCACCCTTGTACAGCTCGTCCATGCCG
iRFP-NLS	Fw	CGCTAGCGCTACCGGTCGCCACCATGCCTGCTGCTAAAAGAGTTAAATTAGATATGGCTGAAGGATCCGTCGCCA
	Rev	TCATGGTGGCGTCGACTGCAGAATTCGAAGCTTGAGCTCGAGATCTGAGTCCGGACTCTTCCATCACGCCGATCTGC

Table 1: The table lists the primer pairs used to PCR amplify the indicated DNA fragments and the sequence of the dsDNA linker described in the "Plasmid constructs" paragraph.

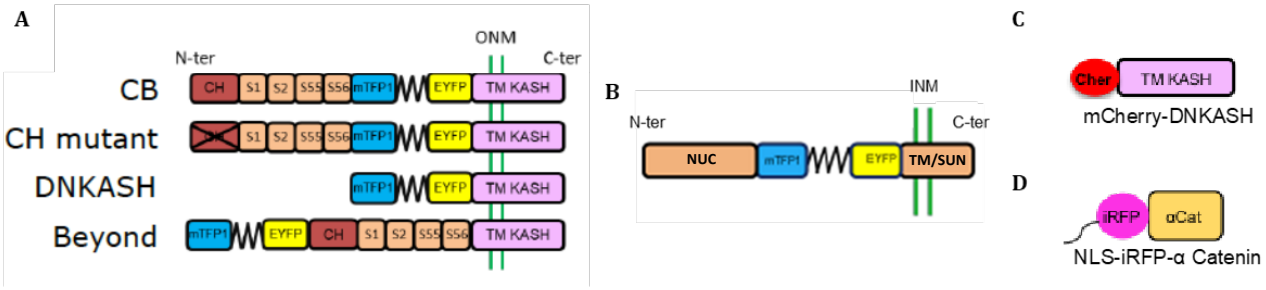

Figure 83: Chimeric constructs. A: the four different MiniN2G FRET TSMod constructs exploited in this work. CB directly derives from MiniN2G (Luxton et al., 2010; Ostlund et al., 2009) plus the insertion of the TSMod (Grashoff, Hoffman, Brenner, Zhou, Parsons, Yang, McLean, Sligar, Chen, Ha, & Schwartz, 2010). Note that the CH mutant, because of its impaired connection to the actin cytoskeleton, is not able to undergo stretching and has been used as "tension-less" control. The other two putative "tension-less" control constructs are DNKASH, where the cytoplasmic domain has been totally removed, and "Beyond", where the TSMod has been cloned "beyond" the CH domain in the N Terminus. N-ter: N terminus; C-ter: C terminus; ONM: Outer Nuclear Membrane. mTFP1 and EYFP proteins are the donor and acceptor fluorophores in the TSMod. B: SUN2-TSMod. SUN/TM: SUN domain and transmembrane domain. NUC: nucleoplasmic domain. INM: Inner Nuclear Membrane. C: mCherry-DNKASH construct.D: NLS-iRFP-α catenin construct. The wavy string attached to iRFP represents the NLS.

3 Transient genetic perturbations

In this work, genetic perturbations comprised either transient expression of mutant as well as chimeric constructs or knocking down the endogenous protein of interest. For transient expression experiments, either mCherry-DNKASH construct or NLS-iRFP-α catenin construct were used. For knockdown experiments, an shRNA construct against α-catenin was exploited. In both cases, transfection was accomplished by using Turbofect reagent according to the instructions provided by the supplier (Thermo Fisher Scientific).

In transient expression experiments, MDCK cells were used during a time window of 48h-72h post-transfection. In the case of knockdown experiments, shRNA construct directed to α-catenin was co-transfected, in a ratio of 1:1, with a plasmid harbouring the plasma membrane protein Lyn fused with an mCherry tag. This in order to visualize co-transfected cells (Fig 84), because of the absence of any fluorescent marker in the shRNA plasmid. In these conditions, more than 90% of co-transfected cells had a decrease of ≈90% in α-catenin content, as shown previously (Nicolas Borghi, Lowndes, Maruthamuthu, Gardel, & Nelson, 2010; Nicolas Borghi et al., 2012). Co-transfected MDCK cells were used 48h post-transfection.

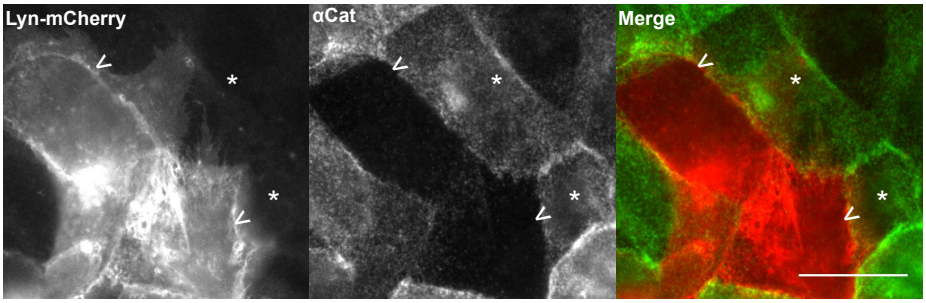

Fig 84: MDCK cells were co-transfected with an shRNA α-catenin plasmid and a Lyn-mCherry plasmid. Arrowheads denote co-transfected cells. Scale bar: 20μm.

4 Pharmacological perturbations

To directly assess the role of the cytoskeleton on the mechanical sensitivity of the LINC complex, Cytochalasin D (to inhibit actin polymerization), Colchicine (to inhibit microtuble polymerization) and Y27632 (to inhibit the RHO kinase ROCK to thus block myosinII activity) were employed. Cytochalasin D was used at 0.5µM final concentration (Sigma, 10 mg/mL in DMSO stock). Colchicine was used at a 1µM final concentration (Sigma, 50 mg/mL in Ethanol stock). Y27632 was used at a 10 µM final concentration (Sigma, 10 mg/mL in water stock). In addition, the lab also evaluated the role of the Ca^{2+}-mediated Adherens Junctions on cytoskeleton/LINC complex force transmission by using EDTA (to chelate Ca^{2+} ions). EDTA was thus used at 1.65 µM final concentration (Invitrogen, 0.5M in water stock).

Finally, to investigate the role β-catenin signalling, I employed LiCl (Lithium Chloride) which, by inhibiting the GSK3 β kinase (Stambolic, Ruel, & Woodgett, 1996), stabilizes β-catenin in its active (neither phosphorylated nor ubiquitinated) form (Van Noort, Meeldijk, Van Der Zee, Destree, & Clevers, 2002) with consequent nuclear β-catenin accumulation (Gayrard et al., 2018). LiCl was used at 30 mM final concentration (105679; Merck Chemicals).

5 Wound Healing and HGF scatter assays

In a cell culture, EMT (Epithelial-Mesenchymal Transition) induction can be achieved through cytokines or growth factors (Thiery & Sleeman, 2006) such as HGF (Hepatocyte Growth Factor) (Weidner et al., 1993), to which I refer to as "HGF scatter assay", as well as by scratching or removing a silicon stamp from a confluent cell monolayer (Stamm et al., 2016), to which I refer to as wound healing (WH) assay. If HGF scatter assay is performed, complete EMT will be promoted (Gayrard et al., 2018)(Fig 85A). If WH assay is carried out, partial EMT will be achieved (Gayrard et al., 2018), which means that only the cells in close proximity to the wound , named as "leaders" (Omelchenko, Vasiliev, Gelfand, Feder, & Bonder, 2003), will display signs of mesenchymal-ness (Fig 85B). The cells present at the back of the wound, namely "followers" (Omelchenko et al., 2003), will not display any typical sign of mesenchymal-ness (Fig 85B).

Since in both HGF and WH assays β-catenin signalling is induced(Gayrard & Borghi, 2016), we thus chose to assess, in these conditions, LINC complex's role in β-catenin signalling as well as to evaluate, in the same context of EMT induction, how the LINC complex tensional state is affected.

To carry out HGF scatter assay, 24 hours before imaging, MDCK cells were plated as $5*10^2/mm^2$ onto round glass coverslips, previously coated with 50µg/mL human type IV collagen (Sigma C7521). MDCK cells were then starved 12h in DMEM supplemented with 0.5% FBS. HGF was finally used at 50ng/mL (Sigma H5691, 20µg/mL in PBS stock).

To perform WH assay, either MDCK cells or NIH 3T3 fibroblasts were cultured at confluence ($5*10^3/mm^2$) around a 5*5mm PDMS (Poly-Di-Methyl-Siloxane,Sylgard 184, Dow Corning) stencil. The PDMS stencil was removed 24h after cell seeding and 48 before imaging. No starvation was carried out in case of WH assay.

It has to be pointed out that in the two assays the starting cell density is different. Indeed, in HGF assay, when the growth factor is added, cells are in small islands of roughly 20cells/island and this allows cells to scatter; in the WH assay, instead, when the PDMS stencil is removed, cells are in a confluent monolayer.

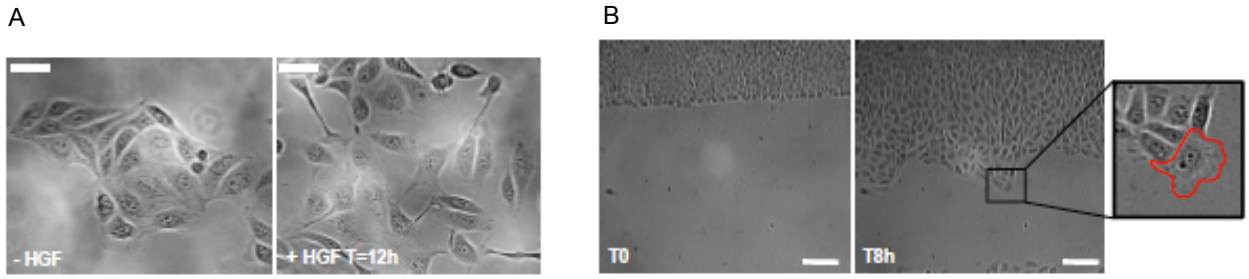

Fig 85: EMT promotion through HGF/WH assays. A: MDCK cells before (left) and 12hours after (right) HGF stimulation. B: MDCK cells imaged at 0h post-wound (left) and at 8h post-wound (right). In the inset, a "leader" cell with visible lamellipodia is shown. Scale bars: A: 20µm; B: 100µm. Adapted from C. Gayrard's PhD manuscript.

6 Nuclear confinement, cell stretching and confined collective migration

To investigate the sensitivity of the LINC complex to extracellular mechanical stimuli, such as nuclear confinement, the lab employed a PDMS microfluidic device -designed by P. Davidson (Davidson, Sliz, Isermann, Denais, & Lammerding, 2015)- with channels consisting of precisely defined constrictions. Basically, the device is made of parallel migration channels with a series of PDMS pillars (Fig 86A and B), which generate different levels of constriction. Seeded cells into the tool can migrate through the constrictions, which deforms the nucleus and makes it adopt an hourglass shape (Fig 86C). The device has made it possible to investigate cell parameters, such as nuclear deformability and cell nucleus velocity through constrictions, over time, with spatially and temporally highly resolved imaging, as demonstrated by Lammerding team (Davidson et al., 2015) (Fig 86C).

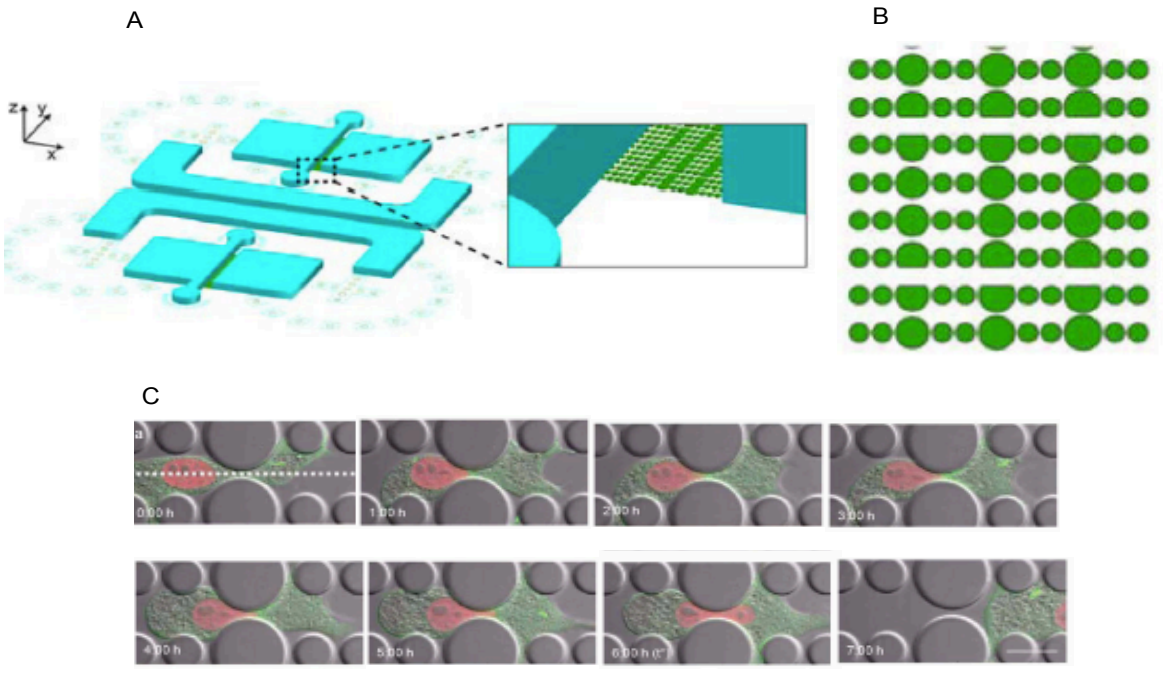

Fig 86: The microfluidic device, with PDMS constrictions to deform cell nucleus. A: schematic bird's eye view of two microfluidic devices with an insight image showing the 5µm-wide constriction channels. B: magnification of the constriction channels. In this case the width, per row, is 2,3 and 5µm, the same that was used in the experiments described in this manuscript. C: 7 h time-lapse imaging showing a fibroblast expressing mCherry-Histone4 (red) and GFP-actin (green) migrating through a 2 µm-wide constriction. Note that nucleus squeezes when cell passes through the constriction. Scale bar: 20µm. Adapted from (Davidson et al., 2015).

In nuclear confinement experiments carried out in our lab, either MDCK cells or NIH 3T3 fibroblasts were seeded into the microfluidic tool, which exhibited 2,3, and 5µm-wide, 5µm high constrictions between adjacent 15-30 µm-wide circular PDMS (Sylgard 184, Dow Corning) pillars.

LINC complex capability to sense cell stretching was also evaluated. To this aim, the lab relied on an experimental design conceived by Damien Cuvelier, from Institut Pierre-Gilles de Gennes, where collagen lines (10µm wide) were micropatterned on thin silicon membranes (Gel pak PF-60-X4; thickness: 150 µm; Teltek (Sonora, CA)) (Fig 87), similarly as shown in Fink's work (Fink et al., 2011). Membranes were thus clamped into a custom-made device, which allowed their stretching through a micrometric screw (Fig 87). In this way, a maximal extension of ~ 25% in ~ 30 s was reached.

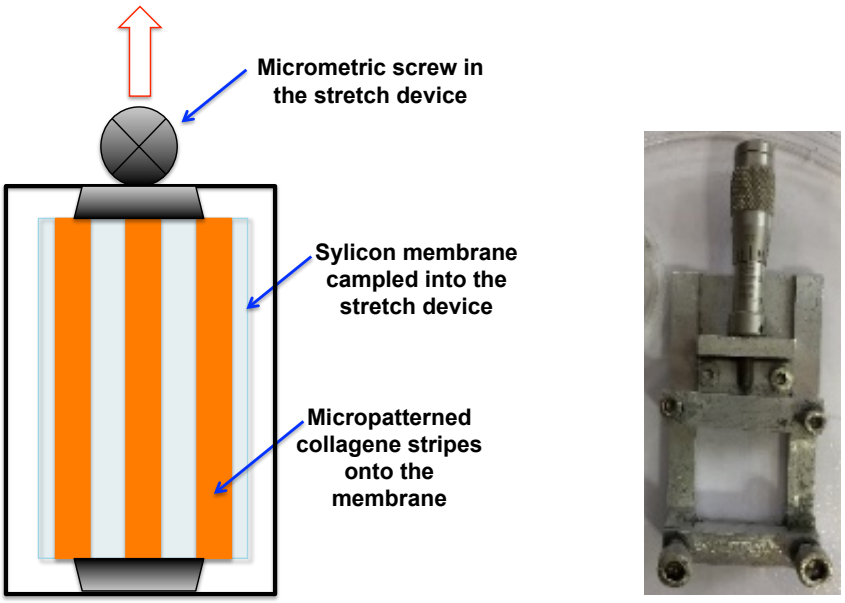

Fig 87: The stretch device (schematic on the left and picture on the right) used in this manuscript. A membrane with micropatterned collagene lines is stretched thanks to the micrometric screw (crossed circle, left image). The arrow points to the direction of the stretch (left image).

A rectangular polydimethylsiloxane 300µL chamber was then attached onto the membrane by using vacuum grease and MDCK cells were seeded for 24 h before stretching. In this setting, FRET was retrieved before (within seconds) and 1 minute after stretching application.

Lastly, to investigate what happens in cells migrating into channels as well as to discriminate which condition -between multicellular unpacking and cell migration speed- affects cytoskeleton-exerted forces on the LINC complex, confined collective migration experiments were carried out. Therefore, MDCK cells were grown at confluence around a PDMS slab exhibiting 100 µm-high, 40 µm-wide micromolded channels (Fig 88) in contact with the coverslip. Cells were then imaged 24 to 48h after seeding.

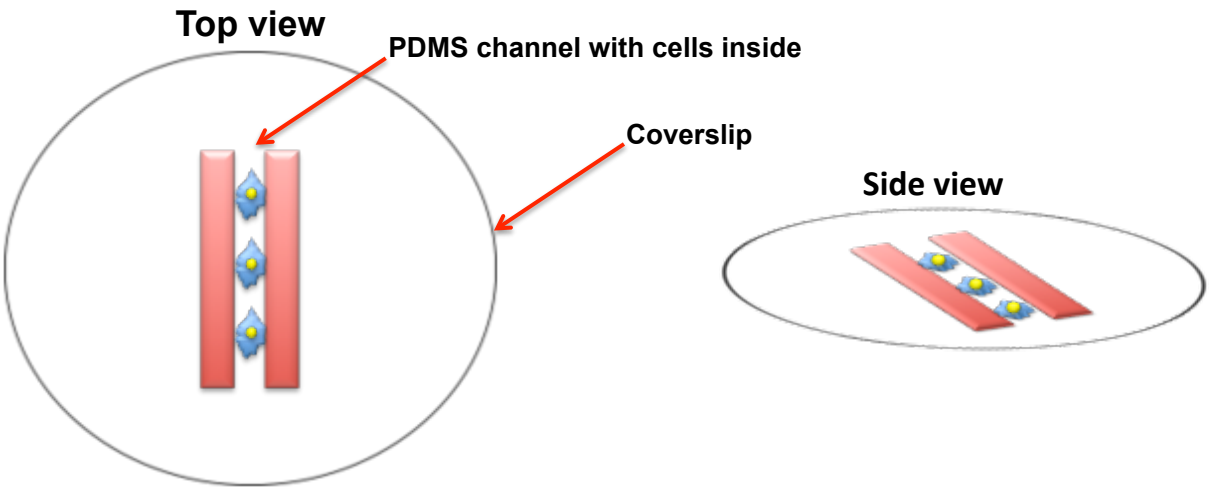

Fig 88: Example of confined collective cell migration within a PDMS micromolded channel.

7 β-catenin dependent gene transcription measurements

In this project, I also focused on evaluating how β-catenin dependent gene transcription is impacted. To test this, I relied on the reporter gene construct TOP-dGFP (Dorsky et al., 2002; Maher, Flozak, Stocker, Chenn, & Gottardi, 2009). Basically, the cDNA sequence of the TOP-dGFP construct comprises four consensus TCF/Lef binding sites and a minimal cFos promoter, which guarantees the transcription of a destabilized GFP (dGFP) transgene (Dorsky et al., 2002) (Fig 89A, B and C). When β-catenin signalling is induced, its nuclear localization allows β-catenin binding to TCF/Lef transcription factors, with consequent dGFP transcription into mRNA and translation into protein (Fig 89C). Once translated, thanks to the presence of the mouse ornithine decarboxylase (MODC) degradation domain, dGFP protein is unstable (hence "destabilized") and rapidly degraded (half-life of 2 hours) compared to wt GFP (X. Li et al., 1998). Thus, the activity of β-catenin dependent gene transcription can be easily assessed and quantified through fluorescence microscopy (Fig 89, right).

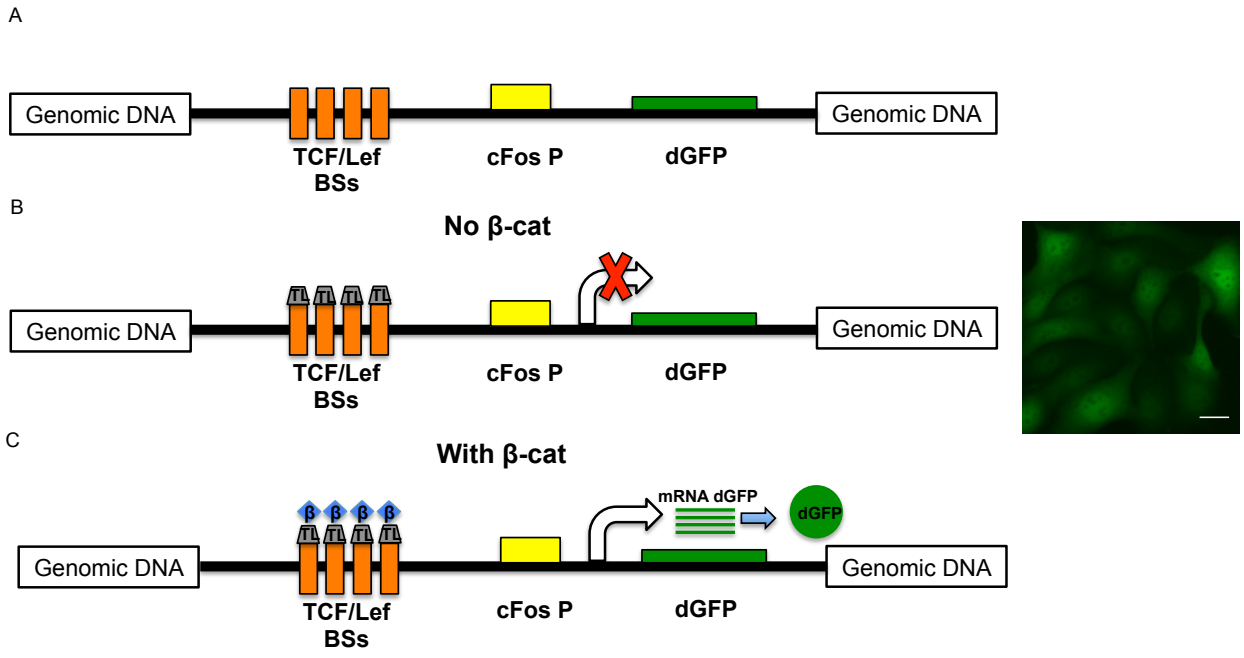

Fig 89: Left: TOP-dGFP reporter construct. A: the construct comprises four TCF/Lef binding sites (BSs) and a c-Fos minimal promoter (P), which regulates dGFP reporter transcription. B: in absence of β-catenin, no transcription of dGFP is carried out. (TL: TCF/Lef transcription factors). C: In presence of β-catenin (β), which binds to TCF/Lef transcription factors, dGFP transcription is activated with subsequent dGFP mRNA translation into protein Right: MDCK cells stably expressing the TOP-dGFP reporter construct. Note that dGFP fluorescence is throughout the cell. Scale bar: 20μm.

8 FRET (Förster Resonance Energy Transfer): background concepts, tension evaluation and image acquisition

8.1 Background concepts

In order to measure forces acting on the LINC complex, this work relied on FRET TSMod biosensors inserted into MiniN2G or SUN proteins. The physical phenomenon of FRET was described and theorized by T. Förster more than 50 years ago (Förster, 1948). Nowadays, FRET is commonly used in biology to study protein-protein interactions and conformational changes (Truong & Ikura, 2001) and it is also exploited in nucleic acids sequencing and Real-Time PCR assays (Didenko, 2001).

Basically, FRET is a physical phenomenon where energy is transferred non-radiatively between two dipoles, the donor (D) and the acceptor (A). In our case, D and A are two fluorescent proteins, namely mTFP1 (Teal Fluorescent Protein 1) and EYFP (Enhanced Yellow Fluorescent Protein) (N. Borghi et al., 2012) or mVenus (Richard N. Day, Booker, & Periasamy, 2008). It has to be noticed that EYFP and mVenus have the same photophysical properties (N. Borghi et al., 2012) and thus can be used interchangeably in FRET biosensors.

If the donor is excited by a photon within its excitation spectrum, it reaches its electronic excited state. Relaxation of this electronic state results in the emission of energy by the donor. If a suitable acceptor is in close proximity to the donor, the energy emission of the latter can be transferred to the former, resulting in acceptor's excitation (Fig 90A) (Gayrard & Borghi, 2016). This reduces both donor's fluorescence lifetime and quantum yield, in comparison to a situation where, in absence of the acceptor, the donor decays only through fluorescence and other non-radiative pathways. While donor is decaying, the acceptor, excited through FRET, decays as well by means of fluorescence (Gayrard & Borghi, 2016).

The rate of energy transfer "k_t" is related to the refractive index "n" of the surrounding molecular environment and to the intrinsic properties of the fluorophores. These are the emission/excitation spectra overlap "J" of the donor and the acceptor and the donor florescence rate "k_f".

The FRET rate is also influenced by the distance "r" between the fluorophores as well as by the angle between the two fluorophores (if the donor and acceptor are parallel, the FRET rate is higher than if they are oriented perpendicularly), namely "orientation factor κ". We can then write the FRET rate as follows: $k_t \approx n^{-4} J k_f * \kappa^2 / r^6$ (1). Consequentially, we can define the FRET Efficiency "E" as the rate of FRET "k_t" normalized to the sum of the rates of FRET, donor fluorescence "k_f" and other non-radiative donor de-excitation pathways (for instance photochemical reactions-such as photobleaching-, dynamic quenching-due to collision between the fluorophores and the quenchers, such as oxygen or halide ions, present in the molecular environment-, intersystem crossing-that is the transition of an excited electron from the singlet to triplet state- (Noomnarm & Clegg, 2009)) "$k_{n\text{-}r}$": $E = k_t / k_f + k_{n\text{-}r} + k_t$ (2)(Gayrard & Borghi, 2016). We can also re-write (2) as follows: $E = 1/[1+(r/R_0)^6]$ (3), where R_0 is defined as the Förster distance, that is the donor/acceptor distance at which FRET Efficiency is 50%(Ni & Zhang, 2010). As evidenced in (3), FRET Efficiency depends on the inverse sixth power of

the intermolecular separation between the fluorophores, which means that small variations in the distance between donor and acceptor can result in sharp variations in FRET Efficiency (Fig 90B).

There exist different ways to acquire FRET signal and compute its Efficiency (see (Gayrard & Borghi, 2016) for an overview). In the experiments present in this manuscript, FRET signal was acquired through acceptor sensitized emission, where a continuous laser is used to excite the donor, with concomitant acquisition of both donor and acceptor emission fluorescence (Gayrard & Borghi, 2016) (Fig 90C). FRET Efficiency was then calculated as follows: $E=(1-a(1-E_R))/(1-b(1-E_R))$ (4). In (4), "E_R" is the FRET Index, that is basically the ratio between the fluorescence emission intensity of the acceptor and the sum of this latter plus the fluorescence emission intensity of the donor (I acceptor/I acceptor+I donor), and a and b account for donor spectral bleed-through, acceptor direct excitation and differences in donor versus acceptor absorption cross-sections and detection efficiencies (N. K. Lee et al., 2005).In order to calculate FRET Efficiency, it is important to calibrate FRET Index by using some FRET biosensor standards. The lab thus relied on two previously described FRET biosensor standards (Richard N. Day et al., 2008): mTFP1-5aa-Venus (referred to as 5aa) and mTFP1-TRAF-Venus (referred to as TRAF) constructs (Fig 90D). Both the constructs have the same donor/acceptor protein pair (Teal Fluorescent Protein 1-hence mTFP1- and Venus, respectively) but a different linker in between: a five amino-acid one in the case of 5aa and a 229 amino-acid one -derived from the Tumor Necrosis Factor Receptor Associated Factor (hence TRAF) domain- in the case of TRAF (Richard N. Day et al., 2008). By virtue of these two different linkers, 5aa works as a High FRET Index standard in comparison to TRAF, which is the Low FRET Index standard. By using these two standards, the above a and b coefficients were calculated as follows: $a=(E_H(1-E_{R,H}) - E_L(1-E_{R,L}) + E_HE_L(E_{R,H} - E_{R,L}))/c$ and $b=(E_H(1-E_{R,L}) - E_L(1-E_{R,H}) + E_{R,L} - E_{R,H})/c$, with $c=(E_H - E_L)(1 - E_{R,H})(1 - E_{R,L})$, where $E_{R,H}$ and $E_{R,L}$ are the 5aa and TRAF FRET Indices measured in the lab, (Fig 90E), and E_H and E_L their FRET Efficiencies, whose values were previously published by Day et al. (Richard N. Day et al., 2008). Then, a and b coefficients were used to calculate FRET Efficiency as shown in (4), where E_R had been previously computed for each single experiment performed (see paragraph 8.3 in this chapter).

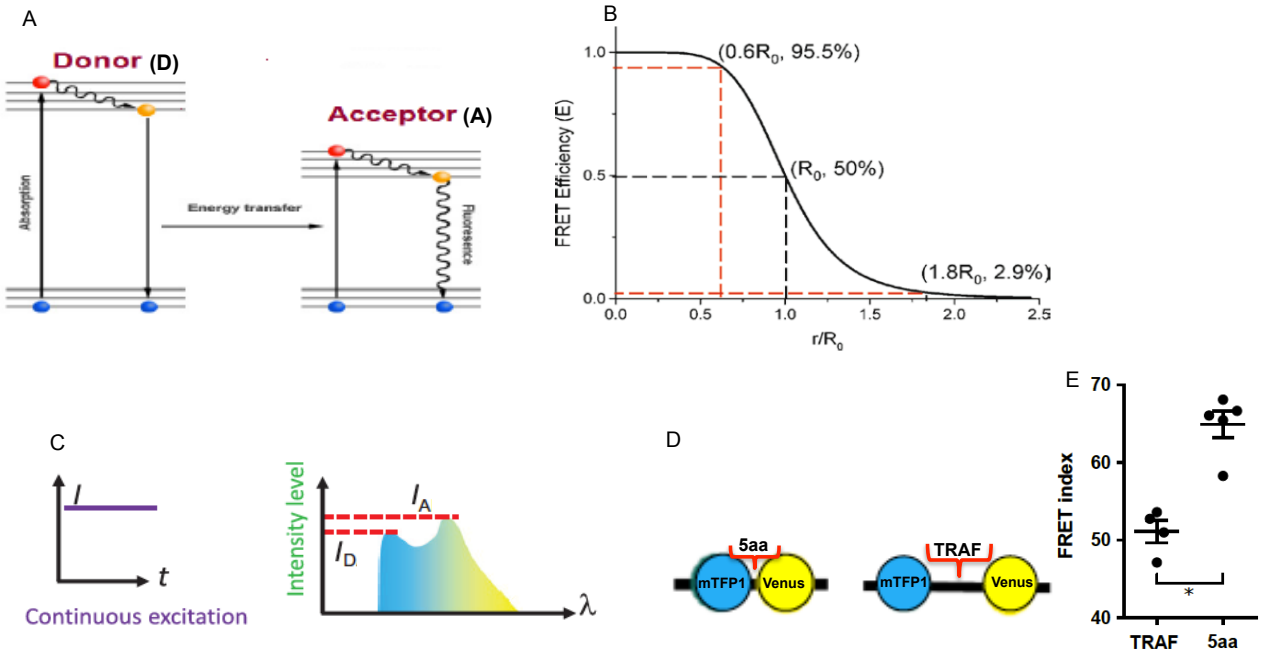

Fig 90: A: Jablonski diagram depicting the FRET phenomenon. When the donor molecule in its electronic excited state relaxes, it emits energy (without emitting a photon) that can be transferred to an acceptor molecule in a non-radiative way. As a result, the excited acceptor fluoresces while relaxing. Adapted from: (Hussain et al.,

2014). B: FRET Efficiency depends on the inverse sixth power of the intermolecular separation between donor and acceptor. Adapted from: (Ni & Zhang, 2010). C: acceptor sensitized emission. Upon continuous donor excitation through time (*I* versus *t* graph), it is possible to retrieve a donor/acceptor emission spectrum (λ) from which I_A (acceptor emission fluorescence intensity) and I_D (donor emission fluorescence intensity) can be estimated. Adapted from: (Gayrard & Borghi, 2016). D: The FRET standards of High (5aa) and Low (TRAF) FRET Index consist of the same donor/acceptor protein pair (mTFP1 as the donor and Venus as the acceptor) but with a different amino-acidic linker in between: 5aa and TRAF. Adapted from: (Gayrard & Borghi, 2016). E: FRET Index of 5aa and TRAF standards expressed in MDCK cells (n(number of cells analyzed for each condition)=4). Mean ± SEM. *p<0.05 with Mann–Whitney.

8.2 Tension evaluation

In this work, we wanted to understand if the LINC complex was under tension. To this aim, we relied on FRET TSMod biosensors inserted into MiniN2G and SUN2 proteins. Specifically, the TSMod biosensor we employed comprises a FRET pair consisting of fluorescent proteins, namely mTFP1 as the donor and EYFP as the acceptor, separated by an elastic linker (Grashoff, Hoffman, Brenner, Zhou, Parsons, Yang, McLean, Sligar, Chen, Ha, & Schwartz, 2010) (Fig 91A). The elastic linker is derived from a 40 amino-acid spider silk flagelliform sequence ($GPGGA_8$), which can act as a linear spring (Brenner et al., 2016) and is suitable for measuring forces in the range of piconewtons (pN) (Becker et al., 2003), with sensitivity to forces from 1 up to 6 pN (Grashoff, Hoffman, Brenner, Zhou, Parsons, Yang, McLean, Sligar, Chen, Ha, & Schwartz, 2010) Indeed, by combining confocal scanning fluorescence microscopy with optical tweezers -a technique referred to as "single-molecule fluorescence force spectroscopy" (Hohng et al., 2007)- Grashoff et al. were able to calibrate the TSMod, thus retrieving the force associated to each single FRET Efficiency value (Grashoff, Hoffman, Brenner, Zhou, Parsons, Yang, McLean, Sligar, Chen, Ha, & Schwartz, 2010). To accomplish this, they generated a version of the TSMod (referred to as TSModCy) by using the organic fluorophores Cy3 and Cy5 instead of fluorescent proteins. This choice was made since fluorescent proteins have low photostability and thus it is difficult to make single-molecule FRET measurements. The elastic linker was placed in between a polymer-coated glass surface and the two fluorophores were attached to DNA tethers, so that Cy3 and Cy5 were in close proximity to the terminal cysteines of the elastic linker. With such a configuration (Fig 91B), Grashoff et al. could estimate the linker end-to-end distance as a function of force from FRET measurements. After several stretch-relax cycles, a calibration curve displaying FRET Efficiency versus Force was determined (Fig 91 C). As the graph points out, the FRET Efficiency is inversely correlated to the Force: the higher the Force, the lower the FRET Efficiency. The researchers were then able to match the values obtained from the FRET Efficiency/Force calibration curve of the TSModCy with the TSMod, since both the sensors had the same Förster distance of ≈6.0 nm. Indeed, even though the zero-force FRET Efficiency of the two sensors was different (≈50% for TSMod and ≈23.5% for TSMod), the addition of 1.3nm to the observed extension in the TSModCy made the zero-force FRET Efficiencies match (Grashoff, Hoffman, Brenner, Zhou, Parsons, Yang, McLean, Sligar, Chen, Ha, & Schwartz, 2010). It is therefore clear that, by taking into account the FRET Efficiency versus Force calibration curve (Fig 91C) and by determining the FRET Efficiency through the FRET Index (see (4) in paragraph 8.2 of this chapter), it is possible to associate a value of Force to an every single FRET Index value that we can compute.

To work properly, the biosensor has to be inserted into a protein site suspected to bear mechanical forces (Gayrard & Borghi, 2016). Therefore, if a target protein harbouring the TSMod construct undergoes mechanical forces, the biosensor will translate these forces into FRET Index variations. TSMod was initially designed to detect tensional forces acting onto proteins of interest, as found for vinculin and E-cadherin (N. Borghi et al., 2012; Grashoff, Hoffman, Brenner, Zhou, Parsons,

Yang, McLean, Sligar, Chen, Ha, & Schwartz, 2010), and, more recently, for Nesprin 2G (Arsenovic et al., 2016). However, TSMod was also reported to be sensitive to mechanical compression. Indeed, TSMod inserted into vinculin exhibited compression in MEFs (murine embryonic fibroblasts) seeded onto micropatterns(Rothenberg, Neibart, LaCroix, & Hoffman, 2015), as well as when cloned into the glycolyx protein MUC1 (present in adhesive contacts with integrins) in non-malignant MECs (mammary epithelial cells) (Paszek et al., 2014).Therefore, if the target protein harbouring the biosensor is compressed, by virtue of the elastic linker the distance between the donor and the acceptor will be decreased with a following FRET Index increase. Conversely, if the protein is stretched, the distance between the donor and the acceptor will be increased with a following decrease in the FRET Index (Gayrard & Borghi, 2016) (Fig 91D). Thus, it is possible to evaluate, in real time, if the protein of interest is under tension or compression.

In order to establish if our protein of interest really senses mechanical cues, it is mandatory to generate some “tension -less" controls. To do so, it is possible to either delete/ mutate protein domains supposed to bear mechanical loading or cloning the TSMod at the N/C termini of the target protein (Gayrard & Borghi, 2016).

Throughout this manuscript, we indicate with “CB” the MiniN2G TSMod construct that can account for mechanical forces and with “CH” the MiniN2G TSMod construct that has an impaired connection to the actin cytoskeleton (see paragraph 2 of this chapter) and thus works as “tension-less” control (Fig 91E). In the DNKASH construct as well as in the Beyond construct, instead, the TSMod is supposed not to be under tension because of either the lack of the CH domains (DNKASH construct) or the different location (at the N-terminus) of the TSMod (Beyond construct). In both cases, no direct actin cystokeleton-generated tension is applied to the biosensor (Fig 91 E).

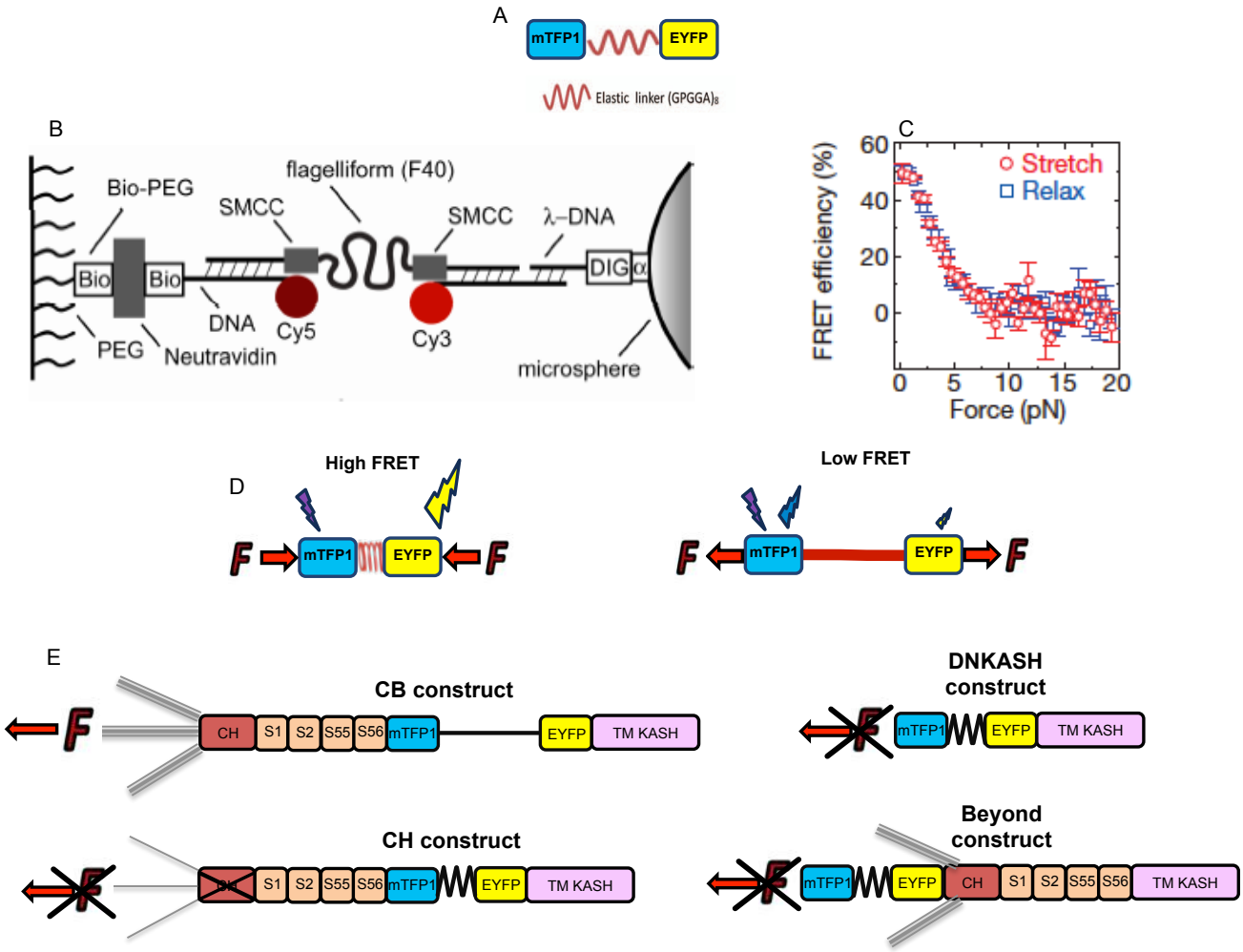

Fig 91: A: schematic of the TSMod biosensor exploited in this manuscript. B and C: TSModCy calibration. B: configuration used to calibrate the TSModCy. C: after cycles of stretch-relax, a calibration curve of FRET Efficiency versus Force is generated. FRET Efficiency and Force are inversely correlated. Adapted from (Grashoff, Hoffman, Brenner, Zhou, Parsons, Yang, McLean, Sligar, Chen, Ha, & Schwartz, 2010). D: Upon compression (left), the FRET phenomenon is high because of the close proximity of the donor to the acceptor. If stretching is applied (right), the increased distance between the donor and the acceptor will determine a lower FRET. E: MiniN2G TSMod constructs used in this work. Actin filaments are depicted in grey. The intensity of the grey lines represents the normal or the impaired connection to the actin cytoskeleton.

8.3 Image Acquisition

We performed spectral acquisition on a confocal microscope (Carl Zeiss LSM 780) with a 63x/1.4NA Plan-Apochromat oil immersion objective. Exciting mTFP1 with the 458 nm line of a 25-mW argon laser, we retrieved donor/acceptor emission at the spectral resolution of 8.7nm within the 476–557nm range (Fig 92). Typically, for timelapse experiments involving nuclear confinement, wound healing and confined cell migration, images were acquired every 10 minutes for a time window of ≈ 15 hours. For experiments involving HGF scatter assay, we set a timelapase acquisition window of 12 hours with images taken every 30 minutes.

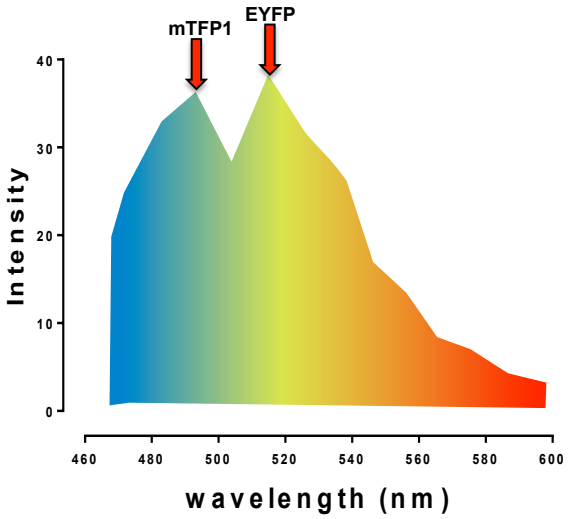

Fig 92: Spectral emission of mTFP1 and EYFP upon excitation of mTFP1. The arrows point to the excitation peaks.

To quantify the FRET signal, fluorescent images were analyzed in Image J by using the Fiji distribution and the PixFRET plugin, even though FRET analyses can be also performed without PixFRET (see Annex 2 in Chapter 8). All the channels were background-subtracted, Gaussian smoothed (radius=1pixel) and thresholded (above ~3-5% of the 12bits range). The FRET Index was then computed pixel-by-pixel as $I_{EYFP}/(I_{mTFP1}+I_{EYFP})$, where I_{mTFP1} and I_{EYFP} are the intensities in 494nm and 521nm donor and acceptor channels, respectively. By doing so, it is possible to generate a FRET Index map which represents, pixel by pixel, the different FRET Index values throughout the image (Fig 93A). Notably, the FRET Index map does not represent fluorescence intensities anymore. For this reason, it is better to select the Region of Interest (ROI) to analyze on the direct fluorescence image -which can be, for instance, the one taken from the acceptor channel-, since it is the most intense and, thus, well suited for choosing ROIs. In our case, ROIs (0.3-0.5 µm in width, that is the average nuclear envelope width) were traced along the nuclear envelope and then reported on the FRET Index map for quantification. The FRET Index was then computed for each single nuclear envelope as the mean of all the pixel values composing that nuclear envelope.

In this manuscript, FRET Index values are displayed with a scatter plot in Graphpad PRISM V. In this specific graph, each single point represents one nuclear envelope and, thus, one cell (Fig 93B). Such a way to visualize values gives us a clear vision of the whole FRET Index values distribution all over an entire cell population. The Standard Error of the Mean (SEM) is reported as well.

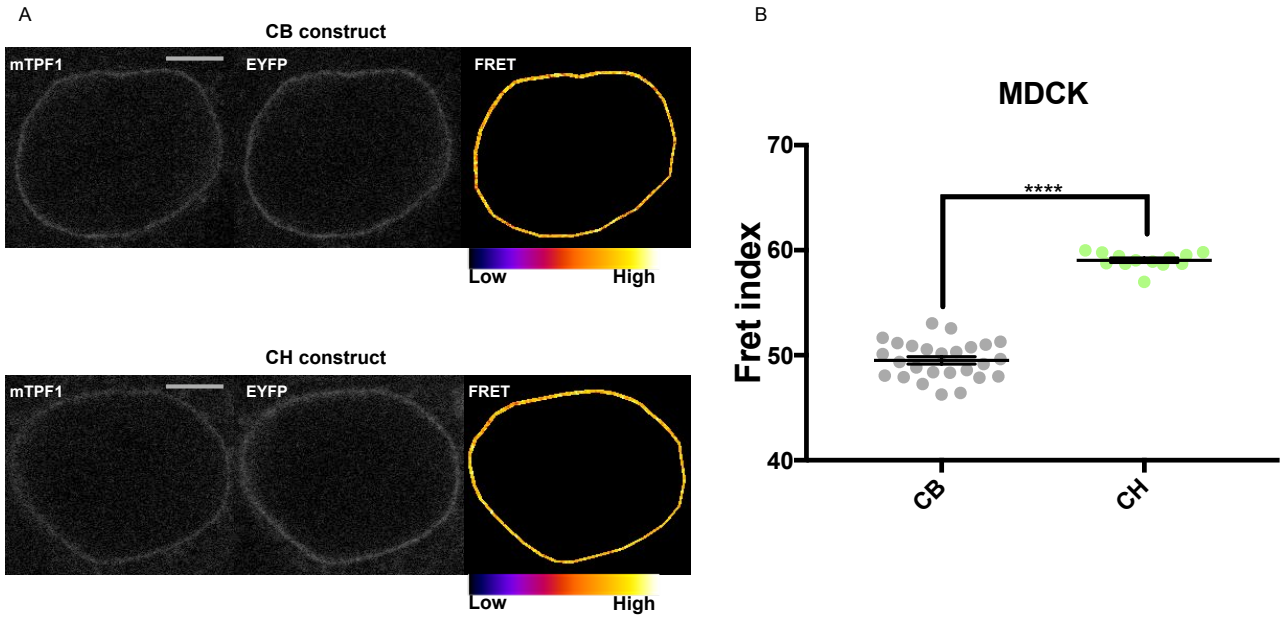

Fig 93: FRET Index measurements for CB and CH constructs. A: for CB and CH constructs, the fluorescence images acquired in both donor (mTFP1) and acceptor (EYFP) channels plus the FRET Index maps are shown. B: FRET Index values in MDCK cells represented as a scatter plot. Note that the "tension-less" CH construct displays higher FRET Index values in comparison to the CB construct. Scale bars: 5µm. "Low" and "High" stand for low and high FRET Index values. (n(number of cells analyzed) CB=26; nCH=16). Mean ± SEM. ****p<0.0001 with Mann–Whitney.

9 Immunostaining

In order to assess α-catenin co-localization with Nesprin 2G as well as the dominant negative effect of the mCherry-DNKASH construct, MDCK cells (either stably expressing α catenin-GFP or transfected with the mCherry-DNKASH construct) were immunostained with the following procedure. Briefly, after rinsing in PBS, cells seeded on glass coverslips were fixed in 4% PFA (Electron Microscopy Science) for 15 min at room temperature, permeabilized with 0.5% Triton X100 in PBS for 5 min at 4°C, incubated with 50mM NH4Cl in PBS and blocked for 30 min at room temperature with 1% BSA (Jackson Immunology) in PBS (blocking solution). Cells were then stained with anti-Nesprin 2G rabbit antibody directed against the CH domain of Nesprin 2G (dilution: 1/500) in blocking solution for 2h at room temperature, followed by incubation with Dylight 650 or Dylight 488 secondary antibody (dilution: 1/500) (ThermoFisher) for 45 min at room temperature. Coverslips were then mounted in Fluoromount medium (Sigma).

10 Fluorescence imaging and analysis

In order to evaluate α/β-catenin signaling in normal, LINC complex disruption and α-catenin knockdown contexts (with or without HGF/LiCl treatments), we also carried out non-FRET fluorescence imaging. We thus performed experiments either on a confocal microscope (Carl Zeiss LSM 780), with a 63x/1.4NA oil immersion objective, or on a widefield microscope (Carl Zeiss Axio Observer Z.1), with a 25x/0.8NA oil immersion objective. On the confocal, GFP in α/β-catenins was excited with the 488nm line of the argon laser; mCherry in the DNKASH construct was excited with the 561nm line of the 15mW DPSS laser and we employed the 633nm line of the 5mW HeNe laser to excite Dylight 650 (to visualize Nesprin 2G in immunostaining). The emissions were then collected between 498-561nm (α catenin-GFP and β catenin-GFP), 570-650nm (mCherry-DNKASH) and 638-755nm (Nesprin 2G) on PMT detectors. On the widefield, the fluorophores were excited with a LED lamp

(CoolLED pE-300 white) by using BP excitation filters 450-490nm (β catenin-GFP and Dylight 488), 538-562nm (mCherry-DNKASH and Lyn-mCherry) and 625-655nm(NLS-iRFP-α catenin). Emissions were then acquired through BP emissions filters 500-550nm (β catenin-GFP and Dylight 488), 570-640nm (mCherry-DNKASH and Lyn-mCherry) and 665-715nm (NLS-iRFP-α catenin) on an sCMOS camera (OrcaFlash4 LT, Hamamatsu).

Fluorescence images were then analyzed in ImageJ, by using the Fiji distribution. All channels were background-subtracted. Mean pixel intensities were measured within the boundaries of the selected ROIs (cytoplasm, nucleus and nuclear envelope, which was segmented from the anti-Nesprin 2 G antibody or mCherry-DNKASH signals).

11 Statistics

Throughout the manuscript, data are presented as mean ± SEM. P-values were calculated from unpaired, non-parametric, two-tailed tests (Mann–Whitney for 2 conditions/experiment or Kruskal-Wallis for more than 2 conditions/experiment) in GraphPad Prism V software. n.s.: statistically non-significant. ****:<0.0001, ***:<0.001, **:<0.01, *<0.05. R was calculated from linear regression by the least-square method.

CHAPTER 6

Results

In this chapter, I will explain the experimental results achieved during my PhD. Most of these results are included in an already submitted manuscript, whose preprint can be reached by the following link: www.biorxiv.org/content/10.1101/744276v1

Table of contents

1 The LINC complex is simultaneously under specific tension and unspecific compression

To assess the tension exerted on the LINC complex, the lab used MDCK type II G (hereafter MDCK) as well as NIH 3T3 (hereafter 3T3) cell lines stably expressing the previously described chimeric constructs (see paragraph 2 in Chapter 5) derived from the short variant of nesprin2G (MiniN2G) - known to rescue the nucleus positioning function of the full-length protein (Luxton et al., 2010)- and harbouring the FRET tension sensor module (TSMod) (Grashoff, Hoffman, Brenner, Zhou, Parsons, Yang, McLean, Sligar, Chen, Ha, & Schwartz, 2010) (Fig 94A). As expected, colonies of MDCK and 3T3 cells stably expressing the construct able to bind the cytoskeleton (CB) exhibited a FRET index significantly lower than that of the CH mutant, supporting that the CB construct is under mechanical tension due to specific interaction with the cytoskeleton (Fig. 94B and C). Surprisingly, the two other control constructs (DNKASH and Beyond) exhibited FRET indices lower than that of the CH mutant and in most cases indistinguishable from that of the CB construct (Fig. 94 B and C). This suggests that the SRs exert or mediate a steric hindrance on the tension sensor module akin to compression that is alleviated upon specific interaction with the cytoskeleton. Altogether, these results show that

nesprin2G appear simultaneously constrained by its SRs and under mechanical tension upon specific binding to the cytoskeleton, which will be further discussed in Chapter 7.

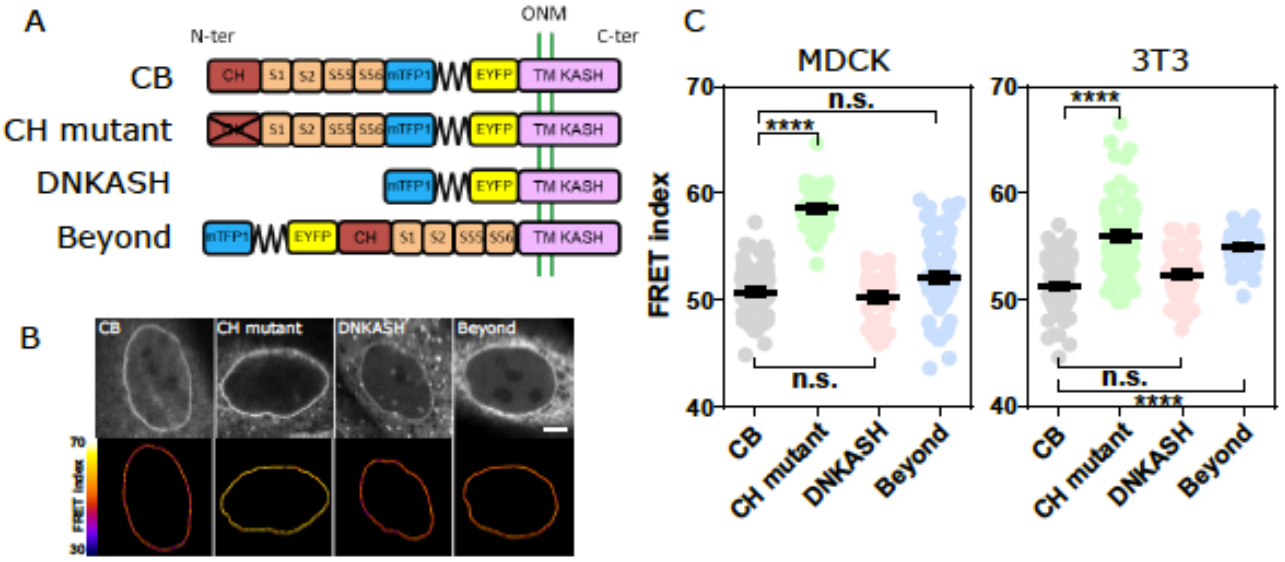

Fig 94: **Nesprin 2 is under cytoskeleton-dependent tension and cytoskeleton-independent compression.** A: schematics of the nesprin constructs. CB: cytoskeleton binding. CH: calponin homology domain. DNKASH: dominant negative KASH. ONM: Outer Nuclear Membrane. S1…S56: Spectrin repeat number. TM: Trans-Membrane. N-term: N-terminus. C-term: C-terminus. B: typical nuclei expressing the nesprin constructs above. Top: direct fluorescence. Bottom: FRET index map. C: FRET index of the nesprin constructs above in MDCK (left) (n(number of cells analyzed)=97 CB, 45 CH mutant, 34 DNKASH, 35 Beyond), and 3T3 (right) (n=88 CB, 89 CH mutant, 60 DNKASH, 62 Beyond) cells. Scale bar=5 µm. Mean ± SEM. Kruskal-Wallis test.

2 Tension on the LINC complex is exerted by contractile cytoskeletal networks and it is balanced by cell adhesion

To assess the influence of the cytoskeleton on nesprin2G tension, MDCK colonies were exposed to pharmacological inhibitors. The CB construct exhibited a significant FRET index increase in MDCK cells exposed to either the actin polymerization inhibitor cytochalasin D, the ROCK inhibitor Y27632 or the microtubule polymerization inhibitor colchicine (Fig. 95A and B). This supports that nesprin2G tension requires myosin contractile activity and intact microtubule and filamentous actin networks. In contrast, the CH mutant did not exhibit significant FRET index changes in those conditions (Fig. 95A and B), indicating that disrupting actomyosin or microtubules does not further relieve tension when the cytoskeletal-binding domain is mutated. The tension generated by the cytoskeleton is thus exerted through the intact CH domain exclusively.

To examine how this cytoskeleton-generated tension exerted onto nesprin2G was balanced, calcium-dependent cell adhesion between MDCK cells was perturbed by exposure to the calcium chelator EDTA. Impaired cell adhesion resulted in an increase of FRET index in the CB construct, but not in the CH mutant (Fig. 95A and B). This supports that cell adhesion is involved in balancing the cytoskeletal tension on nesprin2G.

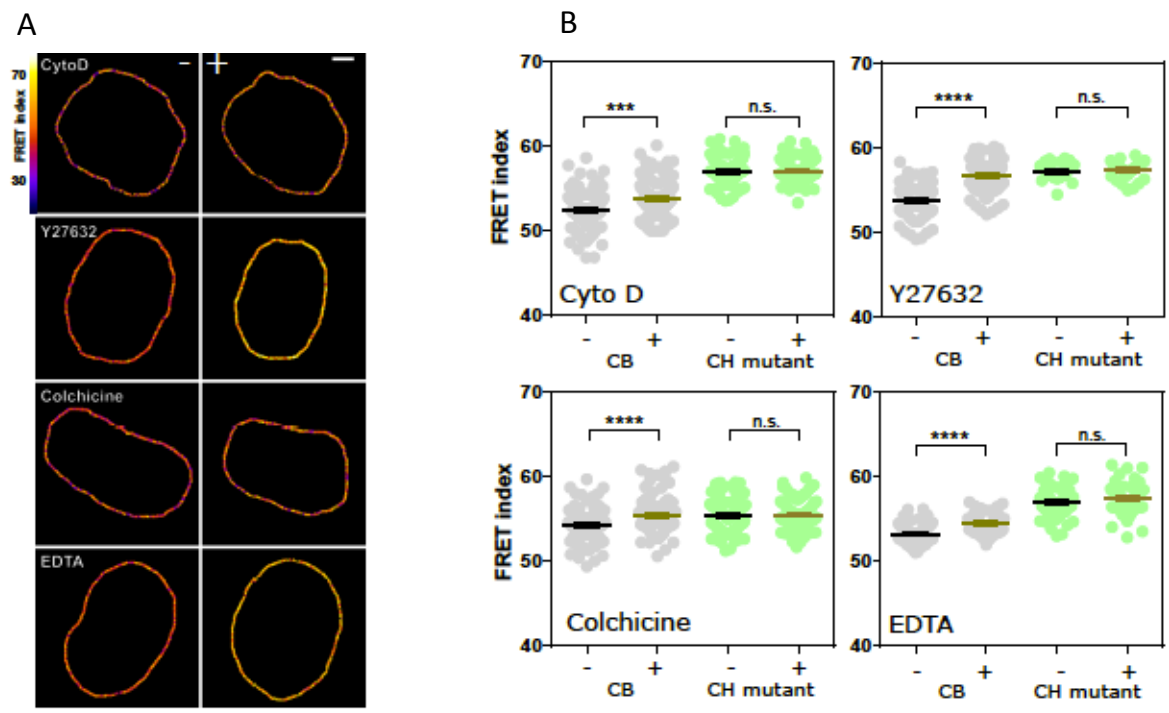

Fig 95: **Tension on nesprin 2 is exerted by contractile cytoskeleton and it is balanced by cell adhesion.** A: FRET index map of the CB construct before (-) and after (+) pharmacological perturbations. Cyto D: cytoshalasin D. B: FRET index of the CB construct and the CH mutant before and 20 min after pharmacological perturbations (n Cyto D = 108 CB, 71 CH mutant, n Y27632 = 74 CB, 30 CH mutant, n Colchicine = 112 CB, 88 CH mutant, n EDTA = 48 CB, 52 CH mutant). Scale bar=5 µm. Mean ± SEM. Mann-Whitney test.

3 Tension on the LINC complex is sensitive to extracellular mechanical cues

To test nesprin2G sensitivity to extracellular mechanical cues, MDCK and 3T3 cells were first allowed to individually migrate through constrictions within the channels of the previously described PDMS microfluidic device (Davidson et al., 2015) (see paragraph 6 in Chapter 5). As cells migrated through constrictions, nucleus squeezing was accompanied by an increase in FRET index of the CB construct in nuclear regions within constrictions compared with regions outside constrictions (Fig. 96A and B). In contrast, the CH mutant exhibited an increase in FRET within constrictions that was not statistically significant. Therefore, these results support that cell migration through narrow constrictions reduces cytoskeleton-generated tension on nesprin2G in the region that is squeezed.

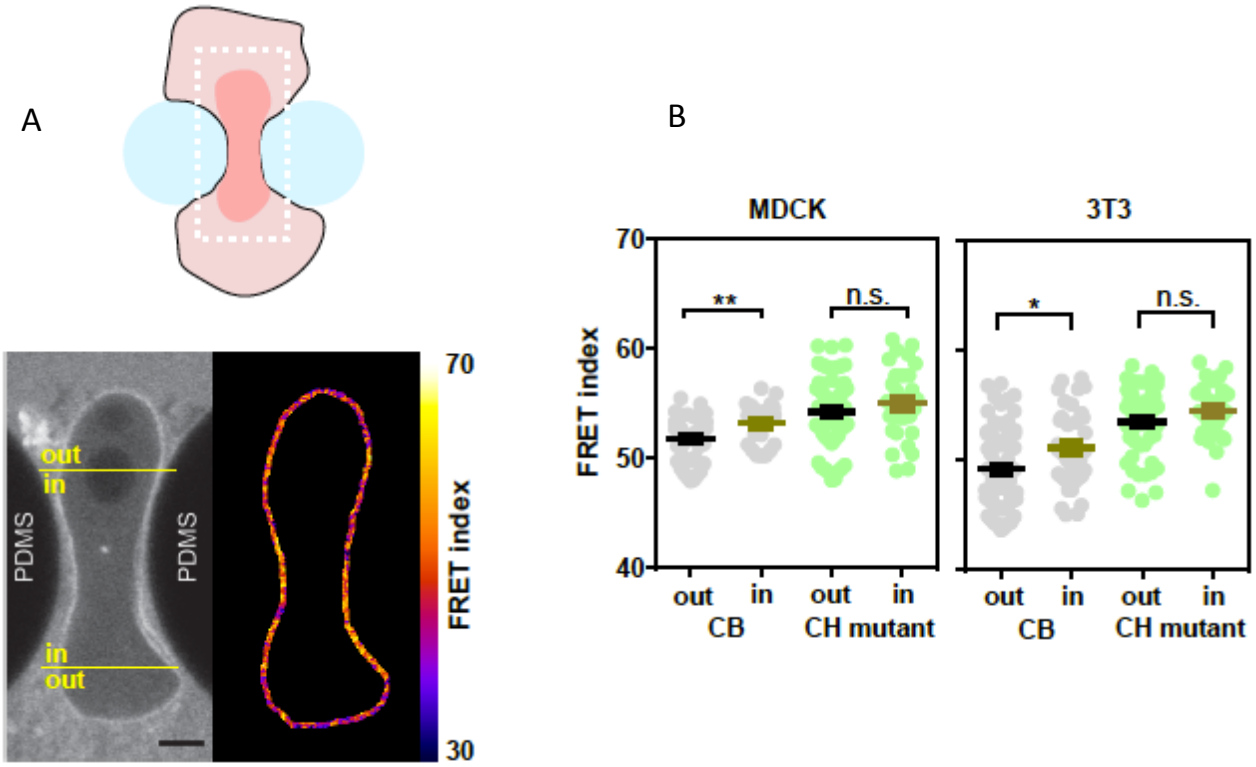

Fig 96: **Nesprin 2 tension is sensitive to extracellular compression.** A, top: schematic of an event of cell migration through a narrow constriction. A, bottom: direct fluorescence image and FRET index map from the dotted box above with boundaries between the region within the constriction and that outside. "PDMS" to indicate the constriction pillars. B: FRET index of the CB construct and the CH mutant inside and outside constrictions, in MDCK (left) (n= 24 CB, 40 CH mutant) and 3T3 (right) (n= 48 CB out, 38 CH mutant) cells. Scale bar=5 µm. Mean ± SEM. Mann-Whitney test.

Next, nesprin2G tension sensitivity to cell substrate stretching was tested. To do so, MDCK cells were plated on adhesive patterns at the surface of a stretchable elastomer sheet substrate (Fink et al., 2011) (see paragraph 6 in Chapter 5). Upon uniaxial substrate stretching, the FRET index in the CB construct significantly decreased in proportion to both cell and nucleus strains, while it did not in the CH mutant (Fig. 97A and B). Thus, nesprin2G tension is sensitive to cell substrate stretching through the cytoskeleton.

Altogether, these results show that nesprin2G tension is sensitive, through the cytoskeleton, to extracellular deformations both in compression and stretch.

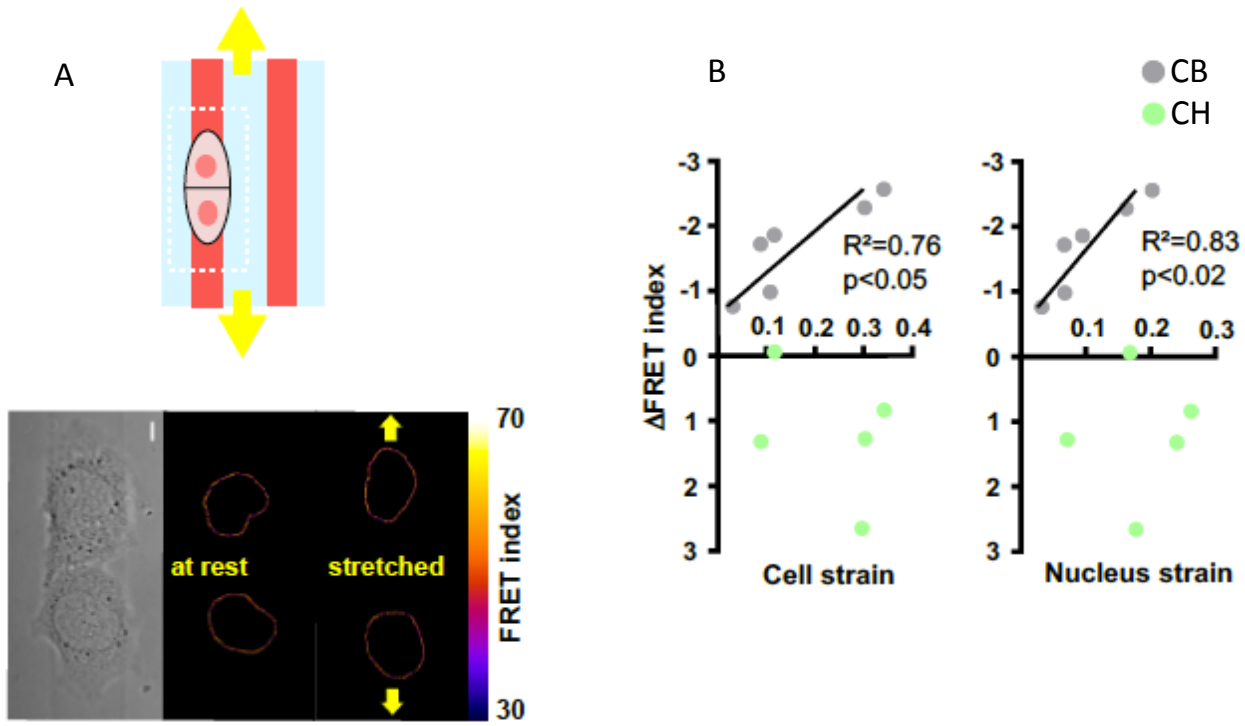

Fig 97: **Nesprin 2 tension is sensitive to extracellular stretch.** A, top: schematic of the cell stretching experiment. Cells are plated on collagen stripes printed on a transparent, elastomeric sheet stretched in the direction of the adhesive stripes. A, bottom: direct fluorescence image and FRET index map from the dotted box above. B: FRET index change upon stretching of the CB construct (gray dots) and the CH mutant (green dots) as a function of cell and nucleus strains. (n= 6 CB, 5 CH mutant). Scale bar=5 µm. Solid lines are linear fits. R was calculated from linear regression by the least-square method.

4 Cells sense cell packing within the nucleus through the cytoskeleton and the LINC complex

To test how nesprin2G responds to cell packing, cells plated at low density in colonies as in previous experiments ($5*10^2$ cells/mm^2, referred to as 1X) were compared with cells at confluence ($5*10^3$ cells/mm^2, referred to as 10X). In cells at confluence, the nucleus cross-sectional area was much smaller (Fig. 98A), and the CB construct exhibited a much higher FRET index than in cells at low density, while the CH mutant did not (Fig. 98B and C). Tension on nesprin2G is thus dependent on cell density, in a manner that depends on cytoskeleton binding.

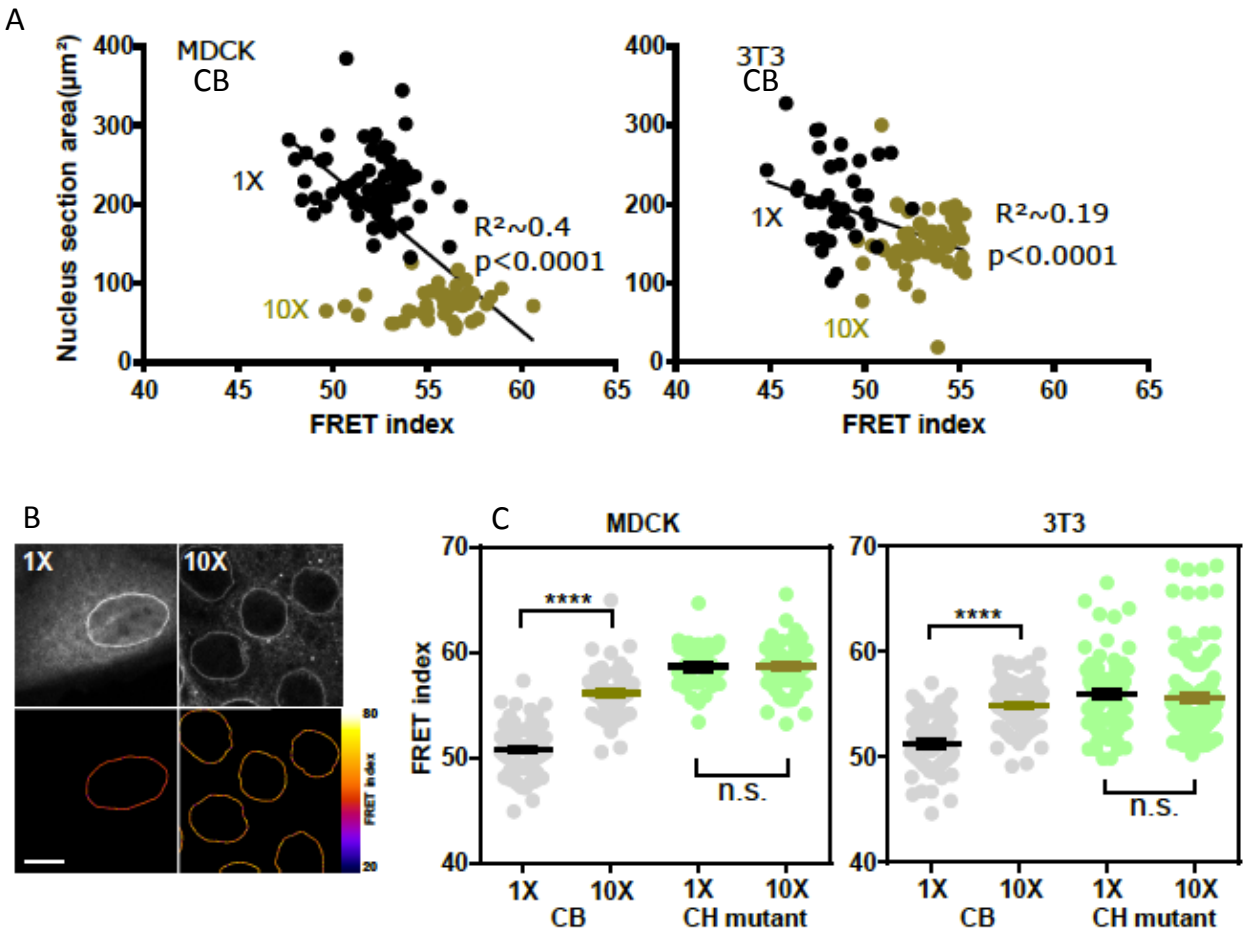

Fig 98: **Nesprin 2 tension is sensitive to cell packing.** A: nucleus section area as a function of FRET index (CB constructs) for low (1X) and high (10X) cell densities for MDCK (left, n= 73 1X, 45 10X) and 3T3 (right, n=36 1X, 59 10X) cells. Solid lines are linear fits. B: MDCK cells expressing the CB construct plated at 1X and 10X. Top: fluorescence. Bottom: FRET index map. C: FRET index of the CB construct and the CH mutant at 1X and 10X densities, in MDCK (left) (n= 97 CB 1X, 82 CB 10X, 45 CH mutant 1X, 61 CH mutant 10X) and 3T3 (right) (n= 88 CB 1X, 120 CB 1X, 89 CH mutant 1X, 152 CH mutant 10X) cells. Scale bar=5 µm. Mean ± SEM. Mann-Whitney test. R was calculated from linear regression by the least-square method.

To assess whether this sensitivity propagated within the nucleus, SUN2-TSMod construct was employed (see paragraph 2 in Chapter 5) (Fig 99). Since the TSMod is inserted between the transmembrane and nucleoplasmic domains of SUN2, forces between the inner nuclear membrane and the nucleoskeleton can be reported (Fig 99). In this construct, the FRET index was higher overall than in the CB construct at equivalent cell density, suggesting a higher level of compression of the sensor not inconsistent with a highly crowded nucleoplasm. Moreover, cell confluence increased the FRET index in this construct compared to cells at low density, consistent with an increase in compression or a release of tension between the inner nuclear membrane and the nucleoskeleton (Fig. 99). Thus, these results support that cell packing is sensed within the nucleus through the cytoskeleton and the LINC complex: the lower the packing, the higher the tension on both sides of the LINC complex.

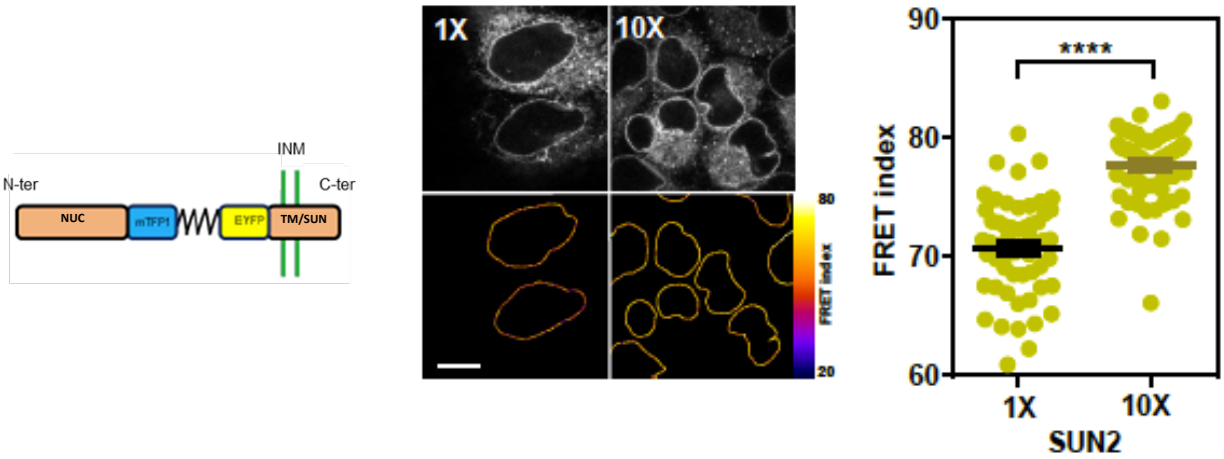

Fig 99: **SUN2 tension is sensitive to cell packing.** Left: SUN2-TSMod. SUN/TM: SUN domain and transmembrane domain. NUC: nucleoplasmic domain. INM: Inner Nuclear Membrane. N-term: N-terminus. C-term: C-terminus. Middle: MDCK cells expressing the SUN2-TSMod construct plated at $5*10^2$ cells/mm^2 (1X) and $5*10^3$ cells/mm^2 (10X). Right: FRET index of the SUN2-TSMod construct at 1X and 10X densities, in MDCK cells (n= 58 1X, 62 10X). Scale bar=5 µm. Mean ± SEM. Mann-Whitney test.

5 Tension in the LINC complex responds to cell packing upon induction of partial EMT

Epithelial sheet wounding results in decreased cell packing at the wound edge, where cells adopt a mesenchymal-like phenotype yet migrate as a cohesive group, a model of partial EMT (Gayrard et al., 2018) (see also paragraph 4 in Chapter 4). In agreement with the ability of nesprin to sense cell packing (see Fig. 98), the FRET index from the CB construct exhibited in wounded MDCK and 3T3 sheets a positive gradient from the wound edge to the back, indicative of a tension at the wound edge higher than in the back of the monolayer (Fig. 100A and B). Edge cells did not exhibit a significant difference in FRET index between the front and back of their nuclei (Fig. 100C). Of note, the CH mutant also exhibited some FRET index decrease toward the wound edge in MDCK (but not 3T3), although to a smaller extent than the CB construct, suggesting a release of some compression independent of cytoskeleton binding in this condition.

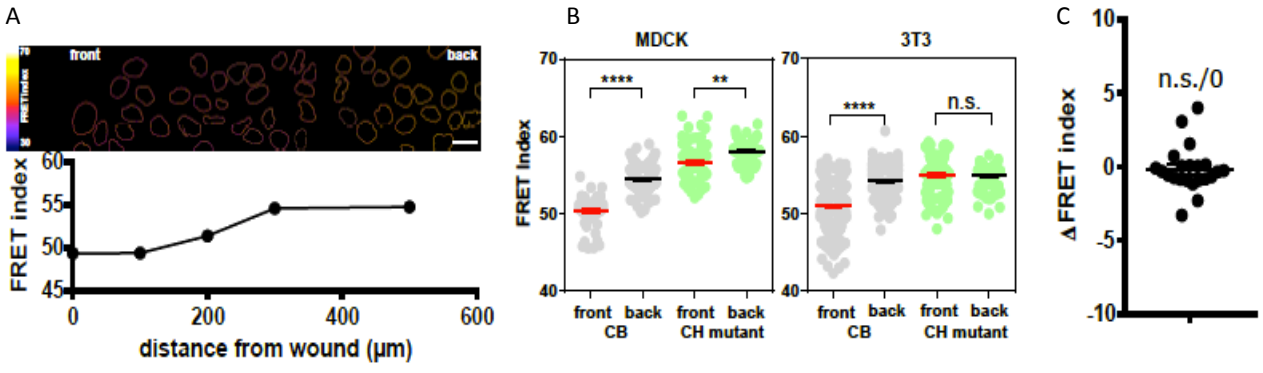

Fig 100: **Nesprin 2 tension is sensitive to induction of partial EMT.** A, top: FRET index map of a wounded MDCK monolayer expressing the CB construct. A,bottom: FRET index as a function of the distance from the front. Solid line to guide the eye. B: FRET index of the CB construct and the CH mutant at the front and back (500 µm) of the monolayer, in MDCK (left) (n= 70 CB front, 130 CB back, 73 CH mutant front, 91 CH mutant back) and 3T3 (right) (n= 363 CB front, 311 CB back, 125 CH mutant front, 143 CH mutant back) cells. C: FRET index difference

between the front and back of a nucleus within leader cells (n= 22). Scale bar=20 µm. Mean ± SEM. Mann-Whitney test.

To assess whether increased cytoskeletal tension on nesprin2G is due to reduction in cell packing and not to increased cell migration velocity, we compared inter-nuclear distance and cell velocity with FRET in cells at the edge and the bulk of a wounded monolayer, in cells at low density (5.10^2 cells/mm^2 (1X)) and at confluence ($5*10^3$ cells/mm^2 (10X)) as above, and in cells collectively migrating within 40 µm-wide channels that maintain cell density while allowing cell migration (see paragraph 6 in Chapter 5)(Fig. 101A and B). From all these conditions, we found that FRET index correlated with inter-nuclear distance but not with cell velocity (Fig. 101A and B).

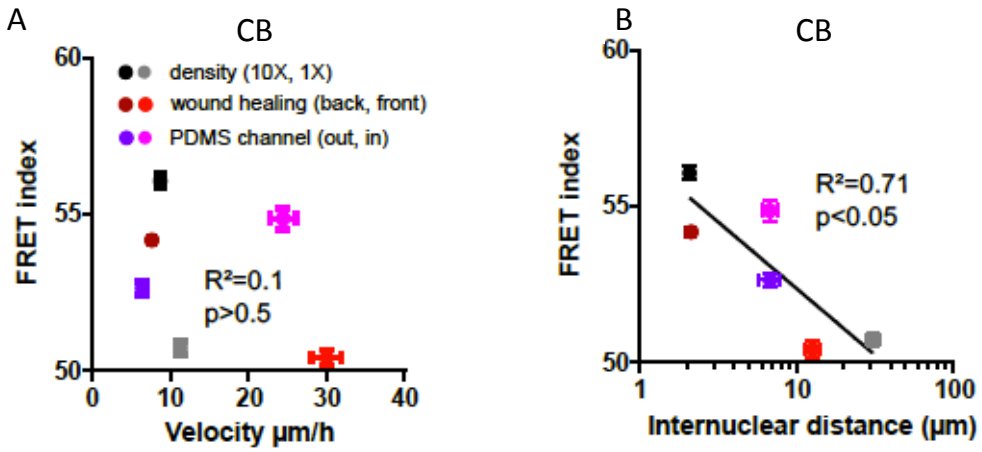

Fig 101: **Decreased cell packing but not cell migration velocity increases cytoskeletal tension on nesprin 2.** A: FRET index of the CB construct in MDCK cells as a function of cell migration velocity from experiments at low and high cell densities, upon epithelial wounding, and collectively migrating from outside (out) to inside (in) 40µm-wide channels (n= 240 1X, 255 10X, 111 front, 110 back, 64 in, 78 out). B: FRET index of the CB construct in MDCK cells as a function of internuclear distance from experiments at low and high cell densities, upon epithelial wounding and upon entering 40µm-wide channels. Solid line is the linear fit (n= 22 1X, 22 10X, 22 front, 22 back, 33 in, 18 out). R was calculated from linear regression by the least-square method.

Altogether these results support that induction of partial EMT in a wound healing model leads to increased tension on the LINC complex due to decreased cell packing rather than cell migration.

6 Tension in the LINC complex does not respond to cell packing upon induction of complete EMT

Exposure of cell colonies to HGF, a model of complete EMT where cells eventually migrate individually (see Chapter 4), induces decreased cell packing in the first hours before cell dissociation (Gayrard et al., 2018). Thus, we expected HGF exposure to induce an increase in tension in the LINC complex. To test this, I monitored how the inter-nuclear distance, the cell spread area and the FRET index of nesprin2G constructs in MDCK colonies changed over time with or without exposure to HGF. Cells exposed to HGF exhibited a significantly larger increase in inter-nuclear distance and cell spread area than non-exposed cells over the same time frame (Fig. 102A-C), which confirms that HGF decreases cell packing. Unexpectedly, the FRET index of the CB, but not the CH construct exhibited an increase over time, whether colonies where exposed to HGF or not (Fig. 102A and D). These results reveal that the cytoskeletal tension exerted on the LINC complex has not reached a steady-state in cell colonies and slowly relaxes over time. Additionally, the lack of difference with or without HGF shows that tension in the LINC complex is not responsive to cell packing upon induction of complete EMT.

Thus, the LINC complex exhibits distinct mechanical responses to cell packing whether it results from induction of partial or complete EMT. While the causes for this differential response may be the focus of future studies, here we focused on its link with EMT-related signaling.

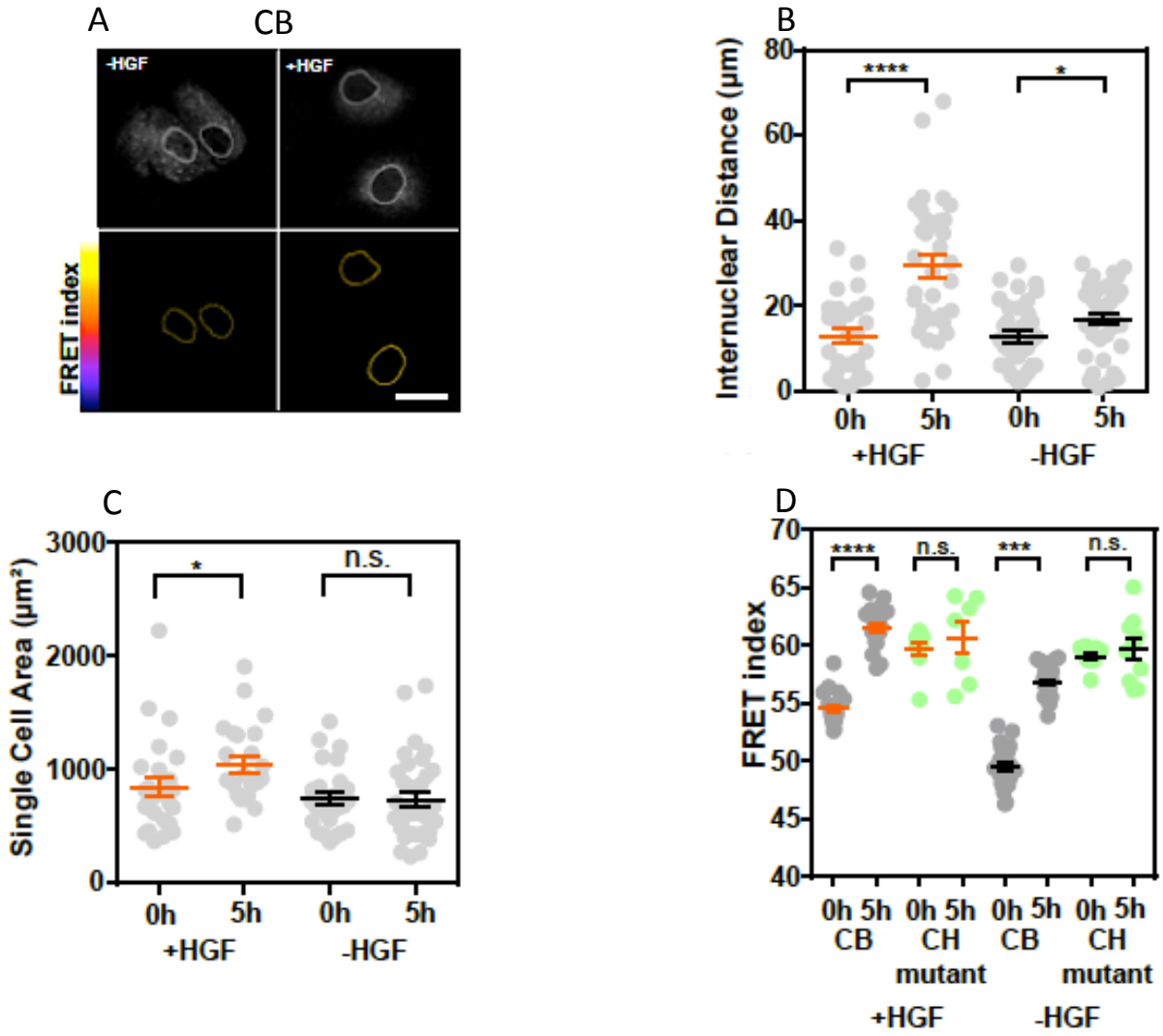

Fig. 102: **Nesprin 2 tension is not sensitive to induction of complete EMT**. A: Direct fluorescence and FRET index maps of the CB construct in MDCK cells after 5hrs with or without HGF. B: Internuclear distance of CB construct-expressing MDCK cells through time with or without HGF addition (n +HGF= 26 0h, 27 5h, n –HGF= 30 0h, 32 5h). C: Single cell area of CB construct-expressing MDCK cells through time with or without HGF addition (n +HGF= 25 0h, 24 5h, n –HGF= 29 0h, 35 5h). D: FRET index of the CB construct and CH mutant in MDCK cells through time with or without HGF addition (n +HGF= 20 CB 0h, 22 CB 5h, 9 CH mutant 0h, 7 CH mutant 5h, n -HGF= 26 CB 0h, 26 CB, 5h, 13 CH mutant 0h, 10 CH mutant 5h). Scale bar=20 µm. Mean ± SEM. Mann-Whitney test.

7 Nesprin cytoplasmic domain defines two mechanisms of β-catenin nuclear translocation differentially activated upon induction of partial or complete EMT

We hypothesized that the distinct mechanical responses of nesprin2G upon induction of partial and complete EMT associated with a differential regulation of β-catenin signaling. The lab had previously shown that, during partial EMT induced by wound healing, the release of catenins from the plasma membrane in leader cells results in nuclear translocation of β-catenin (see Fig 61B in Chapter 3) but in the retention of α-catenin in the cytoplasm (Gayrard et al., 2018). Here, we thus assessed changes in

the nucleo/cytoplasmic balance of α-catenin-GFP and β-catenin-GFP upon HGF stimulation of MDCK cells. HGF stimulation induced β-catenin nuclear translocation, as expected (Gayrard et al., 2018) (see Fig 61E in Chapter 3), but also that of α-catenin (Fig. 103A and B), in stark contrast with the behavior of α-catenin in cells induced to undergo partial EMT in wound healing experiments.

To assess whether this was dependent on nesprins, we transiently expressed mCherry-DNKASH (see paragraph 2 in Chapter 5), which displaces endogenous nesprins from the nuclear envelope (Lombardi et al., 2011; Luxton et al., 2010) (Fig. 103C) (see also paragraph 1.3 in Chapter 2). In agreement, we showed that in cells exposed to HGF, β- and α-catenin nuclear contents were reduced to levels indistinguishable from that of unstimulated cells (Fig. 103A and B).

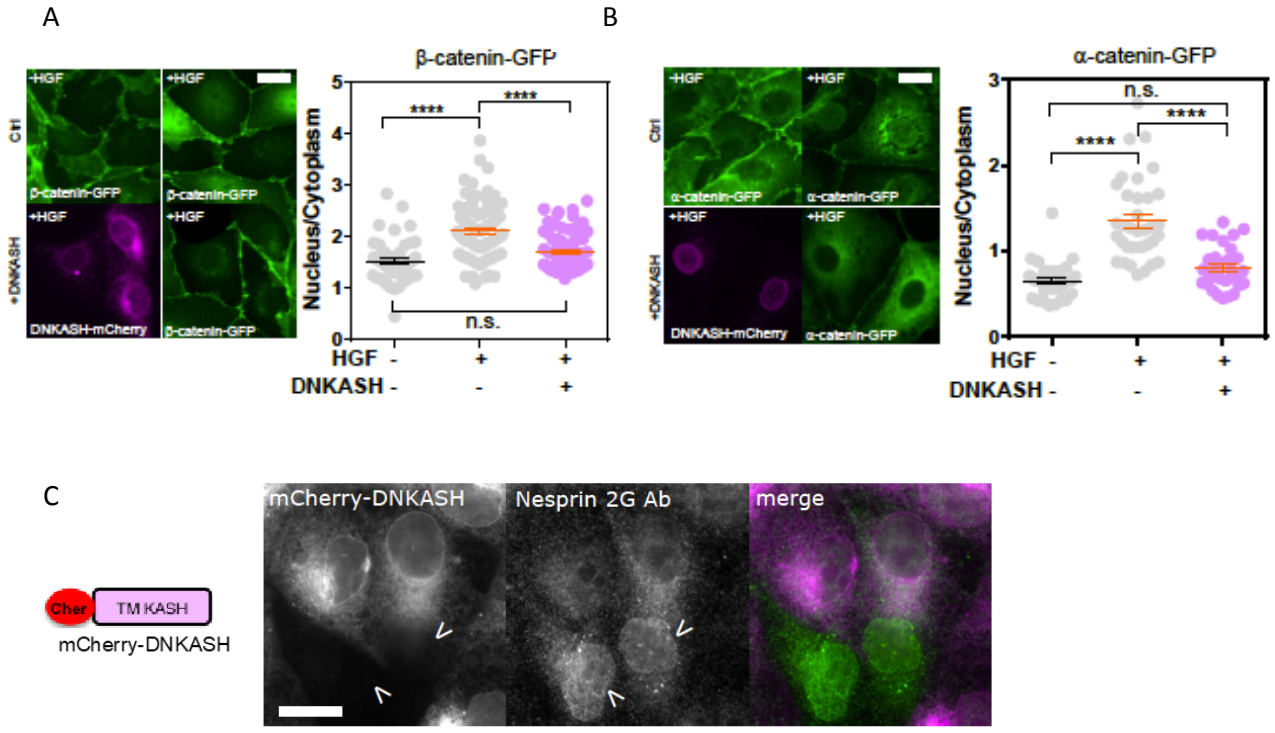

Fig 103: **Nesprin 2 regulates catenins nuclear translocation.** A, left: MDCK cells stably expressing β-catenin-GFP with and without mCherry-DNKASH, with and without HGF addition. A,right: β-catenin nucleus/cytoplasmic balance (GFP intensity ratio) as a function of HGF and DNKASH (n= 43--, 89+-, 65++). B, left: MDCK cells stably expressing α-catenin-GFP with and without mCherry-DNKASH, with and without HGF addition. Right: α-catenin nucleus/cytoplasmic balance (GFP intensity ratio) as a function of HGF and DNKASH (n= 35 --, 36 +-, 31 ++). C, left: schematic of mCherry-DNKASH chimeric construct. TM KASH: Transmembrane/KASH domain. C, right: MDCK cells transiently expressing mCherry-DNKASH and stained for nesprin2G. Only non-transfected cells (arrowhead) show nesprin2G localization at the nuclear envelope. Scale bars=10 µm. Mean ± SEM. Kruskal-Wallis test.

To assess the consequences of LINC complex disruption on β-catenin-dependent transcription, I transiently expressed mCherry-DNKASH in a TOPdGFP cell line, in which dGFP expression is under the control of β-catenin transcriptional activity (Dorsky et al., 2002; Maher et al., 2009) (see paragraph 7 in Chapter 5). These cells were exposed to the β-catenin degradation inhibitior LiCl for 10hrs to increase β-catenin levels. In control cells, LiCl exposure resulted in dGFP expression (Fig. 104), consistent with excess β-catenin accumulation in the nucleus (Gayrard et al., 2018). In mCherry-DNKASH expressing cells, decreased dGFP levels indicated decreased β-catenin transcriptional activity (Fig. 104), consistent with the loss of nuclear β-catenin upon the same perturbation (Fig. 103A).

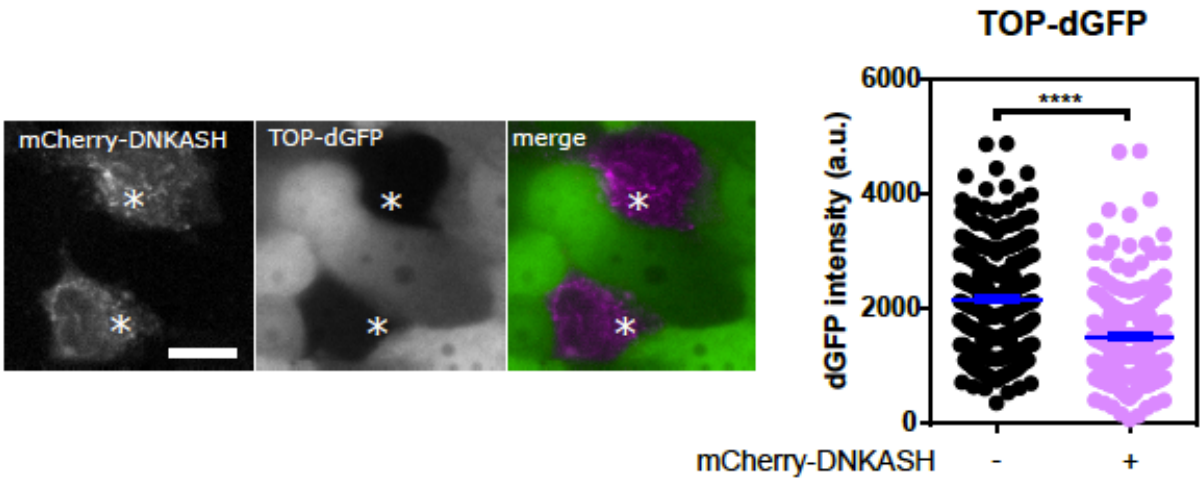

Fig 104: **mCherry-DNKASH negatively impacts β-catenin transcriptional activity.** MDCK cells stably expressing TOP-dGFP and transiently expressing mCherry-DNKASH after 10hrs treatment with LiCl. Cells expressing mCherry-DNKASH (star) show lower dGFP levels (n= 216 +mCherry-DNKASH, 216 -mCherry-DNKASH). Scale bar=10 µm. Mean ± SEM. Mann-Whitney test.

Altogether these results support that β-catenin nuclear translocation and subsequent transcriptional activity can occur through distinct mechanisms: in cells induced to undergo complete EMT, nesprin2G is relaxed and its cytoplasmic domain is required for β- and α-catenin nuclear translocation and β-catenin activity, while in cells induced to undergo partial EMT in wound healing experiments, nesprin2G is tensed and β-catenin translocates into the nucleus alone.

8 Relaxed, but not tensed nesprin2G recruits α-catenin to the nuclear envelope

We then assessed whether the cytoplasmic domain of nesprin2G, which contains a binding site for α-catenin in a complex with β-catenin (Neumann et al., 2010) (see Fig 69 in Chapter 3), contributed to the nuclear translocation of catenins by promoting the recruitment of α-catenin to the nuclear envelope. Consistent with this hypothesis, we found that in HGF-stimulated cells, α-catenin accumulated at the nuclear envelope even more than within the nucleus, and that both these accumulations were abolished in cells expressing mCherry-DNKASH, which lacks the binding site for α-catenin (Fig. 103B, Fig 105 A and B). This suggests that α-catenin nuclear translocation requires its recruitment to the nuclear envelope by nesprins. Consequently, we hypothesized that increased tension on nesprin2G in cells induced to undergo partial EMT could explain the lack of α-catenin nuclear translocation by preventing its recruitment to the nuclear envelope. Consistently, we found no recruitment of α-catenin to the nuclear envelope compared to the cytoplasm in cells at the wound front (Fig. 105 A and B).

Altogether, these results show that in cells induced to undergo complete EMT, relaxed nesprin2G recruits α-catenin to the nuclear envelope, while in cells induced to undergo partial EMT, tensed nesprin2G does not.

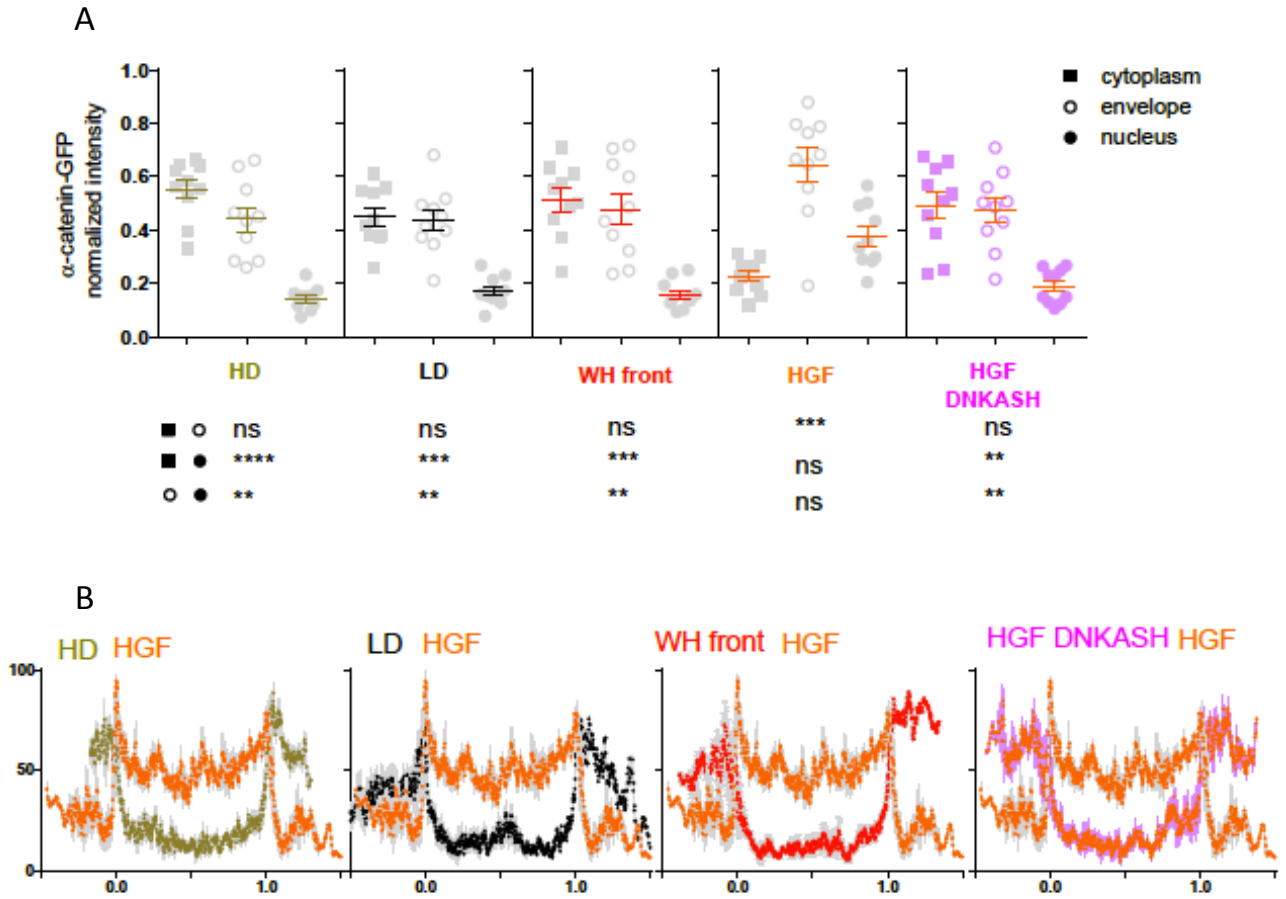

Fig 105: **Nesprin 2 regulates α-catenin recruitment at the nuclear envelope.** A: Relative cytoplasmic, nuclear envelope, and nuclear levels of α-catenin in MDCK cells plated at high density (HD, 10X), low density (LD, 1X), at the wound front, upon HGF exposure, and upon HGF exposure and mCherry-DNKASH expression. n=10 cells for each condition and compartment. B: Normalized α-catenin-GFP intensity along a linescan across the nucleus of cells (MDCK) exposed to HGF compared to that of cells plated at high (HD, 10X) and low (LD, 1X) densities, at the front of an epithelial wound, and expressing mCherry-DNKASH with HGF. Linescans are averages of 3 cells, 5 pixels-window moving-average. 0 and 1 are nuclear envelope positions. Mean ± SEM. Kruskal-Wallis test.

9 Nuclear localization of α-catenin causes β-catenin nuclear retention, but in a transcriptionally less active form

To assess the role of nuclear α-catenin in β-catenin signaling, I transiently expressed NLS-iRFP-α-catenin (Fig 106A) (see paragraph 2 in Chapter 5) in MDCK cells stably expressing β-catenin-GFP. Compared to control cells, NLS-iRFP-α-catenin cells exhibited increased nuclear β-catenin (Fig. 106B). Thus, nuclear α-catenin promotes β-catenin nuclear localization. To determine whether α-catenin is involved in β-catenin translocation or nuclear retention, I examined β-catenin localization in MDCK cells transiently expressing a shRNA against α-catenin (Capaldo & Macara, 2007). These cells displayed higher nuclear β-catenin levels compared to controls (Fig. 106C). This implies that not only α-catenin is dispensable for β-catenin nuclear translocation, but also suggests that its extranuclear pool opposes constitutive β-catenin nuclear localization. Finally, I assessed the effects of nuclear α-catenin on β-catenin transcriptional activity. To do so, I transiently expressed NLS-iRFP-α-catenin in TOPdGFP MDCK cells exposed, or not, to LiCl for 10hrs to increase β-catenin levels. Cells not exposed to LiCl exhibited low levels of dGFP regardless of NLS-iRFP-α-catenin expression, as expected for cells with basal β-catenin levels. In contrast, cells exposed to LiCl exhibited significantly higher dGFP levels, as expected for cells with high β-catenin levels, but to a much lower extent in cells expressing NLS-

iRFP-α-catenin (Fig. 106D). Thus, nuclear α-catenin limits β-catenin transcriptional activity. Altogether, these results support that α-catenin nuclear translocation favors β-catenin nuclear localization, but in a transcriptionally less active form.

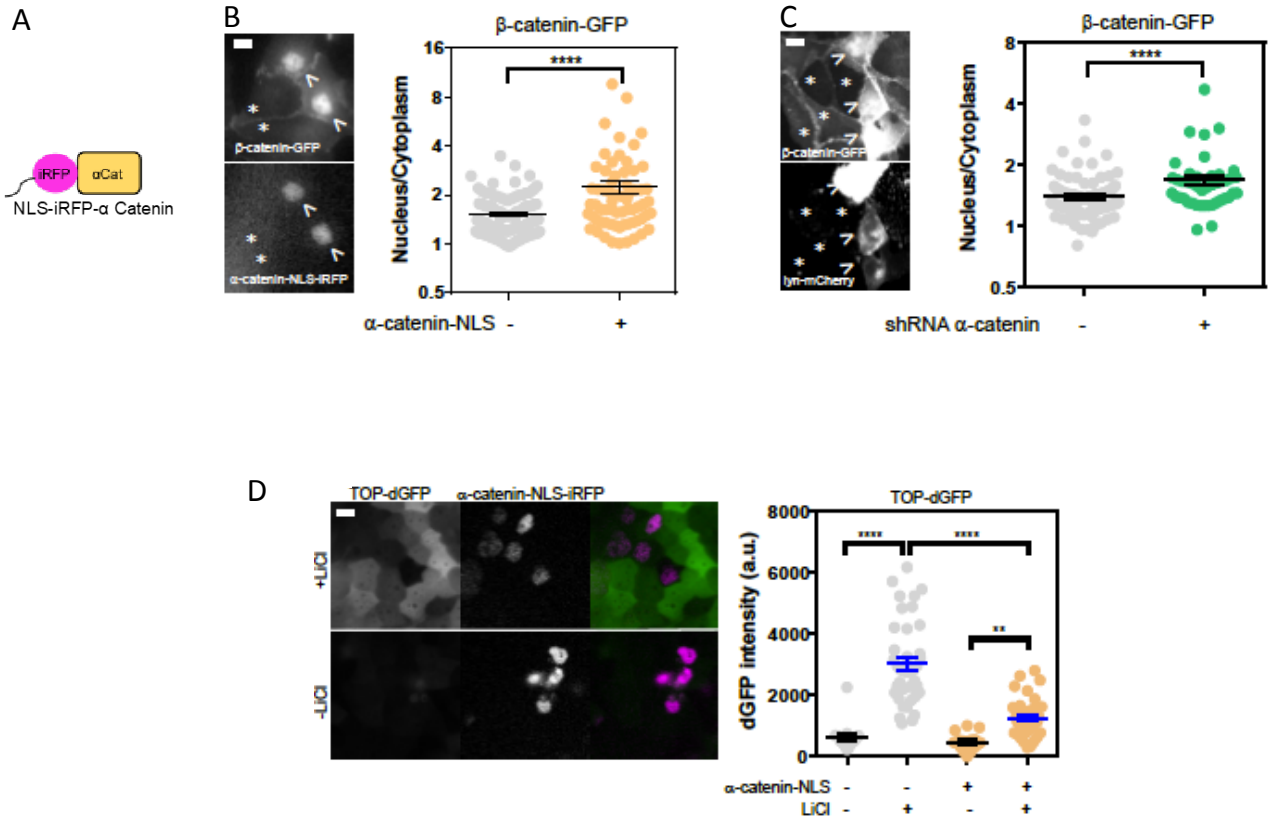

Fig 106: **Nuclear α-catenin sequesters β-catenin in the nucleus in a transcriptionally less active form.** A: NLS-iRFP-α-catenin construct. B, left: MDCK cells stably expressing β-catenin-GFP with transient expression of NLS-iRFP-α-catenin (arrows) and without (stars). B, right: β-catenin nucleus/cytoplasmic balance (GFP intensity ratio) as a function of NLS-iRFP-α-catenin expression (n= 112 -, 66 +). C, left: MDCK cells stably expressing β-catenin-GFP with transient expression of shRNA against α-catenin and lyn-mCherry (arrows) and without (stars). C, right: β-catenin nucleus/cytoplasmic balance (GFP intensity ratio) as a function of shRNA/lyn-mCherry co-transfection (n= 102 -, 44 +). D, left: MDCK cells stably expressing TOP-dGFP and transiently expressing NLS-iRFP-α-catenin after 10hrs with and without LiCl. D, right: dGFP intensity as a function of NLS-α-catenin-iRFP expression and LiCl (n= 17 ---, 39 -+, 17 +-, 39 ++). Scale bars=10 µm. Mean ± SEM. Mann-Whitney and Kruskal-Wallis tests.

In summary

- The LINC complex is under specific cytoskeleton tension and unspecific compression.
- The LINC complex is mechanosensitive to extracellular mechanical cues and cells packing.
- Nesprin2G (N2G) tension is sensitive to cell packing upon partial EMT, but not upon complete EMT.
- When relaxed during complete EMT, N2G recruits α-catenin at the nuclear envelope, with consequent α/β-catenin nuclear translocation.

- When tensed during partial EMT, N2G does not recruit α-catenin with only β-catenin nuclear translocation.

- α-catenin sequesters nuclear β-catenin in a transcriptionally less active form.

CHAPTER 7

Discussion and conclusion

In this chapter, I will discuss the experimental results obtained during my PhD and, on this basis, I will propose a mechanistic model.

Table of contents

Discussion

In this thesis work, we sought to determine whether and how the LINC complex participated in the mechanical regulation of β-catenin signaling during EMT induction. We found that nesprin2G tension increases during partial, but not complete EMT. Upon induction of complete EMT, relaxed nesprin2G recruits α-catenin at the nuclear envelope, which is required for nuclear translocation of both catenins. Upon partial EMT however, tensed nesprin2G does not recruit α-catenin and β-catenin nuclear translocation occurs independently of α-catenin. Once in the nucleus, α-catenin sequesters β-catenin in a transcriptionally less active form.

Using instrument-specific FRET Index to FRET Efficiency calibration and previously published FRET Efficiency to force calibration (see paragraphs 8.1 and 8.2 in Chapter 5), we estimate that forces exerted by the cytoskeleton on nesprin2G can be as high as 8pN, (see paragraph 8.2 in Chapter 5) the full range of the force sensor (see Fig. 94 in Chapter 6). Remarkably, since actin filaments and microtubules interact together (Akhmanova & Steinmetz, 2015; Dugina et al., 2016; Griffith & Pollard, 1978; Griffiths, Pollards, & Fairchild Center, 1982), perturbation of one of these cytoskeletal networks can affect each other as well as nesprin2G tension, and this latter is consistent with the actin- and microtubule-binding properties of CH-domains (Goldsmith et al., 1997; Hayashi & Ikura, 2003). The mechanical, pharmacological and genetic perturbations exploited in this manuscript (aimed at mimicking cell morphological changes in a range of physiological and pathological situations) all result in cytoskeleton-dependent tension changes consistent with that previously observed in cell adhesion proteins (Nicolas Borghi et al., 2012; Grashoff, Hoffman, Brenner, Zhou, Parsons, Yang, McLean, Sligar, Chen, Ha, & others, 2010). Conversely, the SRs exert a constraint on the sensor akin to a compression of magnitude similar to that of cytoskeleton-dependent tension (see Fig. 94 in Chapter 6). Similarly, the sensor response in SUN2 is consistent with a pre-compressed state (see Fig. 99 in Chapter 6). Using the same sensor, protein compression has previously been evidenced in vinculin at Focal Adhesions (Rothenberg et al., 2015; Sarangi et al., 2017) and in the glycocalyx protein MUC1 (Paszek et al., 2014). Our results are consistent with the sensor being sensitive to such a compression and suggest that a steric hindrance akin to a compression occurs constitutively on both sides of the nuclear envelope.

A substantial part of cytoskeleton-dependent nesprin tension is balanced cell-autonomously, as can be seen from individual cells migrating through narrow constrictions (see Fig. 96 in Chapter 6). Focal adhesions (see paragraph 3.1 in Chapter 1), which anchor actin stress fibers to the extracellular matrix, are well positioned to play a role in this balance. Indeed, a number of adherent cells display a nesprin-dependent perinuclear actin cap with fibers terminated by FAs (Chambliss et al., 2013; Khatau et al., 2009; D.-H. Kim et al., 2012), cell stretching with integrin ligand-coated beads results in cytoskeleton- and nesprin-dependent nucleus stretching (Lombardi et al., 2011; Maniotis et al., 1997) and nucleus anchoring to the cytoskeleton affects cell-substrate traction forces (Shiu, Aires, Lin, & Vogel, 2018). Moreover, depletion of nesprin 1 has been associated to increased focal adhesion assembly as well as increased nuclear height as a consequence of impaired actomyosin cytoskeleton-generated tension exerted on the nucleus (Chancellor, Lee, Thodeti, & Lele, 2010). Here, we bring a direct demonstration that nesprin2G tension responds to substrate mechanics: provided that nesprins can bind to the cytoskeleton through their CH domains, their tension increases in remarkable proportion with cell and nucleus strain upon stretching of the cell substrate (see Fig. 97 in Chapter 6).

While previous studies have mostly focused on isolated cells, we also show here how nesprin tension changes in a cell assembly. Remarkably however, this tension does not necessarily correlate with that in E-cadherins, as nesprin and E-cadherin tension gradients are opposite in cells undergoing partial EMT (see Fig. 100 in Chapter 6 and Fig 61A (from (Gayrard et al., 2018) in Chapter 3). This points to a force balance regulation that likely depends on all adhesion complexes and variable fractions of mechanically engaged proteins.

We show that cell packing is a critical determinant of tension in the LINC complex, on both sides of the nuclear envelope (see Fig. 98 and Fig. 99 in Chapter 6). We thus bring a direct demonstration that the LINC complex is a bona fide mechanosensor of cell packing at the nuclear envelope. Nevertheless, a decrease in cell packing results in an increase in nesprin tension at the front of an epithelial monolayer in partial EMT, but does not upon induction of complete EMT by HGF (see Fig. 102 in Chapter 6). This differential response remains unexplained, but it supports that the LINC complex is a mechanosensor able to discriminate between inductions of various EMT programs. This makes nesprin2G tension a better predictor of EMT program than E-cadherin tension or β-catenin nuclear localization. Whether this can be further harnessed in the context of diseases may be the focus of future investigations.

Over the last decade, a number of signaling pathways regulating proliferation have been found to respond to cell confinement, and to depend on the LINC complex, supporting a role of the latter in the former. Confinement modulates YAP/TAZ nuclear translocation and ERK activity cell-autonomously (Dupont et al., 2011; Logue et al., 2015) and in a multicellular context (Aoki et al., 2013; Aragona et al., 2013). Moreover, mechanical induction of YAP nuclear translocation requires the cytoplasmic domain of nesprins at the nuclear envelope (Elosegui-Artola et al., 2017)(see Fig 36 in Chapter 2). However, it does not always appear to require a contractile cytoskeleton. Indeed, when subjected to dynamic stretch in presence of MLCK (myosin-light chain kinase) inhibitor, bovine MSCs (mesenchymal stem cells) still display YAP nuclear translocation (Driscoll, Cosgrove, Heo, Shurden, & Mauck, 2015), which questions whether nesprins bear an actual mechanical function in this process. In addition, cell packing modulates β-catenin signaling downstream of FAK, whose inhibition abolish β-catenin nuclear translocation during EMT induction (Gayrard et al., 2018). Moreover, mechanical induction of β-catenin nuclear translocation is impaired upon disruption of the LINC complex in mouse MSCs (Uzer et al., 2018). While nesprin2G can interact with catenins (Neumann et al., 2010) (see Fig 69 in Chapter 3), it was however unknown whether this interaction could be mechanically

regulated. Here, we took advantage of the differential response of nesprin2G to partial and complete EMT (see Chapter 4) to show that the relaxed cytoplasmic domain of nesprin2G is required for α-catenin recruitment at the nuclear envelope and catenin nuclear translocation, while tensed nesprin2G does not recruit α-catenin at the envelope nor does it allow its nuclear translocation (see Fig. 100A and B, Fig 102A and D, Fig 103B and Fig. 105 in Chapter 6). Thus, nesprin2G tension predicts nuclear translocation of cytoplasmic α-catenin. This supports a model whereby nesprins could capture cytoplasmic catenins at the nuclear envelope for subsequent nuclear translocation in a force-dependent manner by virtue of a higher affinity in a mechanically relaxed state. However, the actual force contribution to catenins' nuclear translocation could be more directly tested by using single molecule force spectroscopy techniques, such as optical as well as magnetic tweezer (Neuman & Nagy, 2008). Remarkably, our proposed mechanism is distinct from that invoked for mechanical induction of YAP nuclear translocation whereby nesprins would transmit cytoskeletal forces to stretch nuclear pores open and sterically facilitate nuclear translocation (Elosegui-Artola et al., 2017). The reason may lie in the fact that β-catenin is its own nuclear transporter that directly interacts with nuclear pore complex (F Fagotto, Glück, & Gumbiner, 1998) (see also paragraph 1.4 in Chapter 2). Additionally, our results support that nuclear localization of α-catenin promotes β-catenin nuclear localization by affinity (see Fig. 106 in Chapter 6). However, we show that nuclear α-catenin limits β-catenin-dependent transcription, consistently with previous reports (Choi et al., 2013; R. L. Daugherty et al., 2014; Ana L. Giannini, Vivanco, & Kypta, 2000; Merdek, Nguyen, & Toksoz, 2004) (see also paragraph 5 in Chapter 3). Since α-catenin needs β-catenin for nuclear localization (R. L. Daugherty et al., 2014), we thus propose that β-catenin piggybacks its own retention, and transcription-limiting factor in a nesprin2G tension-dependent manner.

Based on these results and on Charléne's work (Gayrard et al., 2018), we propose that in a manner dependent on the EMT program, mechanosensitive nesprins may capture, at the nuclear envelope, the catenins released from the plasma membrane when E-cadherin relaxes (see Fig 61D in Chapter 3), and thereby fine-tune their nuclear translocation and activities (Fig. 107).

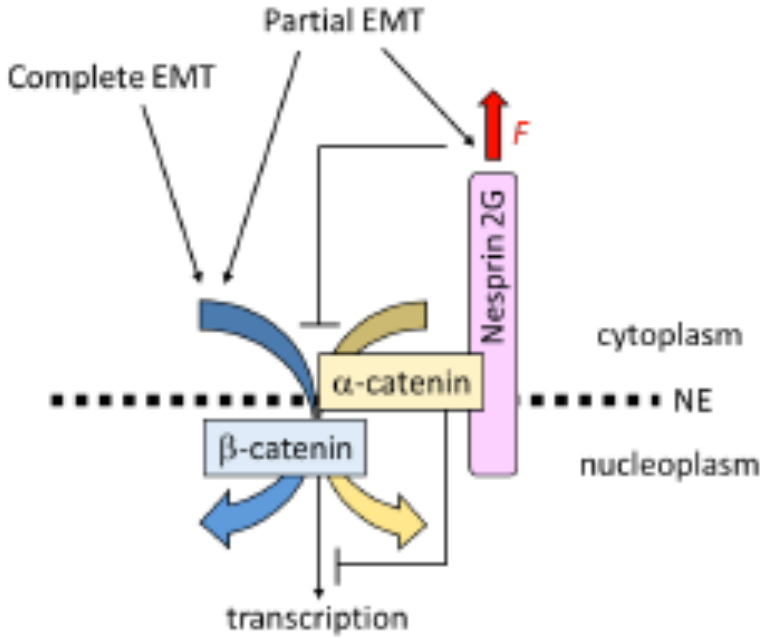

Fig. 107: Proposed mechanism of α/β nuclear translocation and β-catenin transcriptional activity in response to the differential nesprin 2G tensional state following EMT induction. See text for details.

Conclusion

By using a novel encoded FRET biosensor (Grashoff, Hoffman, Brenner, Zhou, Parsons, Yang, McLean, Sligar, Chen, Ha, & Schwartz, 2010) combined with MTM (molecular tension microscopy) (Gayrard & Borghi, 2016), we define a new role of the LINC complex as a mechanotransducer, which regulates catenins signalling in the process of EMT. Firstly referred to as a bridge connecting nucleoskeleton and cytoskeleton (Crisp et al., 2006) and then seen as critical for force transmission between these two compartments (Lombardi et al., 2011), now we know that the LINC complex regulates a plethora of cellular events, ranging form cell signalling (Driscoll et al., 2015; Elosegui-Artola et al., 2017; Neumann et al., 2010; Uzer et al., 2018) to transcriptional regulation (Alam et al., 2016). Moreover, we provide the evidence whereby nesprin2G is differentially sensitive to cell packing, which results in α and β-catenins' nuclear translocation regulation. In addition, we demonstrate that catenins' nuclear translocation during EMT induction is impaired when LINC complex is disrupted. Thus, what we show here is a novel mechanism of catenin's signalling mechanical induction which has never been addressed before and where the LINC complex is found to be the principal regulator.

Since loss of a functional LINC complex affects mechanotransduction as well as cellular signalling, it could be also speculated that LINC complex-disrupted cells, in order to survive, may adapt themselves to this condition by changing their tensional state at the cell-cell contact level, activate pathways to safeguard DNA integrity as well as fine-tune the expression of pro-proliferative genes. Therefore, by addressing these points, a new piece of knowledge could enrich and expand the already wide literature on the LINC complex, in order to better understand the role of the latter in physiological as well as pathological conditions.

CHAPTER 8

Annex 1 and 2

Table of content Annex 1

Here, I will briefly explain some additional experiments carried out during my PhD project, whose rationale can be summarized in the following questions:

- Since both nesprins and E-cadherins are connected to the actin cytoskeleton, does, therefore, LINC complex disruption impact E-cadherin tensional state as a consequence of the lost mechanical tension at the nuclear envelope? And what if nucleo-cytoskeleton connection is enhanced?

- Since depletion of nesprin 1 in humans (Sur, Neumann, & Noegel, 2014) and kms1 (a KASH protein) in yeast *S.Pombe* (Swartz et al., 2014) causes DNA damage response (DDR) signalling (Jackson & Bartek, 2009), is it also the case if the LINC complex is disrupted?

- Since LINC complex disruption impacts β-catenin activity (Neumann et al., 2010) as well as gene transcription (Alam et al., 2016), what happens at the transcription levels of *c-myc* oncogene, which is a direct target of β-catenin (T. C. He et al., 1998), during the induction of complete EMT (Gayrard et al., 2018) and in cells LINC complex- stably disrupted?

- Is it possible to mechanically manipulate miniNesprins2G in order to induce α/β-catenins' signalling?

1 Evaluation of E-cadherin tensional state upon nucleo-cytoskeleton coupling impairement/enhancement.

Since SUN2 null mice-derived primary keratinocytes have been shown to exhibit impaired mechanical stability of intercellular adhesions (R. M. Stewart et al., 2015), we wanted to evaluate if LINC complex disruption could cause a variation in the constitutive tension exerted by the cytoskeleton on E-cadherin at the level of the adherens junctions (AJs) (see paragraph 3.2 in Chapter 1). To this aim, I relied on MDCK type II G cells, stably expressing a full length E-cadherin construct harbouring the TSMod FRET biosensor (E-cadTSMod) and shown to be under constitutive tension at the cell-cell contacts in these same cells (N. Borghi et al., 2012) (see also Fig 14A in Chapter 1). As tension-less control, MDCK type II G cells stably expressing an E-cadherin construct, devoid of the β-catenin

binding domain (βBD) and harbouring the TSMod FRET biosensor (E-cadTSModΔcyto) (N. Borghi et al., 2012) (see also Fig 14A in Chapter 1), were employed.

These cells were transfected with the mCherry-DNKash construct (see paragraphs 2 and 3 in Chapter 5) 48 hours before imaging and then (24 hours before imaging) replated (onto collagen coated coverslips, see paragraph 1 in Chapter 5) in order to reach ≈70% of confluence when imaged. FRET index was then computed at the cell-cell contacts in the same way as previously described (see paragraph 8.3 in Chapter 5 for acquisition parameters and image analysis).

As expected, E-cadTSModΔcyto expressing cells had a higher FRET index (lower tension on E-cadherin) compared to the E-cadTSMod expressing cells, which exhibited a lower FRET index (higher tension) (N. Borghi et al., 2012; Gayrard et al., 2018). Interestingly, however, FRET index measurements between mCherry-DNKASH transfected versus non transfected cells were not statically different, suggesting that LINC complex disruption was not able to alter cytoskeleton-generated tension on E-cadherin (Fig 108).

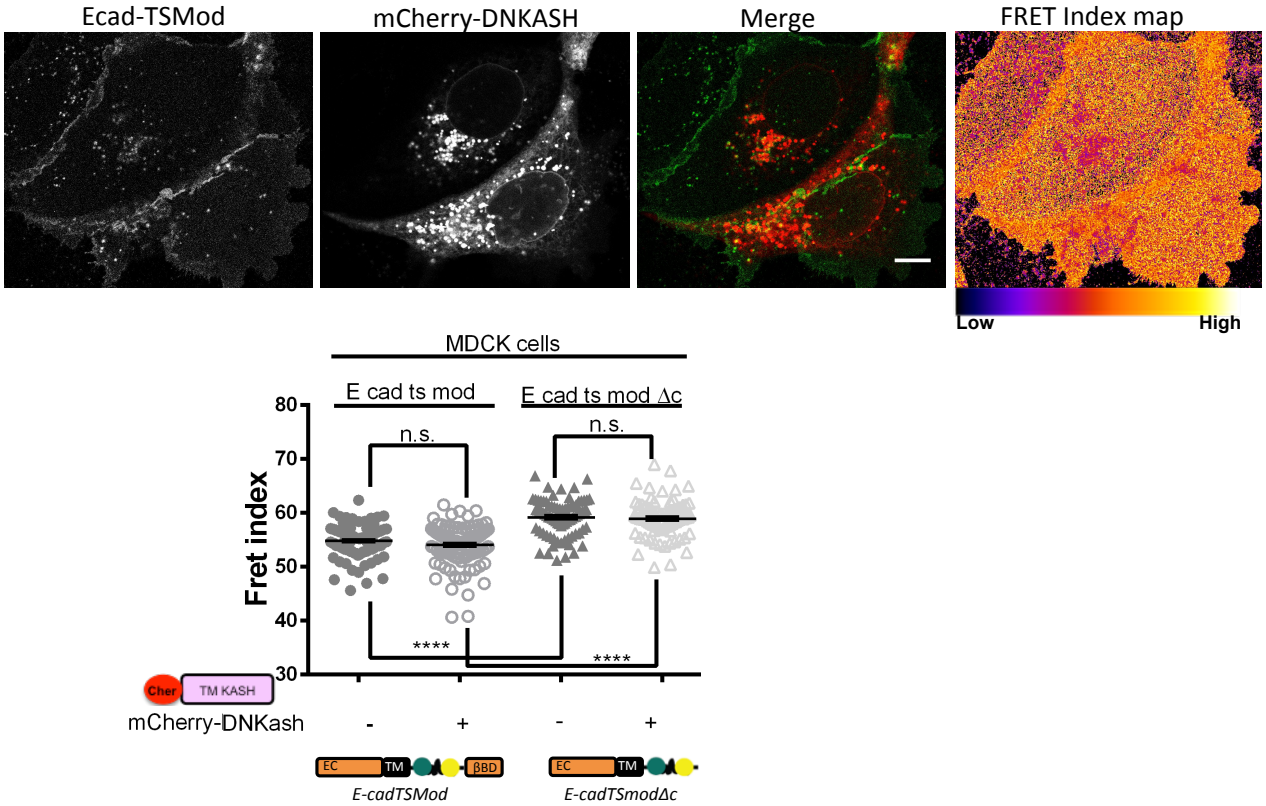

Fig 108: Disruption of the LINC complex via DNKASH does not impair E-cadherin tensional state. Top: live cell imaging and example of FRET index map of MDCK cells, stably expressing E-cadTSMod and transfected with mCherry-DNKASH construct. Scale bar: 10 µm. Bottom: FRET index measurements at the cell-cell contacts of MDCK cells stably expressing either E-cadTSMod or E-cadTSModΔcyto (E-cadTSModΔc) transfected (+) or not transfected (-) with mCherry-DNKASH construct (n(numbers of contacts analysed for)E-cadTSMod(-)=105; nE-cadTSMod(+)=105; nE-cadTSModΔc(-)=81; nE-cadTSModΔc(+)=81). Note that E-cadTSModΔcyto displays a higher FRET index because of the lack of the β-catenin binding domain (βBD). EC: E-cadherin. TM:transmembrane domain. NS:not stastically significant. Mean ± SEM. Kruskal-Wallis test.

This result led us to speculate what could happen if nucleo-cytoskeleton connection was enhanced. To this aim, I relied on overexpressing a miniNesprin 2G construct, which was previously shown to rescue endogenous nesprin 2G (Luxton et al., 2010; Ostlund et al., 2009) and to enhance nucleo-cytoskeleton connection (Lombardi et al., 2011) (see also Fig 33B in Chapter 2).

As in the LINC complex disruption experiment, MDCK cells expressing E-cadTSMod were employed and FRET index was computed at the cell-cell contacts (by using the same imaging acquisition and image analysis parameters as above) following cell transfection with an iRFPminiNesprin 2G construct (same plating conditions as above). Surprisingly, transfected cells did not exhibited any variation in FRET index compared to non transfected cells (Fig 109), suggesting that nucleo-cytoskeleton enhanced connection is not able to influence tension on E-cadherin.

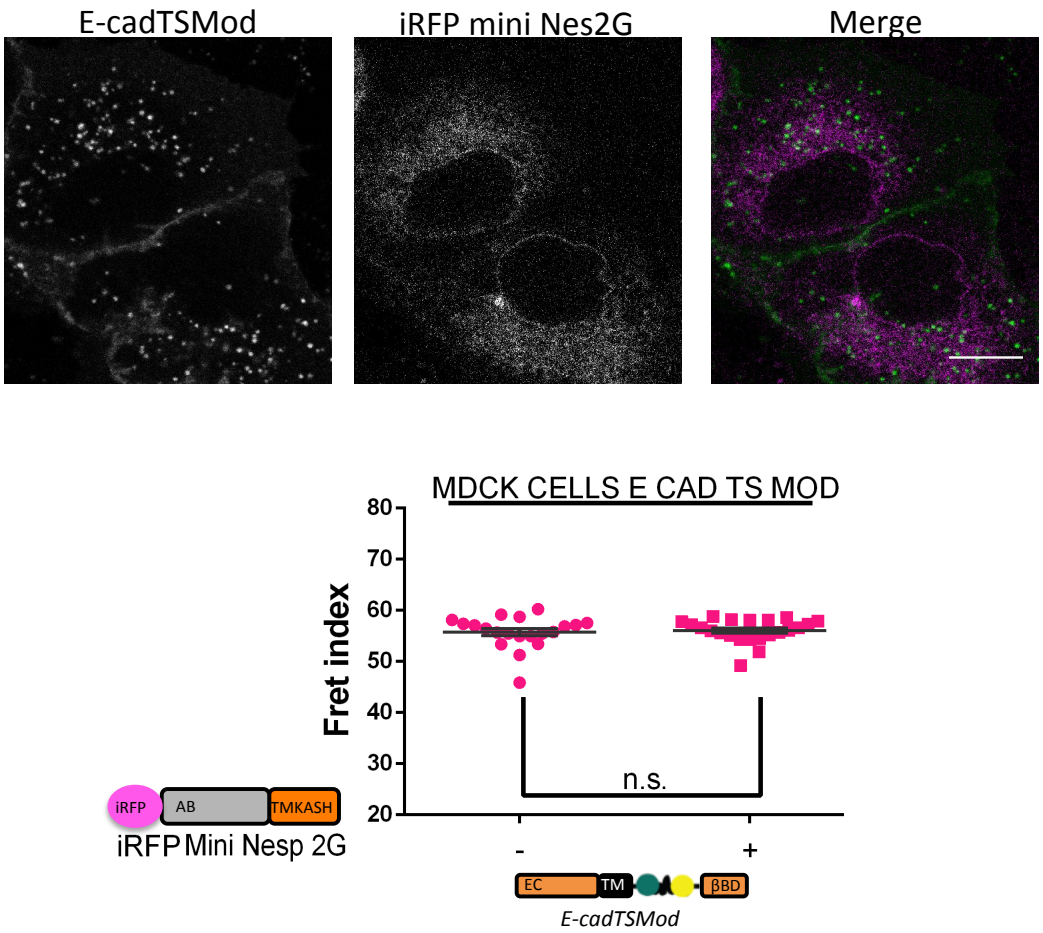

Fig 109: Nucleo-cytoskeleton coupling enhancement does not exert any effects on the tensional state of E-cadherin at the cell-cell contacts. Top: live cell imaging of MDCK cells stably expressing E-cadTSMod and transfected with an iRFP miniNesprin 2G construct. Scale bar: 10 µm. Bottom: FRET index measurements at the cell-cell contacts of MDCK cells, stably expressing E-cadTSMod, transfected (+) or not transfected (-) with iRFPminiNesprin 2G construct (n(numbers of contacts analysed for) E-cadTSMod(-)=21; nE-cadTSMod(+)=24). Ns: not statistically significant. Mean ± SEM. Mann-Whitney test.

Based on the above experimental observations, it could be thought that the cytoskeleton may intervene in order to mitigate force unbalancing that can arise upon nucleo-cytoskeleton coupling disruption/enhancement (Fig 110, see straight and curved white arrows). It could be also reasonable to say that a lower amount of E-cadherins are connected to the nesprins via the actin cytoskeleton (in grey in Fig 110) and, thus, no global variation in E-cadherin tensional state is observed upon nucleo-cytoskeleton coupling disruption/enhancement. Maybe other junctional complexes can be affected by nucleo-cytoskeleton connection perturbation, and, to this regard, the next step in the lab should investigate on the tensional state of focal adhesion proteins (Fig 110, question mark within straight ochre arrows), such as vinculin. In addition, it could be also speculated that variations in E-cadherin

tensional state might happen but they are under the limit of the FRET TSMod sensitivity (see "Discussion" paragraph in Chapter 7) and, thus, these tiny differences, if any, cannot be appreciated.

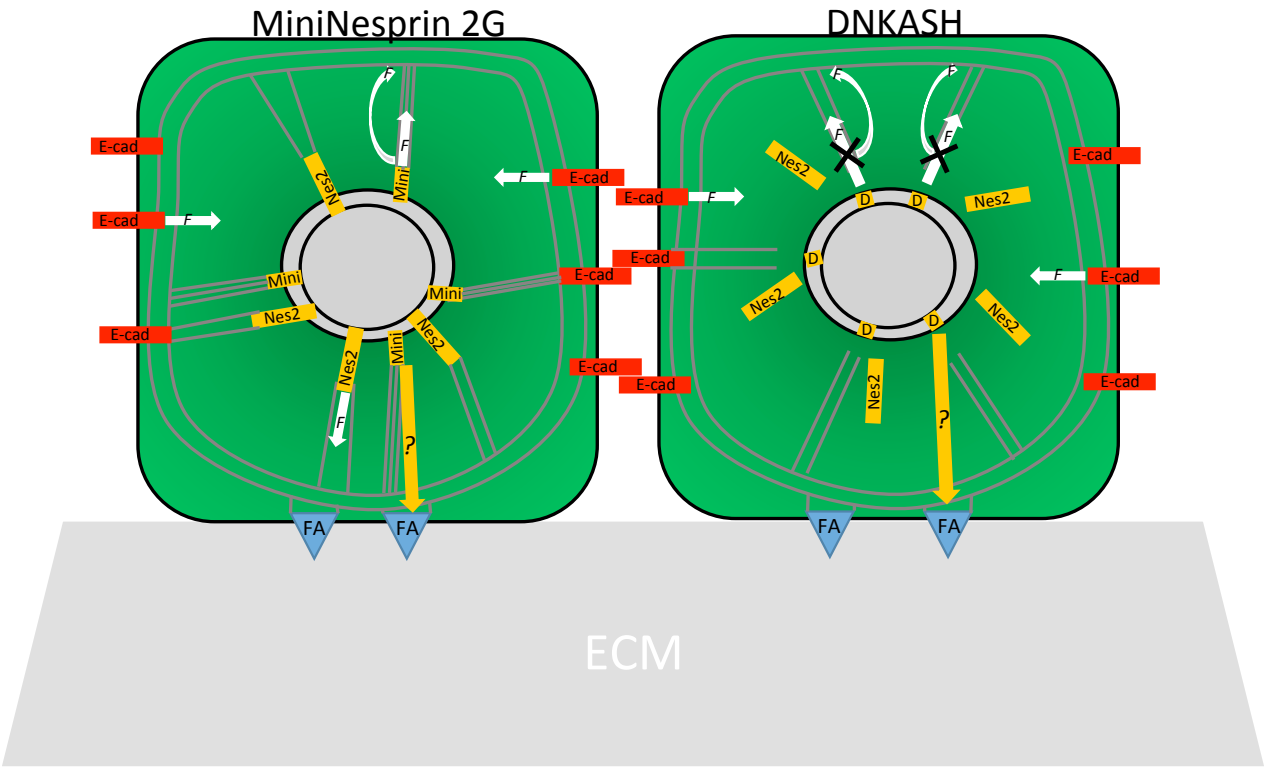

Fig 110: Nucleo-cytoskeleton coupling disruption/enhancement does not impact E-cadherin tensional state. Straight arrows to indicate cytoskeleton tension exerted onto E-cadherin and nesprin proteins; curved arrows to indicate the intervention of the cytoskeleton in balancing forces (F) upon nucleo-cytoskeleton coupling disruption/enhancement. Note that when DNKASH (D) is expressed, endogenous nesprins are dislodged from the nuclear envelope. Up to now, it is unknown if nucleo-cytoskeleton coupling disruption/enhancement has an effect on the tensional state of focal adhension (FA) proteins (straight ochre line with question mark). Actin filaments are depicted in grey. E-cad: E-cadherin. ECM: extracellular matrix. Nes2: Nesprin 2G. Mini: MiniNesprin 2G.

2 Evaluation of DNA damage upon LINC complex disruption

To evaluate if LINC complex disruption could be implied in a possible involvement of the DNA damage response (DDR) pathway (Jackson & Bartek, 2009),I looked for the formation of γH2AX foci -whose presence is indicative of DNA-double strand breaks (Rogakou, Boon, Redon, & Bonner, 1999)-, in MDCK type II G cells stably expressing the mCherry-DNKASH construct (cells were obtained as reported in paragraph 1, Chapter 5), compared to the wt counterparts. Cells were plated onto collagen-coated coverslips 24 hours before PFA fixation (see paragraph 9 in Chapter 5) and a monoclonal antibody recognizing H2AX phosphorylated on serine 139 (namely γH2AX) (Phospho-Histone H2A.X (Ser139) (20E3) Rabbit mAb, Cell signalling) was employed. Once images were acquired (see paragraph 10 in Chapter 5), a home-built macro in ImageJ (Fiji distribution) was used to automatically count single γH2AX foci. As hypothesised, the absolute number of γH2AX foci was higher for MDCK cells stably expressing mCherry-DNKASH compared to wt cells that, however, retained a basal, yet not negligible, level of DNA damage (Fig 111).

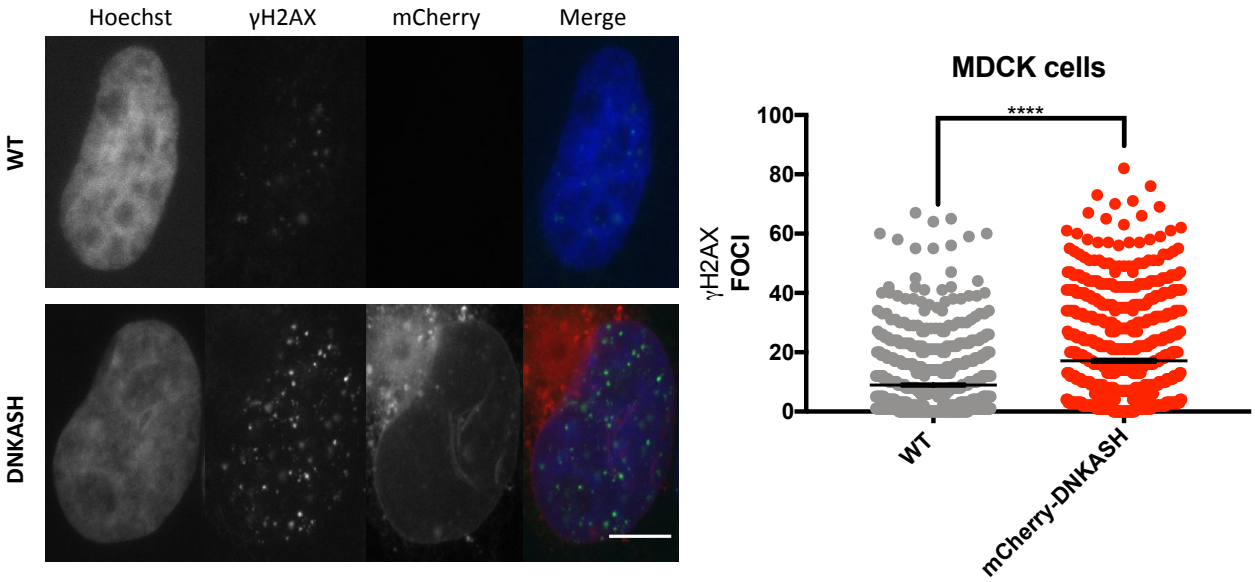

Fig 111: DNA damage evalution via γH2AX foci counting in MDCK cells either wt (n(number of cells analysed)=795) or stably expressing mCherry-DNKASH construct (n= 854). Hoechst 33342 was used to counterstain nuclei. Scale bar: 10 μm. Mean ± SEM. Mann-Whitney test.

Thus, in normal plating condition and without any exposure to DNA damaging agents (Cheung-Ong, Giaever, & Nislow, 2013), LINC complex disruption is able to trigger the first step of DNA damage response, marked by the presence of γH2AX foci (Jackson & Bartek, 2009). The reason of such a response may lay in the fact that, upon LINC complex disruption, nuclear envelope structural organization is altered and this could make DNA undergo damage, which, consequentially, could trigger the activation of the DDR. To this regard, it would be worth analysing p53 transcript/protein levels as well as evaluating cell cycle progression, to determine if these stable cells with disrupted LINC complex behave normally as the wt counterparts, maybe because of the activation of protective mechanisms, or display an altered behaviour.

3 Evaluation of *c-myc* expression upon LINC complex disruption

To evaluate if LINC complex disruption could have an effect on expression of genes directly regulated by β-catenin signalling (see Chapter 3) upon induction of complete EMT (see Chapter 4), I analysed the transcriptional levels of *c-myc* oncogene (Vennstrom, Sheiness, Zabielski, & Bishop, 1982), whose expression depends on β-catenin (T. C. He et al., 1998). To this aim, MDCK type IIG cells, wt or stably expressing mCherry-DNKASH construct, were plated 24 hours before HGF treatment (to induce complete EMT, see paragraph 5 in Chapter 5) in DMED supplemented with 10 %FBS. 12 hours before HGF treatments, cells were starved in DMED supplemented with 0.5% FBS. HGF was then added at 50ng/mL and cells let scatter for 5 hours. Consequentially, cells were harvested and total RNA extraction was accomplished by using NucleoSpin RNAII kit from Machery-Nagel, according to the manufacturer's instruction. Total RNA was retro-transcribed (SuperScript II reverse transcriptase, Invitrogen) and the obtained cDNAs used in qPCR assay (carried out in triplicate with the LightCycler 480 Instrument II, Roche Life Science). As housekeeping gene, *GAPDH* (glyceraldehyde 3-phosphate dehydrogenase) was chosen. The primer pairs used to amplify *c-myc* and *GAPDH* cDNAs are listed in the following table.

Gene		Sequence 5'→3'
c-myc	Fw	GAG CTT CTT TGC CCT GCG TG
	Rev	AGG ATG TAC GCG GTG GCT TT
GAPDH	Fw	AGT GAA GCA GGC ATC GGA GG
	Rev	GGC GTC GAA GGT GGA AGA GT

Table 2: qPCR primers. Note that these primer sequences were designed by using dog genome with Primer-BLAST tool in NCBI.

Relative *c-myc* expression was then calculated by using the $2^{-\Delta\Delta Ct}$ method (Livak & Schmittgen, 2001) as widely found in the literature (Rebecca L Daugherty et al., 2014; Veneziano, Barra, Cilluffo, & Di Leonardo, 2019).

Surprisingly, neither the presence nor the absence of HGF caused a variation of the *c-myc* expression level compared to the control condition (DMEM with 10%FBS, 24 hours) for both the cell lines analysed (Fig 112). However, even though not statistically significant, an increase (≈30%) of *c-myc* expression level was found for the cells stably expressing mCherry-DNKASH construct compared to the wt counterparts (Fig 112).

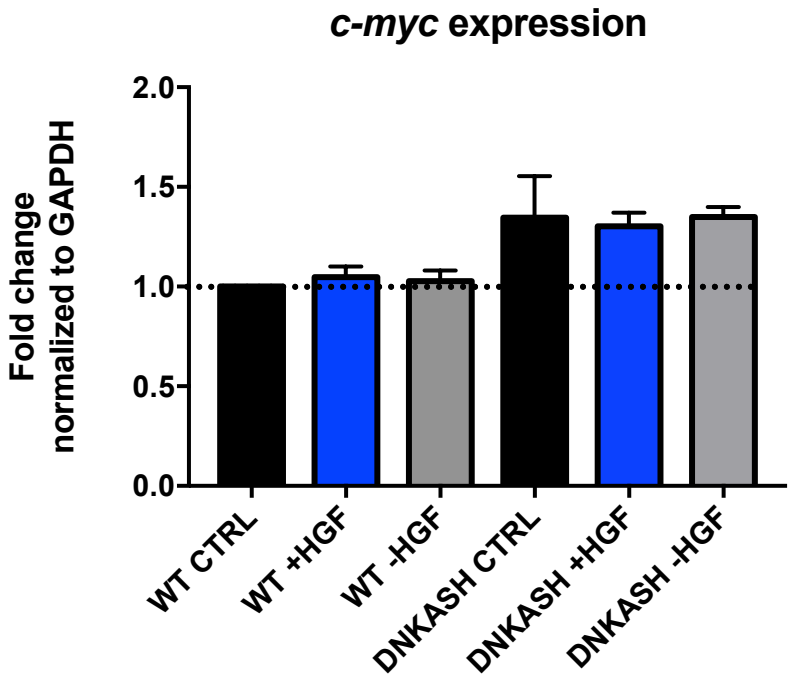

Fig 112: *c-myc* expression level evaluation. Mean ± SEM. Kruskal-Wallis test. N=2 independent experiments.

HGF treatment causes nuclear translocation of β-catenin (Gayrard et al., 2018) (see also Fig 61E in Chapter 3 and Fig 103A in Chapter 6), which can result in β-catenin dependent-gene transcription (Clevers H & Nusse R, 2012) (see also paragraph 3 in Chapter 3). The absence of and increased expression of *c-myc* in HGF conditions may lie in the timing used to carry out the above experiment. Indeed, cells were exposed to HGF only for 5 hours, which may be a too narrow time window to let β-catenin transactivate its target genes. To this regard, in the TOPdGFP cell line we observed increased level of dGFP 10 hours after LiCl treatment (see Fig 104 and Fig 106D in Chapter 6), which can suggest that a 10 hours window is maybe the ideal range of time to observe, if any, an up-regulation of *c-myc* expression.

On the other hand, it is interesting the increased, even though not significant, expression of *c-myc* found in the mCherry-DNKASH cell line. Since β-catenin does not localize in the nucleus when the LINC complex is disrupted (Uzer et al., 2018) (see also Fig 35B in Chapter 2 and Fig 103A in Chapter 6), the found basal *c-myc* up-regulation may be due to other signalling pathways (Shuntaro Yamashita, Ogawa, Ikei, Fujiki, & Katakura, 2014) that can overcome the absence of nuclear β-catenin, thus activating *c-myc*. Therefore, it could be speculated that stable-LINC complex disrupted cells may survive through induction of pro-proliferative mechanisms.

4 Generation of a nanobody construct for miniNesprin 2G mechanical manipulation.

Similarly to Etoc et al. where the researchers used magnetic tweezers to have subcellular control of Rac-GTPase signalling (Etoc et al., 2013),we wanted to micromanipulate GFP-tagged miniNesprin 2G (miniN2G-GFP) protein, in *cellulo*. Magnetic tweezer micromanipulation was supposed to be carried out by using an mCherry-tagged antiGFP nanobody chimeric construct -derived from the pOPINE GFP nanobody vector (Kubala, Kovtun, Alexandrov, & Collins, 2010)- coupled to magnetic nanobeads. Once the above construct was generated, its capability to recognize GFP tag was tested by overexpressing it into an MDCK cell line (type II G) stable for miniN2G-GFP expression. Cells were transfected (as reported in paragraph 3, Chapter 5) and then replated and PFA fixed (as reported in the above paragraph 2 and in paragraph 9,Chapter 5). Once imaged under the confocal microscope (see paragraph 10 in Chapter 5), cells transfected with the chimeric construct displayed a clear red rim around the nuclear envelope, which colocalized with the GFP signal (Fig 113, above). This was not observed in a control condition, where cells were transfected with a vector harbouring the mCherry tag alone, whose fluorescence was then spotted throughout the nucleus (Fig 113, below).

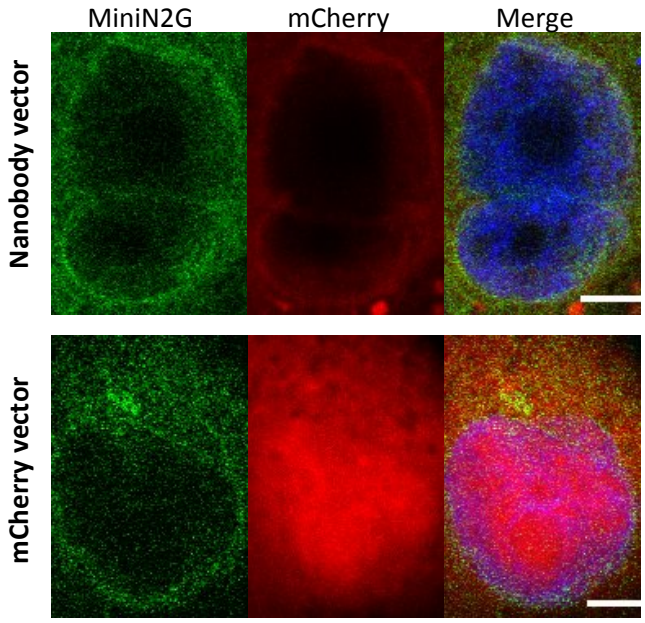

Fig 113: The generated mCherry-tagged antiGFP nanobody localizes around the nuclear envelope of MDCK cells stably expressing miniN2G-GFP (above), whereas the mCherry tag alone localizes throughout the nucleus (below). Scale bars: 5 μm.

Despite this achievement and even though nanobeads microinjection tests in cells were successful (Fig 114), we were not able to couple the nanobody onto the surface of the magnetic nanobeads. Moreover, the magnetic manipulation of the test-microinjected nanobeads resulted extremely difficult to carry out, especially due to the formation of nanobeads clusters stuck onto the

cell membrane and thus impossible to magnetically displace, which made us to pause this project.

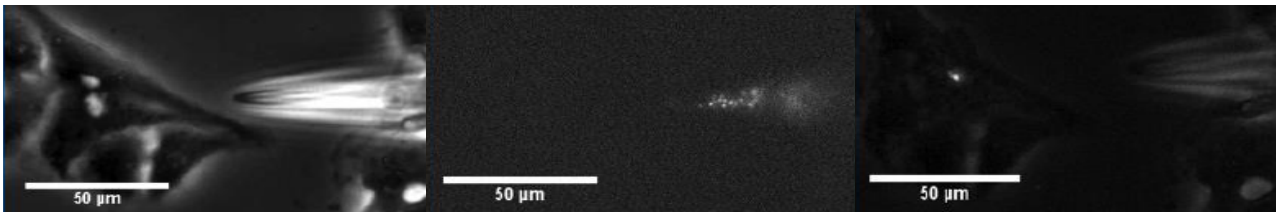

Fig 114: Before (transmission image on the left and fluorescence image in the middle) and after (transmission and fluorescence image on the right) microinjection of FG beads magnetic 200nm Cyanine3 (Tamagawa) nanobeads into MDCK cells. In the images on the left and on the right, it is visible the glass micropipette (at the right side in both images) used to carry out nanobeads microinjection. The image in the middle shows the fluorescent nanobeads within the glass micropipette. Adapted from Jules Caput's M1 report.

Annex 2

Here, it is reported a protocol paper which will appear in "Methods in Molecular Biology" as part of a book on EMT.

Molecular Tension Microscopy of E-cadherin during Epithelial-Mesenchymal Transition

Helena Canever[1], Pietro Salvatore Carollo[1], Romain Fleurisson[1], Philippe P. Girard[1,2], Nicolas Borghi[1,*]

[1] Institut Jacques Monod, CNRS UMR7592, Université de Paris, 75013 Paris, France

[2] Faculty of Basic and Biomedical Sciences, Université Paris Descartes, 45 rue des Saints Pères, 75270 Paris Cedex 06, France.

*correspondence: nicolas.borghi@ijm.fr

Running head: "Molecular Tension Microscopy of E-cadherin during EMT"

Abstract

Molecular Tension Microscopy has been increasingly used in the last years to investigate mechanical forces acting in cells at the molecular scale. Here, we describe a protocol to image the tension of the junctional protein E-cadherin in cultured epithelial cells undergoing Epithelial-Mesenchymal Transition (EMT). We report how to prepare cells and induce EMT, and how to acquire, analyse and quantitatively interpret FRET data.

Keywords: FRET Biosensor, E-cadherin, EMT, Microscopy, Mechanotransduction.

1. Introduction

Molecular Tension Microscopy (MTM) is the microscopy of molecular tension sensors (Gayrard & Borghi, 2016). Molecular tension sensors are a class of Förster Resonance Energy Transfer (FRET) sensors that are sensitive to molecular tension. They consist in a FRET pair of fluorophores separated by an elastic linker. When a force is exerted on the sensor, the rate of FRET, which is sensitive to the distance and orientation between the donor and acceptor fluorophores, decreases. Knowledge of the relationship between a measure of FRET and the force, from in vitro calibration, allows for the determination of molecular tension (Grashoff, Hoffman, Brenner, Zhou, Parsons, Yang, McLean, Sligar, Chen, Ha, & others, 2010). When inserted in a protein of interest, such a sensor can report its tension in live cells.

Molecular tension sensors have been in use for nearly 10 years (Meng, Suchyna, & Sachs, 2008). A variety of sensors with specific operating ranges have been designed (Brenner et al., 2016; Ringer et al., 2017), and have been used to measure tension in matrix, cytoskeleton, adhesion, glycocalyx, kinetochore, membrane-cytoskeleton linker or motor proteins (Grashoff, Hoffman, Brenner, Zhou, Parsons, Yang, McLean, Sligar, Chen, Ha, & others, 2010; Hart et al., 2019; Meng et al., 2008; Paszek et al., 2014; Suzuki et al., 2016; X. Zhang et al., 2019) in cultured cells, C. elegans, Xenopus, Zebrafish or Drosophila (Lagendijk et al., 2017; Lemke, Weidemann, Cost,

Grashoff, & Schnorrer, 2019; Meng et al., 2008; Satoshi Yamashita, Tsuboi, Ishinabe, Kitaguchi, & Michiue, 2016).

Here, we present a protocol to perform MTM of intercellular adhesion proteins E-cadherins (Yoshida & Takeichi, 1982) that experience cytoskeleton-generated tension sensitive to external cues (N. Borghi et al., 2012). During Epithelial-Mesenchymal Transition (EMT), E-cadherin tension relaxes, which associates with the release of its interactant β-catenin and activation of β-catenin dependent transcription (Gayrard et al., 2018).

The protocol describes how to culture epithelial cells (MDCK) stably expressing an E-cadherin tension sensor (E-cadherin-TSMod), induce EMT, and acquire and analyze FRET data using standard confocal microscopy and free image analysis software (Schneider, Rasband, & Eliceiri, 2012) (see Fig. 1). The protocol may be adapted to other proteins or model systems, on different microscopes as well. General considerations about MTM, its strengths and limitations can be found elsewhere (Gayrard & Borghi, 2016).

2. Materials

Store DMEM (Dulbecco's Modified Eagle Medium), trypsin, Dulbecco's Phosphate Buffered Saline (DPBS, that is without Calcium and Magnesium), collagen at 4°C. Store Foetal Bovine Serum (FBS), Penicillin, Streptomycin and Hepatocyte Growth Factor (HGF) solution at -80°C.

2.1 Cell culture

1. Culture medium: low glucose DMEM with phenol red supplemented with 10 % v/v Foetal Bovine Serum (FBS) and Penicillin 10 U/mL + Streptomycin 10 µg/mL.
2. Washing medium: DPBS.
3. 0.05% trypsin-EDTA solution in DPBS.
4. Madin-Darby canine kidney type II (MDCK II) stable cell lines cultured into 25 cm^2 flasks (T25, TPP) at 37°C with 5% CO_2 in humidified atmosphere expressing (see Fig. 2a):

5. E-cadherin-TSMod: E-Cadherin tension sensor containing the donor protein mTFP1 and acceptor protein EYFP separated by a $(GPGGA)_8$ elastic linker (N. Borghi et al., 2012).

6. E-Cadherin-TSModΔcyto: tension-less control construct of the E-Cadherin tension sensor, lacking its cytoplasmic tail (N. Borghi et al., 2012) (see Note 1).

7. mTFP1-GPGGA-Venus: high FRET standard construct made of mTFP1 and Venus separated by a GPGGA amino acid stretch (referred to as 5aa) (R.N. Day, Booker, & Periasamy, 2008).

8. mTFP1-TRAF-Venus: low FRET standard construct made of mTFP1 and Venus separated by a 229 amino acid from Tumor Necrosis Factor Receptor Associated Factor domain (referred to as TRAF) (R.N. Day et al., 2008).

All cell lines and constructs are available on demand.

2.2 Cell imaging

1. Any commercial #1.5 glass-bottomed imaging dish.

2. Collagen from human placenta Bornstein and Traub Type IV (referred to as collagen) 50 µg/mL in acetic acid solution: solubilize 5 mg of collagen in 5 mL of acetic acid (0.5 M) on ice to obtain a 20X stock solution. Dilute in acetic acid (0.5 M) to obtain a solution at the final concentration of 50 µg/mL.

3. Imaging medium: FluoroBrite™ DMEM (or any equivalent product), without phenol red, supplemented with 10 % v/v FBS, 1% v/v PS, 2.5 mM L-Glutamine and 20mM HEPES. Store away from light.

4. Starvation medium: FluoroBrite™ DMEM, without phenol red, supplemented with 0.5 % v/v FBS, 1% v/v PS, 2.5 mM L-Glutamine and 20 mM HEPES. Store away from light.

5. Paraffin oil. Store away from the light at room temperature.

2.3 Cell Scatter assay

1. Hepatocyte Growth Factor (HGF) 10 ng/µL in BSA/DPBS solution: solubilize 1 mg of BSA (Bovine Serum Albumin) in 1 mL of DPBS. Solubilize 10 µg of HGF in the BSA/DPBS solution. Stock as 10 µL aliquots.

2. Stimulation medium: The day of the experiment, dilute an aliquot in 2 mL of starvation medium for a final HGF concentration of 50 ng/mL.

2.4 Wound Healing assay

1. 200 µL pipette tips.

2. Washing medium.

2.5 Microscope

1. Commercial confocal inverted microscope equipped with an incubator (37°C and 5% CO_2 in a humidified atmosphere) and:

2. High numerical aperture immersion objectives (see Note 2).

3. Argon laser -the 458 nm line is optimal for mTFP1 excitation- or equivalent, and a beam splitter that transmits above the excitation wavelength.

4. Spectral acquisition: microscopes that use a grating in the emission path (such as Zeiss or Olympus) allow for simultaneous acquisition of the donor and acceptor emission spectra with a spectral resolution below 10 nm and nm precision (see Fig. 2 b and c).

3. Methods

Carry out all procedures in a cell culture hood unless otherwise specified**.**

3.1 Cell culture maintenance

Pass MDCK II cells three times a week as follows:

1. Prepare a new cell culture flask containing 3 mL of fresh culture medium and put it into the incubator.

2. Remove old culture medium and dead cells from the cell culture flask.

3. Wash once with 1 mL of washing medium and by gently shaking the cell culture flask.

4. Add 1 mL of Trypsin-EDTA solution in DPBS to the cell culture flask.

5. Put the cell culture flask into incubator and wait about 10 minutes for cells to detach from the surface and from each other.

6. Use a microscope to evaluate cell detachment.

7. Once cells are detached, transfer 1:10 of the collected volume into the new flask.

3.2 Collagen preparation and Coverslip coating

1. Take glass-bottomed imaging dishes.
2. Place 1 mL of collagen solution at 50 µg/mL onto the glass-bottomed dish for 10 min at room temperature.
3. Remove collagen solution and let dry for 1 hour (see Note 3).
4. Sterilize the dishes under UV for 20 minutes (see Note 4).
5. Before use, wash the sterilized dishes with at least 1 mL of DPBS, twice.

3.3 Cell seeding for imaging

Seed cells 24 hours before imaging. Prepare separately cells that express the tension sensor as well as cells that express the tension-less control. Follow steps 1 to 6 of the section 3.1 and continue as follows:

1. Collect the cell suspension into a sterile centrifugation tube.
2. Pellet the cells by centrifugation at 60-125 *g* for 5-8 min.
3. Meanwhile, add culture medium onto the collagen coated imaging dishes.
4. Discard the supernatant of the centrifugation tube and re-suspend the pellet with culture medium (see Note 5).
5. Count cells with a hematocytometer or equivalent device.

6. Plate 1:10 of the collected volume in a new flask with culture medium.
7. Plate cells onto collagen coated imaging dishes: 2 x 10^5 for a cell scatter assay or 2 x 10^6 for a Wound Healing assay (see Note 6).

3.4 Cell Scatter assay

1. The day after seeding, starve cells for 12 hrs in 2 mL imaging medium at 0.5 % FBS.
2. Wipe the bottom of the glass-bottomed dish once with optical paper and distilled water, and again with ethanol 70 %.
3. Install the imaging dish on the stage of the microscope.
4. Acquire pre-treatment images (see section 3.6).
5. Replace the imaging medium with stimulation medium (see Note 7).
6. Add 1 mL paraffin oil at the surface of the imaging medium to prevent evaporation (see Note 8).
7. Acquire treatment images (see section 3.6).

It is recommended to perform a mock experiment in parallel by following steps 1-7 except step 5 in which the medium does not contain HGF.

3.5 Wound Healing Assay

1. The day after seeding, wash and leave cells in the washing medium for 5-10 minutes to loosen intercellular contacts (see Note 9).
2. With a 200µL pipette tip, perform a straight scratch in the cell monolayer (see Note 10).
3. Gently wash the dish with imaging medium and leave cells in 2 mL of imaging medium.
4. Any time after the wound, wipe the bottom of the coverslip as in 3.4.2 and install the imaging dish on the stage of the microscope, add paraffin oil and acquire images (see section 3.6).

3.6 Image acquisition

1. Select an objective and exposure time to ensure sufficient signal to noise ratio, negligible fluorophore photobleaching and no saturation, as for standard fluorescence imaging.

2. Specify multi-position settings: if desired, acquiring images from multiple positions can increase your sample size per experiment. Choose between 5 – 10 positions considering that the total acquisition time of each position must not exceed the duration of the time interval between frames (see Note 11).

3. Specify Z-stack settings: if desired, this can alleviate focus drift if auto-focus is out-of-order. Make sure to avoid photobleaching.

4. Specify time-lapse settings: cell scattering by HGF and wound healing typically occur through several hours. Choose a time interval between frames of 10 minutes to 1 hour (see Note 12).

5. Specify spectral acquisition settings: 10 channels in the 473 – 561 nm bandwidth will capture both fluorophores. This will generate a multichannel stack.

3.7 Image analysis

Image analysis can be performed using the free and cross-platform software ImageJ, for instance its FIJI distribution (https://fiji.sc/) (see Fig. 3).

1. Make duplicates of the raw data to avoid losses after permanent modifications (see Note 13). Generate a FRET index image as follows.

2. Open an image file.

3. From the multichannel stack, duplicate the donor and acceptor emission channels (D and A) that correspond to the intensity peaks of the two fluorophores (see Note 14).

4. On both channels, convert image depth to 32-bit. (Image>Type>32-bit)

5. On both channels, subtract background: select a region devoid of cells and measure background level (Analyze>Measure), then subtract the value to the whole image (Process>Math>Subtract [Background value]) (see Note 15).

6. From both channels, generate a donor + acceptor image (D+A) that sums background corrected, donor and acceptor signals pixel by pixel. (Process>Image Calculator>Create new window>32-bit(float) result >[D] Add [A], Create a new window).

7. From the background corrected, acceptor channel and the sum image, generate the FRET index image A/(D+A) (Process>Image Calculator>Create new window>32-bit(float) result>[A] Divide [D+A]).

8. Rescale the pixel values between 0 and 100. (Process>Math>Multiply [100]).

9. Select regions of interest (ROI) with any selection tool, then measure their mean grey value (Analyze>Measure) to get their FRET index.

10. Alternatively, ROI can be defined by segmentation based on fluorescence intensity, size and shape: select the acceptor channel (Note 16), apply a threshold to select bright regions (Image>Adjust>Threshold, set to your taste then Apply) (see Note 17). Choose preferred bright regions according to size and shape by setting their ranges (Analyze>Analyze Particles, check Add to Manager) (see Note 18). In the ROI manager menu, save the ROI set to be able to recall it for future analyses (More>Save). Select/Open the corresponding FRET Index image (3.7.7) and click Measure in the ROI manager menu. You will obtain a measure for each ROI of the set.

3.8. Microscope Calibration

The FRET efficiency E can be related to the FRET index E_R computed as in 3.7 with $E=(1-a(1-E_R))/(1-b(1-E_R))$, where a and b are instrument-dependent coefficients that account for the donor's spectral bleed-through, the acceptor's direct excitation and differences in donor vs acceptor absorption cross-sections and detection efficiencies (N. K. Lee et al., 2005). They can be recovered as follows (see Note 19):

1. Acquire images of the 5aa and TRAF cell lines as in 3.6. There is no need for time-lapse or Z-stack.

2. Analyse images as in 3.7.

3. Compute $a=(E_H(1-E_{R,H}) - E_L(1-E_{R,L}) + E_HE_L(E_{R,H} - E_{R,L}))/c$ and $b= (E_H(1-E_{R,L}) - E_L(1-E_{R,H}) + E_{R,L} - E_{R,H})/c$, with $c=(E_H - E_L)(1 - E_{R,H})(1 - E_{R,L})$, where $E_{R,H}$ and $E_{R,L}$ are the 5aa and TRAF cell lines FRET indices obtained in 3.8.2, and E_H and E_L their FRET efficiencies published elsewhere (R.N. Day et al., 2008).

3.9. Data interpretation

1. For each experimental condition, compute the difference between the tension sensor and tension-less control FRET efficiencies (see Note 20).

2. Use previously published FRET efficiency to force calibration (Grashoff, Hoffman, Brenner, Zhou, Parsons, Yang, McLean, Sligar, Chen, Ha, & others, 2010) to retrieve the force.

3. Mind MTM limitations in your interpretation (Gayrard & Borghi, 2016).

4. Notes

1. There exist other strategies for tension-less constructs, which may or may not give equivalent results depending on the protein of interest, as discussed in (Gayrard & Borghi, 2016).

2. High magnification is irrelevant but comes with high numerical aperture, which increases resolution and signal intensity, and should also come with apochromatic correction. Choose the highest you can, typically 1.4 for standard objectives.

3. Save used collagen solution back in the final concentration solution for later use. Store at 4°C indefinitely.

4. Use the UV light of the cell culture hood. Do not cover the dishes with a plastic lid. Multiple dishes can be prepared in advance and stored on the shelf indefinitely

5. When re-suspending cells, pipette up and down to shear and dissociate cell aggregates. This will facilitate homogenous seeding.

6. When seeding, make sure the cell suspension covers the whole coverslip by gently shaking the dish linearly in X and Y, not circularly as cells would aggregate at the centre of the coverslip.

7. Execute with care and promptly directly on the microscope stage to keep focus, temperature and position the same.

8. Make sure there is enough oil to cover the whole surface of the imaging medium to prevent evaporation.

9. Check that the monolayer is confluent before this step.

10. Two perpendicular scratches maximize wound edge length per coverslip. Use/draw fiducial markers on the coverslip/imaging chamber to easily find the wound once on the microscope stage.

11. Selecting positions in close proximity minimizes the spreading and loss of the objective immersion medium.

12. Consider the total acquisition time per time-point (multiple positions and Z sections), the total duration of the time-lapse, photobleaching and phototoxicity. 20 to 30 minute intervals are adequate for most experiments.

13. Name your processed files consistently with the original files but with a different name to prevent overwriting.

14. Always keep the same donor and acceptor channels throughout all your analyses. You can identify them by plotting the intensity of a region containing fluorophores against the wavelength (or channel number) (select the multichannel stack then Image>Hyperstacks>Hyperstack to Stack, then select a region and Image>Stacks>Plot Z-axis profile). The plot should display two maxima (around 490 and 530nm), if not, do not analyse further: the cell has likely not processed the full construct properly.

15. Before this step, you may filter some noise by local averaging of pixel levels, at the expense of spatial resolution (for instance, Process>Filters>Gaussian Blur).

16. For E-cadherin-TSMod, the donor channel often exhibits intracellular aggregates, probably synthesis or degradation intermediates in which the acceptor fluorophore does not emit. Hence, the acceptor channel is preferred.

17. You can explore the different tools available on Image J to process binary images (Process>Binary>…) to improve segmentation from the thresholded image.

18. More information on how to use the ROI Manager tool can be found here (https://imagej.nih.gov/ij/docs/guide/). Size and shape selection can be very useful to exclude regions too small or round to be cell-cell contacts. In the ROI Manager, you can delete unwanted regions (>Delete) or add missing regions (draw with any selection tool then >Add).

19. This does not need to be done for every experiment but can be performed from time to time to assess the microscope stability.

20. The Ecad-TSModΔcyto is sensitive to intermolecular FRET (N. Borghi et al., 2012). This normalization thus corrects for possible FRET changes due to intermolecular FRET among other causes.

Acknowledgements

This work was supported in part by the Centre national de la recherche scientifique (CNRS), the French National Research Agency (ANR) grants (ANR-17-CE13-0013, ANR-17-CE09-0019, ANR-18-CE13-0008), France BioImaging infrastructure (ANR-10-INBS-04), La Ligue contre le Cancer (Allocation de recherche doctorale to HC), the European Union's Horizon 2020 research and innovation programme (Marie Skłodowska-Curie grant agreement No 665850-INSPIRE to PSC). PSC acknowledges the Ecole Doctorale FIRE-Programme Bettencourt. We acknowledge the ImagoSeine facility, member of the France BioImaging infrastructure (ANR-10-INSB-04).

Figure captions

Figure 1: Experimental workflow for MDCK type II cells sample preparation, EMT induction, image acquisition and image and data analysis.

Figure 2: (a) E-Cadherin-TSMod, tension-less control E-Cadherin-TSModΔcyto, and high and low FRET calibration constructs. Blue squares represent the donor fluorophore mTFP1, yellow squares represent the acceptor fluorophore EYFP/Venus. Linkers $(GPGGA)_8$, 5aa, and TRAF are represented in black. (b) Absorption and emission spectra of mTFP1 and EYFP/Venus. Laser excitation wavelength is indicated by the red dashed line. (c) Spectral emission in the detection bandwidth for mTFP1 and EYFP. Donor and acceptor emission peaks are indicated.

Figure 3: Image analysis workflow for FRET calculation and image segmentation from a multi-channel spectral image.

Fig 1

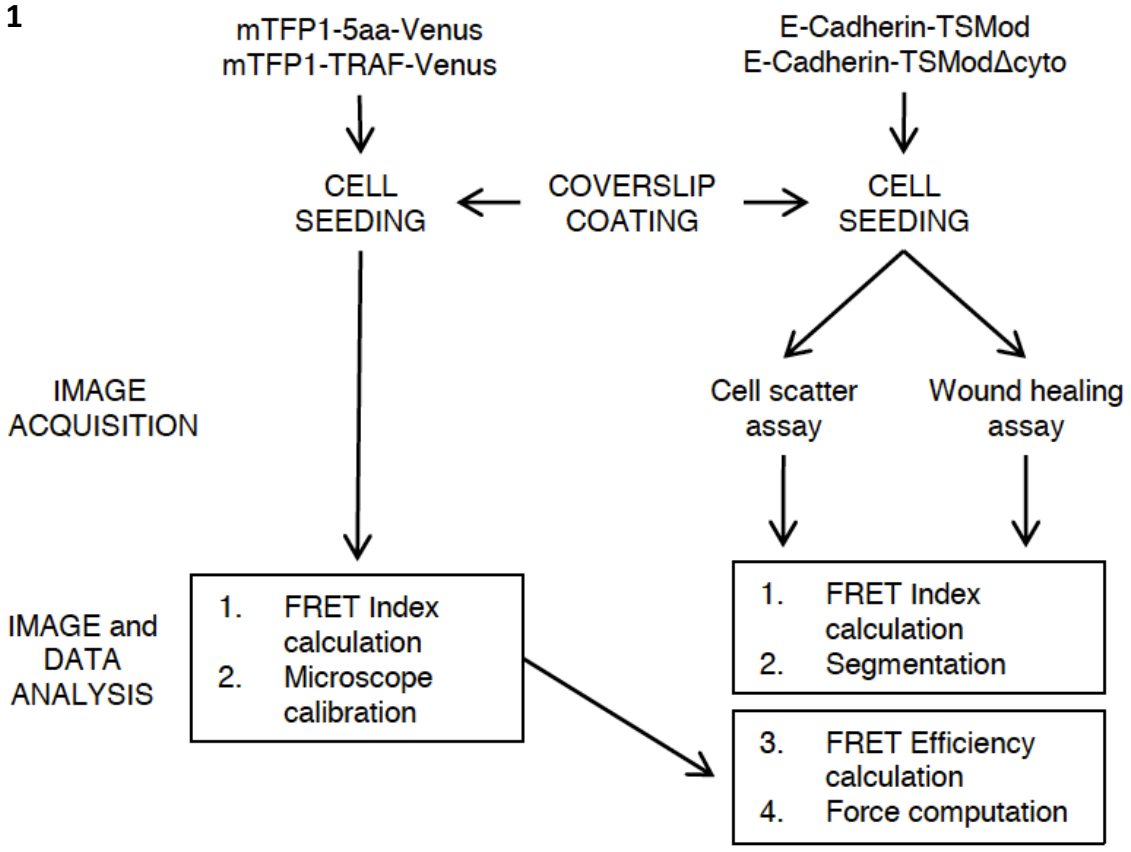

Fig 2

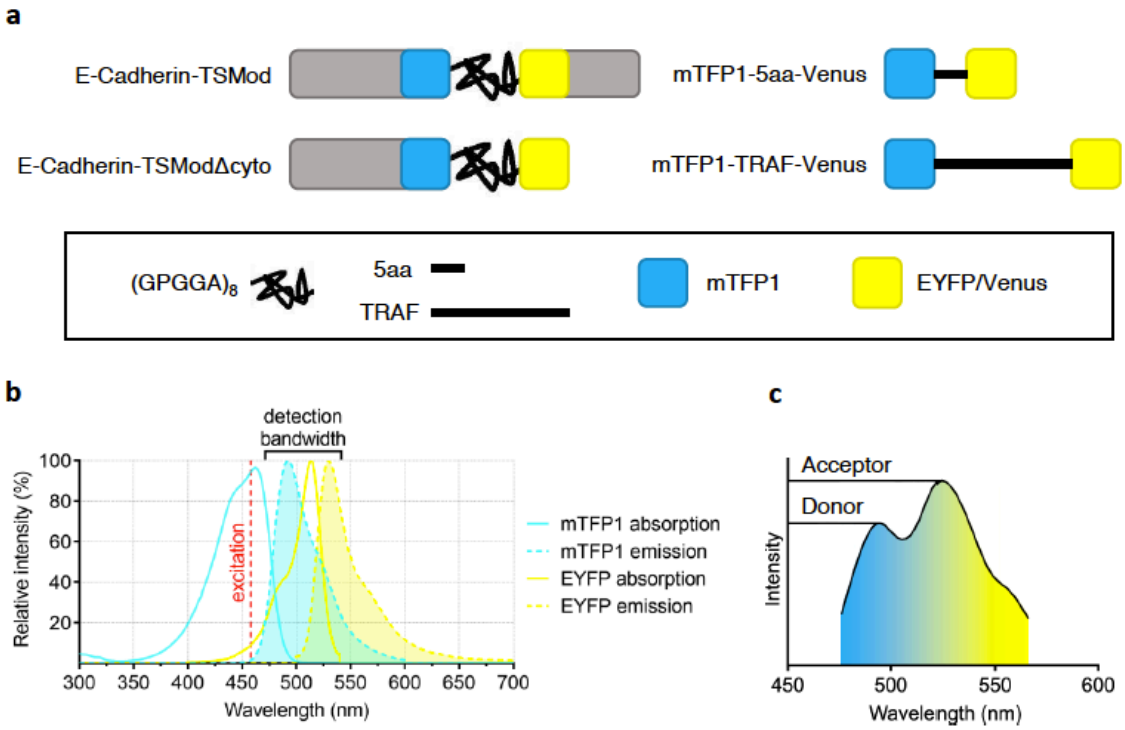
a
E-Cadherin-TSMod
mTFP1-5aa-Venus
E-Cadherin-TSModΔcyto
mTFP1-TRAF-Venus
(GPGGA)8
5aa
TRAF
mTFP1
EYFP/Venus
b
detection bandwidth
Relative intensity (%)
excitation
mTFP1 absorption
mTFP1 emission
EYFP absorption
EYFP emission
Wavelength (nm)
c
Acceptor
Donor
Intensity
Wavelength (nm)

Fig 3

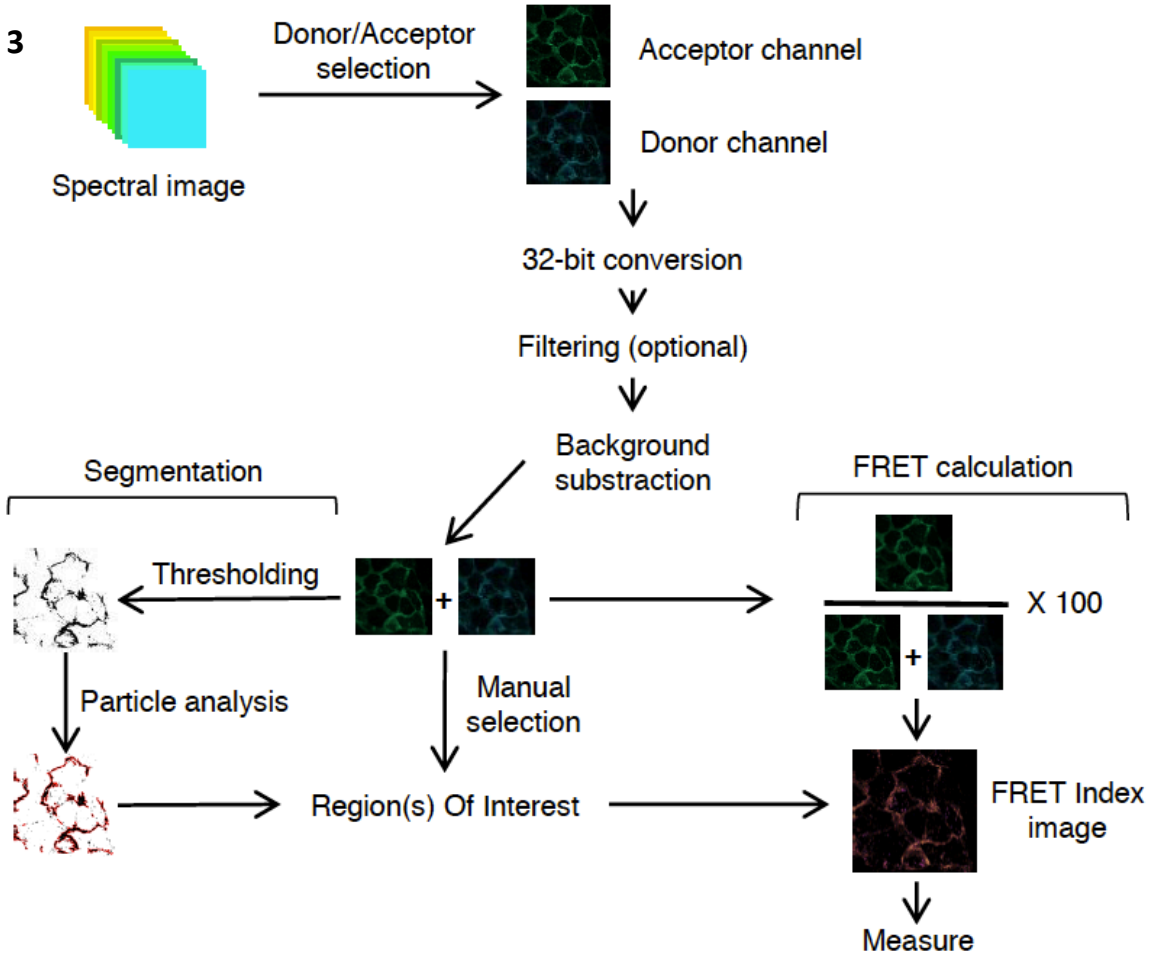
Spectral image
Donor/Acceptor selection
Acceptor channel
Donor channel
32-bit conversion
Filtering (optional)
Background substraction
Segmentation
FRET calculation
Thresholding
X 100
Particle analysis
Manual selection
Region(s) Of Interest
FRET Index image
Measure

Bibliography

Aberle, H, Butz, S., Stappert, J., Weissig, H., Kemler, R., & Hoschuetzky, H. (1994). Assembly of the cadherin-catenin complex in vitro with recombinant proteins. *Journal of Cell Science*.

Aberle, Hermann, Bauer, A., Stappert, J., Kispert, A., & Kemler, R. (1997). β-catenin is a target for the ubiquitin-proteasome pathway. *EMBO Journal*. https://doi.org/10.1093/emboj/16.13.3797

Aiello, N. M., Maddipati, R., Norgard, R. J., Balli, D., Li, J., Yuan, S., … Stanger, B. Z. (2018). EMT Subtype Influences Epithelial Plasticity and Mode of Cell Migration. *Developmental Cell*, *45*(6), 681-695.e4. https://doi.org/10.1016/j.devcel.2018.05.027

Akhmanova, A., & Steinmetz, M. O. (2015, December 1). Control of microtubule organization and dynamics: Two ends in the limelight. *Nature Reviews Molecular Cell Biology*, Vol. 16, pp. 711–726. https://doi.org/10.1038/nrm4084

Alam, S. G., Zhang, Q., Prasad, N., Li, Y., Chamala, S., Kuchibhotla, R., … Lele, T. P. (2016). The mammalian LINC complex regulates genome transcriptional responses to substrate rigidity. *Scientific Reports*. https://doi.org/10.1038/srep38063

Alber, F., Dokudovskaya, S., Veenhoff, L. M., Zhang, W., Kipper, J., Devos, D., … Rout, M. P. (2007). The molecular architecture of the nuclear pore complex. *Nature*, *450*(7170), 695–701. https://doi.org/10.1038/nature06405

Amit, S., Hatzubai, A., Birman, Y., Andersen, J. S., Ben-Shushan, E., Mann, M., … Alkalay, I. (2002). Axin-mediated CKI phosphorylation of β-catenin at Ser 45: A molecular switch for the Wnt pathway. *Genes and Development*. https://doi.org/10.1101/gad.230302

Andrade, M. A., & Bork, P. (1995). HEAT repeats in the Huntington's disease protein. *Nature Genetics*. https://doi.org/10.1038/ng1095-115

Angers, S., & Moon, R. T. (2009). Proximal ev1. Angers, S. & Moon, R. T. Proximal events in Wnt signal transduction. Nat. Rev. Mol. Cell Biol. 10, 468–77 (2009).ents in Wnt signal transduction. *Nature Reviews. Molecular Cell Biology*. https://doi.org/10.1038/nrm2717

Aoki, K., Kumagai, Y., Sakurai, A., Komatsu, N., Fujita, Y., Shionyu, C., & Matsuda, M. (2013). Stochastic ERK activation induced by noise and cell-to-cell propagation regulates cell density-dependent proliferation. *Molecular Cell*, *52*(4), 529–540. https://doi.org/10.1016/j.molcel.2013.09.015

Aragona, M., Panciera, T., Manfrin, A., Giulitti, S., Michielin, F., Elvassore, N., … Piccolo, S. (2013). A mechanical checkpoint controls multicellular growth through YAP/TAZ regulation by actin-processing factors. *Cell*, *154*(5), 1047–1059. https://doi.org/10.1016/j.cell.2013.07.042

Arsenovic, P. T., Ramachandran, I., Bathula, K., Zhu, R., Narang, J. D., Noll, N. A., … Conway, D. E. (2016). Nesprin-2G, a Component of the Nuclear LINC Complex, Is Subject to Myosin-Dependent Tension. *Biophysical Journal*. https://doi.org/10.1016/j.bpj.2015.11.014

Asally, M., & Yoneda, Y. (2005). Beta-catenin can act as a nuclear import receptor for its partner transcription factor, lymphocyte enhancer factor-1 (lef-1). *Experimental Cell Research*, *308*(2), 357–363. https://doi.org/10.1016/j.yexcr.2005.05.011

Bajpai, S., Feng, Y., Krishnamurthy, R., Longmore, G. D., & Wirtz, D. (2009). Loss of α-catenin decreases the strength of single E-cadherin bonds between human cancer cells. *Journal of Biological Chemistry*. https://doi.org/10.1074/jbc.M109.000661

Bamburg, J. R., Harris, H. E., & Weeds, A. G. (1980). Partial purification and characterization of an actin depolymerizing factor from brain. *FEBS Letters*. https://doi.org/10.1016/0014-5793(80)81292-0

Banerjee, I., Zhang, J., Moore-Morris, T., Pfeiffer, E., Buchholz, K. S., Liu, A., … Chen, J. (2014). Targeted Ablation of Nesprin 1 and Nesprin 2 from Murine Myocardium Results in Cardiomyopathy, Altered Nuclear Morphology and Inhibition of the Biomechanical Gene

Response. *PLoS Genetics*, *10*(2). https://doi.org/10.1371/journal.pgen.1004114
Bänziger, C., Soldini, D., Schütt, C., Zipperlen, P., Hausmann, G., & Basler, K. (2006). Wntless, a Conserved Membrane Protein Dedicated to the Secretion of Wnt Proteins from Signaling Cells. *Cell*. https://doi.org/10.1016/j.cell.2006.02.049
Baranwal, S., & Alahari, S. K. (2009). Molecular mechanisms controlling E-cadherin expression in breast cancer. *Biochemical and Biophysical Research Communications*, *384*(1), 6–11. https://doi.org/10.1016/j.bbrc.2009.04.051
Baratchi, S., Khoshmanesh, K., Woodman, O. L., Potocnik, S., Peter, K., & McIntyre, P. (2017). Molecular Sensors of Blood Flow in Endothelial Cells. *Trends in Molecular Medicine*, *23*(9), 850–868. https://doi.org/10.1016/j.molmed.2017.07.007
Bartscherer, K., Pelte, N., Ingelfinger, D., & Boutros, M. (2006). Secretion of Wnt ligands requires Evi, a conserved transmembrane protein. *Cell*, *125*(3), 523–533. https://doi.org/10.1016/j.cell.2006.04.009
Baumann, M., Steichen-Gersdorf, E., Krabichler, B., Petersen, B. S., Weber, U., Schmidt, W. M., … Janecke, A. R. (2017). Homozygous SYNE1 mutation causes congenital onset of muscular weakness with distal arthrogryposis: A genotype-phenotype correlation. *European Journal of Human Genetics*. https://doi.org/10.1038/ejhg.2016.144
Bayliss, R., Littlewood, T., & Stewart, M. (2000). Structural basis for the interaction between FxFG nucleoporin repeats and importin-β in nuclear trafficking. *Cell*. https://doi.org/10.1016/S0092-8674(00)00014-3
Bayliss, R., Littlewood, T., Strawn, L. A., Wente, S. R., & Stewart, M. (2002). GLFG and FxFG nucleoporins bind to overlapping sites on importin-β. *Journal of Biological Chemistry*. https://doi.org/10.1074/jbc.M209037200
Bays, J. L., & DeMali, K. A. (2017). Vinculin in cell–cell and cell–matrix adhesions. *Cellular and Molecular Life Sciences*. https://doi.org/10.1007/s00018-017-2511-3
Becker, N., Oroudjev, E., Mutz, S., Cleveland, J. P., Hansma, P. K., Hayashi, C. Y., … Hansma, H. G. (2003). Molecular nanosprings in spider capture-silk threads. *Nature Materials*, *2*(4), 278–283. https://doi.org/10.1038/nmat858
Behrens, J., Von Kries, J. P., Kühl, M., Bruhn, L., Wedlich, D., Grosschedl, R., & Birchmeier, W. (1996). Functional interaction of β-catenin with the transcription factor LEF- 1. *Nature*. https://doi.org/10.1038/382638a0
Belenkaya, T. Y., Wu, Y., Tang, X., Zhou, B., Cheng, L., Sharma, Y. V, … Lin, X. (2008). The retromer complex influences Wnt secretion by recycling wntless from endosomes to the trans-Golgi network. *Developmental Cell*, *14*(1), 120–131. https://doi.org/10.1016/j.devcel.2007.12.003
Beloussov, L. V, Dorfman, J. G., & Cherdantzev, V. G. (1975). Mechanical stresses and morphological patterns in amphibian embryos. *Journal of Embryology and Experimental Morphology*.
Benham-Pyle, B. W., Pruitt, B. L., & Nelson, W. J. (2015). Mechanical strain induces E-cadherin-dependent Yap1 and β-catenin activation to drive cell cycle entry. *Science*. https://doi.org/10.1126/science.aaa4559
Benham-Pyle, B. W., Sim, J. Y., Hart, K. C., Pruitt, B. L., & Nelson, W. J. (2016). Increasing β-catenin/Wnt3A activity levels drive mechanical strain-induced cell cycle progression through mitosis. *ELife*, *5*(OCTOBER2016). https://doi.org/10.7554/eLife.19799
Berk, J. M., Tifft, K. E., & Wilson, K. L. (2013). The nuclear envelope LEM-domain protein emerin. *Nucleus (United States)*. https://doi.org/10.4161/nucl.25751
Bhanot, P., Brink, M., Samos, C. H., Hsieh, J. C., Wang, Y., Macke, J. P., … Nusse, R. (1996). A new member of the frizzled family from Drosophila functions as a Wingless receptor. *Nature*, *382*(6588), 225–230. https://doi.org/10.1038/382225a0
Bione, S., Maestrini, E., Rivella, S., Mancini, M., Regis, S., Romeo, G., & Toniolo, D. (1994).

Identification of a novel X-linked gene responsible for Emery-Dreifuss muscular dystrophy. *Nature Genetics*, *8*(4), 323–327. https://doi.org/10.1038/ng1294-323
Bolós, V., Peinado, H., Pérez-Moreno, M. A., Fraga, M. F., Esteller, M., & Cano, A. (2003). The transcription factor Slug represses E-cadherin expression and induces epithelial to mesenchymal transitions: a comparison with Snail and E47 repressors. *Journal of Cell Science*, *116*(Pt 3), 499–511. https://doi.org/10.1242/jcs.00224
Borghi, N., Sorokina, M., Shcherbakova, O. G., Weis, W. I., Pruitt, B. L., Nelson, W. J., & Dunn, A. R. (2012). E-cadherin is under constitutive actomyosin-generated tension that is increased at cell-cell contacts upon externally applied stretch. *Proceedings of the National Academy of Sciences*. https://doi.org/10.1073/pnas.1204390109
Borghi, Nicolas, & James Nelson, W. (2009). Intercellular adhesion in morphogenesis: molecular and biophysical considerations. *Current Topics in Developmental Biology*, *89*, 1–32. https://doi.org/10.1016/S0070-2153(09)89001-7
Borghi, Nicolas, Lowndes, M., Maruthamuthu, V., Gardel, M. L., & Nelson, W. J. (2010). Regulation of cell motile behavior by crosstalk between cadherin- and integrin-mediated adhesions. *Proceedings of the National Academy of Sciences of the United States of America*, *107*(30), 13324–13329. https://doi.org/10.1073/pnas.1002662107
Borghi, Nicolas, Sorokina, M., Shcherbakova, O. G., Weis, W. I., Pruitt, B. L., Nelson, W. J., & Dunn, A. R. (2012). E-cadherin is under constitutive actomyosin-generated tension that is increased at cell – cell contacts upon externally applied stretch. *Proceedings of the National Academy of Sciences of the United States of America*, *109*, 12568–12573. https://doi.org/10.1073/pnas.1204390109
Bottaro, D. P., Rubin, J. S., Faletto, D. L., Chan, A. M., Kmiecik, T. E., Vande Woude, G. F., & Aaronson, S. A. (1991). Identification of the hepatocyte growth factor receptor as the c-met proto-oncogene product. *Science (New York, N.Y.)*, *251*(4995), 802–804. https://doi.org/10.1126/science.1846706
Bourret, L. A., & Rodan, G. A. (1976). The role of calcium in the inhibition of cAMP accumulation in epiphyseal cartilage cells exposed to physiological pressure. *Journal of Cellular Physiology*. https://doi.org/10.1002/jcp.1040880311
Brenner, M. D., Zhou, R., Conway, D. E., Lanzano, L., Gratton, E., Schwartz, M. A., & Ha, T. (2016). Spider Silk Peptide Is a Compact, Linear Nanospring Ideal for Intracellular Tension Sensing. *Nano Letters*, *16*(3), 2096–2102. https://doi.org/10.1021/acs.nanolett.6b00305
Brohawn, S. G. (2015). How ion channels sense mechanical force: Insights from mechanosensitive K2P channels TRAAK, TREK1, and TREK2. *Annals of the New York Academy of Sciences*. https://doi.org/10.1111/nyas.12874
Brohawn, S. G., Campbell, E. B., & MacKinnon, R. (2014). Physical mechanism for gating and mechanosensitivity of the human TRAAK K+ channel. *Nature*. https://doi.org/10.1038/nature14013
Buscemi, L., Ramonet, D., Klingberg, F., Formey, A., Smith-Clerc, J., Meister, J. J., & Hinz, B. (2011). The single-molecule mechanics of the latent TGF-β1 complex. *Current Biology*. https://doi.org/10.1016/j.cub.2011.11.037
Cano, A., Pérez-Moreno, M. A., Rodrigo, I., Locascio, A., Blanco, M. J., Del Barrio, M. G., … Nieto, M. A. (2000). The transcription factor Snail controls epithelial-mesenchymal transitions by repressing E-cadherin expression. *Nature Cell Biology*, *2*(2), 76–83. https://doi.org/10.1038/35000025
Cao, Y., Liu, R., Jiang, X., Lu, J., Jiang, J., Zhang, C., … Ning, G. (2009). Nuclear-Cytoplasmic Shuttling of Menin Regulates Nuclear Translocation of -Catenin. *Molecular and Cellular Biology*, *29*(20), 5477–5487. https://doi.org/10.1128/mcb.00335-09
Capaldo, C. T., & Macara, I. G. (2007). Depletion of E-cadherin disrupts establishment but not

maintenance of cell junctions in Madin-Darby canine kidney epithelial cells. *Molecular Biology of the Cell*, *18*(1), 189–200. https://doi.org/10.1091/mbc.e06-05-0471
Cartwright, S., & Karakesisoglou, I. (2014). Nesprins in health and disease. *Seminars in Cell & Developmental Biology*, *29*, 169–179. https://doi.org/10.1016/j.semcdb.2013.12.010
Carver, E. A., Jiang, R., Lan, Y., Oram, K. F., & Gridley, T. (2001). The mouse snail gene encodes a key regulator of the epithelial-mesenchymal transition. *Molecular and Cellular Biology*, *21*(23), 8184–8188. https://doi.org/10.1128/MCB.21.23.8184-8188.2001
Cattaruzza, M., Lattrich, C., & Hecker, M. (2004). Focal Adhesion Protein Zyxin is a Mechanosensitive Modulator of Gene Expression in Vascular Smooth Muscle Cells. *Hypertension*. https://doi.org/10.1161/01.HYP.0000119189.82659.52
Cavalcanti-Adam, E. A., Volberg, T., Micoulet, A., Kessler, H., Geiger, B., & Spatz, J. P. (2007). Cell spreading and focal adhesion dynamics are regulated by spacing of integrin ligands. *Biophysical Journal*. https://doi.org/10.1529/biophysj.106.089730
Cavallo, R. A., Cox, R. T., Moline, M. M., Roose, J., Polevoy, G. A., Clevers, H., … Bejsovec, A. (1998). Drosophila Tcf and Groucho interact to repress wingless signalling activity. *Nature*. https://doi.org/10.1038/26982
Chambliss, A. B., Khatau, S. B., Erdenberger, N., Robinson, D. K., Hodzic, D., Longmore, G. D., & Wirtz, D. (2013). The LINC-anchored actin cap connects the extracellular milieu to the nucleus for ultrafast mechanotransduction. *Scientific Reports*, *3*, 1087. https://doi.org/10.1038/srep01087
Chancellor, T. J., Lee, J., Thodeti, C. K., & Lele, T. (2010). Actomyosin tension exerted on the nucleus through nesprin-1 connections influences endothelial cell adhesion, migration, and cyclic strain-induced reorientation. *Biophysical Journal*, *99*(1), 115–123. https://doi.org/10.1016/j.bpj.2010.04.011
Chen, W., Lou, J., Evans, E. A., & Zhu, C. (2012). Observing force-regulated conformational changes and ligand dissociation from a single integrin on cells. *Journal of Cell Biology*. https://doi.org/10.1083/jcb.201201091
Cheung-Ong, K., Giaever, G., & Nislow, C. (2013, May 23). DNA-damaging agents in cancer chemotherapy: Serendipity and chemical biology. *Chemistry and Biology*, Vol. 20, pp. 648–659. https://doi.org/10.1016/j.chembiol.2013.04.007
Chiarella, S. E., Rabin, E. E., Ostilla, L. A., Flozak, A. S., & Gottardi, C. J. (2018). αT-catenin: A developmentally dispensable, disease-linked member of the α-catenin family. *Tissue Barriers*, *6*(2), e1463896. https://doi.org/10.1080/21688370.2018.1463896
Chikashige, Y., Tsutsumi, C., Yamane, M., Okamasa, K., Haraguchi, T., & Hiraoka, Y. (2006). Meiotic proteins bqt1 and bqt2 tether telomeres to form the bouquet arrangement of chromosomes. *Cell*, *125*(1), 59–69. https://doi.org/10.1016/j.cell.2006.01.048
Cho, M. J., Thompson, D. P., Cramer, C. T., Vidmar, T. J., & Scieszka, J. F. (1989). The Madin Darby canine kidney (MDCK) epithelial cell monolayer as a model cellular transport barrier. *Pharmaceutical Research*, *6*(1), 71–77. Retrieved from http://www.ncbi.nlm.nih.gov/pubmed/2470075
Choi, S. H., Estarás, C., Moresco, J. J., Yates, J. R., & Jones, K. A. (2013). α-Catenin interacts with APC to regulate β-catenin proteolysis and transcriptional repression of Wnt target genes. *Genes and Development*. https://doi.org/10.1101/gad.229062.113
Chuang, H.-H., Wang, P.-H., Niu, S.-W., Zhen, Y.-Y., Huang, M.-S., Hsiao, M., & Yang, C.-J. (2019). Inhibition of FAK Signaling Elicits Lamin A/C-Associated Nuclear Deformity and Cellular Senescence. *Frontiers in Oncology*, *9*, 22. https://doi.org/10.3389/fonc.2019.00022
Cingolani, G., Bednenko, J., Gillespie, M. T., & Gerace, L. (2002). Molecular basis for the recognition of a nonclassical nuclear localization signal by importin beta. *Molecular Cell*, *10*(6), 1345–1353. Retrieved from http://www.ncbi.nlm.nih.gov/pubmed/12504010
Ciruna, B., & Rossant, J. (2001). FGF signaling regulates mesoderm cell fate specification and

morphogenetic movement at the primitive streak. *Developmental Cell*, *1*(1), 37–49. Retrieved from http://www.ncbi.nlm.nih.gov/pubmed/11703922
Clevers H, & Nusse R. (2012). Wnt/β-catenin signaling and disease. *Cell*. https://doi.org/10.1016/j.cell.2012.05.012
Côme, C., Arnoux, V., Bibeau, F., & Savagner, P. (2004). Roles of the transcription factors snail and slug during mammary morphogenesis and breast carcinoma progression. *Journal of Mammary Gland Biology and Neoplasia*, *9*(2), 183–193. https://doi.org/10.1023/B:JOMG.0000037161.91969.de
Comijn, J., Berx, G., Vermassen, P., Verschueren, K., van Grunsven, L., Bruyneel, E., … van Roy, F. (2001). The two-handed E box binding zinc finger protein SIP1 downregulates E-cadherin and induces invasion. *Molecular Cell*, *7*(6), 1267–1278. Retrieved from http://www.ncbi.nlm.nih.gov/pubmed/11430829
Cooper, J. A. (1987). Effects of cytochalasin and phalloidin on actin. *The Journal of Cell Biology*. https://doi.org/10.1083/jcb.105.4.1473
Cramer, L. P., Siebert, M., & Mitchison, T. J. (1997). Identification of novel graded polarity actin filament bundles in locomoting heart fibroblasts: Implications for the generation of motile force. *Journal of Cell Biology*. https://doi.org/10.1083/jcb.136.6.1287
Crisp, M., Liu, Q., Roux, K., Rattner, J. B., Shanahan, C., Burke, B., … Hodzic, D. (2006). Coupling of the nucleus and cytoplasm: Role of the LINC complex. *Journal of Cell Biology*. https://doi.org/10.1083/jcb.200509124
Dahl, K. N. (2004). The nuclear envelope lamina network has elasticity and a compressibility limit suggestive of a molecular shock absorber. *Journal of Cell Science*, *117*(20), 4779–4786. https://doi.org/10.1242/jcs.01357
Dahmen, R. P., Koch, A., Denkhaus, D., Tonn, J. C., Sörensen, N., Berthold, F., … Pietsch, T. (2001). Deletions of AXIN1, a component of the WNT/wingless pathway, in sporadic medulloblastomas. *Cancer Research*, *61*(19), 7039–7043. Retrieved from http://www.ncbi.nlm.nih.gov/pubmed/11585731
Dang, C. V, & Lee, W. M. (1988). Identification of the human c-myc protein nuclear translocation signal. *Molecular and Cellular Biology*, *8*(10), 4048–4054. https://doi.org/10.1128/mcb.8.10.4048
Daniel, J. M., & Reynolds, A. B. (1995). The tyrosine kinase substrate p120cas binds directly to E-cadherin but not to the adenomatous polyposis coli protein or alpha-catenin. *Molecular and Cellular Biology*, *15*(9), 4819–4824. https://doi.org/10.1128/mcb.15.9.4819
Dann, C. E., Hsieh, J. C., Rattner, A., Sharma, D., Nathans, J., & Leahy, D. J. (2001). Insights into Wnt binding and signalling from the structures of two Frizzled cysteine-rich domains. *Nature*. https://doi.org/10.1038/35083601
Daugherty, R. L., Serebryannyy, L., Yemelyanov, A., Flozak, A. S., Yu, H.-J., Kosak, S. T., … Gottardi, C. J. (2014). alpha-Catenin is an inhibitor of transcription. *Proceedings of the National Academy of Sciences*, *111*(14), 5260–5265. https://doi.org/10.1073/pnas.1308663111
Daugherty, Rebecca L, Serebryannyy, L., Yemelyanov, A., Flozak, A. S., Yu, H.-J., Kosak, S. T., … Gottardi, C. J. (2014). α-Catenin is an inhibitor of transcription. *Proceedings of the National Academy of Sciences of the United States of America*, *111*(14), 5260–5265. https://doi.org/10.1073/pnas.1308663111
Davidson, P. M., Sliz, J., Isermann, P., Denais, C., & Lammerding, J. (2015). Design of a microfluidic device to quantify dynamic intra-nuclear deformation during cell migration through confining environments. *Integrative Biology (United Kingdom)*, *7*(12), 1534–1546. https://doi.org/10.1039/c5ib00200a
Day, R.N., Booker, C. F., & Periasamy, A. (2008). Characterization of an improved donor fluorescent protein for Förster resonance energy transfer microscopy. *Journal of*

Biomedical Optics, *13*(3), 031203.
Day, Richard N., Booker, C. F., & Periasamy, A. (2008). Characterization of an improved donor fluorescent protein for Förster resonance energy transfer microscopy. *Journal of Biomedical Optics*, *13*(3), 031203. https://doi.org/10.1117/1.2939094
de Leeuw, R., Gruenbaum, Y., & Medalia, O. (2018). Nuclear Lamins: Thin Filaments with Major Functions. *Trends in Cell Biology*. https://doi.org/10.1016/j.tcb.2017.08.004
De Sandre-Giovannoli, A., Bernard, R., Cau, P., Navarro, C., Amiel, J., Boccaccio, I., … Lévy, N. (2003). Lamin A truncation in Hutchinson-Gilford progeria. *Science*. https://doi.org/10.1126/science.1084125
De Sandre-Giovannoli, A., Chaouch, M., Kozlov, S., Vallat, J. M., Tazir, M., Kassouri, N., … Lévy, N. (2002). Homozygous defects in LMNA, encoding lamin A/C nuclear-envelope proteins, cause autosomal recessive axonal neuropathy in human (Charcot-Marie-Tooth disorder type 2) and mouse. *American Journal of Human Genetics*, *70*(3), 726–736. https://doi.org/10.1086/339274
DeBusk, F. L. (1972). The Hutchinson-Gilford progeria syndrome. Report of 4 cases and review of the literature. *The Journal of Pediatrics*, Vol. 80, pp. 697–724. https://doi.org/10.1016/S0022-3476(72)80229-4
Del Rio, A., Perez-Jimenez, R., Liu, R., Roca-Cusachs, P., Fernandez, J. M., & Sheetz, M. P. (2009). Stretching single talin rod molecules activates vinculin binding. *Science*. https://doi.org/10.1126/science.1162912
Desai, R., Sarpal, R., Ishiyama, N., Pellikka, M., Ikura, M., & Tepass, U. (2013). Monomeric α-catenin links cadherin to the actin cytoskeleton. *Nature Cell Biology*. https://doi.org/10.1038/ncb2685
Desbois-Mouthon, C., Cadoret, A., Blivet-Van Eggelpoël, M. J., Bertrand, F., Cherqui, G., Perret, C., & Capeau, J. (2001). Insulin and IGF-1 stimulate the beta-catenin pathway through two signalling cascades involving GSK-3beta inhibition and Ras activation. *Oncogene*, *20*(2), 252–259. https://doi.org/10.1038/sj.onc.1204064
Diamond, S. L., Eskin, S. G., & McIntire, L. V. (1989). Fluid flow stimulates tissue plasminogen activator secretion by cultured human endothelial cells. *Science (New York, N.Y.)*, *243*(4897), 1483–1485. https://doi.org/10.1126/science.2467379
Didenko, V. V. (2001). DNA Probes Using Fluoresence Resonance Energy Transfer. *Biotechniques*, *31*(5), 1106–1121. https://doi.org/10.2144/01315rv02
Discher, D. E., Janmey, P., & Wang, Y. L. (2005). Tissue cells feel and respond to the stiffness of their substrate. *Science*. https://doi.org/10.1126/science.1116995
Dittmer, T., & Misteli, T. (2011). The lamin protein family. *Genome Biology*, *12*(5). https://doi.org/10.1186/gb-2011-12-5-222
Donald E. Ingber. (2006). Cellular mechanotransduction: putting all the pieces together again. *The FASEB Journal*. https://doi.org/10.1096/fj.05
Dong, Y. Y., Pike, A. C. W., Mackenzie, A., McClenaghan, C., Aryal, P., Dong, L., … Carpenter, E. P. (2015). K2P channel gating mechanisms revealed by structures of TREK-2 and a complex with Prozac. *Science*. https://doi.org/10.1126/science.1261512
Dorner, D., Gotzmann, J., & Foisner, R. (2007, March). Nucleoplasmic lamins and their interaction partners, LAP2α, Rb, and BAF, in transcriptional regulation. *FEBS Journal*, Vol. 274, pp. 1362–1373. https://doi.org/10.1111/j.1742-4658.2007.05695.x
Dorsky, R. I., Sheldahl, L. C., & Moon, R. T. (2002). A transgenic Lef1/beta-catenin-dependent reporter is expressed in spatially restricted domains throughout zebrafish development. *Developmental Biology*, *241*(2), 229–237. https://doi.org/10.1006/dbio.2001.0515
Driscoll, T. P., Cosgrove, B. D., Heo, S. J., Shurden, Z. E., & Mauck, R. L. (2015). Cytoskeletal to Nuclear Strain Transfer Regulates YAP Signaling in Mesenchymal Stem Cells. *Biophysical Journal*. https://doi.org/10.1016/j.bpj.2015.05.010

Duband, J. L., & Thiery, J. P. (1982). Appearance and distribution of fibronectin during chick embryo gastrulation and neurulation. *Developmental Biology*, *94*(2), 337–350. https://doi.org/10.1016/0012-1606(82)90352-9

Duchartre, Y., Kim, Y. M., & Kahn, M. (2016). The Wnt signaling pathway in cancer. *Critical Reviews in Oncology/Hematology*. https://doi.org/10.1016/j.critrevonc.2015.12.005

Dugina, V., Alieva, I., Khromova, N., Kireev, I., Gunning, P. W., & Kopnin, P. (2016). Interaction of microtubules with the actin cytoskeleton via cross-talk of EB1-containing +TIPs and γ-actin in epithelial cells. *Oncotarget*. https://doi.org/10.18632/oncotarget.12236

Dumbauld, D. W., Lee, T. T., Singh, A., Scrimgeour, J., Gersbach, C. A., Zamir, E. A., … García, A. J. (2013). How vinculin regulates force transmission. *Proceedings of the National Academy of Sciences of the United States of America*, *110*(24), 9788–9793. https://doi.org/10.1073/pnas.1216209110

Dunnigan, M. G., Cochrane, M. A., Kelly, A., & Scott, J. W. (1974). Familial lipoatrophic diabetes with dominant transmission. A new syndrome. *The Quarterly Journal of Medicine*, *43*(169), 33–48. Retrieved from http://www.ncbi.nlm.nih.gov/pubmed/4362786

Duong, N. T., Morris, G. E., Lam, L. T., Zhang, Q., Sewry, C. A., Shanahan, C. M., & Holt, I. (2014). Nesprins: Tissue-specific expression of epsilon and other short isoforms. *PLoS ONE*. https://doi.org/10.1371/journal.pone.0094380

Dupont, S., Morsut, L., Aragona, M., Enzo, E., Giulitti, S., Cordenonsi, M., … Piccolo, S. (2011). Role of YAP/TAZ in mechanotransduction. *Nature*. https://doi.org/10.1038/nature10137

Ekblom, P. (1989). Developmentally regulated conversion of mesenchyme to epithelium. *The FASEB Journal*. https://doi.org/10.1096/fasebj.3.10.2666230

Elosegui-Artola, A., Andreu, I., Beedle, A. E. M., Lezamiz, A., Uroz, M., Kosmalska, A. J., … Roca-Cusachs, P. (2017). Force Triggers YAP Nuclear Entry by Regulating Transport across Nuclear Pores. *Cell*. https://doi.org/10.1016/j.cell.2017.10.008

Emery, A. E. (1989). Emery-Dreifuss syndrome. *Journal of Medical Genetics*, *26*(10), 637–641. https://doi.org/10.1136/jmg.26.10.637

Engler, A. J., Sen, S., Sweeney, H. L., & Discher, D. E. (2006). Matrix elasticity directs stem cell lineage specification. *Cell*. https://doi.org/10.1016/j.cell.2006.06.044

Eriksson, M., Brown, W. T., Gordon, L. B., Glynn, M. W., Singer, J., Scott, L., … Collins, F. S. (2003). Recurrent de novo point mutations in lamin A cause Hutchinson-Gilford progeria syndrome. *Nature*, *423*(6937), 293–298. https://doi.org/10.1038/nature01629

Essawy, N., Samson, C., Petitalot, A., Moog, S., Bigot, A., Herrada, I., … Zinn-Justin, S. (2019). An Emerin LEM-Domain Mutation Impairs Cell Response to Mechanical Stress. *Cells*, *8*(6), 570. https://doi.org/10.3390/cells8060570

Etoc, F., Lisse, D., Bellaiche, Y., Piehler, J., Coppey, M., & Dahan, M. (2013). Subcellular control of Rac-GTPase signalling by magnetogenetic manipulation inside living cells. *Nature Nanotechnology*, *8*(3), 193–198. https://doi.org/10.1038/nnano.2013.23

Fagotto, F, Glück, U., & Gumbiner, B. M. (1998). Nuclear localization signal-independent and importin/karyopherin-independent nuclear import of beta-catenin. *Current Biology : CB*, *8*(4), 181–190.

Fagotto, François. (2013). Looking beyond the Wnt pathway for the deep nature of β-catenin. *EMBO Reports*, *14*(5), 422–433. https://doi.org/10.1038/embor.2013.45

Fagotto, François, Glück, U., & Gumbiner, B. M. (1998). Nuclear localization signal-independent and importin/karyopherin-independent nuclear import of β-catenin. *Current Biology*, *8*(4), 181–190. https://doi.org/10.1016/s0960-9822(98)70082-x

Farge, E. (2003). Mechanical induction of Twist in the Drosophila foregut/stomodeal primordium. *Current Biology : CB*, *13*(16), 1365–1377. Retrieved from

http://www.ncbi.nlm.nih.gov/pubmed/12932320
Feng, J., Ito, M., Ichikawa, K., Isaka, N., Nishikawa, M., Hartshorne, D. J., & Nakano, T. (1999). Inhibitory phosphorylation site for Rho-associated kinase on smooth muscle myosin phosphatase. *Journal of Biological Chemistry*. https://doi.org/10.1074/jbc.274.52.37385
Fernández-Sánchez, M. E., Barbier, S., Whitehead, J., Béalle, G., Michel, A., Latorre-Ossa, H., … Farge, E. (2015). Mechanical induction of the tumorigenic β-catenin pathway by tumour growth pressure. *Nature*. https://doi.org/10.1038/nature14329
Filonov, G. S., Piatkevich, K. D., Ting, L. M., Zhang, J., Kim, K., & Verkhusha, V. V. (2011). Bright and stable near-infrared fluorescent protein for in vivo imaging. *Nature Biotechnology*, *29*(8), 757–761. https://doi.org/10.1038/nbt.1918
Fink, J., Carpi, N., Betz, T., Bétard, A., Chebah, M., Azioune, A., … Piel, M. (2011). External forces control mitotic spindle positioning. *Nature Cell Biology*, *13*(7), 771–778. https://doi.org/10.1038/ncb2269
Fitts, R. H., & Widrick, J. J. (1996). Muscle mechanics: adaptations with exercise-training. *Exercise and Sport Sciences Reviews*.
Fletcher, D. A., & Mullins, R. D. (2010). Cell mechanics and the cytoskeleton. *Nature*. https://doi.org/10.1038/nature08908
Förster, T. (1948). Zwischenmolekulare Energiewanderung und Fluoreszenz. *Annalen Der Physik*, *437*(1–2), 55–75. https://doi.org/10.1002/andp.19484370105
Franch-Marro, X., Wendler, F., Guidato, S., Griffith, J., Baena-Lopez, A., Itasaki, N., … Vincent, J.-P. (2008). Wingless secretion requires endosome-to-Golgi retrieval of Wntless/Evi/Sprinter by the retromer complex. *Nature Cell Biology*, *10*(2), 170–177. https://doi.org/10.1038/ncb1678
Frangos, J. A., Eskin, S. G., McIntire, L. V, & Ives, C. L. (1985). Flow effects on prostacyclin production by cultured human endothelial cells. *Science (New York, N.Y.)*, *227*(4693), 1477–1479. https://doi.org/10.1126/science.3883488
Friedl, P. (2004). Prespecification and plasticity: Shifting mechanisms of cell migration. *Current Opinion in Cell Biology*. https://doi.org/10.1016/j.ceb.2003.11.001
Friedland, J. C., Lee, M. H., & Boettiger, D. (2009). Mechanically activated integrin switch controls α 5 β 1 function. *Science*. https://doi.org/10.1126/science.1168441
Funayama, N., Fagotto, F., McCrea, P., & Gumbiner, B. M. (1995). Embryonic axis induction by the armadillo repeat domain of β-catenin: Evidence for intracellular signaling. *Journal of Cell Biology*. https://doi.org/10.1083/jcb.128.5.959
Gao, C., Wang, Y., Broaddus, R., Sun, L., Xue, F., & Zhang, W. (2018). Exon 3 mutations of *CTNNB1* drive tumorigenesis: a review. *Oncotarget*. https://doi.org/10.18632/oncotarget.23695
Garg, A., Vinaitheerthan, M., Weatherall, P. T., & Bowcock, A. M. (2001). Phenotypic Heterogeneity in Patients with Familial Partial Lipodystrophy (Dunnigan Variety) Related to the Site of Missense Mutations in Lamin A/C Gene [1]. *The Journal of Clinical Endocrinology & Metabolism*, *86*(1), 59–65. https://doi.org/10.1210/jcem.86.1.7121
Gatti, R., & Perlman, S. (1993). Ataxia-Telangiectasia. In *GeneReviews*®. Retrieved from http://www.ncbi.nlm.nih.gov/pubmed/20301790
Gayrard, C., Bernaudin, C., Déjardin, T., Seiler, C., & Borghi, N. (2018). Src- and confinement-dependent FAK activation causes E-cadherin relaxation and β-catenin activity. *The Journal of Cell Biology*, *217*(3), 1063–1077. https://doi.org/10.1083/jcb.201706013
Gayrard, C., & Borghi, N. (2016). FRET-based Molecular Tension Microscopy. *Methods (San Diego, Calif.)*, *94*, 33–42. https://doi.org/10.1016/j.ymeth.2015.07.010
Gerber, L. H., Merideth, M. A., Turner, M. L., Cannon, R. O., Gerhard-Herman, M., Gordon, L. B., … Brooks, B. P. (2008). Phenotype and Course of Hutchinson–Gilford Progeria Syndrome. *New England Journal of Medicine*. https://doi.org/10.1056/nejmoa0706898

Giannini, A L, Vivanco, M. d, & Kypta, R. M. (2000). alpha-catenin inhibits beta-catenin signaling by preventing formation of a beta-catenin*T-cell factor*DNA complex. *The Journal of Biological Chemistry*, *275*(29), 21883–21888. https://doi.org/10.1074/jbc.M001929200

Giannini, Ana L., Vivanco, M. d. M., & Kypta, R. M. (2000). α-Catenin Inhibits β-Catenin Signaling by Preventing Formation of a β-Catenin·T-cell Factor·DNA Complex. *Journal of Biological Chemistry*, *275*(29), 21883–21888. https://doi.org/10.1074/jbc.M001929200

Gimpel, P., Lee, Y. L., Sobota, R. M., Calvi, A., Koullourou, V., Patel, R., … Gomes, E. R. (2017). Nesprin-1α-Dependent Microtubule Nucleation from the Nuclear Envelope via Akap450 Is Necessary for Nuclear Positioning in Muscle Cells. *Current Biology*, *27*(19), 2999-3009.e9. https://doi.org/10.1016/j.cub.2017.08.031

Goldman, R. D., Gruenbaum, Y., Moir, R. D., Shumaker, D. K., & Spann, T. P. (2002). Nuclear lamins: building blocks of nuclear architecture. *Genes & Development*, *16*(5), 533–547. https://doi.org/10.1101/gad.960502

Goldsmith, S. C., Fedorov, A. A., Almo, S. C., Pokala, N., Shen, W., Matsudaira, P., … Shen, W. (1997). The structure of an actin-crosslinking domain from human fimbrin. *Nature Structural Biology*, *4*(9), 708–712. https://doi.org/10.1038/nsb0997-708

Görlich, D., Panté, N., Kutay, U., Aebi, U., & Bischoff, F. R. (1996). Identification of different roles for RanGDP and RanGTP in nuclear protein import. *The EMBO Journal*, *15*(20), 5584–5594. Retrieved from http://www.ncbi.nlm.nih.gov/pubmed/8896452

Gottardi, C. J., Arpin, M., Fanning, A. S., & Louvard, D. (1996). The junction-associated protein, zonula occludens-1, localizes to the nucleus before the maturation and during the remodeling of cell-cell contacts. *Proceedings of the National Academy of Sciences of the United States of America*, *93*(20), 10779–10784. https://doi.org/10.1073/pnas.93.20.10779

Grady, R. M., Starr, D. A., Ackerman, G. L., Sanes, J. R., & Han, M. (2005). Syne proteins anchor muscle nuclei at the neuromuscular junction. *Proceedings of the National Academy of Sciences*. https://doi.org/10.1073/pnas.0500711102

Grannas, K., Arngården, L., Lönn, P., Mazurkiewicz, M., Blokzijl, A., Zieba, A., & Söderberg, O. (2015). Crosstalk between Hippo and TGFβ: Subcellular Localization of YAP/TAZ/Smad Complexes. *Journal of Molecular Biology*. https://doi.org/10.1016/j.jmb.2015.04.015

Grashoff, C., Hoffman, B. D., Brenner, M. D., Zhou, R., Parsons, M., Yang, M. T., … others. (2010). Measuring mechanical tension across vinculin reveals regulation of focal adhesion dynamics. *Nature*, *466*(7303), 263–266. https://doi.org/10.1038/nature09198

Grashoff, C., Hoffman, B. D., Brenner, M. D., Zhou, R., Parsons, M., Yang, M. T., … Schwartz, M. A. (2010). Measuring mechanical tension across vinculin reveals regulation of focal adhesion dynamics. *Nature*. https://doi.org/10.1038/nature09198

Green, E. K., Grozeva, D., Forty, L., Gordon-Smith, K., Russell, E., Farmer, A., … Craddock, N. (2013). Association at SYNE1 in both bipolar disorder and recurrent major depression. *Molecular Psychiatry*. https://doi.org/10.1038/mp.2012.48

Greenburg, G., & Hay, E. D. (1982). Epithelia suspended in collagen gels can lose polarity and express characteristics of migrating mesenchymal cells. *Journal of Cell Biology*. https://doi.org/10.1083/jcb.95.1.333

Griffith, L. M., & Pollard, T. D. (1978). Evidence for actin filament-microtubule interaction mediated by microtubule-associated proteins. *Journal of Cell Biology*, *78*(3), 958–965. https://doi.org/10.1083/jcb.78.3.958

Griffiths, L. M., Pollards, T. D., & Fairchild Center, S. (1982). The Interaction of Actin Filaments with Microtubules and Microtubule-associated Proteins*. In *THE JOURNAL 01 BIOLOGICAL CHEMISTRY Printed in U S. A* (Vol. 257).

Gros-Louis, F., Dupré, N., Dion, P., Fox, M. A., Laurent, S., Verreault, S., … Rouleau, G. A. (2007).

Mutations in SYNE1 lead to a newly discovered form of autosomal recessive cerebellar ataxia. *Nature Genetics*, *39*(1), 80–85. https://doi.org/10.1038/ng1927
Grotegut, S., Von Schweinitz, D., Christofori, G., & Lehembre, F. (2006). Hepatocyte growth factor induces cell scattering through MAPK/Egr-1-mediated upregulation of Snail. *EMBO Journal*. https://doi.org/10.1038/sj.emboj.7601213
Gruenbaum, Y., & Foisner, R. (2015). Lamins: Nuclear Intermediate Filament Proteins with Fundamental Functions in Nuclear Mechanics and Genome Regulation. *Annual Review of Biochemistry*. https://doi.org/10.1146/annurev-biochem-060614-034115
Guilluy, C., Osborne, L. D., Van Landeghem, L., Sharek, L., Superfine, R., Garcia-Mata, R., & Burridge, K. (2014). Isolated nuclei adapt to force and reveal a mechanotransduction pathway in the nucleus. *Nature Cell Biology*. https://doi.org/10.1038/ncb2927
Haft, C. R., Sierra, M. d. l. L., Bafford, R., Lesniak, M. A., Barr, V. A., & Taylor, S. I. (2000). Human Orthologs of Yeast Vacuolar Protein Sorting Proteins Vps26, 29, and 35: Assembly into Multimeric Complexes. *Molecular Biology of the Cell*. https://doi.org/10.1091/mbc.11.12.4105
Hagen, T., Daniel, E. Di, Culbert, A. A., & Reith, A. D. (2002). Expression and characterization of GSK-3 mutants and their effect on β-catenin phosphorylation in intact cells. *Journal of Biological Chemistry*. https://doi.org/10.1074/jbc.M201364200
Hajra, L., Evans, A. I., Chen, M., Hyduk, S. J., Collins, T., & Cybulsky, M. I. (2002). The NF-kappa B signal transduction pathway in aortic endothelial cells is primed for activation in regions predisposed to atherosclerotic lesion formation. *Proceedings of the National Academy of Sciences*. https://doi.org/10.1073/pnas.97.16.9052
Hamburger, V. (1997). Wilhelm Roux: visionary with a blind spot. *Journal of the History of Biology*. https://doi.org/10.1023/A:1004231618837
Harada, T., Swift, J., Irianto, J., Shin, J.-W., Spinler, K. R., Athirasala, A., … Discher, D. E. (2014). Nuclear lamin stiffness is a barrier to 3D migration, but softness can limit survival. *The Journal of Cell Biology*, *204*(5), 669–682. https://doi.org/10.1083/jcb.201308029
Harel, A., & Forbes, D. J. (2004). Importin beta: Conducting a much larger cellular symphony. *Molecular Cell*. https://doi.org/10.1016/j.molcel.2004.10.026
Hart, R. G., Kota, D., Li, F., Ramallo, D., Price, A. J., Otterpohl, K. L., … Chandrasekar, I. (2019). Myosin II Tension Sensors Visualize Force Generation within the Actin Cytoskeleton in Living Cells. *BioRxiv*, 623249. https://doi.org/10.1101/623249
Haswell, E. S., Phillips, R., & Rees, D. C. (2011). Mechanosensitive channels: What can they do and how do they do it? *Structure*. https://doi.org/10.1016/j.str.2011.09.005
Hattori, M., & Minato, N. (2003). Rap1 GTPase: functions, regulation, and malignancy. *Journal of Biochemistry*, *134*(4), 479–484. https://doi.org/10.1093/jb/mvg180
Hay, E. D. (1995). An Overview of Epithelio-Mesenchymal Transformation. *Cells Tissues Organs*. https://doi.org/10.1159/000147748
Hayashi, I., & Ikura, M. (2003). Crystal structure of the amino-terminal microtubule-binding domain of end-binding protein 1 (EB1). *Journal of Biological Chemistry*, *278*(38), 36430–36434. https://doi.org/10.1074/jbc.M305773200
He, T. C., Sparks, A. B., Rago, C., Hermeking, H., Zawel, L., Da Costa, L. T., … Kinzler, K. W. (1998). Identification of c-MYC as a target of the APC pathway. *Science*, *281*(5382), 1509–1512. https://doi.org/10.1126/science.281.5382.1509
He, X., Tamai, K., Semenov, M., Kato, Y., Spokony, R., Liu, C., … Saint-Jeannet, J.-P. (2000). LDL-receptor-related proteins in Wnt signal transduction. *Nature*. https://doi.org/10.1038/35035117
Herrmann, H., & Aebi, U. (2016). Intermediate Filaments: Structure and Assembly. *Cold Spring Harbor Perspectives in Biology*, *8*(11). https://doi.org/10.1101/cshperspect.a018242
Hieda, M. (2017). Implications for Diverse Functions of the LINC Complexes Based on the

Structure. *Cells*. https://doi.org/10.3390/cells6010003
Hirano, S., Kimoto, N., Shimoyama, Y., Hirohashi, S., & Takeichi, M. (1992). Identification of a neural α-catenin as a key regulator of cadherin function and multicellular organization. *Cell*. https://doi.org/10.1016/0092-8674(92)90103-J
Hirata, H., Tatsumi, H., Lim, C. T., & Sokabe, M. (2014). Force-dependent vinculin binding to talin in live cells: a crucial step in anchoring the actin cytoskeleton to focal adhesions. *American Journal of Physiology-Cell Physiology*. https://doi.org/10.1152/ajpcell.00122.2013
Hodzic, D. M., Yeater, D. B., Bengtsson, L., Otto, H., & Stahl, P. D. (2004). Sun2 is a novel mammalian inner nuclear membrane protein. *The Journal of Biological Chemistry*, *279*(24), 25805–25812. https://doi.org/10.1074/jbc.M313157200
Hofmann, K. (2000). A superfamily of membrane-bound O-acyltransferases with implications for Wnt signaling. *Trends in Biochemical Sciences*. https://doi.org/10.1016/S0968-0004(99)01539-X
Hofmann, W. A., Stojiljkovic, L., Fuchsova, B., Vargas, G. M., Mavrommatis, E., Philimonenko, V., … de Lanerolle, P. (2004). Actin is part of pre-initiation complexes and is necessary for transcription by RNA polymerase II. *Nature Cell Biology*, *6*(11), 1094–1101. https://doi.org/10.1038/ncb1182
Hohng, S., Zhou, R., Nahas, M. K., Yu, J., Schulten, K., Lilley, D. M. J., & Ha, T. (2007). Fluorescence-force spectroscopy maps two-dimensional reaction landscape of the holliday junction. *Science*, *318*(5848), 279–283. https://doi.org/10.1126/science.1146113
Holaska, J. M., Lee, K. K., Kowalski, A. K., & Wilson, K. L. (2003). Transcriptional repressor germ cell-less (GCL) and barrier to autointegration factor (BAF) compete for binding to emerin in vitro. *Journal of Biological Chemistry*. https://doi.org/10.1074/jbc.M208811200
Horn, H. F., Brownstein, Z., Lenz, D. R., Shivatzki, S., Dror, A. A., Dagan-Rosenfeld, O., … Avraham, K. B. (2013). The LINC complex is essential for hearing. *The Journal of Clinical Investigation*, *123*(2), 740–750. https://doi.org/10.1172/JCI66911
Howard, S., Deroo, T., Fujita, Y., & Itasaki, N. (2011). A positive role of cadherin in wnt/β-catenin signalling during epithelial-mesenchymal transition. *PLoS ONE*, *6*(8). https://doi.org/10.1371/journal.pone.0023899
Hu, S., Eberhard, L., Chen, J., Love, J. C., Butler, J. P., Fredberg, J. J., … Wang, N. (2004). Mechanical anisotropy of adherent cells probed by a three-dimensional magnetic twisting device. *American Journal of Physiology-Cell Physiology*. https://doi.org/10.1152/ajpcell.00224.2004
Huang, J., Wu, S., Barrera, J., Matthews, K., & Pan, D. (2005). The Hippo signaling pathway coordinately regulates cell proliferation and apoptosis by inactivating Yorkie, the Drosophila homolog of YAP. *Cell*, *122*(3), 421–434. https://doi.org/10.1016/j.cell.2005.06.007
Huber, A. H., Nelson, W. J., & Weis, W. I. (1997). Three-dimensional structure of the armadillo repeat region of β-catenin. *Cell*. https://doi.org/10.1016/S0092-8674(00)80352-9
Huels, D. J., Ridgway, R. A., Radulescu, S., Leushacke, M., Campbell, A. D., Biswas, S., … Sansom, O. J. (2015). E-cadherin can limit the transforming properties of activating β-catenin mutations. *The EMBO Journal*, *34*(18), 2321–2333. https://doi.org/10.15252/embj.201591739
Humphries, J. D., Wang, P., Streuli, C., Geiger, B., Humphries, M. J., & Ballestrem, C. (2007). Vinculin controls focal adhesion formation by direct interactions with talin and actin. *Journal of Cell Biology*. https://doi.org/10.1083/jcb.200703036
Hussain, S. A., Dey, D., Chakraborty, S., Saha, J., Roy, A. D., Chakraborty, S., … Bhattacharjee, D.

(2014). *Fluorescence Resonance Energy Transfer (FRET) sensor*. Retrieved from http://arxiv.org/abs/1408.6559
Ikeda, S., Kishida, S., Yamamoto, H., Murai, H., Koyama, S., & Kikuchi, A. (1998). Axin, a negative regulator of the Wnt signaling pathway, forms a complex with GSK-3β and beta-catenin and promotes GSK-3beta-dependent phosphorylation of beta-catenin. *The EMBO Journal*. https://doi.org/10.1093/emboj/16.13.3797
Ingber, D. E. (2003). Tensegrity I. Cell structure and hierarchical systems biology. *Journal of Cell Science*. https://doi.org/10.1242/jcs.00359
Isermann, P., & Lammerding, J. (2013). Nuclear mechanics and mechanotransduction in health and disease. *Current Biology*. https://doi.org/10.1016/j.cub.2013.11.009
Ishiyama, N., Lee, S. H., Liu, S., Li, G. Y., Smith, M. J., Reichardt, L. F., & Ikura, M. (2010). Dynamic and Static Interactions between p120 Catenin and E-Cadherin Regulate the Stability of Cell-Cell Adhesion. *Cell*. https://doi.org/10.1016/j.cell.2010.01.017
Ishiyama, N., Tanaka, N., Abe, K., Yang, Y. J., Abbas, Y. M., Umitsu, M., … Ikura, M. (2013). An autoinhibited structure of α-catenin and its implications for vinculin recruitment to adherens junctions. *Journal of Biological Chemistry*. https://doi.org/10.1074/jbc.M113.453928
Izaurralde, E., Kutay, U., von Kobbe, C., Mattaj, I. W., & Görlich, D. (1997). The asymmetric distribution of the constituents of the Ran system is essential for transport into and out of the nucleus. *The EMBO Journal*, *16*(21), 6535–6547. https://doi.org/10.1093/emboj/16.21.6535
Jaalouk, D. E., & Lammerding, J. (2009). Mechanotransduction gone awry. *Nature Reviews Molecular Cell Biology*. https://doi.org/10.1038/nrm2597
Jackson, S. P., & Bartek, J. (2009, October 22). The DNA-damage response in human biology and disease. *Nature*, Vol. 461, pp. 1071–1078. https://doi.org/10.1038/nature08467
Jahed, Z., Soheilypour, M., Peyro, M., & Mofrad, M. R. K. (2016). The LINC and NPC relationship – it's complicated! *Journal of Cell Science*. https://doi.org/10.1242/jcs.184184
Jainchill, J. L., Aaronson, S. A., & Todaro, G. J. (1969). Murine sarcoma and leukemia viruses: assay using clonal lines of contact-inhibited mouse cells. *Journal of Virology*, *4*(5), 549–553. Retrieved from http://www.ncbi.nlm.nih.gov/pubmed/4311790
Jamali, T., Jamali, Y., Mehrbod, M., & Mofrad, M. R. K. (2011). Nuclear Pore Complex. Biochemistry and Biophysics of Nucleocytoplasmic Transport in Health and Disease. In *International Review of Cell and Molecular Biology*. https://doi.org/10.1016/B978-0-12-386043-9.00006-2
Janda, C. Y., Waghray, D., Levin, a. M., Thomas, C., & Garcia, K. C. (2012). Structural Basis of Wnt Recognition by Frizzled supplementary material. *Science*. https://doi.org/10.1126/science.1222879
Janin, A., Bauer, D., Ratti, F., Millat, G., & Méjat, A. (2017). Nuclear envelopathies: A complex LINC between nuclear envelope and pathology. *Orphanet Journal of Rare Diseases*. https://doi.org/10.1186/s13023-017-0698-x
Janin, A., & Gache, V. (2018). Nesprins and lamins in health and diseases of cardiac and skeletal muscles. *Frontiers in Physiology*. https://doi.org/10.3389/fphys.2018.01277
Janssens, B., Goossens, S., Staes, K., Gilbert, B., van Hengel, J., Colpaert, C., … van Roy, F. (2001). alphaT-catenin: a novel tissue-specific beta-catenin-binding protein mediating strong cell-cell adhesion. *Journal of Cell Science*.
Jechlinger, M., Grunert, S., Tamir, I. H., Janda, E., Lüdemann, S., Waerner, T., … Kraut, N. (2003). Expression profiling of epithelial plasticity in tumor progression. *Oncogene*. https://doi.org/10.1038/sj.onc.1206887
Jiang, X., Cao, Y., Li, F., Su, Y., Li, Y., Peng, Y., … Ning, G. (2014). Targeting β-catenin signaling for therapeutic intervention in MEN1-deficient pancreatic neuroendocrine tumours. *Nature*

Communications, *5*, 5809. https://doi.org/10.1038/ncomms6809
Jin, P., Bulkley, D., Guo, Y., Zhang, W., Guo, Z., Huynh, W., … Cheng, Y. (2017). Electron cryo-microscopy structure of the mechanotransduction channel NOMPC. *Nature*. https://doi.org/10.1038/nature22981
Jolly, M. K., Ware, K. E., Gilja, S., Somarelli, J. A., & Levine, H. (2017). EMT and MET: necessary or permissive for metastasis? *Molecular Oncology*, *11*(7), 755–769. https://doi.org/10.1002/1878-0261.12083
Jung, O., Choi, S., Jang, S.-B., Lee, S.-A., Lim, S.-T., Choi, Y.-J., … Lee, J. W. (2012). Tetraspan TM4SF5-dependent direct activation of FAK and metastatic potential of hepatocarcinoma cells. *Journal of Cell Science*. https://doi.org/10.1242/jcs.100586
Kadowaki, T., Wilder, E., Klingensmith, J., Zachary, K., & Perrimon, N. (1996). The segment polarity gene porcupine encodes a putative multitransmembrane protein involved in Wingless processing. *Genes and Development*. https://doi.org/10.1101/gad.10.24.3116
Kalderon, D., Roberts, B. L., Richardson, W. D., & Smith, A. E. (1984). A short amino acid sequence able to specify nuclear location. *Cell*. https://doi.org/10.1016/0092-8674(84)90457-4
Kalluri, R., & Weinberg, R. a. (2009). Review series The basics o epithelial-mesenchymal transition. *Journal of Clinical Investigation*. https://doi.org/10.1172/JCI39104.1420
Kassianidou, E., Kalita, J., & Lim, R. Y. H. (2019). The role of nucleocytoplasmic transport in mechanotransduction. *Experimental Cell Research*, *377*(1–2), 86–93. https://doi.org/10.1016/j.yexcr.2019.02.009
Khatau, S. B., Hale, C. M., Stewart-Hutchinson, P. J., Patel, M. S., Stewart, C. L., Searson, P. C., … Wirtz, D. (2009). A perinuclear actin cap regulates nuclear shape. *Proceedings of the National Academy of Sciences of the United States of America*, *106*(45), 19017–19022. https://doi.org/10.1073/pnas.0908686106
Kiecker, C., Bates, T., & Bell, E. (2016, March 1). Molecular specification of germ layers in vertebrate embryos. *Cellular and Molecular Life Sciences*, Vol. 73, pp. 923–947. https://doi.org/10.1007/s00018-015-2092-y
Kim, D.-H., Khatau, S. B., Feng, Y., Walcott, S., Sun, S. X., Longmore, G. D., & Wirtz, D. (2012). Actin cap associated focal adhesions and their distinct role in cellular mechanosensing. *Scientific Reports*, *2*(1), 555. https://doi.org/10.1038/srep00555
Kim, D. H., Khatau, S. B., Feng, Y., Walcott, S., Sun, S. X., Longmore, G. D., & Wirtz, D. (2012). Actin cap associated focal adhesions and their distinct role in cellular mechanosensing. *Scientific Reports*. https://doi.org/10.1038/srep00555
Kim, K. K., Kugler, M. C., Wolters, P. J., Robillard, L., Galvez, M. G., Brumwell, A. N., … Chapman, H. A. (2006). Alveolar epithelial cell mesenchymal transition develops in vivo during pulmonary fibrosis and is regulated by the extracellular matrix. *Proceedings of the National Academy of Sciences of the United States of America*, *103*(35), 13180–13185. https://doi.org/10.1073/pnas.0605669103
Kim, K., Lu, Z., & Hay, E. D. (2002). Direct evidence for a role of β-catenin/LEF-1 signaling pathway in induction of EMT. *Cell Biology International*, *26*(5), 463–476. https://doi.org/10.1006/cbir.2002.0901
Kim, N.-G., Koh, E., Chen, X., & Gumbiner, B. M. (2011). E-cadherin mediates contact inhibition of proliferation through Hippo signaling-pathway components. *Proceedings of the National Academy of Sciences*. https://doi.org/10.1073/pnas.1103345108
Kirby, T. J., & Lammerding, J. (2018). Emerging views of the nucleus as a cellular mechanosensor. *Nature Cell Biology*. https://doi.org/10.1038/s41556-018-0038-y
Kishida, S., Yamamoto, H., Hino, S., Ikeda, S., Kishida, M., & Kikuchi, A. (2015). DIX Domains of Dvl and Axin Are Necessary for Protein Interactions and Their Ability To Regulate β-Catenin Stability. *Molecular and Cellular Biology*. https://doi.org/10.1128/mcb.19.6.4414

Koch, A., Waha, A., Tonn, J. C., Sörensen, N., Berthold, F., Wolter, M., … Pietsch, T. (2001). Somatic mutations of WNT/wingless signaling pathway components in primitive neuroectodermal tumors. *International Journal of Cancer*, *93*(3), 445–449. https://doi.org/10.1002/ijc.1342

Koike, J., Takagi, A., Miwa, T., Hirai, M., Terada, M., & Katoh, M. (1999). Molecular cloning of Frizzled-10, a novel member of the Frizzled gene family. *Biochemical and Biophysical Research Communications*. https://doi.org/10.1006/bbrc.1999.1161

Korinek, V., Barker, N., Morin, P. J., Van Wichen, D., De Weger, R., Kinzler, K. W., … Clevers, H. (1997). Constitutive transcriptional activation by a β-catenin-Tcf complex in APC(-/-) colon carcinoma. *Science*. https://doi.org/10.1126/science.275.5307.1784

Koslov, E. R., Maupin, P., Pradhan, D., Morrow, J. S., & Rimm, D. L. (1997). Alpha-catenin can form asymmetric homodimeric complexes and/or heterodimeric complexes with beta-catenin. *The Journal of Biological Chemistry*, *272*(43), 27301–27306. https://doi.org/10.1074/jbc.272.43.27301

Kracklauer, M. P., Link, J., & Alsheimer, M. (2013). LINCing the Nuclear Envelope to Gametogenesis. In *Current Topics in Developmental Biology*. https://doi.org/10.1016/B978-0-12-416024-8.00005-2

Kramps, T., Peter, O., Brunner, E., Nellen, D., Froesch, B., Chatterjee, S., … Basler, K. (2002). Wnt/Wingless signaling requires BCL9/legless-mediated recruitment of pygopus to the nuclear β-catenin-TCF complex. *Cell*. https://doi.org/10.1016/S0092-8674(02)00679-7

Książkiewicz, M., Markiewicz, A., & Zaczek, A. J. (2012). Epithelial-mesenchymal transition: a hallmark in metastasis formation linking circulating tumor cells and cancer stem cells. *Pathobiology : Journal of Immunopathology, Molecular and Cellular Biology*, *79*(4), 195–208. https://doi.org/10.1159/000337106

Kubala, M. H., Kovtun, O., Alexandrov, K., & Collins, B. M. (2010). Structural and thermodynamic analysis of the GFP:GFP-nanobody complex. *Protein Science : A Publication of the Protein Society*, *19*(12), 2389–2401. https://doi.org/10.1002/pro.519

Kukalev, A., Nord, Y., Palmberg, C., Bergman, T., & Percipalle, P. (2005). Actin and hnRNP U cooperate for productive transcription by RNA polymerase II. *Nature Structural and Molecular Biology*. https://doi.org/10.1038/nsmb904

Kutay, U., Bischoff, F. R., Kostka, S., Kraft, R., & Görlich, D. (1997). Export of importin alpha from the nucleus is mediated by a specific nuclear transport factor. *Cell*, *90*(6), 1061–1071. https://doi.org/10.1016/s0092-8674(00)80372-4

Lachowski, D., Cortes, E., Robinson, B., Rice, A., Rombouts, K., & Del Río Hernández, A. E. (2018). FAK controls the mechanical activation of YAP, a transcriptional regulator required for durotaxis. *FASEB Journal*. https://doi.org/10.1096/fj.201700721R

Lagendijk, A. K., Gomez, G. A., Baek, S., Hesselson, D., Hughes, W. E., Paterson, S., … Hogan, B. M. (2017). Live imaging molecular changes in junctional tension upon VE-cadherin in zebrafish. *Nature Communications*, *8*(1), 1402. https://doi.org/10.1038/s41467-017-01325-6

Laity, J. H., Lee, B. M., & Wright, P. E. (2001). Zinc finger proteins: new insights into structural and functional diversity. *Current Opinion in Structural Biology*, *11*(1), 39–46. Retrieved from http://www.ncbi.nlm.nih.gov/pubmed/11179890

Lamouille, S., Xu, J., & Derynck, R. (2014). Molecular mechanisms of epithelial-mesenchymal transition. *Nature Reviews. Molecular Cell Biology*, *15*(3), 178–196. https://doi.org/10.1038/nrm3758

Large-scale, A., Willert, K., Brown, J. D., Danenberg, E., Duncan, A. W., Weissman, I. L., … Nusse, R. (2003). Wnt proteins are lipid-modified and can act as stem cell growth factors. *Nature*. https://doi.org/10.1038/nature01611

Lawson, C., & Schlaepfer, D. D. (2013). Phocal adhesion kinase regulation is on a FERM

foundation. *Journal of Cell Biology*. https://doi.org/10.1083/jcb.201308034
le Duc, Q., Shi, Q., Blonk, I., Sonnenberg, A., Wang, N., Leckband, D., & de Rooij, J. (2010). Vinculin potentiates E-cadherin mechanosensing and is recruited to actin-anchored sites within adherens junctions in a myosin II-dependent manner. *The Journal of Cell Biology*, *189*(7), 1107–1115. https://doi.org/10.1083/jcb.201001149
Lee, J. M., Dedhar, S., Kalluri, R., & Thompson, E. W. (2006). The epithelial-mesenchymal transition: New insights in signaling, development, and disease. *Journal of Cell Biology*. https://doi.org/10.1083/jcb.200601018
Lee, M. S., Gippert, G. P., Soman, K. V, Case, D. A., & Wright, P. E. (1989). Three-dimensional solution structure of a single zinc finger DNA-binding domain. *Science (New York, N.Y.)*, *245*(4918), 635–637. https://doi.org/10.1126/science.2503871
Lee, N. K., Kapanidis, A. N., Wang, Y., Michalet, X., Mukhopadhyay, J., Ebright, R. H., & Weiss, S. (2005). Accurate FRET measurements within single diffusing biomolecules using alternating-laser excitation. *Biophysical Journal*, *88*(4), 2939–2953. https://doi.org/10.1529/biophysj.104.054114
Lemke, S. B., Weidemann, T., Cost, A.-L., Grashoff, C., & Schnorrer, F. (2019). A small proportion of Talin molecules transmit forces at developing muscle attachments in vivo. *PLOS Biology*, *17*(3), e3000057. https://doi.org/10.1371/journal.pbio.3000057
Leptin, M. (1991). twist and snail as positive and negative regulators during Drosophila mesoderm development. *Genes & Development*, *5*(9), 1568–1576. https://doi.org/10.1101/gad.5.9.1568
Lesage, F., Terrenoire, C., Romey, G., & Lazdunski, M. (2000). Human TREK2, a 2P Domain Mechano-sensitive K+ Channel with Multiple Regulations by Polyunsaturated Fatty Acids, Lysophospholipids, and Gs, Gi, and Gq Protein-coupled Receptors. *Journal of Biological Chemistry*. https://doi.org/10.1074/jbc.M002822200
Lewis, J. M., Baskaran, R., Taagepera, S., Schwartz, M. A., & Wang, J. Y. (1996). Integrin regulation of c-Abl tyrosine kinase activity and cytoplasmic-nuclear transport. *Proceedings of the National Academy of Sciences of the United States of America*, *93*(26), 15174–15179. https://doi.org/10.1073/pnas.93.26.15174
Li, Q., Kumar, A., Makhija, E., & Shivashankar, G. V. (2014). The regulation of dynamic mechanical coupling between actin cytoskeleton and nucleus by matrix geometry. *Biomaterials*. https://doi.org/10.1016/j.biomaterials.2013.10.037
Li, X., Zhao, X., Fang, Y., Jiang, X., Duong, T., Fan, C., … Kain, S. R. (1998). Generation of destabilized green fluorescent protein as a transcription reporter. *Journal of Biological Chemistry*, *273*(52), 34970–34975. https://doi.org/10.1074/jbc.273.52.34970
Li, Y., Yang, J., Dai, C., Wu, C., & Liu, Y. (2003). Role for integrin-linked kinase in mediating tubular epithelial to mesenchymal transition and renal interstitial fibrogenesis. *Journal of Clinical Investigation*, *112*(4), 503–516. https://doi.org/10.1172/JCI17913
Liashkovich, I., Pasrednik, D., Prystopiuk, V., Rosso, G., Oberleithner, H., & Shahin, V. (2015). Clathrin inhibitor Pitstop-2 disrupts the nuclear pore complex permeability barrier. *Scientific Reports*, *5*. https://doi.org/10.1038/srep09994
Liem, K. F., Tremml, G., Roelink, H., & Jessell, T. M. (1995). Dorsal differentiation of neural plate cells induced by BMP-mediated signals from epidermal ectoderm. *Cell*, *82*(6), 969–979. https://doi.org/10.1016/0092-8674(95)90276-7
Lim, C.-G., Jang, J., & Kim, C. (2018). Cellular machinery for sensing mechanical force. *BMB Reports*.
Lin, D. H., Stuwe, T., Schilbach, S., Rundlet, E. J., Perriches, T., Mobbs, G., … Hoelz, A. (2016). Architecture of the symmetric core of the nuclear pore. *Science (New York, N.Y.)*, *352*(6283), aaf1015. https://doi.org/10.1126/science.aaf1015
Lindeman, R. E., & Pelegri, F. (2012). Localized products of futile cycle/lrmp promote

centrosome-nucleus attachment in the zebrafish zygote. *Current Biology*. https://doi.org/10.1016/j.cub.2012.03.058

Liu, T. X., Becker, M. W., Jelinek, J., Wu, W. S., Deng, M., Mikhalkevich, N., … Look, A. T. (2007). Chromosome 5q deletion and epigenetic suppression of the gene encoding α-catenin (CTNNA1) in myeloid cell transformation. *Nature Medicine*. https://doi.org/10.1038/nm1512

Liu, W., Dong, X., Mai, M., Seelan, R. S., Taniguchi, K., Krishnadath, K. K., … Thibodeau, S. N. (2000). Mutations in AXIN2 cause colorectal cancer with defective mismatch repair by activating β-catenin/TCF signalling. *Nature Genetics*. https://doi.org/10.1038/79859

Livak, K. J., & Schmittgen, T. D. (2001). Analysis of relative gene expression data using real-time quantitative PCR and the 2-ΔΔCT method. *Methods*, *25*(4), 402–408. https://doi.org/10.1006/meth.2001.1262

Lo, U.-G., Lee, C.-F., Lee, M.-S., & Hsieh, J.-T. (2017). The Role and Mechanism of Epithelial-to-Mesenchymal Transition in Prostate Cancer Progression. *International Journal of Molecular Sciences*, *18*(10). https://doi.org/10.3390/ijms18102079

Logue, J. S., Cartagena-Rivera, A. X., Baird, M. A., Davidson, M. W., Chadwick, R. S., & Waterman, C. M. (2015). Erk regulation of actin capping and bundling by Eps8 promotes cortex tension and leader bleb-based migration. *ELife*, *4*. https://doi.org/10.7554/eLife.08314

Lombardi, M. L., Jaalouk, D. E., Shanahan, C. M., Burke, B., Roux, K. J., & Lammerding, J. (2011). The interaction between nesprins and sun proteins at the nuclear envelope is critical for force transmission between the nucleus and cytoskeleton. *The Journal of Biological Chemistry*, *286*(30), 26743–26753. https://doi.org/10.1074/jbc.M111.233700

Lu, W., Gotzmann, J., Sironi, L., Jaeger, V.-M., Schneider, M., Lüke, Y., … Karakesisoglou, I. (2008). Sun1 forms immobile macromolecular assemblies at the nuclear envelope. *Biochimica et Biophysica Acta (BBA) - Molecular Cell Research*. https://doi.org/10.1016/j.bbamcr.2008.09.001

Lustig, B., Jerchow, B., Sachs, M., Weiler, S., Pietsch, T., Karsten, U., … Behrens, J. (2002). Negative Feedback Loop of Wnt Signaling through Upregulation of Conductin/Axin2 in Colorectal and Liver Tumors. *Molecular and Cellular Biology*. https://doi.org/10.1128/mcb.22.4.1184-1193.2002

Luxton, G. W. G., Gomes, E. R., Folker, E. S., Vintinner, E., & Gundersen, G. G. (2010). Linear arrays of nuclear envelope proteins harness retrograde actin flow for nuclear movement. *Science*. https://doi.org/10.1126/science.1189072

Lygerou, Z., Christophides, G., & Séraphin, B. (1999). A novel genetic screen for snRNP assembly factors in yeast identifies a conserved protein, Sad1p, also required for pre-mRNA splicing. *Molecular and Cellular Biology*, *19*(3), 2008–2020. https://doi.org/10.1128/mcb.19.3.2008

Machin, P., Catasus, L., Pons, C., Muñoz, J., Matias-Guiu, X., & Prat, J. (2002). CTNNB1 mutations and β-catenin expression in endometrial carcinomas. *Human Pathology*. https://doi.org/10.1053/hupa.2002.30723

Maher, M. T., Flozak, A. S., Stocker, A. M., Chenn, A., & Gottardi, C. J. (2009). Activity of the beta-catenin phosphodestruction complex at cell-cell contacts is enhanced by cadherin-based adhesion. *The Journal of Cell Biology*, *186*(2), 219–228. https://doi.org/10.1083/jcb.200811108

Maingret, F, Patel, A. J., Lesage, F., Lazdunski, M., & Honoré, E. (1999). Mechano- or acid stimulation, two interactive modes of activation of the TREK-1 potassium channel. *The Journal of Biological Chemistry*, *274*(38), 26691–26696. https://doi.org/10.1074/jbc.274.38.26691

Maingret, François, Fosset, M., Lesage, F., Lazdunski, M., & Honoré, E. (1999). TRAAK is a mammalian neuronal mechano-gated K+ channel. *Journal of Biological Chemistry*.

https://doi.org/10.1074/jbc.274.3.1381
Malone, C. J., Fixsen, W. D., Horvitz, H. R., & Han, M. (1999). UNC-84 localizes to the nuclear envelope and is required for nuclear migration and anchoring during C. elegans development. *Development (Cambridge, England)*, *126*(14), 3171–3181. Retrieved from http://www.ncbi.nlm.nih.gov/pubmed/10375507
Mandai, K., Nakanishi, H., Satoh, A., Obaishi, H., Wada, M., Nishioka, H., … Takai, Y. (1997). Afadin: A novel actin filament-binding protein with one PDZ domain localized at cadherin-based cell-to-cell adherens junction. *The Journal of Cell Biology*, *139*(2), 517–528. https://doi.org/10.1083/jcb.139.2.517
Maniotis, A. J., Chen, C. S., & Ingber, D. E. (1997). Demonstration of mechanical connections between integrins, cytoskeletal filaments, and nucleoplasm that stabilize nuclear structure. *Proceedings of the National Academy of Sciences*, *94*(3), 849–854. https://doi.org/10.1073/pnas.94.3.849
Mao, J., Wang, J., Liu, B., Pan, W., Farr, G. H., Flynn, C., … Wu, D. (2001). Low-density lipoprotein receptor-related protein-5 binds to Axin and regulates the canonical Wnt signaling pathway. *Molecular Cell*. https://doi.org/10.1016/S1097-2765(01)00224-6
Marfori, M., Mynott, A., Ellis, J. J., Mehdi, A. M., Saunders, N. F. W., Curmi, P. M., … Kobe, B. (2011). Molecular basis for specificity of nuclear import and prediction of nuclear localization. *Biochimica et Biophysica Acta - Molecular Cell Research*. https://doi.org/10.1016/j.bbamcr.2010.10.013
Marikawa, Y., & Elinson, R. P. (1998). beta-TrCP is a negative regulator of Wnt/beta-catenin signaling pathway and dorsal axis formation in Xenopus embryos. *Mechanisms of Development*, *77*(1), 75–80. Retrieved from http://www.ncbi.nlm.nih.gov/pubmed/9784611
Markiewicz, E., Tilgner, K., Barker, N., van de Wetering, M., Clevers, H., Dorobek, M., … Hutchison, C. J. (2006). The inner nuclear membrane protein emerin regulates beta-catenin activity by restricting its accumulation in the nucleus. *The EMBO Journal*, *25*(14), 3275–3285. https://doi.org/10.1038/sj.emboj.7601230
Martinac, B. (2004). Mechanosensitive ion channels: molecules of mechanotransduction. *Journal of Cell Science*. https://doi.org/10.1242/jcs.01232
Martino, F., Perestrelo, A. R., Vinarský, V., Pagliari, S., & Forte, G. (2018). Cellular mechanotransduction: From tension to function. *Frontiers in Physiology*. https://doi.org/10.3389/fphys.2018.00824
Maruyama, K., & Ebashi, S. (1965). α-actinin, a new structural protein from striated muscle: II. action on actin. *Journal of Biochemistry*. https://doi.org/10.1093/oxfordjournals.jbchem.a128158
Maurer, M., & Lammerding, J. (2019). The Driving Force: Nuclear Mechanotransduction in Cellular Function, Fate, and Disease. *Annual Review of Biomedical Engineering*. https://doi.org/10.1146/annurev-bioeng-060418-052139
Mccrea, P. D., Turck, C. W., & Gumbiner, B. (1991). A homolog of the armadillo protein in Drosophila (plakoglobin) associated with E-cadherin. *Science*. https://doi.org/10.1126/science.1962194
McCrea, P D, Brieher, W. M., & Gumbiner, B. M. (1993). Induction of a secondary body axis in Xenopus by antibodies to beta-catenin. *The Journal of Cell Biology*, *123*(2), 477–484. https://doi.org/10.1083/jcb.123.2.477
McCrea, Pierre D., & Gottardi, C. J. (2016). Beyond β-catenin: Prospects for a larger catenin network in the nucleus. *Nature Reviews Molecular Cell Biology*. https://doi.org/10.1038/nrm.2015.3
McEvoy, A. L., Hoi, H., Bates, M., Platonova, E., Cranfill, P. J., Baird, M. A., … Campbell, R. E. (2012). mMaple: A Photoconvertible Fluorescent Protein for Use in Multiple Imaging

Modalities. *PLoS ONE*, *7*(12). https://doi.org/10.1371/journal.pone.0051314
McMahon, A. P. (1992). The Wnt family of developmental regulators. *Trends in Genetics*. https://doi.org/10.1016/0168-9525(92)90393-I
McMahon, A. P., & Moon, R. T. (1989). Ectopic expression of the proto-oncogene int-1 in Xenopus embryos leads to duplication of the embryonic axis. *Cell*. https://doi.org/10.1016/0092-8674(89)90506-0
McMahon, A. P., Takada, S., Ikeya, M., Lee, S. M. K., & Johnson, J. E. (1997). Wnt signalling required for expansion of neural crest and CNS progenitors. *Nature*. https://doi.org/10.1038/40146
Meinke, P., Mattioli, E., Haque, F., Antoku, S., Columbaro, M., Straatman, K. R., … Shackleton, S. (2014). Muscular dystrophy-associated SUN1 and SUN2 variants disrupt nuclear-cytoskeletal connections and myonuclear organization. *PLoS Genetics*, *10*(9), e1004605. https://doi.org/10.1371/journal.pgen.1004605
Mendez, M. G., Kojima, S. I., & Goldman, R. D. (2010). Vimentin induces changes in cell shape, motility, and adhesion during the epithelial to mesenchymal transition. *FASEB Journal*, *24*(6), 1838–1851. https://doi.org/10.1096/fj.09-151639
Meng, F., Suchyna, T. M., & Sachs, F. (2008). A fluorescence energy transfer-based mechanical stress sensor for specific proteins in situ. *The FEBS Journal*, *275*(12), 3072–3087. https://doi.org/10.1111/j.1742-4658.2008.06461.x
Merdek, K. D., Nguyen, N. T., & Toksoz, D. (2004). Distinct activities of the alpha-catenin family, alpha-catulin and alpha-catenin, on beta-catenin-mediated signaling. *Molecular and Cellular Biology*, *24*(6), 2410–2422.
Molenaar, M., Van De Wetering, M., Oosterwegel, M., Peterson-Maduro, J., Godsave, S., Korinek, V., … Clevers, H. (1996). XTcf-3 transcription factor mediates β-catenin-induced axis formation in xenopus embryos. *Cell*. https://doi.org/10.1016/S0092-8674(00)80112-9
Moore, A. R., & Burt, A. S. (1939). On the locus and nature of the forces causing gastrulation in the embryos of Dendraster excentricus. *Journal of Experimental Zoology*. https://doi.org/10.1002/jez.1400820107
Morikawa, Y., Zhang, M., Heallen, T., Leach, J., Tao, G., Xiao, Y., … Martin, J. F. (2015). Actin cytoskeletal remodeling with protrusion formation is essential for heart regeneration in Hippo-deficient mice. *Science Signaling*. https://doi.org/10.1126/scisignal.2005781
Morimoto, A., Shibuya, H., Zhu, X., Kim, J., Ishiguro, K. I., Han, M., & Watanabe, Y. (2012). A conserved KASH domain protein associates with telomeres, SUN1, and dynactin during mammalian meiosis. *Journal of Cell Biology*. https://doi.org/10.1083/jcb.201204085
Morin, P. J., Sparks, A. B., Korinek, V., Barker, N., Clevers, H., Vogelstein, B., & Kinzler, K. W. (1997). Activation of beta-catenin-Tcf signaling in colon cancer by mutations in beta-catenin or APC. *Science (New York, N.Y.)*, *275*(5307), 1787–1790. https://doi.org/10.1126/science.275.5307.1787
Mosimann, C., Hausmann, G., & Basler, K. (2006). Parafibromin/Hyrax activates Wnt/Wg target gene transcription by direct association with beta-catenin/Armadillo. *Cell*, *125*(2), 327–341. https://doi.org/10.1016/j.cell.2006.01.053
Mouw, J. K., Ou, G., & Weaver, V. M. (2014). Extracellular matrix assembly: a multiscale deconstruction. *Nature Reviews. Molecular Cell Biology*, *15*(12), 771–785. https://doi.org/10.1038/nrm3902
Mutsuki, A., Masaaki, I., Kazushi, K., Yuko, F., Kazuyasu, C., Takeshi, N., … Kozo, K. (1996). Phosphorylation and Activation of Myosin by Rho-associated Kinase (Rho-kinase). *Journal of Biological Chemistry*. https://doi.org/10.1074/jbc.271.34.20246
Nagafuchi, A., & Takeichi, M. (1989). Transmembrane control of cadherin-mediated cell adhesion: a 94 kDa protein functionally associated with a specific region of the cytoplasmic domain of E-cadherin. *Cell Regulation*, *1*(1), 37–44. Retrieved from

http://www.ncbi.nlm.nih.gov/pubmed/2519616
Nardone, G., Oliver-De La Cruz, J., Vrbsky, J., Martini, C., Pribyl, J., Skládal, P., … Forte, G. (2017). YAP regulates cell mechanics by controlling focal adhesion assembly. *Nature Communications*. https://doi.org/10.1038/ncomms15321
Naumanen, P., Lappalainen, P., & Hotulainen, P. (2008). Mechanisms of actin stress fibre assembly. *Journal of Microscopy*, *231*(3), 446–454. https://doi.org/10.1111/j.1365-2818.2008.02057.x
Nelson, W. J. (2008). Biochemical Society Annual Symposium No . 75 Regulation of cell – cell adhesion by the cadherin – catenin complex. *Society*. https://doi.org/10.1042/BST0360149
Neuman, K. C., & Nagy, A. (2008, June). Single-molecule force spectroscopy: Optical tweezers, magnetic tweezers and atomic force microscopy. *Nature Methods*, Vol. 5, pp. 491–505. https://doi.org/10.1038/nmeth.1218
Neumann, S., Schneider, M., Daugherty, R. L., Gottardi, C. J., Eming, S. A., Beijer, A., … Karakesisoglou, I. (2010). Nesprin-2 interacts with {alpha}-catenin and regulates Wnt signaling at the nuclear envelope. *The Journal of Biological Chemistry*, *285*(45), 34932–34938. https://doi.org/10.1074/jbc.M110.119651
Ni, Q., & Zhang, J. (2010). Dynamic visualization of cellular signaling. *Advances in Biochemical Engineering/Biotechnology*, *119*, 79–97. https://doi.org/10.1007/10_2008_48
Nieto, M. Angela, Huang, R. Y. Y. J., Jackson, R. A. A., & Thiery, J. P. P. (2016). EMT: 2016. *Cell*. https://doi.org/10.1016/j.cell.2016.06.028
Nieto, M A, Sargent, M. G., Wilkinson, D. G., & Cooke, J. (1994). Control of cell behavior during vertebrate development by Slug, a zinc finger gene. *Science (New York, N.Y.)*, *264*(5160), 835–839. https://doi.org/10.1126/science.7513443
Nix, D. A., & Beckerle, M. C. (1997). Nuclear-cytoplasmic shuttling of the focal contact protein, zyxin: A potential mechanism for communication between sites of cell adhesion and the nucleus. *Journal of Cell Biology*. https://doi.org/10.1083/jcb.138.5.1139
Nollet, F., Berx, G., Molemans, F., & van Roy, F. (1996). Genomic organization of the human beta-catenin gene (CTNNB1). *Genomics*, *32*(3), 413–424. https://doi.org/10.1006/geno.1996.0136
Noomnarm, U., & Clegg, R. M. (2009). Fluorescence lifetimes: fundamentals and interpretations. *Photosynthesis Research*, *101*(2–3), 181–194. https://doi.org/10.1007/s11120-009-9457-8
Noordermeer, J., Klingensmith, J., Perrimon, N., & Nusse, R. (1994). dishevelled and armadillo act in the wingless signalling pathway in Drosophila. *Nature*, *367*(6458), 80–83. https://doi.org/10.1038/367080a0
Norvell, S. M., Alvarez, M., Bidwell, J. P., & Pavalko, F. M. (2004). Fluid shear stress induces beta-catenin signaling in osteoblasts. *Calcified Tissue International*, *75*(5), 396–404. https://doi.org/10.1007/s00223-004-0213-y
Ohashi, K., Nagata, K., Maekawa, M., Ishizaki, T., Narumiya, S., & Mizuno, K. (2000). Rho-associated kinase ROCK activates LIM-kinase 1 by phosphorylation at threonine 508 within the activation loop. *Journal of Biological Chemistry*. https://doi.org/10.1074/jbc.275.5.3577
OKA, M., & YONEDA, Y. (2018). Importin α: functions as a nuclear transport factor and beyond. *Proceedings of the Japan Academy, Series B*. https://doi.org/10.2183/pjab.94.018
Oka, T., & Sudol, M. (2009). Nuclear localization and pro-apoptotic signaling of YAP2 require intact PDZ-binding motif. *Genes to Cells*. https://doi.org/10.1111/j.1365-2443.2009.01292.x
Omelchenko, T., Vasiliev, J. M., Gelfand, I. M., Feder, H. H., & Bonder, E. M. (2003). Rho-dependent formation of epithelial “leader” cells during wound healing. *Proceedings of the*

National Academy of Sciences of the United States of America, *100*(19), 10788–10793. https://doi.org/10.1073/pnas.1834401100
Oria, R., Wiegand, T., Escribano, J., Elosegui-Artola, A., Uriarte, J. J., Moreno-Pulido, C., … Roca-Cusachs, P. (2017). Force loading explains spatial sensing of ligands by cells. *Nature*. https://doi.org/10.1038/nature24662
Orr, A. W., Helmke, B. P., Blackman, B. R., & Schwartz, M. A. (2006). Mechanisms of mechanotransduction. *Developmental Cell*, *10*(1), 11–20. https://doi.org/10.1016/j.devcel.2005.12.006
Orsulic, S., Huber, O., Aberle, H., Arnold, S., & Kemler, R. (1999). E-cadherin binding prevents beta-catenin nuclear localization and beta-catenin/LEF-1-mediated transactivation. *Journal of Cell Science*, *112*(8).
Osorio, D. S., & Gomes, E. R. (2013). The contemporary nucleus: a trip down memory lane. *Biology of the Cell*, *105*(9), 430–441. https://doi.org/10.1111/boc.201300009
Ostlund, C., Folker, E. S., Choi, J. C., Gomes, E. R., Gundersen, G. G., & Worman, H. J. (2009). Dynamics and molecular interactions of linker of nucleoskeleton and cytoskeleton (LINC) complex proteins. *Journal of Cell Science*. https://doi.org/10.1242/jcs.057075
Ozawa, M., Baribault, H., & Kemler, R. (1989). The cytoplasmic domain of the cell adhesion molecule uvomorulin associates with three independent proteins structurally related in different species. *The EMBO Journal*. https://doi.org/10.1002/j.1460-2075.1989.tb03563.x
Ozawa, M., Ringwald, M., & Kemler, R. (1990). Uvomorulin-catenin complex formation is regulated by a specific domain in the cytoplasmic region of the cell adhesion molecule. *Proceedings of the National Academy of Sciences of the United States of America*, *87*(11), 4246–4250. https://doi.org/10.1073/pnas.87.11.4246
Padiath, Q. S., Saigoh, K., Schiffmann, R., Asahara, H., Yamada, T., Koeppen, A., … Fu, Y.-H. (2006). Lamin B1 duplications cause autosomal dominant leukodystrophy. *Nature Genetics*, *38*(10), 1114–1123. https://doi.org/10.1038/ng1872
Park, J., & Schwarzbauer, J. E. (2014). Mammary epithelial cell interactions with fibronectin stimulate epithelial-mesenchymal transition. *Oncogene*. https://doi.org/10.1038/onc.2013.118
Paszek, M. J., DuFort, C. C., Rossier, O., Bainer, R., Mouw, J. K., Godula, K., … Weaver, V. M. (2014). The cancer glycocalyx mechanically primes integrin-mediated growth and survival. *Nature*, *511*(7509), 319–325. https://doi.org/10.1038/nature13535
Patel, A. J., Honoré, E., Maingret, F., Lesage, F., Fink, M., Duprat, F., & Lazdunski, M. (1998). A mammalian two pore domain mechano-gated S-like K+ channel. *EMBO Journal*. https://doi.org/10.1093/emboj/17.15.4283
Peifer, M., Berg, S., & Reynolds, A. B. (1994). A repeating amino acid motif shared by proteins with diverse cellular roles. *Cell*. https://doi.org/10.1016/0092-8674(94)90353-0
Pellegrin, S., & Mellor, H. (2007). Actin stress fibres. *Journal of Cell Science*. https://doi.org/10.1242/jcs.018473
Piao, H.-L., Yuan, Y., Wang, M., Sun, Y., Liang, H., & Ma, L. (2014). α-catenin acts as a tumour suppressor in E-cadherin-negative basal-like breast cancer by inhibiting NF-κB signalling. *Nature Cell Biology*, *16*(3), 245–254. https://doi.org/10.1038/ncb2909
Pickersgill, H., Kalverda, B., De Wit, E., Talhout, W., Fornerod, M., & Van Steensel, B. (2006). Characterization of the Drosophila melanogaster genome at the nuclear lamina. *Nature Genetics*, *38*(9), 1005–1014. https://doi.org/10.1038/ng1852
Pierschbacher, M. D., & Ruoslahti, E. (1984). Cell attachment activity of fibronectin can be duplicated by small synthetic fragments of the molecule. *Nature*, *309*(5963), 30–33. https://doi.org/10.1038/309030a0
Preston, C., & Faustino, R. (2018). Nuclear Envelope Regulation of Oncogenic Processes: Roles

in Pancreatic Cancer. *Epigenomes*. https://doi.org/10.3390/epigenomes2030015
Price, G. J., Jones, P., Davison, M. D., Patel, B., Bendori, R., Geiger, B., & Critchley, D. R. (1989). Primary sequence and domain structure of chicken vinculin. *Biochemical Journal*. https://doi.org/10.1042/bj2590453
Raftopoulos, I., Davaris, P., Karatzas, G., Karayannacos, P., & Kouraklis, G. (1998). Level of alpha-catenin expression in colorectal cancer correlates with invasiveness, metastatic potential, and survival. *Journal of Surgical Oncology*, *68*(2), 92–99. Retrieved from http://www.ncbi.nlm.nih.gov/pubmed/9624037
Rajgor, D., Mellad, J. A., Autore, F., Zhang, Q., & Shanahan, C. M. (2012). Multiple novel nesprin-1 and nesprin-2 variants act as versatile tissue-specific intracellular scaffolds. *PLoS ONE*. https://doi.org/10.1371/journal.pone.0040098
Rajgor, D., & Shanahan, C. M. (2013). Nesprins: from the nuclear envelope and beyond. *Expert Reviews in Molecular Medicine*, *15*, e5. https://doi.org/10.1017/erm.2013.6
Rauch, C., Brunet, A.-C., Deleule, J., & Farge, E. (2002). C 2 C 12 myoblast/osteoblast transdifferentiation steps enhanced by epigenetic inhibition of BMP2 endocytosis . *American Journal of Physiology-Cell Physiology*. https://doi.org/10.1152/ajpcell.00234.2001
Ribbeck, K., & Gorlich, D. (2002). *The permeability barrier of nuclear pore complexes appears.pdf*. *21*(11), 2664–2671. https://doi.org/10.1093/emboj/21.11.2664
Riggleman, B., Wieschaus, E., & Schedl, P. (1989). Molecular analysis of the armadillo locus: uniformly distributed transcripts and a protein with novel internal repeats are associated with a Drosophila segment polarity gene. *Genes & Development*. https://doi.org/10.1101/gad.3.1.96
Rimm, D. L., Koslov, E. R., Kebriaei, P., Cianci, C. D., & Morrow, J. S. (1995). Alpha 1(E)-catenin is an actin-binding and -bundling protein mediating the attachment of F-actin to the membrane adhesion complex. *Proceedings of the National Academy of Sciences*, *92*(19).
Ringer, P., Weißl, A., Cost, A.-L., Freikamp, A., Sabass, B., Mehlich, A., … Grashoff, C. (2017). Multiplexing molecular tension sensors reveals piconewton force gradient across talin-1. *Nature Methods*, *14*(11), 1090–1096. https://doi.org/10.1038/nmeth.4431
Robbins, J., Dilworth, S. M., Laskey, R. A., & Dingwall, C. (1991). Two interdependent basic domains in nucleoplasmin nuclear targeting sequence: identification of a class of bipartite nuclear targeting sequence. *Cell*, *64*(3), 615–623. https://doi.org/10.1016/0092-8674(91)90245-t
Rodan, G., Bourret, L., Harvey, A., & Mensi, T. (1975). Cyclic AMP and cyclic GMP: mediators of the mechanical effects on bone remodeling. *Science*, *189*(4201).
Roelink, H., & Nusse, R. (1991). Expression of two members of the Wnt family during mouse development-restricted temporal and spatial patterns in the developing neural tube. *Genes and Development*. https://doi.org/10.1101/gad.5.3.381
Rogakou, E. P., Boon, C., Redon, C., & Bonner, W. M. (1999). Megabase chromatin domains involved in DNA double-strand breaks in vivo. *The Journal of Cell Biology*, *146*(5), 905–916. https://doi.org/10.1083/jcb.146.5.905
Romano, L. A., & Runyan, R. B. (2000). Slug is an essential target of TGFβ2 signaling in the developing chicken heart. *Developmental Biology*. https://doi.org/10.1006/dbio.2000.9750
Roose, J., Molenaar, M., Peterson, J., Hurenkamp, J., Brantjes, H., Moerer, P., … Clevers, H. (1998). The Xenopus Wnt effector XTcf-3 interacts with Groucho-related transcriptional repressors. *Nature*. https://doi.org/10.1038/26989
Rosanò, L., Spinella, F., Di Castro, V., Nicotra, M. R., Dedhar, S., de Herreros, A. G., … Bagnato, A. (2005). Endothelin-1 promotes epithelial-to-mesenchymal transition in human ovarian cancer cells. *Cancer Research*, *65*(24), 11649–11657. https://doi.org/10.1158/0008-

5472.CAN-05-2123
Rothbächer, U., Laurent, M. N., Deardorff, M. A., Klein, P. S., Cho, K. W. Y., & Fraser, S. E. (2000). Dishevelled phosphorylation, subcellular localization and multimerization regulate its role in early embryogenesis. *EMBO Journal*. https://doi.org/10.1093/emboj/19.5.1010
Rothenberg, K. E., Neibart, S. S., LaCroix, A. S., & Hoffman, B. D. (2015). Controlling Cell Geometry Affects the Spatial Distribution of Load Across Vinculin. *Cellular and Molecular Bioengineering*, *8*(3), 364–382. https://doi.org/10.1007/s12195-015-0404-9
Roux, K. J., Crisp, M. L., Liu, Q., Kim, D., Kozlov, S., Stewart, C. L., & Burke, B. (2009). Nesprin 4 is an outer nuclear membrane protein that can induce kinesin-mediated cell polarization. *Proceedings of the National Academy of Sciences*. https://doi.org/10.1073/pnas.0808602106
Rubinfeld, B., Robbins, P., El-Gamil, M., Albert, I., Porfiri, E., & Polakis, P. (1997). Stabilization of beta-catenin by genetic defects in melanoma cell lines. *Science (New York, N.Y.)*, *275*(5307), 1790–1792. https://doi.org/10.1126/science.275.5307.1790
Rubinfeld, B., Souza, B., Albert, I., Müller, O., Chamberlain, S. H., Masiarz, F. R., … Polakis, P. (1993). Association of the APC gene product with beta-catenin. *Science (New York, N.Y.)*, *262*(5140), 1731–1734. https://doi.org/10.1126/science.8259518
Sakaue-Sawano, A., Kurokawa, H., Morimura, T., Hanyu, A., Hama, H., Osawa, H., … Miyawaki, A. (2008). Visualizing spatiotemporal dynamics of multicellular cell-cycle progression. *Cell*, *132*(3), 487–498. https://doi.org/10.1016/j.cell.2007.12.033
Salpingidou, G., Smertenko, A., Hausmanowa-Petrucewicz, I., Hussey, P. J., & Hutchison, C. J. (2007). A novel role for the nuclear membrane protein emerin in association of the centrosome to the outer nuclear membrane. *Journal of Cell Biology*. https://doi.org/10.1083/jcb.200702026
Sarangi, B. R., Gupta, M., Doss, B. L., Tissot, N., Lam, F., Mège, R.-M., … Ladoux, B. (2017). Coordination between Intra- and Extracellular Forces Regulates Focal Adhesion Dynamics. *Nano Letters*, *17*(1), 399–406. https://doi.org/10.1021/acs.nanolett.6b04364
Sathe, A. R., Shivashankar, G. V., & Sheetz, M. P. (2016). Nuclear transport of paxillin depends on focal adhesion dynamics and FAT domains. *Journal of Cell Science*, *129*(10), 1981–1988. https://doi.org/10.1242/jcs.172643
Satoh, S., Daigo, Y., Furukawa, Y., Kato, T., Miwa, N., Nishiwaki, T., … Nakamura, Y. (2000). AXIN1 mutations in hepatocellular carcinomas, and growth suppression in cancer cells by virus-mediated transfer of AXIN1. *Nature Genetics*, *24*(3), 245–250. https://doi.org/10.1038/73448
Savagner, P, Yamada, K. M., & Thiery, J. P. (1997). The zinc-finger protein slug causes desmosome dissociation, an initial and necessary step for growth factor-induced epithelial-mesenchymal transition. *The Journal of Cell Biology*, *137*(6), 1403–1419. https://doi.org/10.1083/jcb.137.6.1403
Savagner, Pierre, Kusewitt, D. F., Carver, E. A., Magnino, F., Choi, C., Gridley, T., & Hudson, L. G. (2005). Developmental transcription factor slug is required for effective re-epithelialization by adult keratinocytes. *Journal of Cellular Physiology*, *202*(3), 858–866. https://doi.org/10.1002/jcp.20188
Sawada, Y., Tamada, M., Dubin-Thaler, B. J., Cherniavskaya, O., Sakai, R., Tanaka, S., & Sheetz, M. P. (2006). Force sensing by mechanical extension of the Src family kinase substrate p130Cas. *Cell*, *127*(5), 1015–1026. https://doi.org/10.1016/j.cell.2006.09.044
Schiller, H. B., & Fässler, R. (2013). Mechanosensitivity and compositional dynamics of cell-matrix adhesions. *EMBO Reports*. https://doi.org/10.1038/embor.2013.49
Schirmer, E. C., & Gerace, L. (2002). Organellar proteomics: the prizes and pitfalls of opening the nuclear envelope. *Genome Biology*.
Schneider, C. A., Rasband, W. S., & Eliceiri, K. W. (2012). NIH Image to ImageJ: 25 years of

image analysis. *Nature Methods*, *9*(7), 671–675. https://doi.org/10.1038/nmeth.2089
Schuster, J., Sundblom, J., Thuresson, A.-C., Hassin-Baer, S., Klopstock, T., Dichgans, M., … Dahl, N. (2011). Genomic duplications mediate overexpression of lamin B1 in adult-onset autosomal dominant leukodystrophy (ADLD) with autonomic symptoms. *Neurogenetics*, *12*(1), 65–72. https://doi.org/10.1007/s10048-010-0269-y
Seetharaman, S., & Etienne-Manneville, S. (2018). Integrin diversity brings specificity in mechanotransduction. *Biology of the Cell*. https://doi.org/10.1111/boc.201700060
Sen, B., Xie, Z., Case, N., Ma, M., Rubin, C., & Rubin, J. (2008). Mechanical strain inhibits adipogenesis in mesenchymal stem cells by stimulating a durable beta-catenin signal. *Endocrinology*, *149*(12), 6065–6075. https://doi.org/10.1210/en.2008-0687
Sen, B., Xie, Z., Case, N., Styner, M., Rubin, C. T., & Rubin, J. (2011). Mechanical signal influence on mesenchymal stem cell fate is enhanced by incorporation of refractory periods into the loading regimen. *Journal of Biomechanics*. https://doi.org/10.1016/j.jbiomech.2010.11.022
Seong, J., Tajik, A., Sun, J., Guan, J.-L., Humphries, M. J., Craig, S. E., … Wang, Y. (2013). Distinct biophysical mechanisms of focal adhesion kinase mechanoactivation by different extracellular matrix proteins. *Proceedings of the National Academy of Sciences*. https://doi.org/10.1073/pnas.1307405110
Shang, S., Hua, F., & Hu, Z.-W. (2017). The regulation of β-catenin activity and function in cancer: therapeutic opportunities. *Oncotarget*, *8*(20), 33972–33989. https://doi.org/10.18632/oncotarget.15687
Shapiro, L., & Weis, W. I. (2009). and Catenins. *Spring*. https://doi.org/10.1101/cshperspect.a003053
Shattil, S. J., Kim, C., & Ginsberg, M. H. (2010). The final steps of integrin activation: The end game. *Nature Reviews Molecular Cell Biology*. https://doi.org/10.1038/nrm2871
Shibamoto, S., Hayakawa, M., Takeuchi, K., Hori, T., Miyazawa, K., Kitamura, N., … Takeichi, M. (1995). Association of p120, a tyrosine kinase substrate, with E-cadherin/catenin complexes. *The Journal of Cell Biology*, *128*(5), 949–957. https://doi.org/10.1083/jcb.128.5.949
Shiloh, Y., & Ziv, Y. (2013). The ATM protein kinase: Regulating the cellular response to genotoxic stress, and more. *Nature Reviews Molecular Cell Biology*. https://doi.org/10.1038/nrm3546
Shindo, Y., Kim, M. R., Miura, H., Yuuki, T., Kanda, T., Hino, A., & Kusakabe, Y. (2010). Lrmp/Jaw1 is expressed in sweet, bitter, and umami receptor-expressing cells. *Chemical Senses*. https://doi.org/10.1093/chemse/bjp097
Shiu, J. Y., Aires, L., Lin, Z., & Vogel, V. (2018). Nanopillar force measurements reveal actin-cap-mediated YAP mechanotransduction. *Nature Cell Biology*. https://doi.org/10.1038/s41556-017-0030-y
Shumaker, D. K., Lee, K. K., Tanhehco, Y. C., Craigie, R., & Wilson, K. L. (2001). LAP2 binds to BAF·DNA complexes: Requirement for the LEM domain and modulation by variable regions. *EMBO Journal*, *20*(7), 1754–1764. https://doi.org/10.1093/emboj/20.7.1754
Siegfried, E., Chou, T. Bin, & Perrimon, N. (1992). wingless signaling acts through zeste-white 3, the drosophila homolog of glycogen synthase kinase-3, to regulate engrailed and establish cell fate. *Cell*. https://doi.org/10.1016/S0092-8674(05)80065-0
Singh, M., Yelle, N., Venugopal, C., & Singh, S. K. (2018). EMT: Mechanisms and therapeutic implications. *Pharmacology & Therapeutics*, *182*, 80–94. https://doi.org/10.1016/j.pharmthera.2017.08.009
Slack-Davis, J. K., Martin, K. H., Tilghman, R. W., Iwanicki, M., Ung, E. J., Autry, C., … Parsons, J. T. (2007). Cellular characterization of a novel focal adhesion kinase inhibitor. *The Journal of Biological Chemistry*, *282*(20), 14845–14852. https://doi.org/10.1074/jbc.M606695200

Snider, N. T., & Omary, M. B. (2014). Post-translational modifications of intermediate filament proteins: Mechanisms and functions. *Nature Reviews Molecular Cell Biology*. https://doi.org/10.1038/nrm3753

Sosa, B. A., Rothballer, A., Kutay, U., & Schwartz, T. U. (2012). LINC complexes form by binding of three KASH peptides to domain interfaces of trimeric SUN proteins. *Cell*. https://doi.org/10.1016/j.cell.2012.03.046

Spagnoli, F. M., Cicchini, C., Tripodi, M., & Weiss, M. C. (2000). Inhibition of MMH (Met murine hepatocyte) cell differentiation by TGF(beta) is abrogated by pre-treatment with the heritable differentiation effector FGF1. *Journal of Cell Science*, *113 (Pt 20)*, 3639–3647. Retrieved from http://www.ncbi.nlm.nih.gov/pubmed/11017879

Städeli, R., Hoffmans, R., & Basler, K. (2006). Transcription under the Control of Nuclear Arm/β-Catenin. *Current Biology*. https://doi.org/10.1016/j.cub.2006.04.019

Stambolic, V., Ruel, L., & Woodgett, J. R. (1996). Lithium inhibits glycogen synthase kinase-3 activity and mimics wingless signalling in intact cells. *Current Biology : CB*, *6*(12), 1664–1668. https://doi.org/10.1016/s0960-9822(02)70790-2

Stamm, A., Reimers, K., Strauß, S., Vogt, P., Scheper, T., & Pepelanova, I. (2016, May 1). In vitro wound healing assays - State of the art. *BioNanoMaterials*, Vol. 17, pp. 79–87. https://doi.org/10.1515/bnm-2016-0002

Stamos, J. L., & Weis, W. I. (2013). The β-catenin destruction complex. *Cold Spring Harbor Perspectives in Biology*, *5*(1), a007898. https://doi.org/10.1101/cshperspect.a007898

Starr, D. A., & Han, M. (2002). Role of ANC-1 in tethering nuclei to the actin cytoskeleton. *Science*. https://doi.org/10.1126/science.1075119

Stewart-Hutchinson, P. J., Hale, C. M., Wirtz, D., & Hodzic, D. (2008). Structural requirements for the assembly of LINC complexes and their function in cellular mechanical stiffness. *Experimental Cell Research*. https://doi.org/10.1016/j.yexcr.2008.02.022

Stewart, C. L., & Burke, B. (2014). The missing LINC. *Nucleus*. https://doi.org/10.4161/nucl.27819

Stewart, M. (2007). Molecular mechanism of the nuclear protein import cycle. *Nature Reviews Molecular Cell Biology*. https://doi.org/10.1038/nrm2114

Stewart, R. M., Zubek, A. E., Rosowski, K. A., Schreiner, S. M., Horsley, V., & King, M. C. (2015). Nuclear-cytoskeletal linkages facilitate cross talk between the nucleus and intercellular adhesions. *Journal of Cell Biology*, *209*(3), 403–418. https://doi.org/10.1083/jcb.201502024

Straßburger, K., Tiebe, M., Pinna, F., Breuhahn, K., & Teleman, A. A. (2012). Insulin/IGF signaling drives cell proliferation in part via Yorkie/YAP. *Developmental Biology*, *367*(2), 187–196. https://doi.org/10.1016/j.ydbio.2012.05.008

Strohmeyer, N., Bharadwaj, M., Costell, M., Fässler, R., & Müller, D. J. (2017). Fibronectin-bound α5β1 integrins sense load and signal to reinforce adhesion in less than a second. *Nature Materials*, *16*(12), 1262–1270. https://doi.org/10.1038/nmat5023

Ström, A. C., & Weis, K. (2001). Importin-beta-like nuclear transport receptors. *Genome Biology*.

Strutz, F., Zeisberg, M., Ziyadeh, F. N., Yang, C.-Q., Kalluri, R., Müller, G. A., & Neilson, E. G. (2002). Role of basic fibroblast growth factor-2 in epithelial-mesenchymal transformation. *Kidney International*, *61*(5), 1714–1728. https://doi.org/10.1046/j.1523-1755.2002.00333.x

Su, L. K., Vogelstein, B., & Kinzler, K. W. (1993). Association of the APC tumor suppressor protein with catenins. *Science (New York, N.Y.)*, *262*(5140), 1734–1737. https://doi.org/10.1126/science.8259519

Su, T.-H., Chang, J.-G., Yeh, K.-T., Lin, T.-H., Lee, T.-P., Chen, J.-C., & Lin, C.-C. (2003). Mutation analysis of CTNNB1 (beta-catenin) and AXIN1, the components of Wnt pathway, in

cervical carcinomas. *Oncology Reports*, *10*(5), 1195–1200. Retrieved from http://www.ncbi.nlm.nih.gov/pubmed/12883680
Sur, I., Neumann, S., & Noegel, A. A. (2014). Nesprin-1 role in DNA damage response. *Nucleus (United States)*, *5*(2). https://doi.org/10.4161/nucl.29023
Suzuki, A., Badger, B. L., Haase, J., Ohashi, T., Erickson, H. P., Salmon, E. D., & Bloom, K. (2016). How the kinetochore couples microtubule force and centromere stretch to move chromosomes. *Nature Cell Biology*, *18*(4), 382–392. https://doi.org/10.1038/ncb3323
Swartz, R. K., Rodriguez, E. C., & King, M. C. (2014). A role for nuclear envelope-bridging complexes in homology-directed repair. *Molecular Biology of the Cell*. https://doi.org/10.1091/mbc.e13-10-0569
Tabdanov, E., Borghi, N., Brochard-Wyart, F., Dufour, S., & Thiery, J. P. (2009). Role of E-cadherin in membrane-cortex interaction probed by nanotube extrusion. *Biophysical Journal*. https://doi.org/10.1016/j.bpj.2008.11.059
Tajik, A., Zhang, Y., Wei, F., Sun, J., Jia, Q., Zhou, W., … Wang, N. (2016). Transcription upregulation via force-induced direct stretching of chromatin. *Nature Materials*, *15*(12), 1287–1296. https://doi.org/10.1038/nmat4729
Takeichi, M. (1988). The cadherins: cell-cell adhesion molecules controlling animal morphogenesis. *Development (Cambridge, England)*.
Takeichi, M. (1995). Morphogenetic roles of classic cadherins. *Current Opinion in Cell Biology*, *7*(5), 619–627. Retrieved from http://www.ncbi.nlm.nih.gov/pubmed/8573335
Takeichi, Masatoshi. (2018). Multiple functions of α-catenin beyond cell adhesion regulation. *Current Opinion in Cell Biology*, *54*, 24–29. https://doi.org/10.1016/j.ceb.2018.02.014
Takeichi, Masatoshi, Atsumi, T., Yoshida, C., Uno, K., & Okada, T. S. (1981). Selective adhesion of embryonal carcinoma cells and differentiated cells by Ca 2+ -dependent sites. *Developmental Biology*. https://doi.org/10.1016/0012-1606(81)90157-3
Tamai, K., Zeng, X., Liu, C., Zhang, X., Harada, Y., Chang, Z., & He, X. (2004). A Mechanism for Wnt Coreceptor Activation. *Molecular Cell*. https://doi.org/10.1016/S1097-2765(03)00484-2
Tanaka, K., Kitagawa, Y., & Kadowaki, T. (2002). Drosophila segment polarity gene product porcupine stimulates the posttranslational N-glycosylation of wingless in the endoplasmic reticulum. *Journal of Biological Chemistry*. https://doi.org/10.1074/jbc.M200187200
Tanja Mierke, C. (2018). Physical role of nuclear and cytoskeletal confinements in cell migration mode selection and switching. *AIMS Biophysics*. https://doi.org/10.3934/biophy.2017.4.615
Tapley, E. C., & Starr, D. A. (2013). Connecting the nucleus to the cytoskeleton by SUN-KASH bridges across the nuclear envelope. *Current Opinion in Cell Biology*. https://doi.org/10.1016/j.ceb.2012.10.014
Taranum, S., Vaylann, E., Meinke, P., Abraham, S., Yang, L., Neumann, S., … Noegel, A. A. (2012). LINC complex alterations in DMD and EDMD/CMT fibroblasts. *European Journal of Cell Biology*, *91*(8), 614–628. https://doi.org/10.1016/j.ejcb.2012.03.003
Theys, J., Jutten, B., Habets, R., Paesmans, K., Groot, A. J., Lambin, P., … Vooijs, M. (2011). E-Cadherin loss associated with EMT promotes radioresistance in human tumor cells. *Radiotherapy and Oncology*, *99*(3), 392–397. https://doi.org/10.1016/j.radonc.2011.05.044
Thiery, J. P. (2002). Epithelial–mesenchymal transitions in tumour progression. *Nature Reviews Cancer*, *2*(6), 442–454. https://doi.org/10.1038/nrc822
Thiery, J. P., Acloque, H., Huang, R. Y. J., & Nieto, M. A. (2009). Epithelial-Mesenchymal Transitions in Development and Disease. *Cell*. https://doi.org/10.1016/j.cell.2009.11.007
Thiery, J. P., & Sleeman, J. P. (2006). Complex networks orchestrate epithelial-mesenchymal

transitions. *Nature Reviews. Molecular Cell Biology*, *7*(2), 131–142. https://doi.org/10.1038/nrm1835
Thompson, D. W. (1995). On growth and form, new ed. *Cambridge,Canto*. https://doi.org/10.1017/CBO9781107325852
Tojkander, S., Gateva, G., & Lappalainen, P. (2012). Actin stress fibers - assembly, dynamics and biological roles. *Journal of Cell Science*. https://doi.org/10.1242/jcs.098087
Torgan, C. E., Burge, S. S., Collinsworth, A. M., Truskey, G. A., & Kraus, W. E. (2000). Differentiation of mammalian skeletal muscle cells cultured on microcarrier beads in a rotating cell culture system. *Medical and Biological Engineering and Computing*. https://doi.org/10.1007/BF02345757
Tortelote, G. G., Reis, R. R., de Almeida Mendes, F., & Abreu, J. G. (2017). Complexity of the Wnt/β-catenin pathway: Searching for an activation model. *Cellular Signalling*. https://doi.org/10.1016/j.cellsig.2017.08.008
Truong, K., & Ikura, M. (2001). The use of FRET imaging microscopy to detect protein-protein interactions and protein conformational changes in vivo. *Current Opinion in Structural Biology*, *11*(5), 573–578. Retrieved from http://www.ncbi.nlm.nih.gov/pubmed/11785758
Turgay, Y., Eibauer, M., Goldman, A. E., Shimi, T., Khayat, M., Ben-Harush, K., … Medalia, O. (2017). The molecular architecture of lamins in somatic cells. *Nature*, *543*(7644), 261–264. https://doi.org/10.1038/nature21382
Turner, C. E., Glenney, J. R., & Burridge, K. (1990). Paxillin: A new vinculin-binding protein present in focal adhesions. *Journal of Cell Biology*. https://doi.org/10.1083/jcb.111.3.1059
Udatsu, Y., Kusafuka, T., Kuroda, S., Miao, J., & Okada, A. (2001). High frequency of beta-catenin mutations in hepatoblastoma. *Pediatric Surgery International*, *17*(7), 508–512. Retrieved from http://www.ncbi.nlm.nih.gov/pubmed/11666046
Uzer, G., Bas, G., Sen, B., Xie, Z., Birks, S., Olcum, M., … Rubin, J. (2018). Sun-mediated mechanical LINC between nucleus and cytoskeleton regulates βcatenin nuclear access. *Journal of Biomechanics*. https://doi.org/10.1016/j.jbiomech.2018.04.013
Valenta, T., Hausmann, G., & Basler, K. (2012). The many faces and functions of β-catenin. *The EMBO Journal*. https://doi.org/10.1038/emboj.2012.150
Van Noort, M., Meeldijk, J., Van Der Zee, R., Destree, O., & Clevers, H. (2002). Wnt signaling controls the phosphorylation status of β-catenin. *Journal of Biological Chemistry*, *277*(20), 17901–17905. https://doi.org/10.1074/jbc.M111635200
van Steensel, B., & Belmont, A. S. (2017, May 18). Lamina-Associated Domains: Links with Chromosome Architecture, Heterochromatin, and Gene Repression. *Cell*, Vol. 169, pp. 780–791. https://doi.org/10.1016/j.cell.2017.04.022
Veneziano, L., Barra, V., Cilluffo, D., & Di Leonardo, A. (2019). Proliferation of aneuploid cells induced by CENP-E depletion is counteracted by the p14 ARF tumor suppressor. *Molecular Genetics and Genomics*, *294*(1), 149–158. https://doi.org/10.1007/s00438-018-1495-5
Vennstrom, B., Sheiness, D., Zabielski, J., & Bishop, J. M. (1982). Isolation and characterization of c-myc, a cellular homolog of the oncogene (v-myc) of avian myelocytomatosis virus strain 29. *Journal of Virology*, *42*(3), 773–779. Retrieved from http://www.ncbi.nlm.nih.gov/pubmed/6284994
Vermeulen, S. J., Bruyneel, E. A., Bracke, M. E., De Bruyne, G. K., Vennekens, K. M., Vleminckx, K. L., … Mareel, M. M. (1995). Transition from the noninvasive to the invasive phenotype and loss of alpha-catenin in human colon cancer cells. *Cancer Research*, *55*(20), 4722–4728. Retrieved from http://www.ncbi.nlm.nih.gov/pubmed/7553655
Vermeulen, S. J., Nollet, F., Teugels, E., Vennekens, K. M., Malfait, F., Philippé, J., … Mareel, M. M.

(1999). The alphaE-catenin gene (CTNNA1) acts as an invasion-suppressor gene in human colon cancer cells. *Oncogene*, *18*(4), 905–915. https://doi.org/10.1038/sj.onc.1202348
Vite, A., Li, J., & Radice, G. L. (2015). New functions for alpha-catenins in health and disease: from cancer to heart regeneration. *Cell and Tissue Research*, *360*(3), 773–783. https://doi.org/10.1007/s00441-015-2123-x
Walker, R. G., Willingham, A. T., & Zuker, C. S. (2000). A Drosophila mechanosensory transduction channel. *Science*. https://doi.org/10.1126/science.287.5461.2229
Wall, M., Butler, D., El Haj, A., Bodle, J. C., Loboa, E. G., & Banes, A. J. (2018). Key developments that impacted the field of mechanobiology and mechanotransduction. *Journal of Orthopaedic Research*. https://doi.org/10.1002/jor.23707
Wang, N., Butler, J. P., & Ingber, D. E. (1993). Mechanotransduction across the cell surface and through the cytoskeleton. *Science*. https://doi.org/10.1126/science.7684161
Wang, N., & Suo, Z. (2005). Long-distance propagation of forces in a cell. *Biochemical and Biophysical Research Communications*, *328*(4), 1133–1138. https://doi.org/10.1016/j.bbrc.2005.01.070
Wang, N., Tytell, J. D., & Ingber, D. E. (2009). Mechanotransduction at a distance: Mechanically coupling the extracellular matrix with the nucleus. *Nature Reviews Molecular Cell Biology*. https://doi.org/10.1038/nrm2594
Wang, S., Stoops, E., Unnikannan, C. P., Markus, B., Reuveny, A., Ordan, E., & Volk, T. (2018). Mechanotransduction via the LINC complex regulates DNA replication in myonuclei. *Journal of Cell Biology*. https://doi.org/10.1083/jcb.201708137
Wang, Y. K., Samos, C. H., Peoples, R., Pérez-Jurado, L. A., Nusse, R., & Francke, U. (1997). A novel human homologue of the Drosophila frizzled wnt receptor gene binds wingless protein and is in the Williams syndrome deletion at 7q11.23. *Human Molecular Genetics*. https://doi.org/10.1093/hmg/6.3.465
Wang, Y, Macke, J. P., Abella, B. S., Andreasson, K., Worley, P., Gilbert, D. J., … Nathans, J. (1996). A large family of putative transmembrane receptors homologous to the product of the Drosophila tissue polarity gene frizzled. *The Journal of Biological Chemistry*, *271*(8), 4468–4476. https://doi.org/10.1074/jbc.271.8.4468
Wang, Yanshu, Chang, H., Rattner, A., & Nathans, J. (2016). Frizzled Receptors in Development and Disease. In *Current Topics in Developmental Biology*. https://doi.org/10.1016/bs.ctdb.2015.11.028
Wang, Zhenghe, Vogelstein, B., & Kinzler, K. W. (2003). Phosphorylation of beta-catenin at S33, S37, or T41 can occur in the absence of phosphorylation at T45 in colon cancer cells. *Cancer Research*, *63*(17), 5234–5235. Retrieved from http://www.ncbi.nlm.nih.gov/pubmed/14500351
Wang, Ziyi, Zhang, H., Hou, J., Niu, J., Ma, Z., Zhao, H., & Liu, C. (2015). Clinical implications of β-catenin protein expression in breast cancer. *International Journal of Clinical and Experimental Pathology*, *8*(11), 14989–14994. Retrieved from http://www.ncbi.nlm.nih.gov/pubmed/26823833
Watabe-Uchida, M., Uchida, N., Imamura, Y., Nagafuchi, A., Fujimoto, K., Uemura, T., … Takeichi, M. (1998). α-Catenin-vinculin interaction functions to organize the apical junctional complex in epithelial cells. *Journal of Cell Biology*. https://doi.org/10.1083/jcb.142.3.847
Watanabe, N., Madaule, P., Reid, T., Ishizaki, T., Watanabe, G., Kakizuka, A., … Narumiya, S. (1997). p140mDia, a mammalian homolog of Drosophila diaphanous, is a target protein for Rho small GTPase and is a ligand for profilin. *The EMBO Journal*, *16*(11), 3044–3056. https://doi.org/10.1093/emboj/16.11.3044
Weidner, K. M., Hartmann, G., Naldini, L., Comoglio, P. M., Sachs, M., Fonatsch, C., … Birchmeier, W. (1993). Molecular characteristics of HGF-SF and its role in cell motility and invasion.

EXS, *65*, 311–328. Retrieved from http://www.ncbi.nlm.nih.gov/pubmed/8380739
Wheeler, M. A., Davies, J. D., Zhang, Q., Emerson, L. J., Hunt, J., Shanahan, C. M., & Ellis, J. A. (2007). Distinct functional domains in nesprin-1α and nesprin-2β bind directly to emerin and both interactions are disrupted in X-linked Emery-Dreifuss muscular dystrophy. *Experimental Cell Research*. https://doi.org/10.1016/j.yexcr.2007.03.025
Whitehurst, A. W., Wilsbacher, J. L., You, Y., Luby-Phelps, K., Moore, M. S., & Cobb, M. H. (2002). ERK2 enters the nucleus by a carrier-independent mechanism. *Proceedings of the National Academy of Sciences of the United States of America*, *99*(11), 7496–7501. https://doi.org/10.1073/pnas.112495999
Wiese, K. E., Nusse, R., & van Amerongen, R. (2018). Wnt signalling: conquering complexity. *Development*. https://doi.org/10.1242/dev.165902
Wilhelmsen, K., Litjens, S. H. M., Kuikman, I., Tshimbalanga, N., Janssen, H., Van Bout, I. Den, … Sonnenberg, A. (2005). Nesprin-3, a novel outer nuclear membrane protein, associates with the cytoskeletal linker protein plectin. *Journal of Cell Biology*. https://doi.org/10.1083/jcb.200506083
Wilson, K. L., Holaska, J. M., Montes de Oca, R., Tifft, K., Zastrow, M., Segura-Totten, M., … Bengtsson, L. (2005). Nuclear membrane protein emerin: roles in gene regulation, actin dynamics and human disease. *Novartis Foundation Symposium*, *264*, 51–58; discussion 58-62, 227–230. Retrieved from http://www.ncbi.nlm.nih.gov/pubmed/15773747
Wolff, J. (2010a). The classic: on the inner architecture of bones and its importance for bone growth. 1870. *Clinical Orthopaedics and Related Research*. https://doi.org/10.1007/s11999-010-1239-2
Wolff, J. (2010b). The classic: on the theory of fracture healing. 1873. *Clinical Orthopaedics and Related Research*. https://doi.org/10.1007/s11999-010-1240-9
Wolff, J. (2011). The classic: On the significance of the architecture of the spongy substance for the question of bone growth: a preliminary publication. 1869. *Clinical Orthopaedics and Related Research*, *469*(11), 3077–3078. https://doi.org/10.1007/s11999-011-2041-5
WOLFF, & J. (1892). Das Gesetz der Transformation der Knochen. *A Hirshwald*, *1*, 1–152.
Worman, H. J. (2012). Nuclear lamins and laminopathies. *Journal of Pathology*. https://doi.org/10.1002/path.2999
Wu, G., Huang, H., Abreu, J. G., & He, X. (2009). Inhibition of GSK3 phosphorylation of β-catenin via phosphorylated PPPSPXS motifs of Wnt coreceptor LRP6. *PLoS ONE*. https://doi.org/10.1371/journal.pone.0004926
Wu, R., Zhai, Y., Fearon, E. R., & Cho, K. R. (2001). Diverse mechanisms of beta-catenin deregulation in ovarian endometrioid adenocarcinomas. *Cancer Research*, *61*(22), 8247–8255. Retrieved from http://www.ncbi.nlm.nih.gov/pubmed/11719457
Xia, J., Urabe, K., Moroi, Y., Koga, T., Duan, H., Li, Y., & Furue, M. (2006). beta-Catenin mutation and its nuclear localization are confirmed to be frequent causes of Wnt signaling pathway activation in pilomatricomas. *Journal of Dermatological Science*. https://doi.org/10.1016/j.jdermsci.2005.09.005
Xing, Y., Takemaru, K. I., Liu, J., Berndt, J. D., Zheng, J. J., Moon, R. T., & Xu, W. (2008). Crystal Structure of a Full-Length β-Catenin. *Structure*. https://doi.org/10.1016/j.str.2007.12.021
Xue, C., Plieth, D., Venkov, C., Xu, C., & Neilson, E. G. (2003). The gatekeeper effect of epithelial-mesenchymal transition regulates the frequency of breast cancer metastasis. *Cancer Research*, *63*(12), 3386–3394. Retrieved from http://www.ncbi.nlm.nih.gov/pubmed/12810675
Yamashita, H., Ichikawa, T., Matsuyama, D., Kimura, Y., Ueda, K., Craig, S. W., … Kioka, N. (2014). The role of the interaction of the vinculin proline-rich linker region with vinexin in sensing the stiffness of the extracellular matrix. *Journal of Cell Science*.

https://doi.org/10.1242/jcs.133645
Yamashita, Satoshi, Tsuboi, T., Ishinabe, N., Kitaguchi, T., & Michiue, T. (2016). Wide and high resolution tension measurement using FRET in embryo. *Scientific Reports*, *6*(1), 28535. https://doi.org/10.1038/srep28535
Yamashita, Shuntaro, Ogawa, K., Ikei, T., Fujiki, T., & Katakura, Y. (2014). FOXO3a potentiates hTERT gene expression by activating c-MYC and extends the replicative life-span of human fibroblast. *PLoS ONE*, *9*(7). https://doi.org/10.1371/journal.pone.0101864
Yan, C., Grimm, W. A., Garner, W. L., Qin, L., Travis, T., Tan, N., & Han, Y. P. (2010). Epithelial to mesenchymal transition in human skin wound healing is induced by tumor necrosis factor-α through bone morphogenic protein-2. *American Journal of Pathology*. https://doi.org/10.2353/ajpath.2010.090048
Yokoya, F., Imamoto, N., Tachibana, T., & Yoneda, Y. (1999). beta-catenin can be transported into the nucleus in a Ran-unassisted manner. *Molecular Biology of the Cell*, *10*(4), 1119–1131. https://doi.org/10.1091/mbc.10.4.1119
Yonemura, S., Wada, Y., Watanabe, T., Nagafuchi, A., & Shibata, M. (2010). α-Catenin as a tension transducer that induces adherens junction development. *Nature Cell Biology*. https://doi.org/10.1038/ncb2055
Yoshida, C., & Takeichi, M. (1982). Teratocarcinoma cell adhesion: identification of a cell-surface protein involved in calcium-dependent cell aggregation. *Cell*, *28*(2), 217–224.
Yu, F. X., Zhao, B., & Guan, K. L. (2015). Hippo Pathway in Organ Size Control, Tissue Homeostasis, and Cancer. *Cell*. https://doi.org/10.1016/j.cell.2015.10.044
Zanconato, F., Forcato, M., Battilana, G., Azzolin, L., Quaranta, E., Bodega, B., … Piccolo, S. (2015). Genome-wide association between YAP/TAZ/TEAD and AP-1 at enhancers drives oncogenic growth. *Nature Cell Biology*. https://doi.org/10.1038/ncb3216
Zeisberg, M., Yang, C., Martino, M., Duncan, M. B., Rieder, F., Tanjore, H., & Kalluri, R. (2007). Fibroblasts derive from hepatocytes in liver fibrosis via epithelial to mesenchymal transition. *The Journal of Biological Chemistry*, *282*(32), 23337–23347. https://doi.org/10.1074/jbc.M700194200
Zhang, J., Guo, W.-H., & Wang, Y.-L. (2014). Microtubules stabilize cell polarity by localizing rear signals. *Proceedings of the National Academy of Sciences*. https://doi.org/10.1073/pnas.1410533111
Zhang, L., & Min, W. (2017). Bioorthogonal chemical imaging of metabolic changes during epithelial–mesenchymal transition of cancer cells by stimulated Raman scattering microscopy. *Journal of Biomedical Optics*, *22*(10), 1. https://doi.org/10.1117/1.jbo.22.10.106010
Zhang, Q, Skepper, J. N., Yang, F., Davies, J. D., Hegyi, L., Roberts, R. G., … Shanahan, C. M. (2001). Nesprins: a novel family of spectrin-repeat-containing proteins that localize to the nuclear membrane in multiple tissues. *Journal of Cell Science*, *114*(Pt 24), 4485–4498. Retrieved from http://www.ncbi.nlm.nih.gov/pubmed/11792814
Zhang, Qiuping, Bethmann, C., Worth, N. F., Davies, J. D., Wasner, C., Feuer, A., … Shanahan, C. M. (2007). Nesprin-1 and -2 are involved in the pathogenesis of Emery Dreifuss muscular dystrophy and are critical for nuclear envelope integrity. *Human Molecular Genetics*, *16*(23), 2816–2833. https://doi.org/10.1093/hmg/ddm238
Zhang, X., Li, G., Guo, Y., Song, Y., Chen, L., Ruan, Q., … Guo, J. (2019). Regulation of ezrin tension by S-nitrosylation mediates non-small cell lung cancer invasion and metastasis. *Theranostics*, *9*(9), 2555–2571. https://doi.org/10.7150/thno.32479
Zhang, Y., Zhang, H., & Zhao, B. (2018). Hippo Signaling in the Immune System. *Trends in Biochemical Sciences*. https://doi.org/10.1016/j.tibs.2017.11.009
Zhao, K., Wang, W., Rando, O. J., Xue, Y., Swiderek, K., Kuo, A., & Crabtree, G. R. (1998). Rapid and phosphoinositol-dependent binding of the SWI/SNF-like BAF complex to chromatin

after T lymphocyte receptor signaling. *Cell*, *95*(5), 625–636. https://doi.org/10.1016/s0092-8674(00)81633-5

Zhong, Z., Chang, S. A., Kalinowski, A., Wilson, K. L., & Dahl, K. N. (2010). Stabilization of the spectrin-like domains of nesprin-1α by the evolutionarily conserved "adaptive" domain. *Cellular and Molecular Bioengineering*, *3*(2), 139–150. https://doi.org/10.1007/s12195-010-0121-3

Zhou, C., Rao, L., Shanahan, C. M., & Zhang, Q. (2018). Nesprin-1/2: roles in nuclear envelope organisation, myogenesis and muscle disease. *Biochemical Society Transactions*, *46*(2), 311–320. https://doi.org/10.1042/BST20170149

Zhou, J., Aponte-Santamaría, C., Sturm, S., Bullerjahn, J. T., Bronowska, A., & Gräter, F. (2015). Mechanism of Focal Adhesion Kinase Mechanosensing. *PLoS Computational Biology*, *11*(11), e1004593. https://doi.org/10.1371/journal.pcbi.1004593